UNIVERSITY OF LONDON THESIS

Degree MD Year 2008 Name of Author TOWNLEY, WILLIAM, ARTHUR.

An Investigation into the Role of Matrix Metalloproteinases in Matrix Remodelling and Contraction by Dupuytren's Fibroblasts

William Townley MRCS

2007

A thesis submitted to the University of London
for the degree of
Doctor of Medicine (MD)

The RAFT Institute of Plastic Surgery
The Leopold Muller Building
Mount Vernon Hospital
Northwood
Middlesex
UK
&
Ocular Repair & Regeneration Biology Unit (ORB)
Institute of Ophthalmology
University College London
UK

ProQuest LLC
789 East Eisenhower Parkway
P.O. Box 1346
Ann Arbor, MI 48106-1346

ABSTRACT

Dupuytren's disease is a common fibroproliferative condition of the hand that results in disability through progressive digital contracture. Despite advances in operative technique, recurrence remains an unsolved problem. The matrix metalloproteases (MMPs) are a large family of proteolytic enzymes that have been shown to play a critical role in cell-mediated collagen contraction and tissue scarring. The aim of this project was to investigate the effect of ilomastat, a broad-spectrum MMP inhibitor, on matrix contraction and remodelling by Dupuytren's fibroblasts in vitro.

Paired nodule and cord-derived fibroblasts were isolated by explant culture from five Dupuytren's patients, carpal ligament fibroblasts acted as the control. We employed two different in vitro models to assess the effect of ilomastat on contraction and remodelling by each cell population. A stress-release fibroblast populated collagen lattice (FPCL) model was employed to assess collagen contraction. Generation of mechanical tension was determined using a culture force monitor (CFM). Following dynamic force generation, treatment with cytochalasin-D was used to assess residual matrix tension (RMT) in the collagen lattice, allowing quantification of matrix remodelling. The expression of a range of MMPs (MMP-1, MMP-2, MT1-MMP) and Tissue Inhibitors of Metalloproteinases (TIMP-1, TIMP-2), was established by RT-PCR. Protein levels and enzyme activity were assessed by western blotting, zymography and ELISA.

In the FPCL model, ilomastat significantly ($p<0.01$) inhibited contraction by all tissue-derived fibroblasts at 100μM. In the CFM model, ilomastat significantly reduced force development by cord and nodule-derived fibroblasts ($p<0.01$), but did not significantly affect RMT. In both models, treatment with ilomastat suppressed activity of MMP-1 and MMP-2, however gene expression and levels of secreted protein were unaffected. Conversely, the expression and activity of MT1-MMP was upregulated in response to ilomastat, whereas, TIMP-1 and TIMP-2 were unaffected.

Our findings demonstrate an important role for MMP activity in matrix processing and organisation by Dupuytren's fibroblasts in vitro and suggest that inhibition of MMP activity may well provide a means of controlling or reducing contracture in vivo, by reducing fibroblast-mediated matrix contraction and remodelling.

ACKNOWLEDGEMENTS

This thesis was the product of the collective support, enthusiasm and goodwill of many people. I would like to begin by expressing my sincere gratitude to Mr. Adriaan Grobbelaar for being an inspiring and motivating supervisor throughout this project. I am also indebted to my scientific supervisor, Dr. Alison Cambrey, who demonstrated considerable patience and skill in guiding me through my two years as an MD student. She set high standards for my work and provided the necessary support and encouragement to help me realise them. Part of the work involved collaborating with the Institute of Ophthalmology and I received great help from all members of Professor Khaw's team.

The environment at RAFT was a pleasure to work in and many others contributed to my experience including both members of the administrative team (Hilary, Stephanie, Amanda, Christine, Sheila) as well as scientists (Miss J Richardson, Mrs. E. Clayton, Mr. J. Shelton, Dr. C. Linge). Dr K. Rolfe was instrumental in imparting her technical wisdom in the laboratory especially with regard to PCR and proved very tolerant of my incessant questioning. I am also grateful to Kate Beckett, the previous Dupuytren's fellow, whose thesis inspired this work and who has continued to provide valuable support despite busy clinical commitments.

This work would not have been completed without the valuable financial support from the Royal College of Surgeons of England, The Dunhill Trust, and all the Trustees of the Restoration and Function Trust

DECLARATION OF ORIGINALITY

I declare that the laboratory research for this thesis is original and that the ideas were developed in conjunction with my supervisors. I performed the experiments myself with the guidance and technical assistance of the laboratory and scientific staff at the Restoration of Appearance and Function Trust (RAFT) Institute, Mount Vernon Hospital, and the Institute of Ophthalmology at Moorefield's Eye Hospital.

This thesis is dedicated to my

loving and beautiful wife

Nathalie

ABBREVIATIONS

5-FU	5-Flourouracil
bFGF	Basic fibroblast growth factor
BSA`	Bovine serum albumin
CFM	Culture force monitor
CM	Cell-conditioned media
DEPC	Diethylprocarbonate
DMSO	Dimethyl sulphoxide
DNA	Deoxyribonucleic acid
ECM	Extracellular matrix
EGF	Epidermal growth factor
ELISA	Enzyme-linked immunosurbent assay
FCS	Fetal calf serum
FPCL	Fibroblast-populated collagen lattice
GFM	Gelatinase-free media
MCPJ	Metacarpophalangeal joint
MMP	Matrix metalloproteinase
MPI	Matrix metalloproteinase inhibitor
mRNA	Messenger ribonucleic acid
NGM	Normal fibroblast growth medium
OD	Optical density
PBS	Phosphate buffered saline
PCR	Polymerase chain reaction
PDGF	Platelet-derived growth factor
PFC	Palmar fascial complex
PIPJ	Proximal interphalangeal joint
RMT	Residual matrix tension
RT	Reverse transcriptase
SEM	Standard error of the mean
SMA	Smooth muscle actin
TBS	Tris buffered saline
TEMED	Tetramethylethylenediamine
TGF	Transforming growth factor
TIMP	Tissue inhibitor of metalloproteinase

CONTENTS

INDEX OF FIGURES

CHAPTER 1

CHAPTER 2

CHAPTER 3

CHAPTER 4

CHAPTER 5

CHAPTER 6

INDEX OF TABLES

CHAPTER 1

CHAPTER 2

CHAPTER 1

INTRODUCTION

1.1 OVERVIEW

Dupuytren's disease is a common fibrocontractile condition of the hand that causes disability through progressive digital contracture. Through its numerous associations, Dupuytren's disease crosses all borders of medicine and is frequently encountered by surgeon, physician and general practitioner alike. It tends to affect mainly the elderly, although younger patients carry a worse prognosis. The clinical significance of Dupuytren's primarily lies in the vast number of people affected (an estimated 2 million in the UK), accounting for lost workdays in the young and stolen dignity and diminished independence in the elderly.

The only widely accepted mode of treatment is surgery. Although surgery readily corrects contracture, the disease frequently recurs, as is often the case with fibroproliferative conditions. Unfortunately, the operative risks associated with recurrent procedures mount as the chance of delivering a fully functioning hand dwindles. Untreated, the disease can progress, leading to irreversible joint deformity and in severe cases, the prospect of amputation. Hence the quandary: of the current treatments, surgery undoubtedly provides the best outcome, but may lead to a vicious cycle of recurrent disease followed by surgical correction, that results in a spiralling deterioration in function. Hence, there is considerable impetus to develop a non-operative adjunct to surgery that will prevent both disease progression and recurrence and thereby allow patients to maintain hand function.

There is considerable evidence that MMPs play an important role in normal wound healing and in fibrocontractile scarring such as that found in Dupuytren's disease. This thesis intends to investigate the effects of ilomastat, a broad-spectrum MMP inhibitor, on matrix contraction and remodelling by Dupuytren's fibroblasts in vitro, with the aim of establishing its possible therapeutic potential as an agent to prevent recurrence and progression of contracture.

1.2 AETIOLOGY

Dupuytren's disease typically affects elderly men of Northern European descent. Prevalence varies widely according to the selected population, ranging from 2 to 42% (Ross 1999). This is not purely an environmental coincidence: it is underpinned by a genetic predisposition, since the high prevalence follows Northern Europeans to warmer climes such as Australia (Hueston 1962). The possible mode of inheritance appears, in several cases, to conform to a Mendelian autosomal dominant trait with variable penetrance (Ling 1963; Matthews 1979).

Genetic studies have yet to detect a specific gene or set of genes as the primary origin of Dupuytren's disease, although research into possible associations with different genetic polymorphisms may provide the first breakthrough. Bayat and colleagues (Bayat et al. 2003) have unravelled an association between Dupuytren's disease and allele frequency of a transcription factor (Zinc finger 9) for transforming growth factor β (TGF β), a pro-fibrotic gene. More recently, Hu and colleagues (Hu et al. 2005) established genetic linkage in a Swedish family affected by Dupuytren's, pinpointed to a region on chromosome 16. The locus harbours several interesting candidate genes, including some encoding matrix metalloproteinases.

Development of disease appears to be contingent on an environmental trigger as well as a genetic predisposition. Smoking and excessive alcohol intake are independent risk factors for disease development, and in both cases the relation is dose dependent (Godtfredsen et al. 2004). Chronic liver disease is not a risk factor independent of alcohol consumption (Attali et al. 1987). The condition is more prevalent among diabetics, especially those dependent on insulin (Godtfredsen et al. 2004). Controversy exists as to the significance of either anticonvulsant drugs or epilepsy (Critchley et al. 1976; Arafa et al. 1992). As many studies have established a relation between Dupuytren's disease and manual labour as have refuted one (McFarlane 1991). Most experts would concede, however, that a one-off hand injury can rarely trigger Dupuytren's disease, but that a history of manual labour indicates a worse prognosis.

1.3 ANATOMY

1.3.1 Normal anatomy

An appreciation of the normal anatomy is key to understanding the deformities associated with Dupuytren's disease and the surgical basis of their correction. Dupuytren's disease affects the palmar fascial complex (PFC) – a tough aponeurotic sheet that lies deep to the dermis and fans outwards from the wrist, taking origin from the palmaris longus tendon, where present (Ritter 1973), or, if absent, from the flexor retinaculum. The PFC proceeds distally across the volar aspect of the palm as a woven 3-dimensional fascial framework terminating in the digital fascia. The PFC serves to support the palmar skin against compressive and shearing forces, to protect deeper structures, and to maintain the transverse arch and cupping of the hand through fixation to the metacarpals. It also allows conformation of the palmar skin to assist grasping objects.

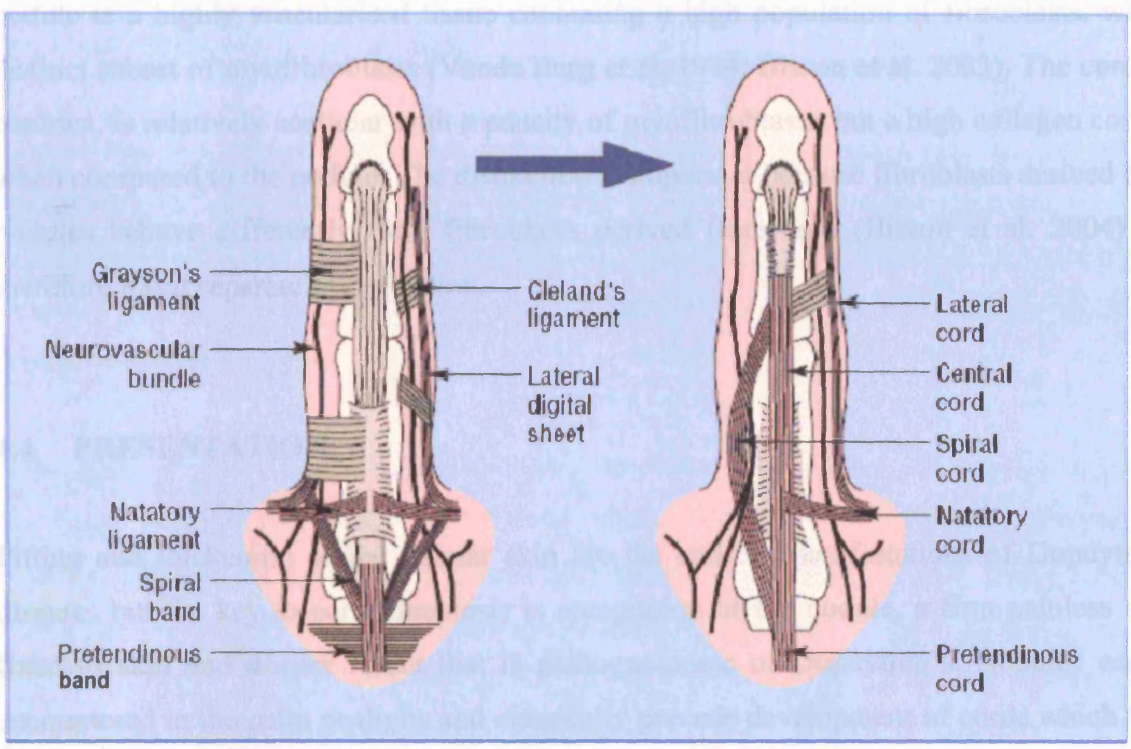

Figure 1. Normal anatomy of the digital fascia (left) and pathological fascial structures associated with Dupuytren's disease (right).

1.3.2 Pathological anatomy

The lesions of Dupuytren's disease can be explained in terms of involvement of different elements of the PFC. The normal bands and ligaments of the PFC are the precursors of the diseased nodules and cords, the two main lesions observed in Dupuytren's disease (Figure 1). Nodules are firm fleshy masses that form along the lines of the longitudinal fibres of the palm (McGrouther 1982), usually superficial to the pretendinous band. Cord is the term used to describe affected bands (Luck 1959). Cords are prone to contracture, resulting in progressive shortening of the diseased fascia and subsequent digital flexion deformity. The continuity between palmar and digital fascia ensures that contracture is continuous from palm to digit.

1.3.3 Microscopic anatomy

Nodules and cords are discrete entities that relate to different stages of disease, which can be readily distinguished by histological analysis in addition to clinical observation. The nodule is a highly vascularised tissue containing a high population of fibroblasts, with a distinct subset of myofibroblasts (Vande Berg et al. 1984; Bisson et al. 2003). The cord, by contrast, is relatively acellular with a paucity of myofibroblasts, but a high collagen content when compared to the nodule. The distinction is important because fibroblasts derived from nodules behave differently from fibroblasts derived from cord (Bisson et al. 2004) and therefore merit separate investigation.

1.4 PRESENTATION

Pitting and thickening of the palmar skin are the earliest manifestations of Dupuytren's disease, but the key to early diagnosis is recognition of the nodule, a firm painless mass fixed to skin and deeper fascia that is pathognemonic of Dupuytren's. Nodules can be encountered in the palm or digits and classically precede development of cords which form firm tendon-like structures (Rayan 1999). Contraction of cords results in predictable deformity as they cross joints (Table 1): the palmar cords (pretendinous) cause flexion contracture at the metacarpophalangeal (MCP) joint; the digital cords (lateral, central,

spiral) contribute to proximal interphalangeal (PIP) joint contracture. The spiral cord is responsible for both PIPJ contracture and superficial displacement of the neurovascular bundle, making it more susceptible to accidental division at surgery.

NORMAL STRUCTURE	PATHOLOGIC CORD	CLINICAL EFFECT
Pretendinous band	Pretendinous cord	MCPJ deformity
Central fibrofatty tissue	Central cord	PIPJ deformity
Spiral band	Spiral cord	Displaces neurovascular bundle superficially
Lateral digital sheet	Lateral cord	PIPJ/DIPJ contracture

Table 1. The normal anatomical palmar fascial precursors of the pathological structures observed in Dupuytren's disease and their clinical effect.

Contracture is a common presenting complaint (Figure 2), although it may be the fear of malignancy or embarrassment of a handshake that precipitates initial consultation. The main consequence is impaired function. Contractures can affect activities at the work place (manual labour, wearing gloves) and in the home (washing, dressing), posing a threat to independence and dignity.

The condition is frequently bilateral and often associated with involvement of other areas of the body, so called ectopic disease; Garrod's knuckle pads (44-54%), plantar fibromatosis (Ledderhose disease, 6-31%) and penile fibromatosis (Peyronie's disease, 2-8%) (Rayan 1999). A diathesis is recognised in Dupuytren's and describes disease affecting young Caucasian men with a strong family history, bilateral involvement, severe disease and ectopic manifestations. Recognition of this clinical type is essential as it carries with it a more serious prognosis and warrants aggressive follow-up and treatment.

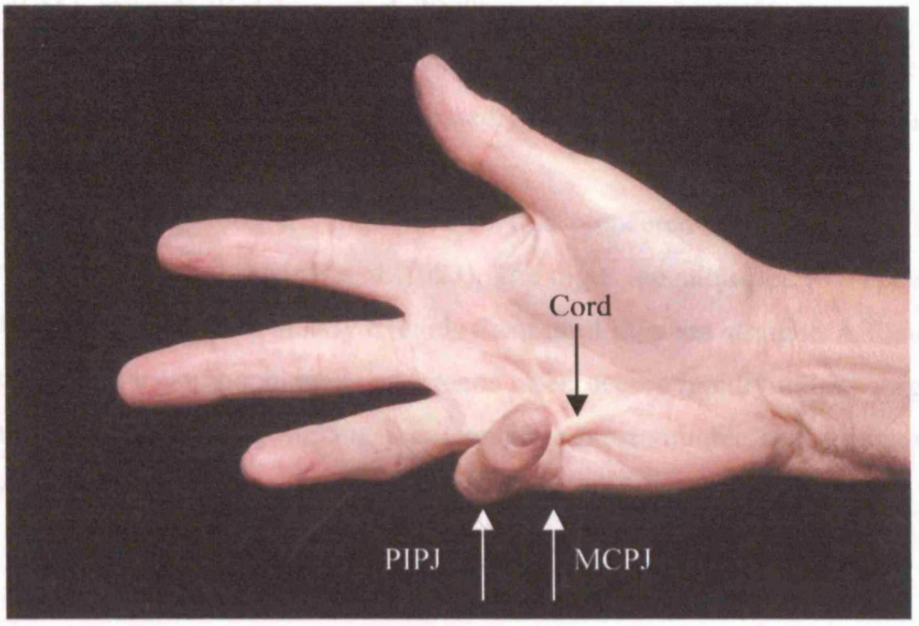

Figure 2. Dupuytren's disease affecting the little finger. MCPJ and PIPJ contracture due to a tight cord of tissue.

1.5 TREATMENT

The majority of patients with Dupuytren's disease do not require treatment and can be managed expectantly as disease often remains confined to the palm and does not progress to digital flexion deformity (Rayan 1999). Intervention is almost exclusively surgical and should be considered where function is impeded or where deformity is disabling. Referral to a specialist is advisable when contracture develops, because the longer deformity prevails, the greater the chance of joint contracture becoming irreversible, with ligaments remodelling in the contracted position.

1.5.1 Non-operative management

Despite much unravelling of the biochemical and cellular processes underlying Dupuytren's Disease, there has so far been no translation into medical treatment. Several non-operative treatments, including radiotherapy (Keilholz et al. 1996), ultrasonic therapy

(Stiles 1966), steroids (Ketchum et al. 2000), topical vitamin A (Shelley et al. 1993), 5-FU (Bulstrode et al. 2004), gamma interferon (Pittet et al. 1994) and the enzyme, collagenase (Badalamente et al. 2002) have been assessed. However, none has gained popularity.

The continuous elongation technique (TEC) was pioneered as a non-operative means of correcting contracture (Messina et al. 1993). The digits are subjected to mechanical tension on an adjustable frame that slowly extends them until they are straight. Although reduction in contracture is usually achieved, recurrence often occurs rapidly unless surgical excision is subsequently performed, making this technique most suitable as a preparatory step for surgery.

1.5.2 Surgical correction

The aim of surgery is to restore function and correct deformity with minimal complications. Broadly speaking, surgical options involve either fasciotomy, in which the cord is simply divided, or fasciectomy, in which the diseased fascia is excised. Fasciectomy can be either limited, where all macroscopically diseased tissue is excised, or segmental, where only segments of the diseased tissue are removed (Moermans 1996). Intraoperative complications are rare (1-2%) but include digital nerve or vessel injury and buttonholing of skin flaps (Bulstrode et al. 2005). In the early postoperative period, heamatoma, infection and flap necrosis occur relatively frequently (19%) (McFarlane 1983). Such wound complications may be reduced by segmental fasciectomy, which involves a more minimal dissection compared to limited fasciectomy (Moermans 1996).

1.5.3 Recurrence

Although surgery corrects contracture, it does not cure disease. Over time, recurrence is likely, with new Dupuytren's tissue appearing within areas previously cleared at operation, and the disease extending into previously untreated areas (Figure 3, Table 2). Recurrence appears to be an early postoperative event that particularly affects young patients (Hueston 1963) and those with aggressive disease (Rodrigo et al. 1976).

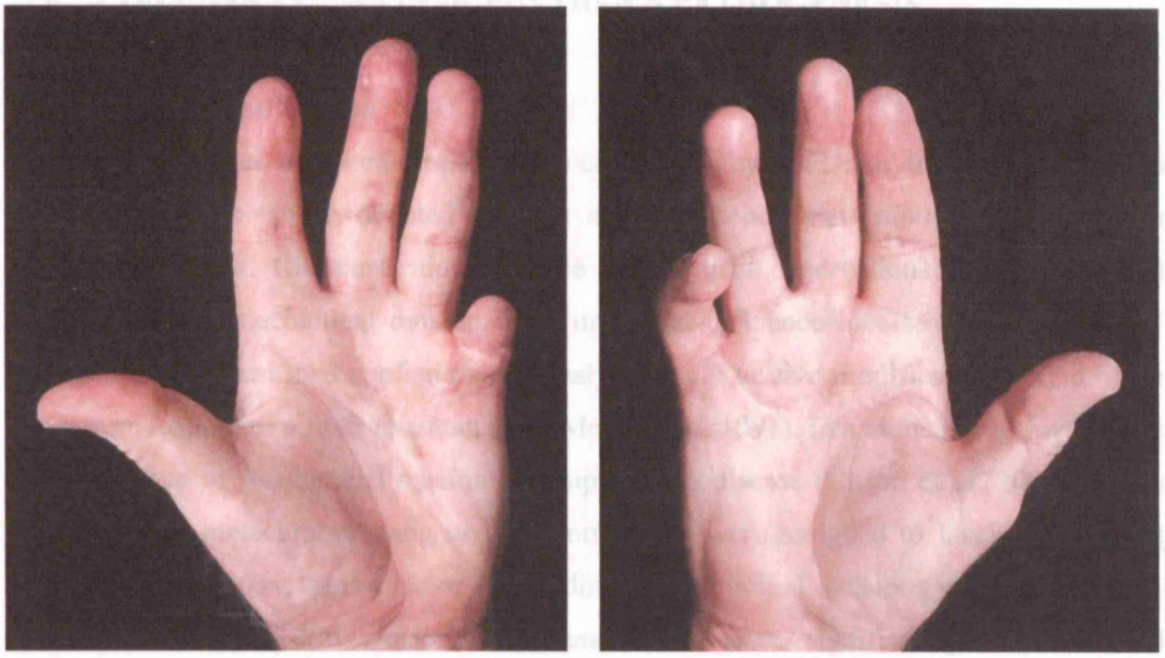

Figure 3. Recurrent Dupuytren's disease affecting the little fingers. Multiple recurrences of Dupuytren's disease in the left hand has led to amputation.

STUDY	PATIENTS *(hands)*	FOLLOW-UP (years)	RECURRENCE (%)	EXTENSION (%)
FASCIOTOMY				
(Foucher et al. 2003)	100	3.2	58	11
LIMITED FASCIECTOMY				
(Rombouts et al. 1989)	63 *(77)*	5.3	39	32
(Makela et al. 1991)	127 *(153)*	3.2	27	7
(Foucher et al. 1992)	54 *(67)*	5.6	41	39
(Moermans 1996)	141 *(173)*	2.9	47	31
(Armstrong et al. 2000)	103 *(143)*	5.8	8.4	*

Table 2. Reported recurrence and extension rates of Dupuytren's disease.

*Numbers not available in published series.

1.6 CONSIDERATIONS IN DUPUYTREN'S PATHOGENESIS

1.6.1 Mechanical tension

Mechanical tension has been proposed as a cause or trigger of Dupuytren's disease. In part, this relates to the much debated possible association between Dupuytren's and manual labour or trauma. Circumstantial evidence and clinical observations add weight to the suggestion that mechanical tension is an important influence in disease pathogenesis. A reduced mechanical load applied exogenously to a scar in vivo modifies the wound healing response, leading to a finer resultant scar (Meyer et al. 1991). In a clinical trial investigating the influence of mechanical tension on Dupuytren's disease (Citron et al. 2003), patients with isolated metacarpophalangeal joint contracture were assigned to fasciotomy through one of two incisions, transverse or longitudinal. Longitudinal incisions were closed with z-plasties to reduce skin tension. Recurrence rates were significantly reduced in the longitudinal incision group leading the investigators to propose that mechanical tension is a contributing factor to Dupuytren's pathogenesis. This observation has not been substantiated by further clinical studies (Citron et al. 2005). However, as will be subsequently shown, mechanical tension is an important influence on fibroblast behaviour in vitro although its role in disease pathogenesis remains to be determined.

1.6.2 Similarities with wound healing

Although Dupuytren's tissue appears to have several features in common with neoplastic conditions (McFarlane 1990; Jemec et al. 1999), the disease evolves at the cellular and connective tissue level, similar to a healing wound (Fitzgerald et al. 1999). As well as fibroblast proliferation, both conditions are marked by extracellular matrix deposition. Similarly, the myofibroblast, a fibroblast derivative associated with contractile force, is prominent in both granulation tissue, where it assists wound closure, and Dupuytren's tissue. Growth factor production, stimulated by injury, is essential for coordinating repair in the healing wound. Similarly, upregulation of various growth factors and their receptors also occurs in Dupuytren's tissue (Baird et al. 1993) and may propagate the disease process.

The above observations suggest that many of the matrix and cellular events that are common to wound healing also occur in Dupuytren's disease, but without the same level of control. Whereas wound healing is induced by dermal injury, there is no obvious precipitating event identifiable in Dupuytren's disease, although hypoxia-induced free radicals and microtrauma to collagen fibres have been identified as possible triggers (McGrouther 1982; Murrell et al. 1987). Moreover, wound healing proceeds in a very regulated manner, delivering new epithelialised dermis in a very time-specific and controlled way. The response subsides as wound closure occurs and resolution or repair is achieved. By contrast, the disease process in Dupuytren's is uncontrolled, leading to a persistent or progressive response similar to the pathological healing response that defines keloid and hypertrophic scarring.

1.7 THE EXTRACELLULAR MATRIX

The extracellular matrix (ECM) is the environment in which cells are embedded. It provides a supportive scaffold through a network of macromolecules and acts as an important reservoir of biologically active molecules. It therefore contains the necessary components to protect and guide cell movement and provides an intricate molecular milieu capable of influencing and participating in cell signalling as well as facilitating cell behaviour such as growth, differentiation and migration (Lin et al. 1993). The ECM is not a passive, static structure, but rather a dynamic organisation, evolving to meet the requirements of an environment subject to mechanical and biological changes. Together, the ECM and the cells embedded in it form connective tissue, which provides the connecting and structural framework of the body. An appreciation of the reciprocal relationship between cells and the ECM is integral to gaining insight into the abnormalities underlying connective tissue diseases such as Dupuytren's disease. Cells such as fibroblasts produce matrix components and can therefore determine ECM composition. Conversely, the ECM can influence cell behaviour by sequestering signalling molecules, such as growth factors and growth-factor binding proteins, and by acting as ligands for cellular adhesion receptors, such as integrins, that transduce signals to the interior (Streuli 1999).

There are four major classes of macromolecules that make up the ECM – collagens, proteoglycans, glycoproteins and elastin (Haralson et al. 1995). Collagen is the most abundant protein in the body (van der Rest et al. 1991). Collagen in fact encompasses a large family of structurally similar molecules predominantly synthesised by fibroblasts that share a characteristic triple helical arrangement. Type I is found in all connective tissues (skin, tendon, bone etc.); type II occurs in hyaline cartilage, and type III in distensible tissues (skin, lung, vessels). Collagen types I, II and III are the major fibrous collagens providing structural support, whereas, type IV has a mesh-like structure and is an important constituent of basement membranes where it aids filtration (e.g. glomeruli in the kidney). Alterations in collagen structure account for numerous diseases; for example, osteogenesis imperfecta and Ehlers-Danlos syndrome. The glycoproteins include fibronectin, an important cell-adhesion molecule, and laminin, another component of basement membranes. Elastin is a structural protein that confers distensibility on tissues. ECM production is controlled by cell type, cell number and many growth factors, whereas matrix breakdown is controlled by specific proteases, the matrix metalloproteases (Haralson et al. 1995).

All matrix proteins can interact both with cells, through specific cell surface receptors, and, other matrix molecules through specific binding domains. The result is a fusion of matrix molecules and cells that are in constant communication, enabling maintenance of tissue structure and adaptation of function. These qualities are especially important in guiding embryogenesis and tissue repair. However, changes in matrix metabolism (both in synthesis and degradation) are associated with a number of acquired diseases, including Dupuytren's contracture (Tomasek et al. 2002).

1.8 CHANGES IN THE ECM IN DUPUYTREN'S DISEASE

1.8.1 Collagen

There are two major abnormalities of collagen synthesis in Dupuytren's tissue compared to normal palmar fascia. Firstly, there is an overall increase in the collagen content of

Dupuytren's tissue and secondly, there is an abundance of type-III collagen, which is virtually absent in normal palmar fascia (Menzel et al. 1979; Gelberman et al. 1980; Brickley-Parsons et al. 1981). These changes mirror those occurring in the granulation tissue of dermal wounds and hypertrophic scars (Bailey et al. 1975). However, whereas the stimulus for continued type III collagen disappears in a normal healing wound as the scar matures, such stimulus inexplicably persists in Dupuytren's disease. It has been proposed that the increase in newly synthesised collagen encountered in Dupuytren's tissue may be accounted for by an increase in fibroblast density rather than an aberration in collagen production (Murrell et al. 1991).

A defining feature of Dupuytren's disease is tissue contracture, specifically a progressive shortening of the longitudinal axis of the palmar fascia. In theory, this contracture could result from a change in the collagen organisation through either fibril plication or shortening by disruption of the triple helical structure of collagen. However, x-ray diffraction studies indicate that there is no evidence of either plication or collagen denaturation (Brickley-Parsons et al. 1981). In fact, the alignment of collagen fibrils in Dupuytren's palmar fascia is, if anything, better than seen in controls and is therefore an unlikely source of contracture.

1.8.2 Proteoglycans

Kozma (Kozma et al. 2005) demonstrated significant differences in the proteoglycan profile of Dupuytren's tissue compared to normal palmar fascia. Specifically, increased amounts of biglycan and chondroitin sulphate were found in Dupuytren's tissue, together with significant alterations in the chain structure of decorin. Proteoglycans play a role in matrix

assembly and can influence matrix permeability. It was therefore postulated that the observed proteoglycan changes might affect the matrix properties and disease progression.

1.9 MYOFIBROBLASTS

The term 'myofibroblast' derives from the morphological features the cell shares in common with both fibroblasts and smooth muscle cells. Myofibroblasts were first observed in the granulation tissue of healing wounds (Gabbiani et al. 1971), but have subsequently been identified in many fibrotic tissues, including Dupuytren's (Gabbiani et al. 1972). Rayan and Tomasek (Rayan et al. 1994) demonstrated that myofibroblasts in Dupuytren's disease are likely to derive from differentiation of fibroblasts, as opposed to smooth muscle cells. Fibroblasts from normal palmar aponeurosis cultured within a collagen lattice acquired morphological characteristics, including stress fibres similar to myofibroblasts in Dupuytren's diseased fascia.

Myofibroblasts are virtually absent from normal dermis and normal palmar fascia (Bisson et al. 2003). They do occur in normal wound healing as the differentiation of fibroblast to myofibroblast facilitates wound contraction and re-epithelialisation. After successful resolution or repair of a wound, myofibroblasts undergo apoptosis and disappear. However, in pathological scarring conditions such as keloid and hypertrophic scars, myofibroblasts persist (Ehrlich et al. 1994). The presence of myofibroblasts is in fact a common finding in many fibrotic diseases (Thannickal et al. 2004) including Dupuytren's disease, they have been associated both with the involutional stage of disease (Meister et al. 1979) and with nodule phenotype (Hueston et al. 1976). Furthermore, McCann (McCann et al. 1993) suggested that the presence of dermal myofibroblasts may be linked to recurrence after surgery. The role of myofibroblasts in generating contractile force will be discussed in subsequent sections.

1.10 GROWTH FACTOR CHANGES IN DUPUYTREN'S DISEASE

Growth factors are naturally occurring polypeptides that influence a wide range of cellular activities such as migration, proliferation, differentiation and matrix synthesis. There is increasing evidence that various growth factors play an important role in the pathophysiology of Dupuytren's disease (Badalamente et al. 1999; Cordova et al. 2005).

Similar to the healing wound, Dupuytren's tissue is an environment rich in biologically active molecules. Platelet-derived growth factor B (PDGF-B), basic fibroblast growth factor (bFGF), and transforming growth factor-β1 (TGF-β1) have been found in increased levels in Dupuytren's tissue, together with increased levels of their receptors (Gonzalez et al. 1992; Terek et al. 1995; Badalamente et al. 1996). PDGF-α stimulates cellular proliferation, whereas TGF-β1 induces myofibroblast differentiation and collagen production (Alioto et al. 1994; Tomasek et al. 2002) – all fundamental processes in Dupuytren's pathogenesis. Augoff (Augoff et al. 2005) observed that epidermal growth factor (EGF) varies with the stage of disease and may be particularly important in contracture development.

1.11 MATRIX REMODELLING

Fibroblasts possess the ability to remodel the surrounding extracellular matrix through a combination of matrix degradation, synthesis and organisation. These activities are critical for maintaining tissue homeostasis during development and in response to injury. The interaction nurtured between cells and the ECM is both dynamic and reciprocal. The matrix communicates with cells both directly, through interaction with cell surface proteins to initiate signal transduction pathways and indirectly, through release or activation of sequestered growth factors. Hence, modulation of the ECM through the remodelling of its structure and activity can profoundly influence function of both the matrix and the cells residing within it. Any remodelling process inevitably involves the removal of matrix

molecules and although many enzymes participate, matrix degradation is largely mediated by matrix metalloproteinases.

1.12 MATRIX METALLOPROTEINASES (MMPS)

The matrix metalloproteinases (MMP) are a family of zinc-dependent endopeptidases that cleave extracellular matrix (ECM) components and participate in many biological processes. Several reviews have been consulted to crystallise information in this section (Nagase et al. 1999; Visse et al. 2003; Lemaitre et al. 2006; Nagase et al. 2006). Through matrix resorption, MMPs facilitate tissue remodelling, cell migration and release of biologically active molecules that regulate fundamental cellular processes such as proliferation, growth, signalling and differentiation. In addition to matrix substrates, MMPs also cleave cell surface molecules and pericellular non-matrix proteins such as clotting factors and other proteinases. At the tissue level, MMPs influence diverse physiological processes such as embryonic development, tissue morphogenesis and wound repair. There is also an accumulating body of evidence that implicates MMP activity in numerous pathological processes such as arthritis, glaucoma, atherosclerosis and cancer.

MMPs are distinguished from other metalloproteinases by a highly conserved motif containing three histidines that bind zinc at the catalytic site and by a conserved methionine turn that sits beneath the active site zinc. Figure 4 illustrates the generic domain structure of MMPs. They are either secreted from the cell as inactive zymogens, requiring activation, or anchored to the cell membrane. Each MMP has distinct but often overlapping substrate-specificities and together they can cleave all ECM proteins (Sternlicht et al. 2001). The characteristic of redundancy safeguards against any loss of MMP activity but underlines the complexity of the MMP family, making it difficult to associate individual MMPs with specific functions or disease processes.

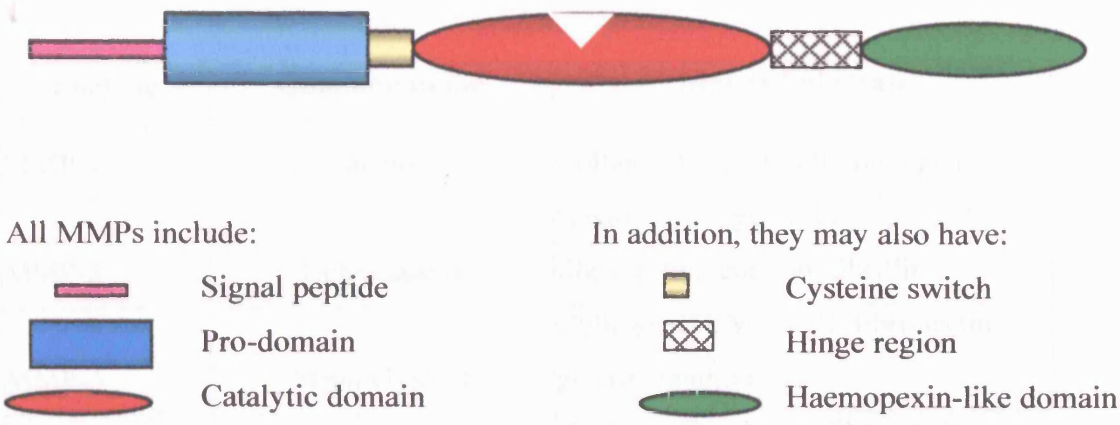

Figure 4. General domain structures of MMPs. The lengths of the domains are not drawn in proportion to the actual number of amino acid residues.

Twenty-three MMPs have been described in humans, which, depending on substrate specificity, sequence similarity and domain structure, are assigned to different groups – collagenases, gelatinases, stromelysins, matrilysins and membrane-bound MMPs. Table 2 illustrates the common MMPs described in humans.

Collagenases are distinguished by the ability to cleave the triple helix of interstitial collagens I, II and III. Gelatinases readily digest denatured collagens and gelatins. Stromelysins share similar structure and substrate specificity, and, in addition to digesting ECM components, stromelysin-1 activates several proMMPs, such as MMP-1. Matrilysins process cell surface molecules and ECM components. The membrane-type MMPs (MT-MMPs) are characterised by the presence of a transmembrane domain and are involved in the activation of proMMPs as well as matrix processing.

Enzyme	Common name	Matrix Substrates
MMP-1	Collagenase-1	Collagen I, II, III, VII, aggregan
MMP-2	Gelatinase A	Gelatin, Collagen I, IV, V, VII, X, fibronectin, tenascin, fibrillin
MMP-3	Stromelysin-1	Collagen IV, V, IX, X, fibronectin, gelatin, laminin
MMP-7	Matrilysin	Collagen IV, elastin, fibronectin, laminin, tenascin
MMP-8	Collagenase-2	Collagen I, II, III, aggregan
MMP-9	Gelatinase B	Gelatin, Collagen IV, V, VII, XI, elastin, fibrillin
MMP-10	Stromelysin-2	Collagen IV, V, IX, X, fibronectin, gelatin, laminin
MMP-11	Stromelysin-3	Fibronectin, laminin
MMP-12	Metalloelastase	Collagen IV, fibronectin, gelatin, laminin, elastin, fibrillin
MMP-13	Collagenase-3	Collagen I, II, III, IV, VII, IX, X, gelatin, fibronectin, laminin
MMP-14	MT1-MMP	Collagen I, II, III, gelatin, laminin, vitronectin
MMP-15	MT2-MMP	Fibronectin, laminin, aggrecan, tenascin, nidogen
MMP-16	MT3-MMP	Collagen III, fibronectin, gelatin, cartilage, proteoglycan
MMP-17	MT4-MMP	Gelatin
MMP-20	Enamelysin	Amelogenin

Table 3. A list of MMPs that have been demonstrated in humans.

1.12.1 Regulation of MMP activity

In order that MMP proteolysis does not lead to widespread matrix destruction, MMPs must be activated or inhibited appropriately. Control is essential. Hence, MMPs are tightly regulated at the transcriptional and post-transcriptional levels. Control is also exercised at the protein level via activators and inhibitors (Figure 5).

The level of MMP expression is very low in vivo and in unstimulated cells in vitro. However, MMP expression is induced by various signals, including growth factors, cytokines, physical stress and cell-matrix and cell-cell interactions. In fact, the biologic function of individual MMPs is largely dictated by their differential patterns of expression, since substrate specificities often overlap and are therefore not necessarily distinguishing features. Thus, most MMPs are tightly regulated at the level of transcription, with the exception of MMP-2, which is often controlled through enzyme activation. Post-transcriptional mechanisms of control include stabilisation of mRNA transcripts by phorbol esters (MMP-1, MMP-3) or hormones (e.g. glucocorticoids, MMP-13). Following translation of mRNA transcripts, most MMPs are constitutively secreted with the exception of those integrated into the cell membrane.

MMPs are secreted as inactive zymogens that are mostly subsequently activated by cleavage of a pro-domain. Exceptions include MMP-11 and MT1-MMP, which are activated intracellularly by Golgi-associated proteases prior to secretion (MMP-11) or membrane expression (MT1-MMP). Individual enzyme activation occurs in a stepwise fashion whilst collectively, MMPs are activated in a cascade, enabling finer regulatory control. Activated MMPs can participate in the processing of other MMPs. Activation by plasma proteinases such as plasmin appears to be an important physiological pathway *in vivo*. ProMMP-2 is not readily activated by general proteinases. Instead, activation of pro-MMP-2 takes place on the cell surface and is mediated by MT-MMPs including MT1-MMP.

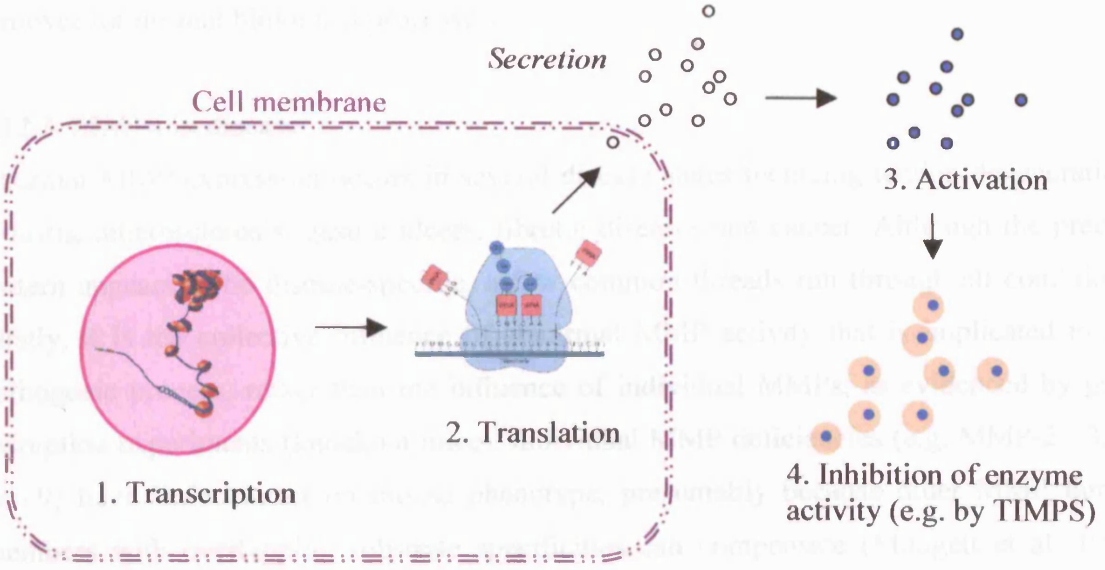

Figure 5. Regulation of MMP activity occurs at many different levels ranging from gene transcription, through protein production, to activation and inhibition of secreted enzymes. Most MMPs are constitutively secreted.

1.12.2 Endogenous MMP inhibitors

The tissue inhibitors of matrix metalloproteinases (TIMPs) represent a family of at least four secreted proteins that are the major endogenous inhibitors of MMP activity in the tissue. They reversibly inhibit MMPs in a 1:1 stoichiometric fashion. Individual TIMPs differ in their tissue-specific patterns of gene expression, as well as in their ability to inhibit various MMPs. In addition to their metalloproteinase inhibitory activity, TIMPs demonstrate additional biological functions. TIMP-1 and TIMP-2 have growth-promoting effects that are independent of their effect on MMP activity. Conversely, TIMP-3 has been shown to induce apoptosis of human colon carcinoma cells (Smith et al. 1997). Furthermore, TIMP-2 is required in the activation of proMMP-2 mediated by MT1-MMP (Wang et al. 2000). The plasma protein, α2-macroglobulin, is an additional MMP inhibitor that may be important in tissue fluids, whereas TIMPs may act more locally.

The net balance of MMP activity in the extracellular space is therefore the result of an intricate, multidimensional system of regulation that sets a physiological level of matrix turnover for normal biological processes.

1.12.3 MMPs in disease

Aberrant MMP expression occurs in several disease states including tendon degeneration, arthritis, atherosclerosis, gastric ulcers, fibrotic diseases and cancer. Although the precise pattern appears to be disease-specific, a few common threads run through all conditions. Firstly, it is the collective influence of abnormal MMP activity that is implicated in the pathogenic process, rather than the influence of individual MMPs, as evidenced by gene disruption experiments (knockout mice). Individual MMP deficiencies (e.g. MMP-2, -3, -7 or –9) have little impact on mouse phenotype, presumably because other MMP family members with overlapping substrate specificities can compensate (Mudgett et al. 1998; Haro et al. 2000; Itoh et al. 2002). Secondly, the ratio of MMP-to-TIMP activity is frequently modified, favouring a net increase in MMP activity and unregulated ECM turnover.

Neely (Neely et al. 1999) demonstrated that MMP-2 activity is increased in hypertrophic and keloid scar tissue, two fibroproliferative conditions similar to Dupuytren's disease. Riley (Riley et al. 2002) established an increase in MMP-1activity associated with rotator cuff tendon degeneration and rupture. Furthermore, distinct MMP gene expression profiles have been demonstrated for normal, painful and rupture Achilles tendons (Jones et al. 2006). In rheumatoid arthritis, active forms of MMPs (1, 3, 9) are expressed by synovial cells and are upregulated by inflammatory cytokines such as interleukin-1 (IL-1) and tumour necrosis factor α (TNFα) (Mengshol et al. 2002), which has been the focus of s possible therapeutic strategy (Jain et al. 2002). By contrast, TIMP levels do not appreciably increase, or may even decrease, leading to an imbalance in the MMP-to-TIMP ratio, which favours MMP-mediated joint destruction (Malemud 2006). MT1-MMP knockout mice develop dwarfism, arthritis and a prominent fibrotic synovitis (Holmbeck et al. 1999). Conversely, treatment with a broad-spectrum MMP inhibitor, GI168, significantly reduced

ankle swelling and cartilage destruction in an experimental arthritis model (Conway et al. 1995).

There is an abundance of circumstantial clinical evidence to suggest that MMPs play a salient role in cancer progression. MMPs can degrade basement membrane ECM proteins that may facilitate tumour invasion into surrounding connective tissues (Zucker et al. 2004). MMP-2, which is normally expressed in stromal cells, where it promotes migration (Giannelli et al. 1997), is highly elevated adjacent to metastasising carcinomas (Li et al. 2005). Similarly, serum MMP-2 levels have been shown to correlate with both the presence of pulmonary metastases and the response to therapy (Garbisa et al. 1992). In addition, MMP-2 and MMP-9 have been associated with progression from benign to advanced ovarian carcinoma (Schmalfeldt et al. 2001) and with survival in gastric carcinoma (Sier et al. 1996).

1.12.4 MMPs in Dupuytren's Disease

Little work has been undertaken to establish the precise role of MMPs in Dupuytren's disease. A few studies have looked directly at tissue levels and serum MMP expression. Qian (Qian et al. 2004) demonstrated an upregulation of MMP-2 expression in Dupuytren's tissue excised at surgery, compared to adjacent (uninvolved) tendon. Furthermore, in one study (Tarlton et al. 1998), a direct relationship was found between mechanical stress and release of MMP-2 by Dupuytren's tissue in vitro. However, the pattern of tissue-level mRNA expression does not appear to match serum MMP levels. Ulrich and colleagues (Ulrich et al. 2003) measured serum MMP levels in 22 Dupuytren's patients by enzyme-linked immunosorbent assay. Dupuytren's patients were shown to have elevated TIMP-1 serum levels compared to controls, but no significant differences in MMP-1, MMP-2 and MMP-9 serum concentrations. Furthermore, Dupuytren's patients had a significantly lower MMP-to-TIMP ratio compared to controls, which was postulated to reflect increased collagen synthesis over degradation, thus favouring matrix deposition. However, snapshot systemic enzyme levels may be a poor reflection of localised tissue activity. Furthermore, many external factors influence MMP expression, including conditions of blood collection

(Meisser et al. 2005) and associations such as smoking, diabetes and alcohol consumption, that are common to this population.

1.13 MODELS OF TISSUE ORGANISATION

Fibroblast-populated collagen lattices (FPCLs) have been developed as in vitro models of wound contraction, enabling cell-matrix interactions to be studied (Bell et al. 1979) and fibroblast-mediated matrix contraction to be quantified. Fibroblasts cultured in three-dimensional collagen lattices demonstrate an ability to reorganise the collagen fibril network into a dense, tissue-like structure (Elsdale et al. 1972). Furthermore, fibroblasts exhibit functional, morphologic and metabolic characteristics, which are distinct from cells cultured in monolayer in vitro (Grinnell 2003). FPCLs therefore provide a valuable model for studying cell-mediated tissue organisation.

Changes in the mechanical environment can influence fibroblast behaviour (Brown et al. 1998). Therefore, three variations of FPCLs (Figure 6) have been developed to investigate how mechanical load influences fibroblast-mediated matrix contraction (Grinnell 1994, 1999, 2000, 2003). In the free-floating model, the fibroblast-embedded matrix is released from the culture-dish surface immediately after lattice polymerisation. The fibroblasts extend fine protrusions (stellate morphology) and remain mechanically unloaded as they contract the matrix. In these circumstances, they do not differentiate into myofibroblasts. In the attached model, the collagen lattice remains attached to the culture dish. Isometric tension develops as cells become bipolar in morphology, forming large extensions and stress fibres that are oriented along lines of tension. In the stress-release model, the lattice is attached to the culture dish for one or two days before release. Cells in the stress-release model develop stress fibres and isometric tension during lattice attachment, which is then dissipated on release as the cells revert to a stellate morphology concomitant with contraction.

Each model is thought to represent a different stage of wound contraction (Grinnell 1999). The free-floating lattice model resembles initial wound contraction, whereas, granulation tissue formation is represented by the attached lattice model and granulation tissue contraction, by the stress-release model. Contraction can be estimated either by reduction in lattice area (free-floating, stress-release models) or by lattice height (attached model). Although FPCLs provide a simple in vitro model of fibroblast-mediated tissue organisation, they do not allow precise quantification of matrix contraction, direction of force or subtle manipulation of mechanical load.

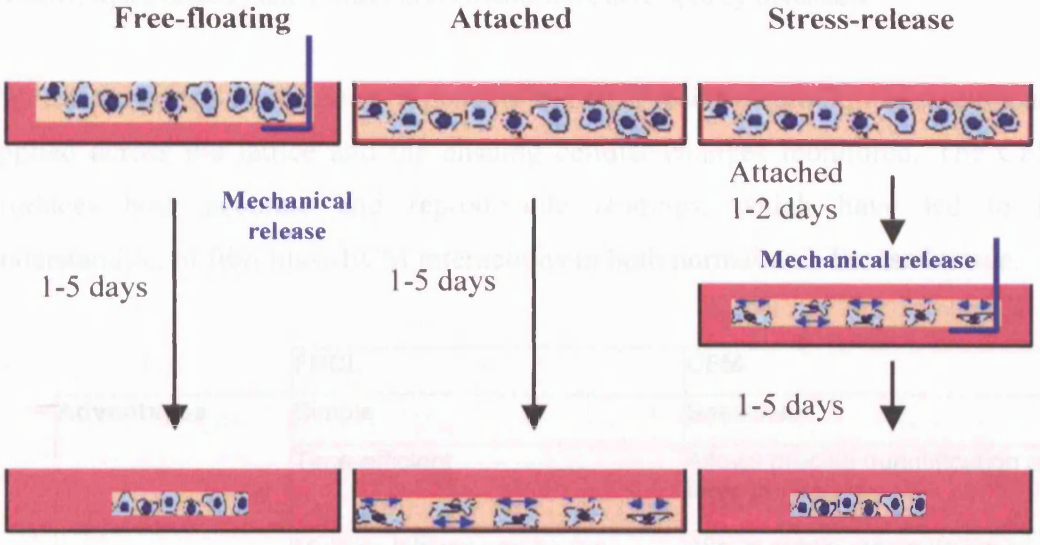

Figure 6. The three FPCL models. In the free-floating model, lattices are released from the well periphery and allowed to contract immediately after lattice polymerisation. In the attached model, lattices remain attached, enabling the development of isometric tension. Lattices in the stress-release model are allowed to develop tension over 1 or 2 days before being released. Adapted from (Howard et al. 2003).

More recently, the culture force monitor (CFM, Figure 7), an in vitro kinetic model of lattice contraction, has been developed (Eastwood et al. 1994; Eastwood et al. 1996; Eastwood et al. 1998). The CFM allows both precise quantification of contraction and manipulation of mechanical load. In this model, a fibroblast-populated lattice is attached at one end to a fixed strut and at the other, to a strain gauge, which detects lattice contraction. Unidirectional mechanical tension develops across the lattice by virtue of its fixed attachments. The CFM model most closely approximates the attached FPCL model. Both

can be used in parallel as they yield complementary information on the contractile behaviour of fibroblasts.

Figure 7. Culture Force Monitor. Collagen lattices are attached to a fixed strut at one end and a strain gauge at the other, which detects finite changes in contractile force developed by fibroblasts.

Table 4 provides a comparison of the two models. Precise external mechanical loads can be applied across the lattice and the ensuing cellular changes monitored. The CFM model produces both accurate and reproducible readings, which have led to improved understanding of fibroblast-ECM interactions in both normal and diseased tissue.

	FPCL	CFM
Advantages	Simple	Sensitive
	Time-efficient	Allows precise quantification of force generation
	Multiple lattices can be run simultaneously	Allows subtle manipulation of mechanical load
	Ease of sampling with minimal disruption	Sampling disrupts mechanical environment due to sensitivity of equipment
Disadvantages	Relatively insensitive to changes in force development	Time-inefficient as only one lattice can be run at once
	Mechanical load fixed	Expensive

Table 4. Comparison of benefits and drawbacks of FPCL and CFM models of matrix contraction.

1.14 GENERATION OF CONTRACTILE FORCE

Myofibroblasts are characterised by the presence of a contractile apparatus containing bundles of actin microfilaments (termed 'stress fibres') and associated contractile proteins (Tomasek et al. 2002). Several studies have demonstrated that, in vitro, myofibroblasts can generate contractile force (Gabbiani et al. 1972; Hueston et al. 1976). In addition to expressing the β- and γ- cytoplasmic actins that are found in fibroblasts, myofibroblasts also express α-smooth muscle actin (Darby et al. 1990), which is considered to be the most reliable marker of myofibroblast differentiation (Serini et al. 1999). The actin bundles are arranged parallel to the long axis of the cell and terminate at the cell surface in the fibronexus, a specialised adhesion complex that links intracellular actin with extracellular fibronectin fibrils. In vivo, by contrast, fibroblasts in connective tissues lack the stress fibres observed in myofibroblasts.

Some have suggested that the increased contractile ability of myofibroblasts over fibroblasts may relate directly to α-SMA expression. Fibroblasts transfected with α-SMA cDNA exhibit significantly increased collagen lattice contraction compared to transfection with β- or γ- cytoplasmic actins (Hinz et al. 2001). Furthermore, expression of α-SMA by Dupuytren's fibroblasts cultured in vitro has been shown to correlate with increased contractility (Tomasek et al. 1995).

Another distinguishing feature, indicative of their contractile nature, is that myofibroblasts are connected directly to each other through gap junctions (Gabbiani et al. 1978). This finding suggests the possibility that myofibroblasts can form multicellular contractile units during contraction, similar to smooth muscle cells.

The transformation of the fibroblast into the myofibroblast phenotype has been the subject of many studies reviewed by Gabbiani (Gabbiani 2003). The first changes in fibroblast modulation involve development of stress fibres, probably induced by mechanical stress (Tomasek et al. 2002). At this transient stage, the cell phenotype is termed protomyofibroblast. Under the influence of growth factors (e.g. TGF-β1) or a mechanical

change in the extracellular matrix, the protomyofibroblast may further develop into a myofibroblast (Figure 8). The myofibroblast at this stage is characterised by the de-novo expression of α-smooth muscle actin, and large supermature focal adhesion complexes. Bisson (Bisson et al. 2003) demonstrated that stimulation with TGF-β1 resulted in an increase in the myofibroblast phenotype of cultured Dupuytren's tissue (both cord and nodule), but not of control flexor retinaculum. As discussed previously, TGF-β upregulation and mechanical tension are both important features of Dupuytren's pathogenesis that may create an environment which, compared to normal palmar fascia, facilitates myofibroblast differentiation and the generation of contractile force.

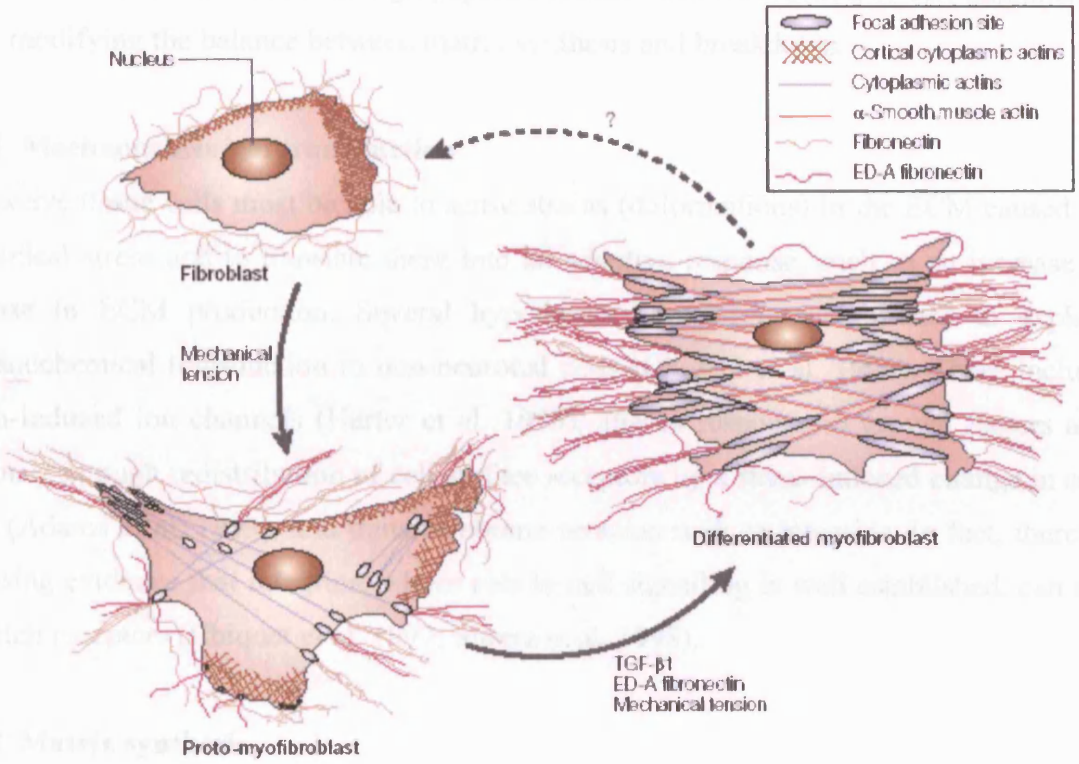

Figure 8. Myofibroblast differentiation. Adapted from Tomasek et al. 2002.

1.15 THE INFLUENCE OF MECHANICAL TENSION ON MATRIX REMODELLING

A key parameter underlying regulation of tissue homeostasis and matrix remodelling is mechanical tension. All connective tissues appear to be under some sort of mechanical tension, even at rest: blood vessels dissected free of their fascial attachments have resting lengths 25-30% shorter than their in situ length (Tomasek et al. 2002). Fibroblasts are sensitive to mechanical forces and can change their surrounding ECM in response to changes in their mechanical environment (Brown et al. 1998). Responses to mechanical stimulation are dependent on cell type. However, in general, fibroblasts can respond to mechanical stimulation either through physical means - cell contraction or cell alignment - or, by modifying the balance between matrix synthesis and breakdown.

1.15.1 Mechanochemical transduction

Connective tissue cells must be able to sense strains (deformations) in the ECM caused by mechanical stress and to translate these into an adaptive response, such as an increase or decrease in ECM production. Several hypotheses have been put forward to explain mechanochemical transduction in non-neuronal cells (Chiquet et al. 1996). These include stretch-induced ion channels (Harter et al. 1995), altered response to growth factors and hormones through redistribution of cell surface receptors by a stress-induced change in cell shape (Adams et al. 1993), and transmembrane proteins such as integrins. In fact, there is increasing evidence that integrins, whose role in cell signalling is well established, can act as stretch receptors (Chiquet et al. 1997; Sheetz et al. 1998).

1.15.2 Matrix synthesis

Detection of a mechanical stimulus leads to an adaptive response that can activate ECM gene expression - a prerequisite for matrix remodelling. Mechanical load has been shown to promote procollagen synthesis in dermal fibroblasts both by enhancing gene expression and by posttranslational processing of procollagen (Parsons et al. 1999). Ultimately, regulation of gene expression by mechanical stress can occur indirectly, by stimulating release of growth factors, or directly, by triggering an intracellular signalling pathway. Expression of

most ECM components is likely to be controlled indirectly by mechanical stress, for example, by TGF-β-dependent induction of the procollagen I gene (Lindahl et al. 2002). However, evidence suggests that tenascin-C, a large ECM protein, is an example of a gene directly regulated by mechanical stress (Chiquet et al. 2003). In the latter, induction of tenascin-C mRNA was found to occur rapidly in fibroblasts under tension both in vivo and in vitro and to be independent of prior protein synthesis or growth factors released into the medium.

1.15.3 Matrix degradation - mechanical tension and MMP activity

MMP activity can also be regulated by mechanical tension, enabling fibroblasts to alter cell-matrix attachments, to influence cell movement and therefore adapt to the mechanical demands of the matrix. Dermal fibroblasts, seeded in a collagen lattice, were found to upregulate MMP-9 on cyclical loading, whereas, MMP-3 activity was reduced (Prajapati et al. 2000). Similarly, an upregulation of MMP-1 mRNA expression by dermal fibroblasts was detected on application of a biaxial load (Derderian et al. 2005). Conversely, in a stress-release collagen lattice model, release of mechanical tension resulted in an upregulation of MMP-3, -9, -13 and MT1-MMP (Lambert et al. 2001). Other studies have focused on the effect of mechanical load, as well as cell alignment on MMP expression in three-dimensional collagen lattices (Mudera et al. 2000). Fibroblasts aligned parallel to the load down-regulated MMP expression, whereas non-aligned fibroblasts increased MMP expression, perhaps to facilitate cell movement and remodelling and to promote alignment and stress shielding. Interestingly, TIMP activity was found to be poorly mechano-responsive, further highlighting the importance of MMP over TIMP activity in matrix remodelling.

1.15.4 Tensional homeostasis

Fibroblasts respond mechanically to mechanical signals in the matrix in order to maintain tension equilibrium in the tissue, a characteristic referred to as tensional homeostasis (Brown et al. 1998). Using a culture force monitor model, Brown and colleagues determined quantitatively how fibroblasts respond mechanically to defined tensional loads. This study demonstrated that fibroblasts seeded in a collagen lattice react to modify tension

in the opposite direction from externally applied loads, thus maintaining a constant level of endogenous matrix tension or tensional homeostasis. Each tissue type has a distinct endogenous matrix tension, which is 'set' to meet specific functional requirements; for example, the resting tension maintained by aortic smooth muscle cells is likely to be much greater than exhibited by colonic smooth muscle cells. Failure of cell-mediated tensional homeostasis may therefore be important in disease.

1.16 EFFECT OF MECHANICAL TENSION ON DUPUYTREN'S FIBROBLASTS

Using an FPCL model, Howard (Howard et al. 2003) demonstrated that the synthetic capacity of Dupuytren's fibroblasts varies with changes in isometric tension. Specifically, the expression of two ECM components associated with remodelling, β-catenin and fibronectin, increased in lattices cultured under stress (attached), but decreased following a reduction in isometric tension (release). On the other hand, expression by control fibroblasts was not sensitive to changes in mechanical tension. Similarly, Bailey and colleagues (Bailey et al. 1994) demonstrated an increase in MMP activity and new collagen synthesis in tissue samples excised from patients subjected preoperatively to TEC (and therefore to prolonged exposure to mechanical tension). The results suggested that mechanical tension induced a remodelling response in Dupuytren's fibroblasts.

Studies on Dupuytren's fibroblasts also suggest that defects in tensional homeostasis may occur in Dupuytren's disease. Bisson (Bisson et al. 2004) demonstrated that Dupuytren's fibroblasts contract in response to an externally applied mechanical load, in contrast to dermal fibroblasts, which respond by reducing tension (Brown et al. 1998). Similarly, Beckett (Beckett 2005) demonstrated that Dupuytren's fibroblasts, seeded in a collagen lattice in the culture force model, continue developing tension over a 48-hour period, failing to reach a plateau phase of force generation. In contrast, control carpal ligament and dermal fibroblasts attained a plateau phase of force generation, assumed to be analogous to endogenous tissue tension.

1.17 GENERATION OF CONTRACTURE: CONTRACTION AND REMODELLING

The hallmark of Dupuytren's disease is connective tissue contracture. Contracture implies a process of permanent tissue shortening that cannot be explained either by increased matrix synthesis, which does not necessarily lead to tissue shortening (Brickley-Parsons et al. 1981; Glimcher et al. 1990), or by cellular contraction, which is a rapid, reversible process and too energy-consuming to maintain tissue shortening long term. However, contractile force generated by myofibroblasts is a prominent feature of Dupuytren's disease (Bisson et al. 2004) and likely to contribute to contracture, as myofibroblasts are frequently associated with scar formation and fibrocontractile conditions such as keloid scarring. Furthermore, contraction by myofibroblasts differs from that by smooth muscle cells, which can contract connective tissue for decades in the gut or vascular wall without leading to contracture (Tomasek et al. 2002). Collagen deposition is also a prominent feature of Dupuytren's disease and an inseparable part of contracture, although it is not the root of tissue shortening, since the deposited collagen is neither folded nor plicated (Brickley-Parsons et al. 1981).

In fact, researchers (Guidry et al. 1987; Flint et al. 1990) have proposed that contracture is a result of two different processes working in parallel, that together lead to incremental, anatomical tissue shortening. The process is initiated by fibroblast contraction, which, through cell-matrix attachments, can exert a mechanical force or deformation on the matrix, leading to shortening. Remodelling of the matrix leads to synthesis of new matrix components that stabilise the new matrix configuration, holding it in the shortened position. This proposed cycle of myofibroblast contraction and matrix remodelling (Figure 9), coined 'slip and ratchet theory' (Tomasek et al. 2002), can be repeated perpetually, leading to small incremental changes and eventual tissue contracture, without the loss of load-carrying function.

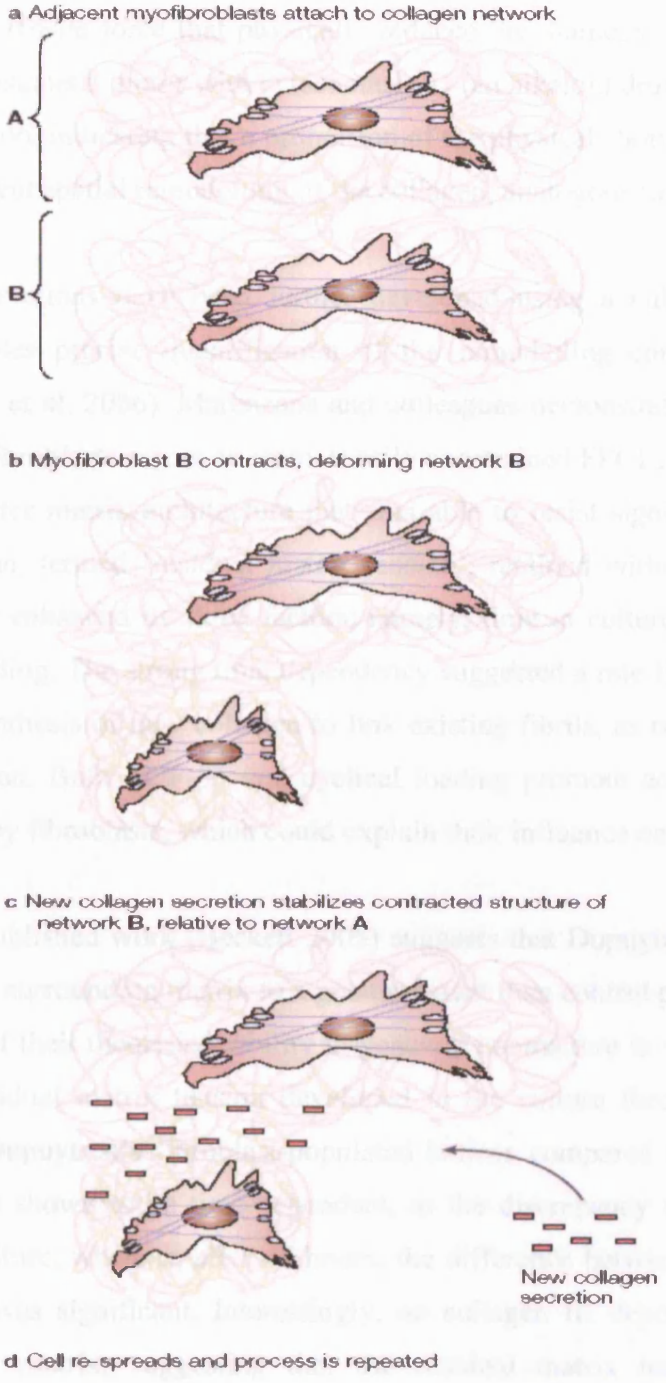

Figure 9. 'Slip and ratchet' theory of matrix contracture. Taken from (Tomasek et al. 2002).

Evidence that force generated by myofibroblasts can be translated into a shortened collagen matrix that no longer requires active cellular contraction comes from stress-release collagen

lattice models (Grinnell et al. 2002). Dermal fibroblasts seeded in a collagen lattice generated a tensile force that physically reduced the diameter of the lattice. Disruption of the cell cytoskeletal motor with cytochalasin-D (an alkaloid drug) resulted in an incomplete loss of tension, indicating that a proportion of the physical shortening of the lattice was due to a permanent spatial remodelling of the collagen, analogous to in vitro contracture.

These observations have been further developed using a culture force monitor model, which enables precise quantification of the remodelling component of lattice tension (Marenzana et al. 2006). Marenzana and colleagues demonstrated that the force generated by dermal fibroblasts across an isometrically constrained FPCL, was stabilised over time by a new, shorter matrix architecture that was able to resist significant tensional force. The fixed tension, termed 'residual matrix tension', retained within the remodelled collagen matrix, was enhanced by three factors: namely, time in culture, exposure to TGF-β1 and cyclical loading. The strong time dependency suggested a rate-limiting process, such as the need for synthesis of new collagen to link existing fibrils, as required for dynamic spatial reorganisation. Both TGF-β1 and cyclical loading promote collagen synthesis and force generation by fibroblasts, which could explain their influence on residual matrix tension.

Recent unpublished work (Beckett 2005) suggests that Dupuytren's fibroblasts are able to remodel the surrounding matrix to a greater extent than control palmar fascia fibroblasts, an indication of their theoretical ability to generate contracture in vivo. Beckett demonstrated that the residual matrix tension developed in the culture force model was significantly greater in Dupuytren's fibroblast-populated lattices compared to control fibroblasts. This process was shown to be time-dependent, as the discrepancy was not perceptible after 8 hours of culture, whereas, after 48 hours, the difference between Dupuytren's and control fibroblasts was significant. Interestingly, no collagen III deposition was detected in the surrounding matrix, suggesting that the residual matrix tension was due to spatial reorganisation of the existing collagen I lattice, as opposed to new collagen synthesis.

As discussed, any remodelling process inevitably requires matrix turnover, which is largely mediated by MMPs. The precise MMPs involved in matrix degradation leading to

contracture is unknown, although MMP-1, -2, -3, and -9 have been proposed as possible candidates (Tomasek et al. 2002).

1.18 MMP INHIBITORS

As more has been uncovered about the functions and influence of MMP activity, various MMP inhibitors have been developed in anticipation of a potential clinical role in the prevention of progression of various diseases, notably cancer and arthritis.

1.18.1 Synthetic MMP inhibitors

Naturally occurring inhibitors, including TIMP-1 and TIMP-2, were initially considered as potential therapeutic agents for cancer and other diseases. However, technical difficulties have prevented their development into useful drugs. Subsequently, small molecules containing both hydroxamate and non-hydroxamate zinc bindings sites have been developed as synthetic MMP inhibitors (MPIs). These agents include ilomastat (N-L-tryptophan methylamide), batimastat and marimastat, which typically inhibit a broad-spectrum of MMPs, since the substrate structure can be recognised by multiple MMP family members (Skiles et al. 2004). The structure and substrate specificity of ilomastat are demonstrated in Figure 10. Ilomastat is also known as galardin or GM6001. However, for the purposes of this thesis, it will, for consistency, henceforth be referred to as ilomastat.

1.18.2 Contraction

Several studies have demonstrated that inhibition of MMP activity reduces FPCL contraction in vitro and modulates the wound healing response in experimental in vivo models. Scott (Scott et al. 1998) demonstrated that FPCL contraction mediated by dermal fibroblasts was inhibited by marimastat. Sheridan (Sheridan et al. 2001) investigated the effects of galardin as well as various MMP antibodies on lattice contraction mediated by ocular fibroblasts. Collectively, antibodies to MMP-1, -2, -3 and -9 inhibited lattice contraction, although individually, they had no effect. Ilomastat inhibited contraction to an even greater extent than the combination of MMP antibodies, suggesting that numerous

MMPs are involved in processing and remodelling of the collagen lattice during contraction. Daniels (Daniels et al. 2003) demonstrated a dose-dependent inhibition of ocular fibroblast-mediated FPCL contraction by ilomastat. The effect was reversible upon removal of ilomastat, suggesting that MMP activity plays an important role in lattice contraction.

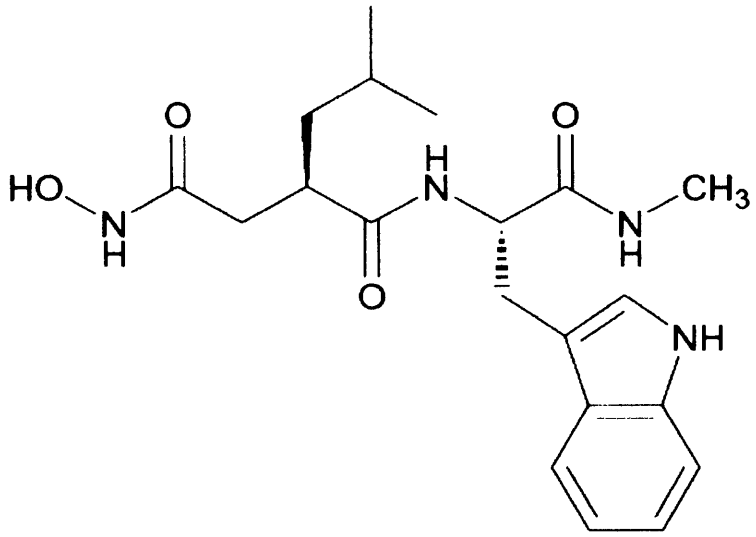

Selectivity of ilomastat (K_i values)

MMP-1= 400 pM	MMP-8 =100pM
MMP-2 = 500pM	MMP-9 = 200pM
MMP-3 = 27nM	

Figure 10. Structure and selectivity of ilomastat. Picture taken from (Mirastschijski et al.), K_i values from www.merckbiosciences.co.uk.

Ilomastat has also been shown to affect epithelial cell migration, a prerequisite for wound healing and an integral part of the contraction process (Wong et al. 2004). In an experimental model of wound healing, Mirastschijski (Mirastschijski et al. 2004) demonstrated that ilomastat inhibited wound repair, specifically epithelialisation, granulation tissue development and wound contraction, illustrating the importance of MMP function on remodelling processes. Interestingly, in this study, ilomastat did not affect TGF-β1 mediated lattice contraction by dermal fibroblasts in the CFM model, suggesting that ilomastat does not directly block TGF-β1 promotion of myofibroblast formation.

However, ilomastat reduced α-SMA expression by fibroblasts in granulation tissue as well as wound contraction, and may therefore act indirectly by preventing TGF-β1 release from the ECM. In another study (Wong et al. 2003), ilomastat was found to reduce the postoperative scarring response following experimental glaucoma filtration surgery.

1.18.3 Clinical trials

The association of MMPs with tumour invasion, together with the positive results of preclinical studies on cancer models, has led to numerous clinical trials being undertaken. There have been some positive results of MPIs suggesting a survival advantage in advanced gastric carcinoma (Brown 2000) and a possible delay in progression in relapsed prostate cancer (Rosenbaum et al. 2005), although several trials have demonstrated no clear clinical benefit (Bramhall et al. 2001). Musculoskeletal side effects such as myalgia and arthralgia may limit use of MPIs to sub-therapeutic tissue levels (Wojtowicz-Praga et al. 1998; Rosemurgy et al. 1999; Hande et al. 2004). Furthermore, most trials recruit patients with advanced disease, although the therapeutic benefit of MPIs would be predicted to wane in the late stages of disease, after widespread tumour dissemination has occurred (Coussens et al. 2002). Clinical trials are ongoing in the expectation that MPIs have a definite place in cancer treatment. Through modification of trial design to recruit patients with earlier stage disease as well as improving the selectivity profile of MPIs to limit side effects, a framework will be created for uncovering the clinical potential of MPIs.

1.19 INTRODUCTION TO THESIS

This thesis intends to investigate the effects of ilomastat, a broad-spectrum MMP inhibitor, on matrix contraction by Dupuytren's fibroblasts in vitro, using two different collagen lattice models. In particular, we aim to determine the influence of MMP activity on spatial remodelling as well as cell-mediated contractile force development. It is intended that the results from this in vitro study will help to outline the possible therapeutic potential of an MMP inhibitor as an agent to prevent recurrence and progression of contracture.

1.20 QUESTIONS TO BE ANSWERED

1. Does ilomastat affect cell proliferation? **Chapter 3**
2. Does ilomastat mediate inhibition of FPCL contraction in a dose-dependent manner? **Chapter 3**
3. Define differences in matrix contraction by cord, nodule and control fibroblasts and assess the pattern of inhibition by ilomastat for the three fibroblast types. **Chapter 4**
4. Which MMPs are important in matrix contraction by Dupuytren's and control fibroblasts and how does ilomastat affect their pattern of activity and secretion? **Chapter 4**
5. Does ilomastat affect both components of lattice contraction, namely cell-mediated contraction and matrix remodelling, in the CFM model? **Chapter 5**
6. Does ilomastat modulate MMP activity at the pre or post-transcriptional level? **Chapter 5**

CHAPTER 2

MATERIALS AND METHODS

2.1 GENERAL CELL CULTURE

2.1.1 Tissue selection

Following local ethics committee approval (reference EC2002/97) and informed consent, fresh tissue specimens were collected from Mount Vernon Hospital theatres. Dupuytren's tissue was obtained from patients undergoing primary fasciectomy; tissue from recurrent procedures was discarded. In addition, only specimens that included both an identifiable nodule and a length of pathological cord were selected. Identification of cord and nodule was carried out by the senior operating surgeon and the primary researcher per-operatively and confirmed by subsequent histological evaluation. Paired samples, in other words, cord and nodule tissue from the same patient, were chosen to limit interpatient variability and therefore to improve the strength of comparisons. When dissected of surrounding fatty and loose connective tissue, the specimen would often resemble a 'drumstick' shape (Figure 1). The tissue was sectioned longitudinally and one half was then used to establish cell cultures. The other half was fixed in 5ml 10% formal saline for 2 hours at room temperature prior to embedding in paraffin wax for subsequent histological examination. Carpal ligament was selected as the control tissue and obtained from carpal tunnel release in patients unaffected by Dupuytren's disease.

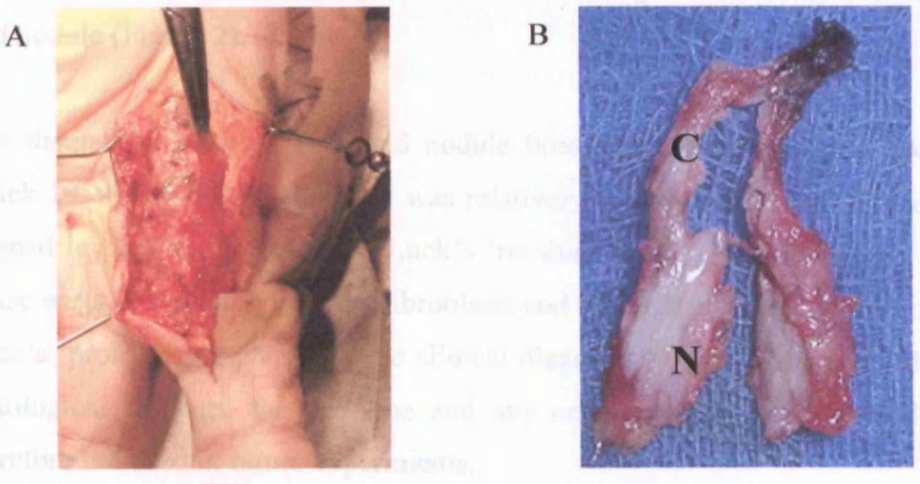

Figure 1. Illustration of Dupuytren's tissue. Panel A illustrates removal of Dupuytren's tissue at primary fasciectomy. Panel B demonstrates diseased fascia dissected free of fatty tissue revealing a distinct cord (C) and nodule (N).

2.1.2 Histology

The fixed specimens of Dupuytren's tissue were embedded in paraffin blocks with a known orientation marked by ink, enabling accurate identification of the areas from which cells were harvested for explant culture. Representative sections of the embedded tissue were cut and stained with haematoxylin and eosin to confirm clinical typecasting of tissue as either nodule or cord. Paraffin blocks were sectioned at 4μm using a Reichert-Jung Microtome (Leica Instruments, Germany) and were mounted on glass slides (VWR International, Leuven, Belgium). Sections were dewaxed by bathing in xylene (No. 202-422-2, Genta Medical, York, UK) for 10 minutes, then rehydrated through bathing in a series of ethanol (Hayman Ltd, Essex, UK) dilutions, from 100%, 90%, 70% through to tap water. The sections were stained in Harris Haematoxylin (BDH, Poole, Dorset, UK) for one minute, differentiated in 1% alcohol for 10 seconds, washed well in running tap water for 3 minutes and then immersed in Eosin (1% solution; BDH, UK) for a further minute. After a further wash, slides were dehydrated in alcohol solutions, cleared in xylene and mounted using DPX (DiaCheM, London, UK) and 22x30 mm cover slips (Menzel-glazer). Examination at 100x and 200x magnification (Zeiss Axioscope 20, Carl Zeiss, Germany) enabled confirmation of histological differences between regions clinically corresponding to cord and nodule (Figure 2).

The distinction between cord and nodule broadly corresponded to Luck's classification (Luck 1959). Cord-derived tissue was relatively acellular with large amounts of collagen, aligned in parallel, representing Luck's 'residual phase'. Nodule-derived tissue contained dense nests of randomly aligned fibroblasts and minimal collagen deposition, correlating to Luck's 'proliferative phase'. If the clinical diagnosis of cord or nodule did not correlate to histological findings, the cell line and any cell strains isolated were discontinued and therefore not used in future experiments.

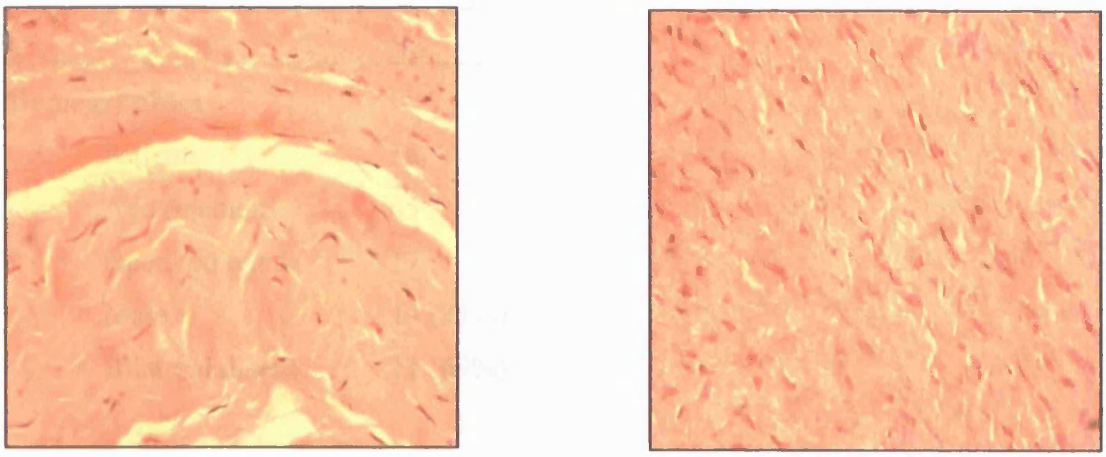

Figure 2. Haematoxylin and eosin-stained section of a Dupuytren's cord (left) and nodule (right) x 200 magnification. Cord-derived tissue was relatively acellular with an abundance of aligned collagen fibrils, whereas nodule-derived tissue was highly cellular with a relative paucity of extracellular matrix.

2.1.3 Cell strains

In all, tissue samples were harvested from 17 patients with Dupuytren's disease and 5 patients undergoing carpal tunnel release. Table 1 illustrates the demographics and risk factors for the Dupuytren's patients. Some tissue samples were unpaired (cord and nodule not easily distinguished on clinical or histological observation). Furthermore, some paired samples yielded only one cell strain as either cord or nodule-derived fibroblasts grew poorly in the culture medium or underwent premature senescence. Analysis was therefore confined to cell strains from 5 paired nodule and cord samples. The unpaired cell strains were used to validate assays.

	No.
Demographics	
Patients	16
Age (median)	65
Operated hands	17
Male	14 (81%)
Bilateral disease	11 (69%)
Associations	
Smoking	5 (31%)
Alcohol excess	3 (19%)*
Diabetes Mellitus	1 (6%)
Epilepsy	0

Table 1. Table illustrating the demographics and associations of Dupuytren's patients who donated fascia samples to the tissue bank for fibroblast isolation. *represents consumption of alcohol above current recommended guidelines (28u/week for males, 21u/week for females).

2.1.4 Isolation of cells from explant tissue

An explant method was used to establish primary cell cultures from the harvested material (Jones et al. 1979). Cord, nodule and carpal ligament-derived tissue was prepared separately. Each surgical specimen was minced into 1-2mm^2 pieces using a scalpel and forceps, which had been previously sterilized in 70% Industrial Methylated Spirits (IMS) and allowed to air dry. Each piece of macerated tissue was placed on the base of a T25cm^2 tissue culture flask (Greiner Labortechnik, Greiner bio one, Germany) and allowed to adhere for 2 minutes, before dispensing 5ml of normal fibroblast growth medium (NGM) into the flask. NGM consisted of Dulbecco's Modified Eagle's Medium (DMEM, Gibco, UK) supplemented with glutamax (dipeptide L-Alanyl-L-Glutamine), 10% (vol/vol) fetal calf serum (FCS), penicillin (100U/ml), and streptomycin (100µg/ml, all Gibco, UK). The

flask was incubated in a Heraeus humidified incubator, maintained at 37^0C and 5% CO_2. After fibroblasts were observed migrating from the specimen, media changes were carried out twice weekly.

Cells were passaged successively into T75cm^2, then T175cm^2 (Greiner Labortechnik, Germany) and finally T225cm^2 tissue culture flasks (Corning, New York, USA) just prior to confluence. Subsequent routine propagation of cell cultures involved splitting each T225cm^2 tissue culture flasks into three. Culture medium was aspirated and the cell monolayer washed with 5ml ethylenediaminetetraacetic acid (EDTA) to chelate calcium and magnesium ions. Following washing of the monolayer, 2.5ml of 0.25% trypsin (Gibco, UK) in versene (Gibco, UK) was dispensed into the flask, and the flask was incubated at 37^0C until all cells had lost contact with the flask surface, forming a single cell suspension. The trypsin solution was neutralized with 20ml of NGM, and the resulting cell suspension immediately aspirated from the flask into a 50ml centrifuge tube. The suspension was then centrifuged at 1000 rpm for 5 minutes to pellet the cells and remove traces of the active trypsin. The supernatant was discarded, and the cell pellet resuspended in 12ml of NGM, before being evenly distributed between three T225cm^2 cell culture flasks. The flasks were returned to the incubator after the final NGM volume had been made up to 35ml. The media was changed twice weekly until confluent, at which point the cells were passaged again, used for experiments, or prepared for cryostorage. Only cells from passages 3-5 were used for experiments as passage number has been shown to influence the efficiency of fibroblasts at remodelling matrices (Steinberg et al. 1980).

2.1.5 Cryostorage of cells

A cell suspension was obtained by trypsination of the cell monolayer, as previously described, followed by neutralisation and centrifugation at 1000rpm for 5 minutes to pellet the cells. The supernatant was discarded, and the cell pellet resuspended in 3ml of cryopreservation medium: 10% DMSO (Dimethyle sulphoxide, Sigma, Poole, Dorset) and 90% fetal calf serum (FCS, Gibco, Paisley, Scotland). The cell suspension was dispensed into 3 labelled cryovials, detailing cell strain, passage number and date. The usual cell density for cryopreservation was 1x10^{6}cells/ml. The cryovials were insulated with paper

wadding and placed at -80^{0}C, the wadding aids gradual freezing over 24 hours to ensure optimal survival during the cryopreservation process. Once frozen, the samples were transferred to liquid nitrogen for long-term storage until required.

2.1.6 Propagation of cells from cryostorage

The cryovial was rapidly thawed in a 37^{0}C water bath. The cell suspension was transferred to a 15ml centrifuge tube, and 10ml of NGM added drop-wise, slowly, with agitation to prevent osmotic stress. The resulting cell suspension was centrifuged at 1000 rpm for 5 minutes and the supernatant aspirated and discarded to remove traces of DMSO. The cell pellet was washed of any remaining cryopreservative with a further 10ml of NGM and then recentrifuged. The supernatant was discarded and the cell pellet was resuspended in 13ml of NGM, then dispensed into a T75cm^2 flask for incubation.

2.1.7 Cell viability and counting

Cells were stained with Trypan Blue to determine viability and then counted using a haemocytometer (improved Neubauer). An aliquot of 20µl of cell suspension was diluted 1:1 with 20µl of Trypan Blue (0.4%, Sigma, Dorset, UK) and then drawn between the haemocytometer (Nebauer) and the cover slip by capillary action. This was examined under an inverted phase contrast microscope (Olympus CK2, Olympus Optical Co., Japan.). Live cells appeared phase bright, as they retain the ability to pump out the Trypan blue, whereas dead cells stained blue, as the dye is not removed. The number of viable cells contained within 1 large grid of the haemocytometer was counted and, the count repeated in 3 further grids. The cell density of the suspension was then calculated as follows:

Mean cell number of 4 grids x 2 (dilution factor) x 10^4 = Number of viable cells/ml

2.2 ASSESSMENT OF CELL PROLIFERATION

Ilomastat (GM6001; Calbiochem, UK) and the control peptide (GM6001 negative control, Calbiochem, UK) are poorly soluble in aqueous solution and therefore prepared in dimethyl

sulfoxide (DMSO, Sigma Chemical Co., Dorset, UK) at stock concentrations of 100mM. Although DMSO is an excellent organic solvent and vehicle for delivery of ilomastat, it has been shown to be cytotoxic to fibroblasts at higher concentrations (Berliner et al. 1967). Similarly, synthetic MMP inhibitors have been reported to affect cell proliferation (Mannello et al. 2005). Any effect of ilomastat or DMSO on fibroblast proliferation could influence matrix contraction. A proliferation assay was therefore undertaken to determine the effect of ilomastat on proliferation by nodule, cord (unpaired sample) and carpal ligament-derived fibroblasts so that an appropriate dose could be selected for subsequent experiments that was neither toxic nor a stimulant to proliferation.

2.2.1 Background to the metabolic proliferation assay

Cell proliferation was assessed using a metabolic reagent, WST-1 (Roche Molecular Diagnostics and Biochemicals, Lewes, UK). WST-1 is a tetrazolium salt that is cleaved to formazan by cellular enzymes (Figure 3). An expansion in the number of viable cells results in an increase in the overall activity of mitochondrial dehydrogenases, which increase the amount of formazan produced. Formazan production directly correlates with the number of metabolically active cells in the culture. The reaction is accompanied by a colour change, enabling precise quantification of the formazan formed, through measuring change in absorbance (optical density, OD) spectrophotometrically at 450nm.

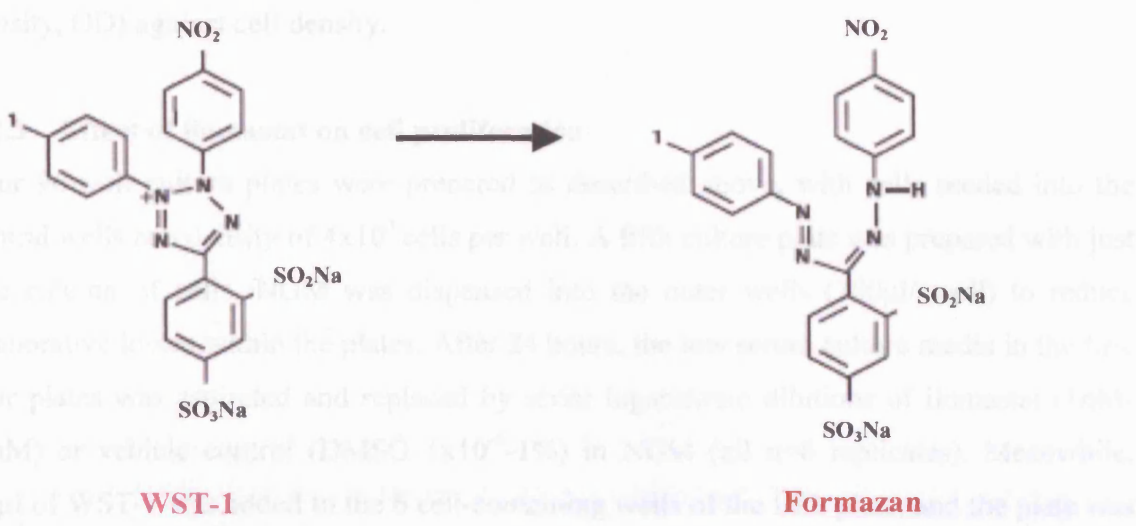

Figure 3. Cleavage of the tetrazolium salt WST-1 (4-[3-(4-Iodophenyl)-2-(4-nitrophenyl)-2H-5-tetrazolio]-1,3-benzene disulfonate) to formazan was accompanied by a colour change from light red to dark red, which was detected spectrophotometrically at 450nm.

2.2.2 Correlation of cell density with optical density

Initially, the optimal detection limits of the WST-1 proliferation assay were investigated by assessing the effect of cell density (number of fibroblasts seeded in each well) on optical density.

A single cell suspension of fibroblasts was prepared as described previously and the number of viable cells determined using Trypan Blue exclusion. The cell suspension was centrifuged at 1000rpm for 5 minutes and the pellet resuspended in DMEM supplemented with 0.5% FCS. This medium is sufficient to promote cellular adhesion whilst retaining cells in a quiescent, non-proliferating state over the initial 24-hour culture period. Serial dilutions of the cell suspension enabled fibroblasts to be seeded into the central 60 wells ($4x10^3$ cells per well) of a 96-well culture plate at a range of cell densities (2-20,000 fibroblasts in 100µl/ well). DMEM was dispensed into the outer wells (100µl/ well) to reduce evaporative losses within the plate. The plates were incubated at 37°C overnight to allow cells to adhere to the well base. After 24 hours, 10µl of WST-1 was added to all cell-containing wells. The tissue culture plate was then incubated at 37°C for 2 hours. The absorbance, related to the number of viable cells converting WST-1 to coloured formazan crystals, was determined at 450nm with a spectrophotometer (Model 550, BioRad, UK) using 630nm as a reference wavelength. A graph was plotted of absorbance (optical density, OD) against cell density.

2.2.3 Effect of ilomastat on cell proliferation

Four 96-well culture plates were prepared as described above, with cells seeded into the central wells at a density of $4x10^3$ cells per well. A fifth culture plate was prepared with just one column of cells. NGM was dispensed into the outer wells (100µl/ well) to reduce evaporative losses within the plates. After 24 hours, the low serum culture media in the first four plates was aspirated and replaced by serial logarithmic dilutions of ilomastat (1nM-1mM) or vehicle control (DMSO $1x10^{-6}$-1%) in NGM (all n=6 replicates). Meanwhile, 10µl of WST-1 was added to the 6 cell-containing wells of the fifth plate, and the plate was incubated for 2 hours. The OD value at 450nm provided the t=0 measurement i.e. corresponding to cell number at the start of the experiment. The WST-1 assay was

subsequently performed at 24 or 48 hours on the first four plates to provide a t=24 hr and t=48 hr reading for both ilomastat and DMSO dilutions. A graph was plotted of change in OD from the initial t=0 value over time, comparing basal conditions with serial dilutions of ilomastat or vehicle control (DMSO). Increases in OD above the t=0 value related to increases in cell biomass as an indicator of cell proliferation. OD values at 24 and 48 hr below the initial t=0 value indicated cell death over the exposure period.

The proliferation assay established the upper limit of ilomastat at which fibroblasts remained viable and functional for use in subsequent experiments aimed at investigating the effects of ilomastat on matrix contraction.

2.3 MODELS OF MATRIX CONTRACTION

Two models of fibroblast-mediated matrix contraction were employed, the fibroblast-populated collagen lattice (FPCL) and the culture force monitor (CFM). The two models were used to assess the differential contractile abilities of Dupuytren's (cord and nodule) and control fibroblasts as well as the effects of ilomastat on fibroblast-mediated tissue remodelling and contraction.

2.4 FIBROBLAST-POPULATED COLLAGEN LATTICE (FPCL)

Matrix contraction was assessed using a stress-release fibroblast-populated collagen lattice (FPCL) model. A single cell suspension of fibroblasts was prepared as previously described in section 2.2.1. Cell viability and number were determined using Trypan Blue and a Neubauer haemocytometer. The cell suspension was centrifuged at 1000rpm for 5 minutes. The supernatant was aspirated and the pellet washed in phosphate-buffered saline (PBS, Gibco, Scotland) to remove traces of FCS. The suspension was recentrifuged, the supernatant discarded and the pellet resuspended at $2x10^6$ cells in 0.6ml GFM (gelatinase-free growth medium).

GFM was used as the main stimulant for matrix contraction to enable accurate assessment of gelatinase (MMP-2, -9) production by fibroblasts during the experiment, without interference from the gelatinases that occur naturally in fetal-calf serum. Gelatinase-free fetal calf serum was prepared as follows: 1ml gelatin sepharose 4B (in 60% ethanol; Amersham Biosciences, UK) was dispensed into two 15ml centrifuge tubes. The liquid was centrifuged at 1000rpm for 5 minutes, and the resultant supernatant was discarded. The pellet was resuspended in 10ml PBS, to wash away all ethanol remnants, and was then recentrifuged. The supernatant was aspirated and discarded. The pellet was resuspended in 9ml fetal calf serum (Gibco, UK) and incubated at 4^0C on a vertical rotary shaker for 2 hours. During this time, gelatine sepharose binds the gelatinases (mainly MMP-2, MMP-9). The mixture was centrifuged at 1000rpm for 5 minutes, and the supernatant (gelatinase-free fetal calf serum) was then aspirated and used to make GFM. All other ingredients of GFM were identical to NGM.

2.4.1 Construction of FPCL model

A stress-release FPCL model was constructed as follows. A 1.1ml FPCL lattice mixture was prepared by mixing 150µl cell suspension, as prepared above, with 350µl of 10x Dulbeccos' Modification of Eagle's Medium (DMEM, Sigma, UK) and 600µl of 5mg/ml type I collagen (Sigma, UK) in 0.01% acetic acid. The solution was neutralised by drop-wise addition of 0.1M NaOH until a colour change from yellow to just pink was observed, indicative of the adjustment of pH from 1.0 to 7–7.5. The liquid lattice was gently agitated and 150µl of lattice mixture dispensed per well of a 48-well plate, rotating the plate to ensure the lattice was evenly spread throughout the well. The plate was incubated for 1 hour at 37°C to allow the lattices to polymerise. After 1 hour, test medium (depending on individual experiment) was dispensed into wells. FPCLs were allowed to develop mechanical tension over 48 hours before being gently released from the well periphery with a 200µl Gilson pipette tip and returned to the incubator.

2.4.2 Assessment of matrix contraction

Lattices were photographed (Figure 4) at point of release, and then every 24 hours, using a camera system (UVP Bioimaging System, Epi Chemi II Darkroom), linked to a computer. The lattice area was measured in pixels (ImageTool 3.0) and the degree of contraction calculated as the change in lattice area was compared to well circumference over time.

2.4.3 Determination of appropriate time course

A stress-release FPCL model was prepared as described above to assess the rate of lattice contraction mediated by cord, nodule (paired, n=4 replicates) and carpal ligament-derived fibroblasts (n=4 replicates) over time. After lattice polymerisation, 0.5ml GFM was dispensed into each well and the lattices were allowed to develop mechanical tension for 48 hours before release. The media was changed at point of release and subsequently every 2 days. The lattices were photographed at daily intervals over 5 days and the lattice area was plotted against time, yielding rate of lattice contraction from the slope of the curve. This enabled selection of an appropriate incubation time correlating to the maximal rate of contraction for subsequent FPCL experiments.

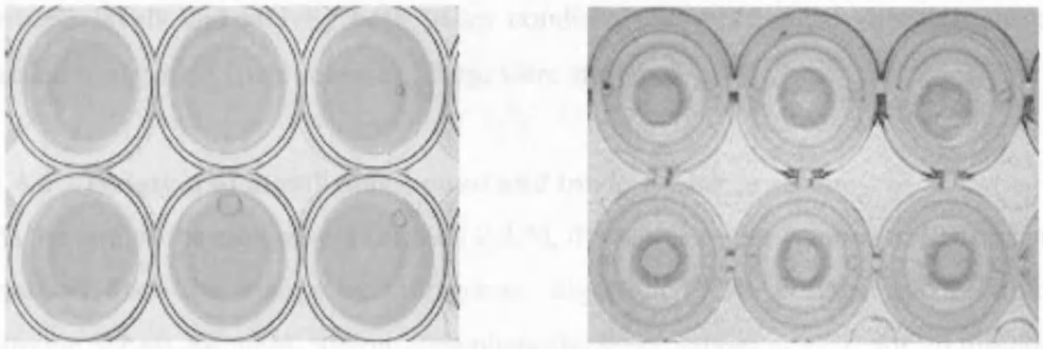

Figure 4. Photograph of stressed lattices (left), anchored to the well, and contracting lattices (right), 48 hours after release from the well periphery.

2.4.4 Optimal ilomastat dose determination

Ilomastat has been shown to suppress FPCL contraction in a dose-dependent manner (Daniels et al. 2003). A stress-release FPCL model was employed to determine the dose of ilomastat that yielded maximal suppression of matrix contraction. FPCLs were prepared as described above. After lattice polymerisation, 0.5ml of test medium (0, 100nM, 1μM,

10μM or 100μM ilomastat) was dispensed into wells in quadruplicate. FPCLs were allowed to develop mechanical tension over 48 hours prior to release. Lattice contraction was monitored over a further 48 hours enabling selection of the maximum dose of ilomastat that suppressed matrix contraction without affecting cell proliferation or viability.

2.4.5 Effect of ilomastat on matrix contraction

A comparison was made between FPCL contraction under basal conditions (GFM) and under treatment with ilomastat, control peptide or vehicle control. FPCLs were prepared as described above with fibroblasts derived from paired cord and nodule samples (n=5) and carpal ligament (n=5). After lattice polymerisation, 0.5ml of test medium (0, 100μM ilomastat, 100μM control peptide or 0.1% DMSO in GFM) was dispensed into wells in quadruplicate. As before, the lattices were released after 48 hours and then allowed to contract for a further 48 hours before termination of the experiment. A graph of lattice area was plotted against time. The results were pooled for each cell type so that a comparison of contractile ability and effect of ilomastat could be made between cord, nodule and carpal ligament. Cell-conditioned media samples were collected in quadruplicate to assess MMP protein levels and activity both under conditions of mechanical stress (pre-release) and lattice contraction (post-release). These were stored at -20°C.

2.4.6 Isolation of membrane-bound and intracellular proteins

At the end of the experiment (section 2.4.5), the lattices were washed in PBS and then cells isolated from the matrix by collagenase digestion (0.5% collagenase D, Roche; 0.5% Bovine Serum Albumin, Sigma; Phosphate Buffered Saline) at 37°C for 20 minutes or until the collagen was completely dissolved. After the lattices had been dissolved, 5ml PBS was added to the resultant cell suspension to terminate the reaction. The mixture was centrifuged at 1200rpm for 5 minutes, and the supernatant aspirated to remove traces of collagenase. The resultant pellet was resuspended in 0.5ml minimal lysis buffer (50mM tris-buffered saline pH7.6, 1.5mM NaCl, 0.5mM $CaCl_2$, 1μM Zn Cl_2, 0.1% Brij-35, 0.25% Triton X-100) to isolate membrane-bound and intracellular proteins. The suspension was incubated at 4°C for 10 minutes to allow cell lysis, and then centrifuged at 13000rpm for 5 minutes. The supernatant containing the isolated membrane-bound proteins was aspirated

and stored at -20°C, prior to determination of protein concentration and type 1 membrane-bound MMP (MT1-MMP) activity.

Whilst the FPCL is an efficient model for providing data on fibroblast-mediated matrix contraction and allowing media analysis at multiple time points, it is not very sensitive and allows only limited analysis of the contraction profile. The culture force monitor was therefore introduced to yield accurate kinetic information and enable differentiation of the cellular and remodelling components of matrix contraction.

2.5 CULTURE FORCE MONITOR (CFM)

The culture force monitor (Figure 4) is an in vitro kinetic model designed to measure contractile forces generated by cells within a three-dimensional matrix in real time (Eastwood et al. 1994).

The CFM model involves a fibroblast-seeded collagen lattice that resides within a rectangular well filled with growth medium providing a friction-free environment. The well was carved out of a single rectangular block of polytetrafluoroethylene (PTFE; RS components) and had standard dimensions 7.5 x 2.5 x 1.5cm to a depth of 1.5cm. The PTFE ensured a hydrophobic well environment, thus inhibiting cell attachment. The collagen lattice was suspended longitudinally between two hydrophilic flotation bars, which were connected to the culture force monitor by means of two 'A' frames of stainless steel suture wire (Figures 5, 6). One frame was attached to a fixed strut and the other, to a strain gauge by means of a small hook (Figure 7). The block was positioned on a platform with a mounting stage, which enabled fine adjustments to ensure that the lattice was accurately aligned between the fixed strut and the strain gauge. The whole apparatus was incubated at 37°C, 5% CO_2, with constant humidity within an incubator (Innova CO-48, NewBrunswick Scientific Co., NJ, USA).

The CFM was powered by a 12V power supply, which applied a high input signal, increased by a strain gauge amplifier. The output from the amplifier was channelled into a voltmeter, and through an analogue digital converter, which provided a force reading every 800 milliseconds. The data were transferred to a laptop computer (PP01A, Dell; Windows 2000) and recorded by a computer software programme (Chart Recorder, Grey Institute, UK). As the cell-seeded lattice contracts, the strain gauge lever is deflected horizontally, resulting in a positive force reading. Any manual forces on the strain gauge lever or transducer, or prolonged time at a temperature different from 37°C can cause inaccuracies of the transducer's readings. The force transducer was therefore regularly calibrated against a series of known weights in order to ensure linearity of displacement of the strain gauge.

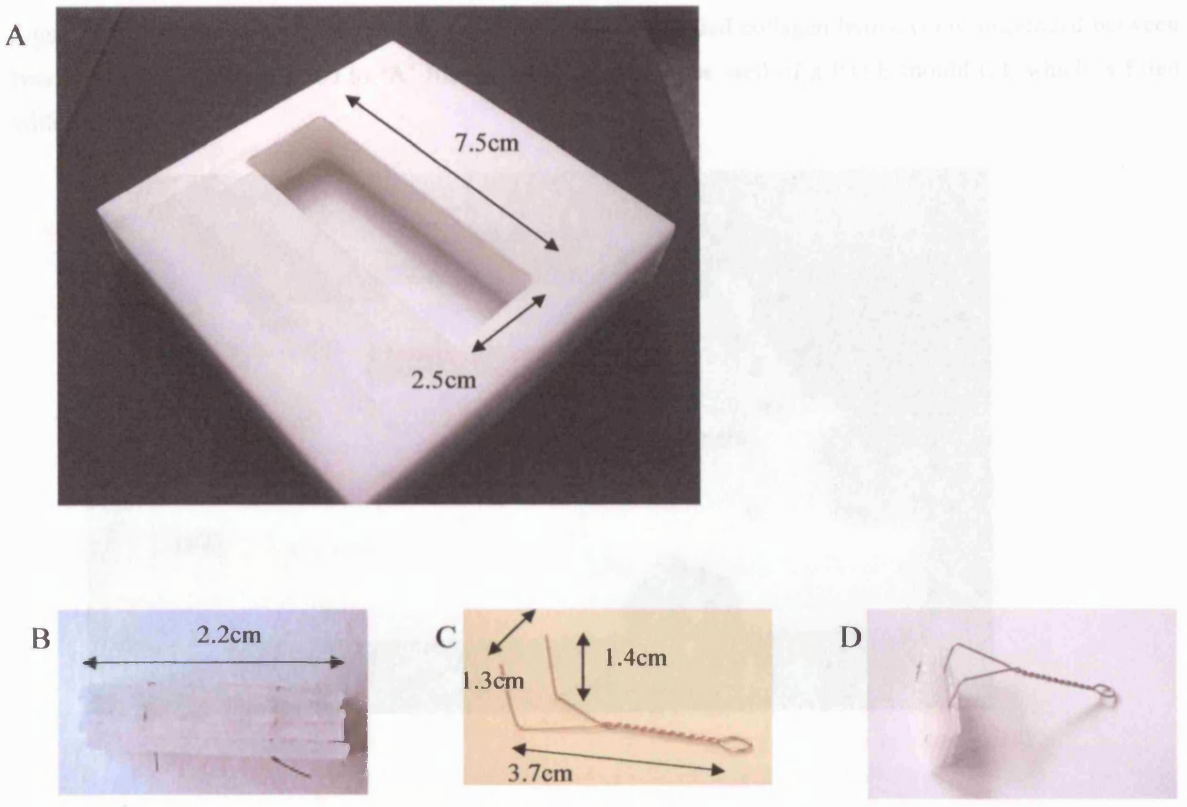

Figure 5. Components of the culture force monitor. Panel A demonstrates a PTFE mould. The depth of the chamber was 1.5cm. Panel B demonstrates a flotation bar, constructed from plastic canvas squares (Haberdashery department, John Lewis Department Store, UK). Four 6 by 3 square rectangles were joined together to form each bar using nylon non-absorbable sutures. Panel C shows an 'A frame' and panel D demonstrates how the flotation bar and 'A frame' were connected.

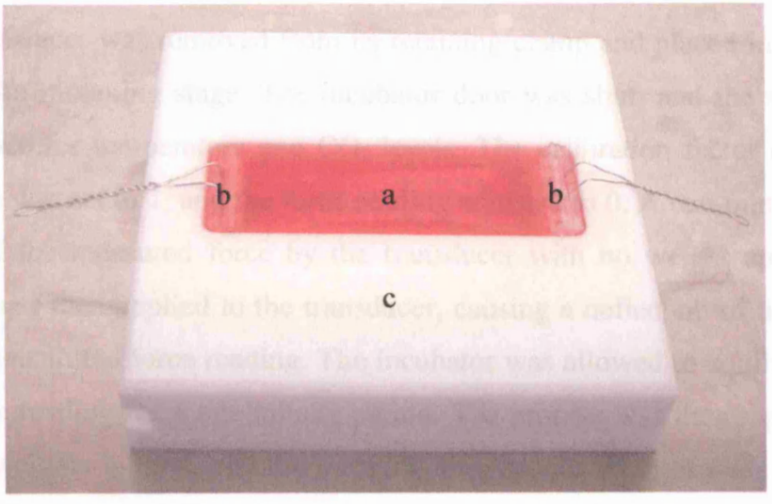

Figure 6. Demonstration of lattice position in well. The cell seeded collagen lattice (a) is suspended between two flotation bars (b) attached to 'A' frames. It floats within the well of a PTFE mould (c), which is filled with test media.

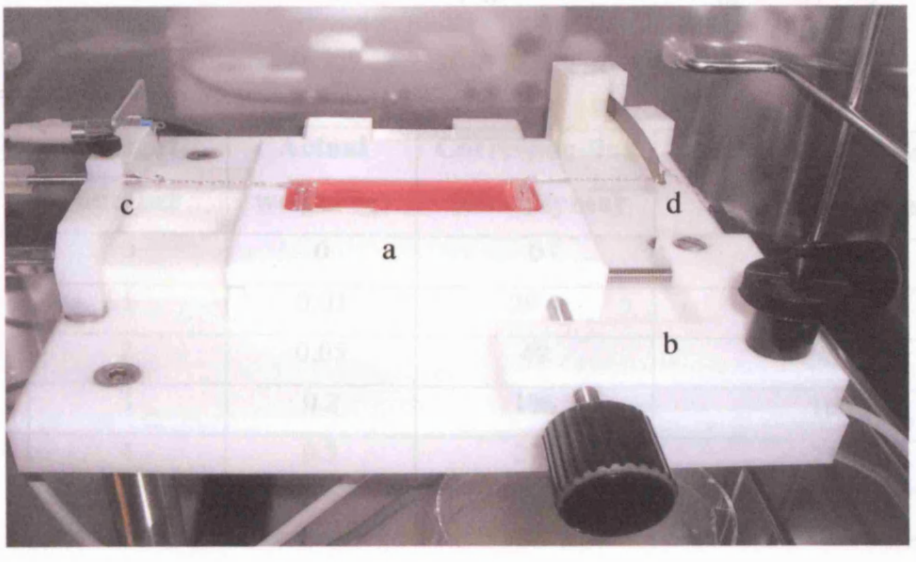

Figure 7. Illustration of the culture force monitor positioned in the incubator. The PTFE mould (a) is positioned on a platform with a moveable mounting stage (b). One 'A' frame is attached to a fixed strut on the platform (c), whilst the other is attached to the strain gauge (d).

2.5.1 Calibration of the Culture Force Monitor

The transducer was removed from its retaining clamp and placed in a vertical direction on top of the mounting stage. The incubator door was shut, and the system was allowed to equilibrate for temperature and CO_2 levels. The calibration factor on the Chart Recorder program was set to 1, and the force reading adjusted to 0. A one-minute recording was then made of the measured force by the transducer with no weight applied. A small known weight was then applied to the transducer, causing a deflection of the arm and an increase in the transmitted force reading. The incubator was allowed to equilibrate before recording the force reading for a one-minute period. The process was then repeated for a series of 5 known weights in total, and the mean reading calculated to provide a mean force for each weight. The standard force for each weight was calculated from the equation below and a table constructed as illustrated in Table 2. One dyne is equivalent to 10^{-5} Newtons.

Force (Newtons) = Mass (kg) x Acceleration (gravity, 9.8)

Weight number	Actual weight (g)	Corresponding force (dynes)	Mean force transducer reading (dynes)
0	0	0	0
1	0.03	29.4	25
2	0.05	49	43
3	0.2	196	166
4	0.3	294	235
5	0.5	490	403

Table 2. Table illustrating the mean force recorded by the CFM for each known weight and the equivalent calculated force.

A scatter graph was then plotted of force recorded by the culture force monitor against the standard force for each weight (Figure 8). A line of best fit was drawn, yielding the calibration factor from the slope of the graph. The correlation coefficient (R^2) was also

calculated to ensure that a linear relationship was established. The calibration factor was then entered directly into the Chart Recorder software.

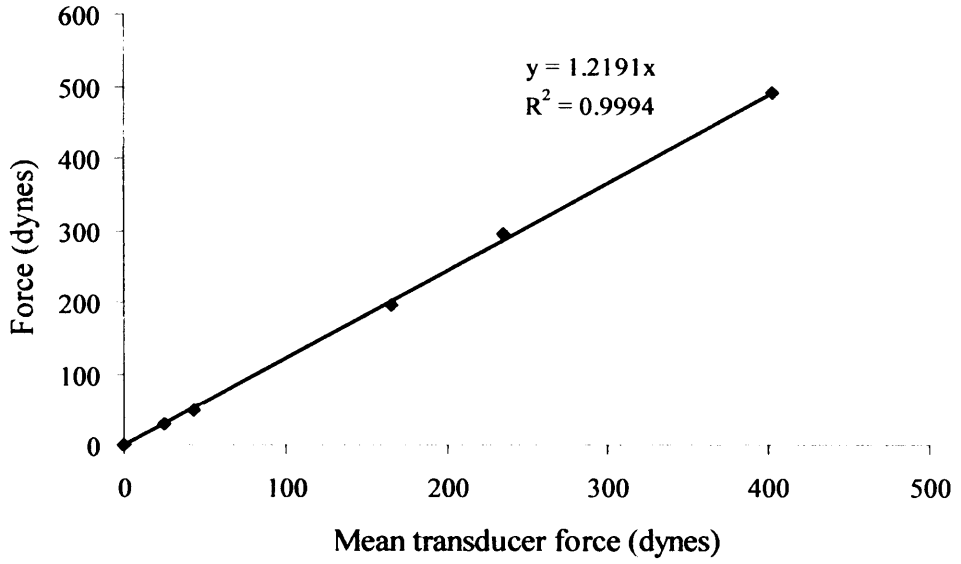

Figure 8. Scattergraph of calibrating force in dynes plotted against the mean CFM force transducer reading. The slope of the curve gives the calibration factor (1.22 in this example). The correlation coefficient (R^2) was also calculated.

2.5.2 Construction of the CFM lattice

A cell suspension of fibroblasts was prepared from two sub-confluent T225cm^2 (Corning, NY, USA) tissue culture flasks, as described previously. Cell viability and number were determined using Trypan Blue and a Neubauer haemocytometer. The cell suspension was centrifuged at 1000rpm for 5 minutes, the supernatant discarded, and the pellet washed in PBS, then resuspended in GFM at 10x10^{6}cells/ ml.

Meanwhile the mould and flotation bars were prepared. The flotation bars were attached to the 'A' frames and checked for symmetry and correct height relative to the mould. They were then immersed in 70% IMS to sterilise them, and left on a sterile petri dish to air-dry, before being placed at either end of the mould. The mould and 'A' frames were autoclaved prior to use.

Lattices were prepared by mixing 700µl of 10x concentrated DMEM (Sigma, Dorset, UK) and 6ml Collagen type 1 solution (2.16mg/ml in 0.6% acetic acid, First link, UK). The solution was neutralised by drop-wise addition of 5M NaOH, then 1M NaOH, until a colour change from yellow to just pink was observed, indicative of the adjustment of pH from 1.0 to 7-7.5. Some of the neutralised solution was then pipetted into the flotation bars (1ml each) and the rest mixed carefully with 500µl of the cell suspension ($5x10^6$ fibroblasts). The resultant cell suspension was then dispensed into the well between the two flotation bars and the mould, rotated to ensure even lattice distribution throughout the well. The mould was placed in an incubator for 30 minutes at 37°C to polymerise the lattice. An inverted 9cm Petri dish base placed over the mould was used as a protective lid.

After 30 minutes, the polymerised lattice was released from the well using a sterile green needle and 20ml of GFM dispensed into the well. The lattice then floated to the surface between the flotation bars. The mould was transferred to the culture force monitor situated within a humidified incubator maintained at 37°C, and 5% CO_2. The eye of one 'A' frame was attached to the fixed strut of the platform and the other was hooked onto the strain gauge. The position of the mould on the platform was adjusted to ensure precise longitudinal alignment of the flotation bars and platform, to enable frictionless movement of the lattice.

2.5.3 Contraction profile determination

The apparatus was allowed to equilibrate in the incubator for 10 minutes before data recording commenced. The force at equilibrium was set at zero and subsequent readings were recorded every 800ms by a computer software programme (Chart Recorder, Grey Institute, UK), which converted the voltage reading into a force measurement in dynes. The whole system was maintained at 37°C and 5% CO_2 for the duration of the experiment. The lattice was allowed to contract for 48 hours, producing a contraction profile over time for each cell line and experimental condition investigated. The data for each experiment were converted to a mean reading every 15 minutes using the Chart Recorder software and a graph of force plotted against time using Microsoft Excel software (Microsoft Corporation).

2.5.4 Effect of ilomastat on force generation

A comparison was made between force generated by Dupuytren's (paired cord and nodule, n=5) and control fibroblasts (carpal ligament, n=5) under basal conditions (GFM) and treatment with ilomastat, control peptide or vehicle control. CFM lattices were prepared as described above. After lattice polymerisation, 20ml of test media (0, 100μM ilomastat, 100μM control peptide or 0.1% DMSO in GFM) was dispensed into the chamber of the PTFE mould and force generation recorded over 48 hours.

2.5.5 Effect of ilomastat on matrix remodelling by addition of Cytochalasin-D

After allowing lattices to contract for 48hours, a single dose of cytochalasin-D (Sigma, Poole, Dorset, UK), 20μl of 60mM in 0.5ml of GFM, was added to the cell-conditioned test media giving an overall concentration of 60μM within the chamber. This was added rapidly in order to minimise disruption to the incubator temperature and CO_2 levels. Readings were recorded for a further 2 hours until the force had reached a plateau, revealing a residual force termed 'residual matrix tension' (RMT). Cytochalasin-D specifically targets the actin-dependent processes required for contraction generated by fibroblasts, but not remodelling of the collagen matrix. Therefore, the reduction in force after addition of cytochalasin-D was equivalent to the cellular component of contraction. A graph was plotted of force against time, yielding maximum force generated as well as differentiation of the cellular and matrix components (Figure 9).

The results were pooled for each cell type so that a comparison of the effects of ilomastat on maximum force generation and RMT could be made for each cell type (cord, nodule and carpal ligament).

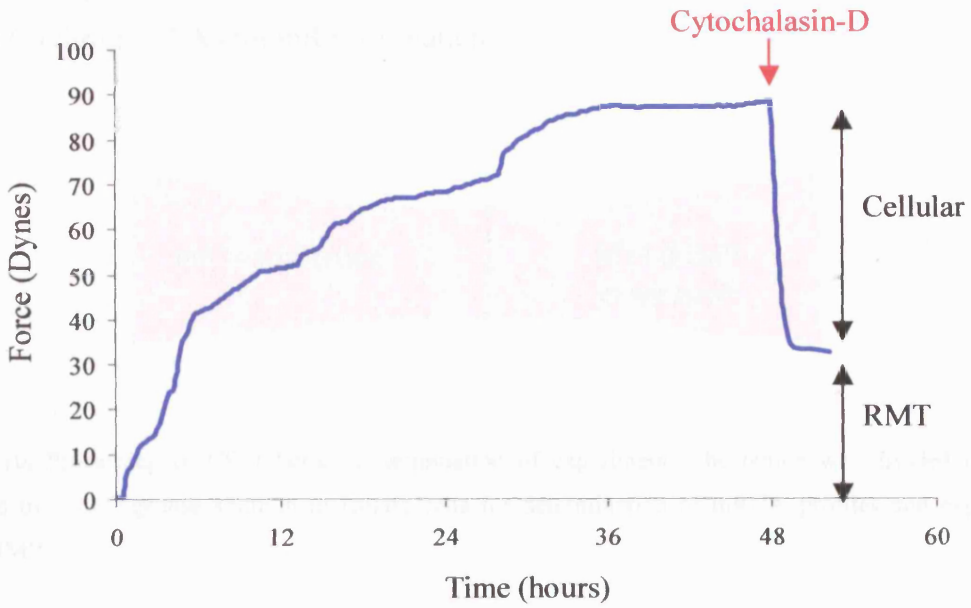

Figure 9. Demonstration of force generated by fibroblasts over time in the CFM model. On addition of Cytochalasin-D after 48 hours, the force drastically reduces revealing the separate components of residual matrix tension (RMT) and cellular contraction.

2.5.6 Removal and processing of lattices from the CFM

At the conclusion of each experiment, cell-conditioned media samples were collected and stored in labelled eppendorfs at -20°C, so that the effect of ilomastat on MMP protein levels and activity could subsequently be determined. The lattice was removed from the CFM mould and examined under light microscopy, to ensure that there was no evidence of contamination or infection. The culture force monitor apparatus is not a closed system, and therefore susceptible to contamination, which could cause erroneous results. Any infected lattices were therefore discarded and the experiment was rerun.

Lattices were washed in PBS, divided in two (Figure 10) and then cells isolated from the matrix by collagenase digestion (0.5% collagenase D, Roche; 0.5% Bovine Serum Albumin, Sigma; Phosphate Buffered Saline). PBS (30ml) was added to each cell suspension and the two suspensions were centrifuged at 1200rpm for 5 minutes. The supernatant was aspirated. One pellet was resuspended in 1ml lysis buffer (50mM tris-buffered saline pH7.6, 1.5mM NaCl, 0.5mM $CaCl_2$, 1µM Zn Cl_2, 0.1% Brij-35, 0.25%

Triton X-100) to isolate membrane-bound and intracellular proteins and the other in 1ml Tryzol (Invitrogen, UK) for mRNA isolation.

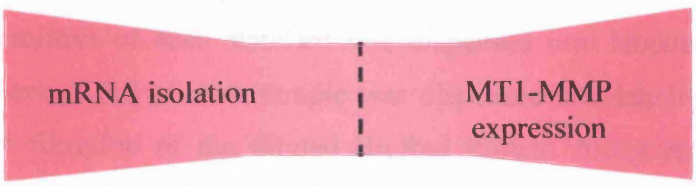

Figure 10. Processing of CFM lattice at termination of experiment. The lattice was divided in two and digested by a collagenase solution to isolate cells for determination of mRNA profiles and expression of MT1-MMP.

The lysis suspension was incubated at 4°C for 10 minutes to achieve cell lysis, and then centrifuged at 13000rpm for 5 minutes. The supernatant was aspirated and stored at -20°C prior to determination of protein concentration and MT1-MMP activity. The Tryzol suspension was incubated at room temperature for 5 minutes and then stored at -20°C prior to mRNA extraction at a later stage.

2.6 DETERMINATION OF MMP SECRETION AND ACTIVITY

2.6.1 Determination of protein concentration

The total protein concentration of conditioned media and cell lysate samples was estimated using a commercial protein assay reagent based on the Bradford method (BioRad, UK). This enabled MMP activity to be normalised against total protein concentration, as protein levels affect MMP binding and therefore observed MMP levels and activity.

Cell-conditioned media (CM) samples contained levels of protein in excess of that accurately determined by the assay, therefore, samples were diluted 6-fold (40µl CM in 200µl distilled water). This dilution factor was previously determined by assay validation. CM and cell lysate samples were thawed on ice. A 2mg/ml standard protein solution was

prepared (50mg BSA dissolved in 25ml distilled water). Serial dilutions (0, 0.2, 0.4, 0.6, 0.8. 1.0, 1.2 mg/ml in 500µl distilled water) of the standard protein solution were prepared. The BioRad Protein Assay Reagent was diluted 1:4 with distilled water, and then filtered through a Whatman No. 1 filter paper (Whatman International, UK) to remove particulate matter. Ten microlitres of each standard was dispensed into labelled replicate tubes (in duplicate). Similarly, 10µl of each sample was dispensed into labelled replicate tubes (in duplicate). After filtration of the diluted BioRad Protein Assay reagent was complete, 500µl was dispensed into each tube and mixed thoroughly. After 5 minutes incubation at room temperature, the tubes were mixed again to ensure a homogeneous solution and then transferred to a 96-well plate (2x100µl of each standard or sample, repeated with each replicate). The absorbance at 595nm was determined in a microtitre plate spectrophotometer (Model 550, BioRad, UK), and the data transferred to a microsoft excel spreadsheet, which enabled calculation of the mean absorbance per standard/sample. Absorbance (measured as optical density, OD) was plotted against standard protein concentration (mg/ml) and regression analysis used to calculate and plot a line of best fit, yielding a regression equation (Figure 11).

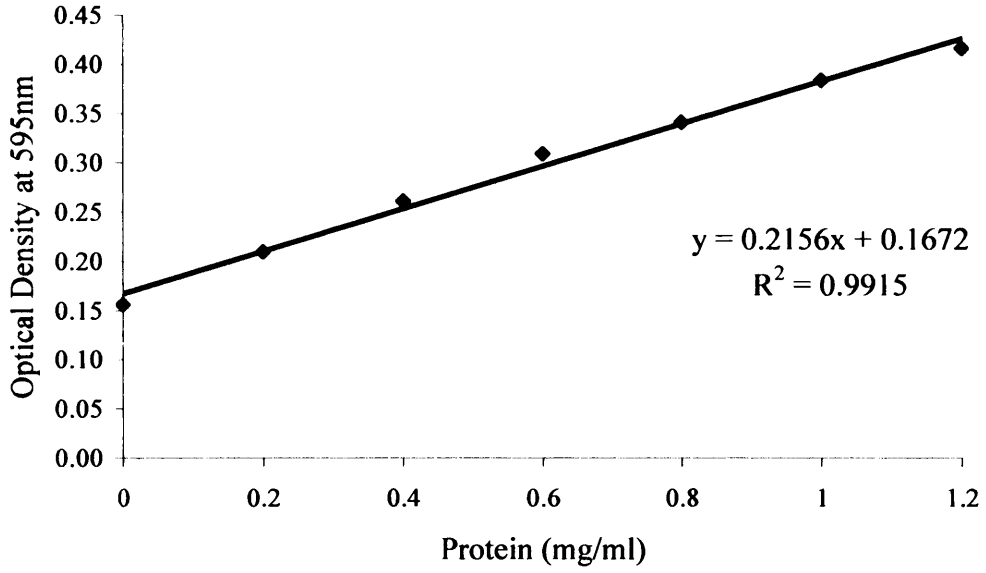

Figure 11. Example of protein standard curve. A line of best fit was plotted, yielding a regression formula, allowing the protein concentration in unknown samples to be calculated.

The regression formula was used to calculate the protein concentration from the OD values obtained for each replicate sample. The CM sample concentrations were then multiplied by 6 to correct for the initial dilution.

2.6.2 Western Blot analysis

The relative expression of specific MMP protein levels was detected in conditioned media samples collected from stressed and contracting FPCLs by western blotting. Western blotting is a technique that involves the immunochemical detection of a target antigen that has been resolved by sodium dodecyl sulphate – polyacrylamide gel electrophoresis (SDS-PAGE). This assay did not yield any information on the enzyme activity levels associated with expression of the target MMP.

2.6.2.1 SDS gel formulation

Resolving SDS separating gels were cast into a 1.5mm gel mould (BioRad, UK) with a 15-well comb and SDS stacking gel. Generally, the separating gel comprised 10% acrylamide (Sigma), 0.4M tris pH8.8, 0.001% SDS, 0.0003% ammonium persulfate (APS) and 0.001% tetramethylethylenediamine (TEMED, Invitrogen). However, a 15% acrylamide separating gel was used to separate low molecular weight molecules (TIMP-1, -2). The stacking gel consisted of 5% acrylamide, 0.125M tris pH6.8, 0.001% SDS, 0.0005% APS and 0.001% TEMED.

Once polymerised, the comb was gently removed, and the glass plates assembled within the gel running tank with running buffer (25mM tris base, 192mM Glycine, 0.1% SDS). Kaleidoscope Marker (10µl mix of colour-tagged proteins approximately 14.3 – 220kDa, BioRad, UK) was dispensed into the first lane of the gel so that the molecular weight of bands revealed by western blotting could be estimated. Estimation of protein content in each sample, as previously described, enabled loading of equal amounts of protein (10µg) per lane for comparative purposes. Each sample was mixed 1:1 with sample buffer (120mM tris pH6.8, 4 % SDS, 10% glycerol, 0.01% bromophenol blue; 12.5µl per sample) and then loaded into successive lanes of the gel. The entire gel tank was connected to a power pack

(BioRad, UK), and run at 200V for 60 minutes, or until the dye front had reached the base of the gel.

After electrophoresis, the gel was briefly soaked in fresh transfer buffer (25mM tris base; 192mM Glycine; 20% methanol, 70% dH_2O). Simultaneously, six pieces of pre-cut filter paper (3mm; Whatman, UK) and one pre-cut nitrocellulose membrane (Hybond-ECL; Amersham Biosciences, UK) were soaked in transfer buffer. Three filter pads were placed onto the base (anode) of the semi-dry blotter, and on top, the nitrocellulose membrane, the gel and a further three filter pads. Air bubbles were removed and the protein transferred for 60mins at 25V. Once the transfer was complete, the nitrocellulose membrane was placed in blocking buffer, which consisted of BSA (5%) in TBS (10mM tris base, 13.8mM NaCl, 2.7mM KCL), and set for 1 hour on a rotary shaker at room temperature.

2.6.2.2 Antibody detection

Following blocking of non-specific binding, the membrane was washed three times (10 minutes per wash) in TTBS wash buffer (TBS + 0.1% Tween-20) with shaking. The membrane was then incubated in the relevant primary antibody (diluted in blocking buffer, Table 3) overnight at room temperature on the rotary shaker.

Following incubation with the primary antibody, the membrane was washed three times (10 minutes each) in fresh TTBS and incubated with the relevant secondary antibody (diluted in blocking buffer, Table 3) for one hour at room temperature on the rotary shaker.

After incubation with the secondary antibody, the membrane was washed again in TTBS as previously described. The presence of the protein of interest was then visualised with an alkaline phosphatase III substrate kit (Vector Laboratories, SK5300), according to the kit instructions. Briefly, 4 drops of each of the three alkaline phosphatase reagents (1, 2 and 3) were diluted in 20ml tris pH8.2 and applied to the membrane. The membrane was placed on a rotary shaker and covered to block light. The membrane was checked frequently for the appearance of bands. After optimal development of the bands, the reagents were

removed and the membrane was then placed in dH_2O to prevent overexposure, before being air-dried and photographed.

MMP	Primary Antibody	Antibody recognition	Dilution	Secondary Antibody	Dilution
MMP-1	Mouse monoclonal (Calbiochem)	proenzyme (55 kDa) active (43 kDa)	1:1000	Rabbit anti-mouse IgG (Dako)	1:500
MMP-2	Mouse monoclonal (Calbiochem)	proenzyme (72 kDa) active (66 kDa)	1:1000	Goat anti-mouse IgG (Sigma)	1:1000
MT1-MMP	Rabbit polyclonal (Chemicon)	proenzyme (65 kDa) active (63 kDa)	1:1000	Goat anti-rabbit IgG (Sigma)	1:1000
TIMP-1	Mouse monoclonal (Calbiochem)	TIMP-1 protein (30 kDa)	1:1000	Goat anti-mouse IgG (Sigma)	1:1000
TIMP-2	Mouse monoclonal (Calbiochem)	TIMP-2 protein (21 kDa)	1:400	Goat anti-mouse IgG (Sigma)	1:1000

Table 3. Details of the primary MMP antibodies and corresponding secondary antibodies used, including specific enzyme forms recognised, their respective molecular weights and dilution factors.

2.6.3 Gelatin zymography

Conditioned media samples collected from stressed and contracting FPCLs were analysed for MMP activity by gelatin zymography. Gelatin zymography is an electrophoretic technique, based on SDS-PAGE, that involves an MMP substrate (gelatin) copolymerised with the polyacrylamide gel. Zymography enabled detection of gelatinase (MMP-2, -9) activity through digestion of the gelatin substrate.

Resolving SDS separating gels were cast into a 1.5mm gel mould (BioRad, UK) with a 15-well comb and SDS stacking gel. The SDS gel comprised 10% acrylamide (Sigma), 0.15% gelatine (Type A, Sigma), 0.4M tris pH8.8, 0.001% SDS, 0.0007% ammonium persulfate (APS) and 0.003% tetramethylethylenediamine (TEMED, Invitrogen). The separating gel consisted of 5% acrylamide, 0.125M tris pH6.8, 0.001% SDS, 0.0005% APS and 0.001% TEMED.

2.6.3.1 Zymographic analysis

The gels were assembled into a running tank with running buffer (2.5mM tris base, 19.2mM Glycine, 0.01% SDS). After removal of the combs from the separating gel, 10µl of Kaleidoscope Marker (mix of colour-tagged proteins approximately 14.3 – 220kDa; BioRad, UK) was dispensed into the first lane of the gel, so that the molecular weight of bands in the sample lanes could subsequently be determined. Estimation of protein content in each sample, as previously described, enabled loading of equal amounts of protein (20µg) per lane for comparative purposes. Each sample was mixed 1:1 with sample buffer (0.145M tris pH6.8, 4.6% SDS, 23& glycerol, 0.001% bromophenol blue; 12.5µl per sample) and then loaded into successive lanes of the gel. The entire gel tank was connected to a power pack (BioRad, UK), placed on ice to prevent enzymatic degradation and then run at 25mA for 150 minutes.

The gels were then placed in 100ml renaturation buffer (2.5% Triton X-100, 1µM zinc chloride in distilled water) per gel and incubated at room temperature on an orbital shaker for 1 hour. The renaturation process replaces the SDS in the gel with Triton. The renaturation buffer was decanted and replaced with 20ml development buffer (50mM TRIS base, 200mM sodium chloride, 5mM calcium chloride (anhydrous), 1µM zinc chloride, in distilled water). After 30 minutes, the buffer was decanted and replaced with fresh development buffer, and the zymogram was then incubated at 37°C overnight with shaking. Incubation with the development buffer allowed the proteins to re-fold and re-establish their tertiary structure becoming enzymatically active

The gels were stained with Coomasie Brilliant Blue (0.5% Coomasie Brilliant Blue R-250, Sigma; 40% methanol, 10% acetic acid in distilled water) for 1hr, and then destained (40% methanol, 10% acetic acid in distilled water) by shaking for 30-60 minutes with several changes of destain solution. The gels were deemed to have destained sufficiently when clear gelatinolytic bands were visible. The gels were then placed in dH_2O to prevent further destaining before being photographed.

2.6.4 Enzyme-linked immunosurbent assay (ELISA)

Zymography demonstrates gelatinolytic activity and so is a poor method of quantifying non-gelatinolytic MMP activity. It was therefore necessary to assess the activity of other relevant MMPs. We used an Activity ELISA, which was a modified ELISA system involving activation of a detection enzyme by the bound target MMP rather than a secondary anti-MMP antibody (Figure 12). This was preformed on conditioned media and cell lysate samples using a commercially available ELISA kit (Amersham, UK). The instructions provided by the manufacturer were followed precisely.

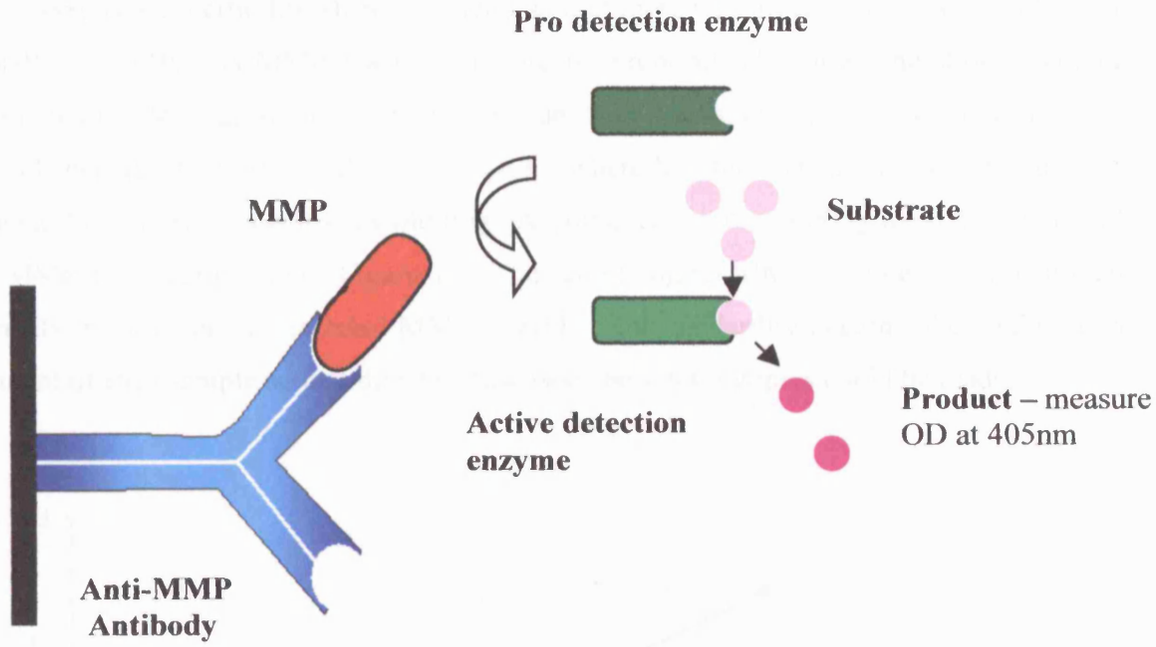

Figure 12. Identification of active MMP enzymes in CM or cell lysate derived from contracting FPCLs. MMPs bind to the anti-MMP antibody, which is adherent to the microplate well. The active MMP complex activates a detection enzyme, which in turn, activates a specific chromogenic peptide substrate. The net result is a product that can be detected by absorbance at 405nm in a spectrophotometer.

2.6.4.1 Detection of MMP-1 activity

Purified MMP-1 working standards were prepared from stock solutions (0.1-1.56ng/ml), then 100µl of each standard and undiluted CM sample was dispensed into a 96-well microplate in duplicate. The plate was covered and incubated at 4°C overnight to allow any active MMP-1 present to bind to the immobilised antibody. Afterwards, the wells were washed and aspirated 4 times with wash buffer, ensuring that all wells were completely

filled and emptied at each wash. The detection reagent was prepared by mixing 100µl of the detection enzyme with the substrate reconstituted in 5.1ml of assay buffer. Assay buffer (50µl) and detection reagent (50µl) were then dispensed into all wells. Absorbance at 405nm was read by a spectrophotometer to obtain a t=0 value (Model 550, BioRad, UK). The plate was then covered and incubated at 4°C for 4 hours again before recording the absorbance at 405nm.

The assay was specific for MMP-1 activity so that there was no cross-reactivity with other MMPs or TIMPs. As MMP-1 activity is directly proportional to the generation of colour through the cleavage of the substrate, it can be represented by the rate of change of absorbance at 405nm (i.e. $\delta Absorbance_{405}/ h^2$, where h is the incubation time in hours). A standard curve was generated by plotting $\delta Absorbance_{405}/ h^2 \times 1000$ (y axis) against ng/ml of MMP-1 standard (x axis, Figure 13). The sample ng/ml MMP-1 values were then read directly from the graph. Secreted MMP-1 levels were standardised against the total protein content of each sample so that direct comparisons between samples could be made.

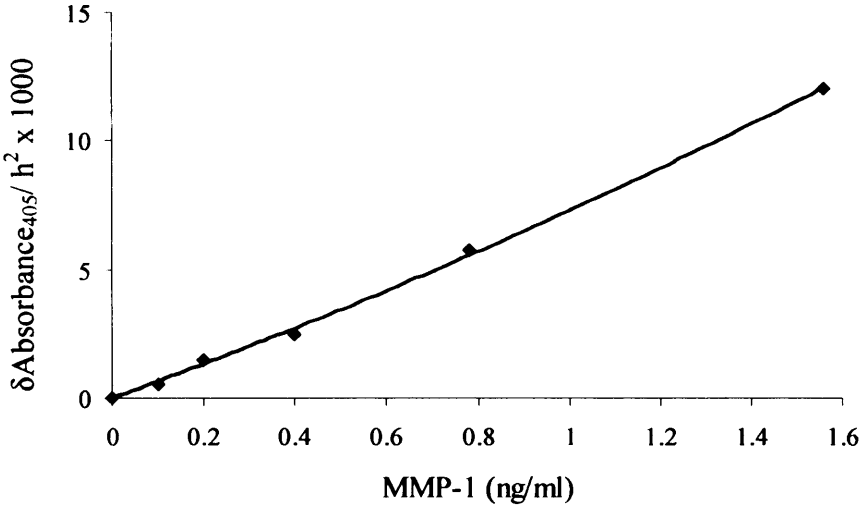

Figure 13. Standard curve for MMP-1 activity.

2.6.4.2 Detection of MMP-2 activity

Purified MMP-2 working standards were prepared from stock solutions (0.7-12ng/ml), then 100µl of each standard and undiluted CM sample was dispensed into a 96-well microplate in duplicate. The assay was specific for MMP-2 activity so that there was no cross-reactivity with other MMPs or TIMPs. After incubation overnight and thorough washing, assay buffer (50µl) and detection reagent (50µl) were dispensed into all wells as previously described. Absorbance at 405nm was read by a spectrophotometer to obtain a t=0 value (Model 550, BioRad, UK). The plate was then covered and incubated at 4°C for 3 hours before recording the absorbance at 405nm again. A standard MMP-2 curve was generated as previously described and the sample ng/ml MMP-2 values read directly from the graph (Figure 14). Secreted MMP-2 levels were standardised against the total protein content of each sample so that direct comparisons between samples could be made.

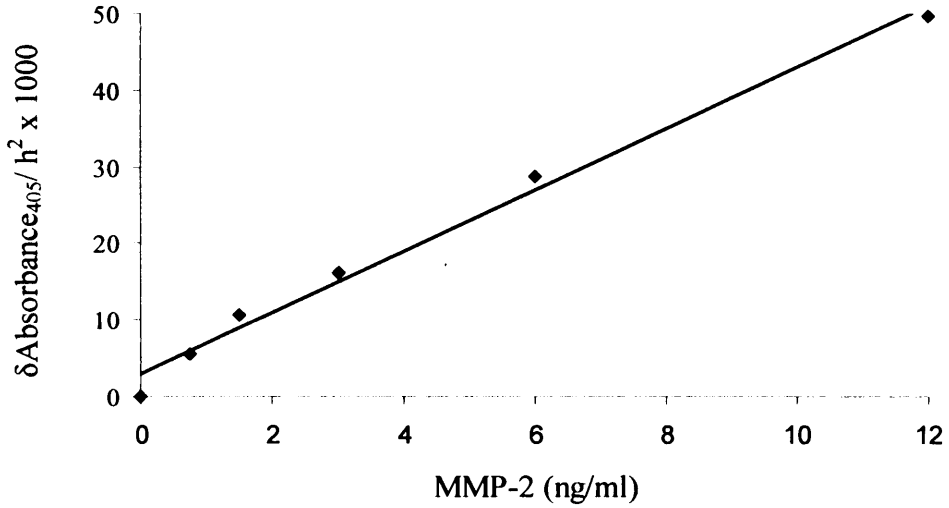

Figure 14. Standard curve for MMP-2 activity.

2.6.4.3 Detection of MT1-MMP activity

MT1-MMP working standards were prepared from stock solutions (1-32ng/ml). Cell lysate samples required a 10x dilution in order for estimates of activity to fall within the active detection range of the assay. The dilution factor was validated in preliminary experiments

(data not shown). 100µl of each standard and 100µl of each diluted lysate sample were dispensed into a 96-well microplate in duplicate. After incubation overnight and thorough washing, assay buffer (50µl) and detection reagent (50µl) were dispensed into all wells as previously described. Absorbance at 405nm was read by a spectrophotometer to obtain a t=0 value (Model 550, BioRad, UK). The plate was then covered and incubated at 4°C for 2.5 hours before again recording the absorbance at 405nm. A standard MT1-MMP curve was generated as previously described and the sample ng/ml MT1-MMP values read directly from the graph (Figure 15). Values were subsequently normalised against protein concentration. MT1-MMP levels were standardised against the total protein content of each sample so that direct comparisons between samples could be made.

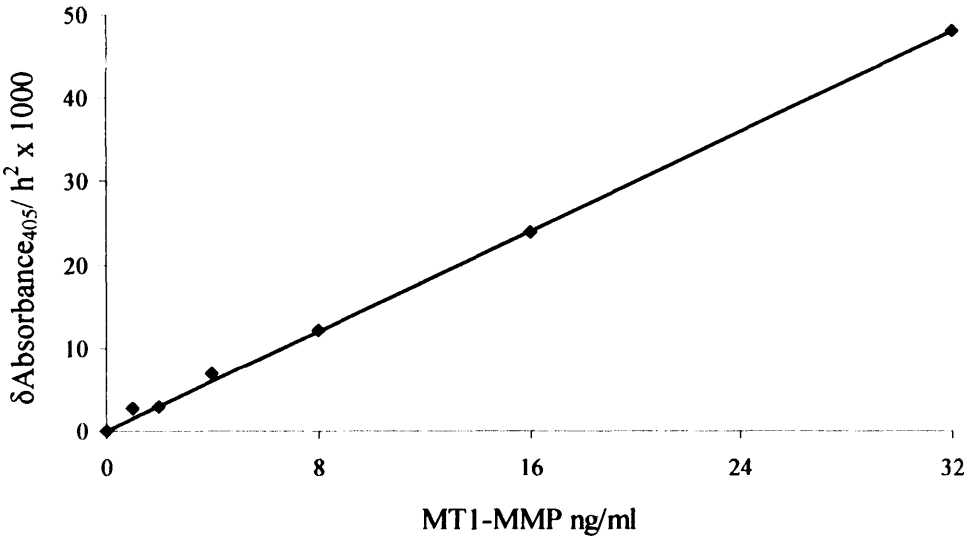

Figure 15. Standard curve for MT1-MMP activity.

Western blotting, zymography and ELISA enabled determining of MMP protein and activity levels by contracting fibroblasts in both CFM and FPCL models. Subsequently, an assessment of MMP gene expression by fibroblasts in the CFM model was undertaken by RT-PCR (real time polymerase chain reaction) to determine whether any differences in pre-

transcriptional control existed between different cell types and in their response to ilomastat.

2.7 DETERMINATION OF MMP GENE EXPRESSION

2.7.1 General precautions to prevent contamination

To avoid contamination from RNA degrading enzymes, diethylprocarbonate (DEPC)-treated water was used as a solvent for RNA extraction, as it is DNAase and RNAase-free. DEPC water was made by adding 2ml DEPC (0.2%; Sigma, UK) to 1 litre of ultra pure (18MΩ) water and shaking vigorously. The mixture was incubated overnight at 37°C and then autoclaved and stored at room temperature until use. Furthermore, all equipment and apparatus was designated for RNA use only and pre-incubated with DEPC water before autoclaving.

2.7.2 mRNA extraction

After thawing of the cell suspensions (in Tryzol, Gibco), 200µl of chloroform was added to each sample and the resultant mixture was shaken vigorously. After incubation at room temperature for 3 minutes, the mixture was centrifuged at 11,000 rpm at 4°C for 15 minutes to separate the phases. The upper clear phase was transferred carefully to a fresh eppendorf and mixed with 0.5ml of 80% isopropanol. After a further 10 minutes incubation at room temperature, the mixture was centrifuged at 11,000 rpm for 30 minutes to pellet the RNA. The supernatant was aspirated and the pellet resuspended in 1ml of 75% DEPC-ethanol to wash the pellet. The RNA suspension was vortexed on low for 10-15 seconds and then centrifuged at 4°C for 5 minutes to re-pellet the RNA. The supernatant was discarded and the pellet air-dried at room temperature for 10 minutes, then dissolved in 60µl DEPC-water by gentle pipetting and finally stored at -80°C in preparation for making cDNA.

2.7.3 Determination of RNA yield and quality

A 1µl aliquot of the extracted RNA was diluted with 999µl of DEPC water and its absorbance determined spectrophotometrically. The spectrophotometer (ComSpec M330)

was zeroed by making a reference against DEPC water alone, then absorbance readings (optical density, OD) were observed at 260nm and at 280nm. One absorbance unit (OD_{260}) represents 40μg of single stranded RNA per ml (Sambrook 1989).

The purity of the extracted RNA was estimated by comparing the ratio of absorbencies OD_{260}:OD_{280}, which provided an estimate of contamination due to DNA or protein and therefore a measure of the accuracy of the extraction procedures. Pure RNA gives a ratio of 2.0; however sample ratios between 1.7 and 2.1 were deemed acceptable (Sambrook 1989).

The concentration of RNA isolated pre sample, and subsequently the total yield of RNA were calculated from the OD_{260} values as detailed in the equation below. The dilution factor accounts for the initial 1:1000 dilution of RNA in DEPC water prior to absorbance measurement.

$$\text{mRNA concentration } (\mu g/\mu l) = OD_{260} \times 40 \times \text{dilution factor (1000)}$$

$$\text{mRNA yield } (\mu g) = \text{mRNA concentration} \times \text{total volume of isolated RNA}$$

After isolation of mRNA from the cell suspensions, it was necessary to convert RNA into cDNA by the reverse transcriptase reaction (RT) as the PCR method involves multiplying copies of single-stranded DNA (cDNA) rather than RNA.

2.7.4 Obtaining cDNA from RNA

All reagents were thawed on ice except for reverse transcriptase. The heating block was set to 65°C. Five micrograms of RNA from the stock solutions was first diluted in DEPC water in fresh sterile PCR grade eppendorf tubes to give a total volume of 8μl. The samples were heated at 65°C for 10 minutes and then placed on ice for a further 5 minutes.

The RT working mix was prepared in a separate tube as detailed in Table 4. Ten microlitres of working mix was added to each RNA sample and mixed by pipetting. Reverse transcriptase (MMLV Reverse transcriptase, 1μl of 200U/ml, Gibco) was then added fresh

from the freezer, mixed carefully and the samples were then pulse-spun in a centrifuge for 60 seconds. Finally, the samples were then incubated at 37°C for one hour.

REAGENTS	QUANTITY	VOLUME	SOURCE
Oligo-dT primers	200µg/ml	1µl	Gibco
0.1M DTT		2µl	Gibco
5 x RT buffer		4µl	Gibco
DEPC water		1µl	-
10mM dNTPs		2µl	Pharmacia (100mM kit)
RNAse inhibitor	30U/µl	1µl	Pharmacia (porcine)

Table 4. The constituents of the reverse transcriptase working mix.

The reaction was terminated by heating samples to 75°C in a heating block (Techne DRI) for 10 minutes. cDNA samples were spun at 13,000 rpm for 1 minute at 4°C, then diluted 1:1 with DEPC water. The samples were then ready to undergo PCR, which enabled relative quantification of cDNA and therefore an estimate of the original RNA content of each sample.

2.7.5 The polymerase chain reaction (PCR)

Gene expression was determined by quantitative PCR using SYBR Green I (Stratagene, USA), a dye that fluoresces when bound non-specifically to double-stranded DNA. The following components were added to each well of a 96-well PCR plate: 12.5µl of SYBR Green QPCR master mix (Stratagene, USA), 0.375µl reference dye (ROX, 30nM final concentration, Stratagene), forward and reverse primers (exact volumes primer-specific as determined through preliminary optimisation; data not shown) and DEPC water to make a total reaction volume of 25µl. The SYBR Green QPCR master mix included *Taq* DNA polymerase. Aliquots (2µl) of each experimental cDNA sample or negative control were dispensed into wells in duplicate. A negative control (non-template control, DEPC water) was used for each primer to screen for contamination of reagents or false amplification

(primer-dimers). The PCR plate was placed in the PCR machine (MX3000P™, Strategene, USA), and the amplification protocol run for a total of 40 cycles.

Each PCR cycle involved 3 stages (Figure 16): *denaturing*, the solution was heated to 95°C to denature the two strands of the target cDNA (SYBR Green I dye remained unbound); *annealing*, the solution was cooled to 60°C to enable the primers to bind to the DNA strand ends (fluorescence occurred on binding of the SYBR Green I dye to double-stranded DNA), and *extension*, reheating to 72°C was accompanied by synthesis of complementary copies of each DNA strand. Fluorescence, as measured by an amplification plot, increases as the double-stranded DNA extends, but remains unchanged in the non-template control which is devoid of DNA.

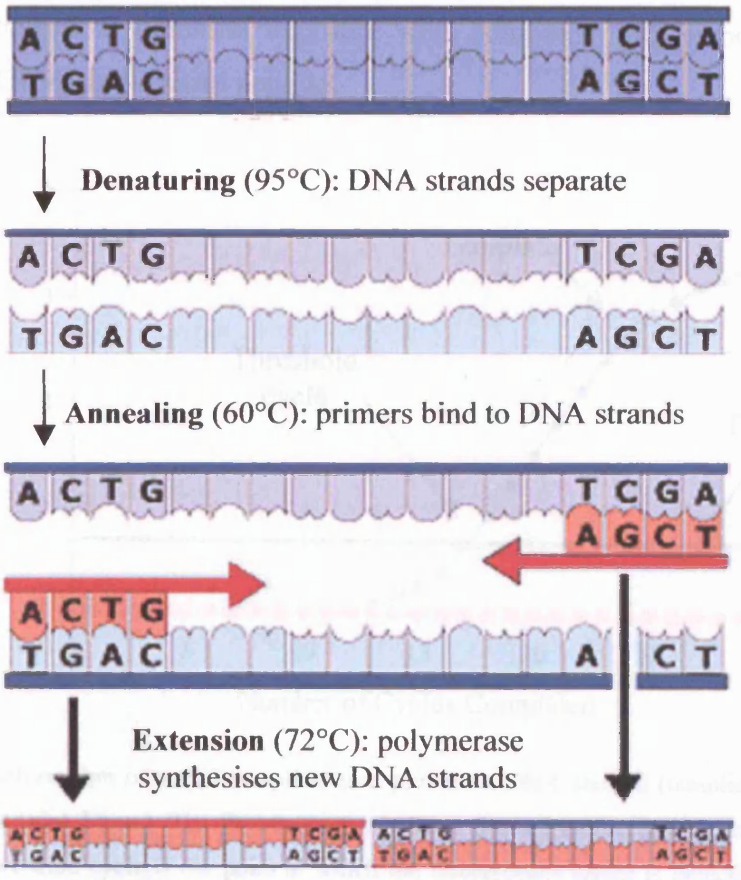

Figure 16. An illustration of the three stages of PCR. Denaturing: solution is heated to 95°C to denature the two strands of the target DNA. Annealing: solution is cooled to 60°C to allow the primers to anneal to the ends of the DNA strands. Extension: solution is reheated to 72°C to allow polymerase to synthesise complementary copies of each strand.

2.7.6 Amplification plot

The fluorescence was monitored in real-time and displayed as an amplification plot (Figure 17), which correlated with the number of copies of DNA synthesised. The initial copy number was quantified, based on the threshold cycle, which is defined as the cycle number at which fluorescence is determined to be statistically significant above background. The threshold cycle has been shown to be inversely proportional to the log of the initial copy number (Higuchi et al. 1993). Furthermore, threshold cycle is a more accurate parameter than information based on endpoint determinations, which may be influenced by limiting reagents. The more template that is initially present, the fewer the number of cycles it takes to reach threshold. Ultimately, the threshold cycle value was used to compare RNA expression levels between contracting Dupuytren's and control fibroblasts in the CFM model. Responses to ilomastat exposure were compared with responses to basal media conditions (GFM) and control peptide.

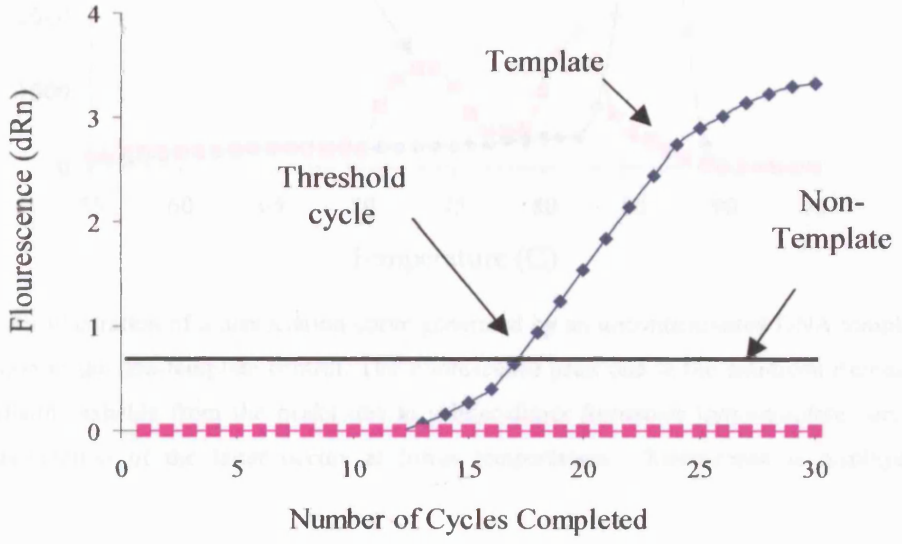

Figure 17. An illustration of a PCR amplification plot for a DNA sample (template, blue boxes) and non-template control (pink boxes). The fluorescence of SYBR Green I increases with each cycle as the template extends. The threshold cycle is the point at which the fluorescence signal is detectable above a background threshold signal (horizontal black line).

Contamination from primer-dimer formation can result in generation of an amplification curve in the absence of cDNA. A dissociation profile was therefore generated to determine whether amplification was due to template extension or contamination from primer-dimers (Figure 18). The melting of products results in a drop in fluorescence which is recorded on the dissociation curve. Primer-dimers generally dissociate at lower temperatures than the desired PCR products. Any DNA sample with evidence of primer-dimer formation on the dissociation curve was discarded and the PCR repeated.

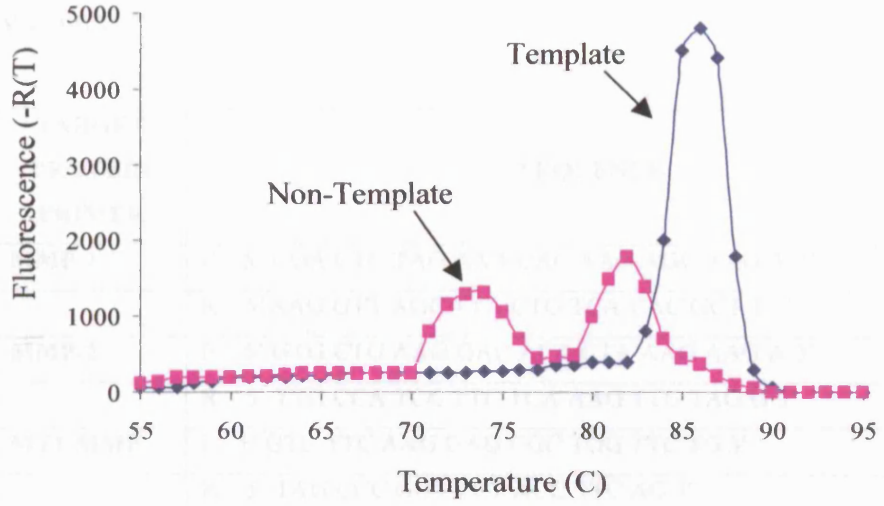

Figure 18. An illustration of a dissociation curve generated by an uncontaminated DNA template sample and contamination in the non-template control. The fluorescence peak due to the amplicon (template curve, blue boxes) is distinguishable from the peaks due to primer-dimer formation (non-template curve, pink boxes) because dissociation of the latter occurs at lower temperatures. Fluorescence is displayed as the first derivative.

2.7.7 Oligonucleotide primers

Specific human oligonucleotide primers were used to amplify the variable portions of MMP-1, -2, MT1-MMP, TIMP-1 and 2. GAPDH was the housekeeping gene used as an internal cellular control. All primers were ordered and synthesised commercially by MWG Biotech. An internal control, or housekeeping gene, is required to determine baseline RNA expression so that comparisons of MMP expression under different sets of conditions can

be objectively made. The two main prerequisites of a housekeeping gene in our experiment were met by GAPDH; it is expressed by palmar fascia (Beckett 2005) and it does not vary with changes in mechanical tension (Mudera et al. 2000; Cheema et al. 2003).

The optimal concentration of each reverse and forward primer pair was established to avoid primer-dimer formation, as SYBR Green I will bind to any double-stranded DNA. This was determined empirically; serial primer concentrations in the range 50nM to 300nM were run with standard cDNA for 40 cycles (data not shown). The optimal concentration was the lowest concentration that resulted in the lowest cycle threshold (amplification plot) and an adequate fluorescence, with minimal or no primer-dimer formation as determined by the dissociation curve.

TARGET PROTEIN PRIMER	SEQUENCE
MMP-1	F – 5' CGA CTC TAG AAA CAC AAG AGC AAG A 3'
	R – 5'AAG GTT AGC TTA CTG TCA CAC GCT T 3'
MMP-2	F – 5' GTG CTG AAG GAC ACA CTA AAG AAG A 3'
	R – 5' TTG CCA TCC TTC TCA AAG TTG TAG G 3'
MT1-MMP	F –5' GTC TTC AAG GAG CGC TGG TTC TG 3'
	R – 5' TAG CCC GGT TCT ACC TTC AG 3'
TIMP-1	F – 5' ACC ACC TTA TAC CAG CGT TAT GAG 3'
	R – 5' GAG GAG CTG GTC CGT CCA CAA GCA 3'
TIMP-2	F – 5' CGC TGG ACG TTG GAG GAA AGA AGG 3'
	R – 5' GGG TCC TCG ATG TCG AGA AAC TCC 3'
GAPDH	F – 5' AAG AAG ATG CGG CTG ACT GTC GAG CCA CAT 3'
	R – 5' TCT CAT GGT TCA CAC CCA TGA CGA ACA TG 3'

Table 5. Table demonstrating primer sequences for the target MMP and TIMP target genes. F denotes forward sequences and R reverse sequences. The sequences were designed by previous investigators in our research institute (Beckett 2005).

2.7.8 Data Analysis

The relative expression software tool (REST©) was used for the calculation of relative MMP and TIMP gene expression levels in real-time PCR (Pfaffl et al. 2002). This mathematical model is based on the mean threshold cycle between the treated and the control cells. The target gene expression was normalised against our housekeeping gene, GAPDH. Statistical analysis of group differences was performed by Pair Wise Fixed Reallocation Randomization Test©, implemented in the REST-XL software (Pfaffl et al. 2002).

2.8 STATISTICAL ANALYSIS

All data underwent statistical evaluation. Statistical analysis was performed using a statistical software package (Sigmastat 2.0). A two-tailed student t-test was used to compare treatments between two groups whilst a one-way ANOVA was employed to compare results derived from multiple groups. Probabilities with $p<0.05$ were considered statistically significant.

CHAPTER 3

OPTIMISATION OF CONDITIONS FOR MATRIX CONTRACTION IN THE FPCL MODEL

3.1 INTRODUCTION

In this chapter we set out to establish the optimum conditions for use of ilomastat in subsequent models of fibroblast-mediated matrix contraction. Matrix contraction in vitro is a complex process that involves numerous cellular processes including migration, cellular contraction and matrix reorganisation (Tomasek et al. 2002; Grinnell 2003). Cell density has been shown to be an additional key parameter that influences both the mechanism and extent of lattice contraction (Ehrlich et al. 2000).

As discussed earlier (section 1.15), two of the three variations of FPCL, the free-floating and stress-release models, allow simple quantification of contraction (Grinnell 2003). In this thesis, we used the stress-release model as it most closely mimics Dupuytren's contracture following surgical release and has been favoured by previous investigators studying Dupuytren's fibroblasts (Howard et al. 2003; Tse et al. 2004).

3.2 AIMS

Initially, our aim was to determine whether ilomastat was cytotoxic or affected proliferation and therefore density of Dupuytren's and carpal ligament-derived fibroblasts (section 2.2.3). Secondly, we set out to define an appropriate time course for FPCL contraction by Dupuytren's and control fibroblasts. Finally, we aimed to demonstrate a dose-dependent inhibition of fibroblast lattice contraction mediated by ilomastat (section 2.4.4). These preliminary experiments were designed so that the optimum dose of ilomastat could be selected that suppressed matrix contraction without affecting cell proliferation or viability for use in subsequent experiments.

3.3 METHODS

A WST-1 metabolic assay was performed to assess both cytotoxicity and cell proliferation. After determining the optimal detection limits of the WST-1 proliferation assay, the effect of serial concentration of DMSO and ilomastat on fibroblast viability and proliferation were investigated. Fibroblast-mediated matrix contraction in a stress-

release FPCL model was characterised over time and then a dose-response effect of ilomastat-mediated suppression of FPCL contraction was established.

3.4 RESULTS

Although 17 Dupuytren's tissue samples were harvested for explant culture, the number of cells available for experiments was limited to five paired sets of cord and nodule due to difficulty in delineating cord from nodule, cellular senescence and over-passage of cells. Therefore, unpaired nodule and cord cell strains were selected for use in the preliminary experiments to test cytotoxicity and establish conditions for the FPCL model.

3.4.1 Optimal cell density for proliferation assay

The WST-1 assay is a metabolic proliferation assay that relies on the conversion of a tetrazolium salt (WST-1) to formazan by cellular enzymes. The amount of formazan produced is related to the number of viable cells present; an increase in cell number is estimated by increasing absorbance (or optical density, OD) at 450nm. Conversely, cell death is determined as a decrease in OD 450nm at the end-point of the assay compared with the t=0 value (section 2.2.3). At higher cell densities, substrate availability may become a rate limiting step in the reaction preventing accurate determination of cell number from formazan production. Fibroblasts derived from different tissues vary in both their size and metabolic activities, which could affect the cell density at which substrate availability becomes limiting. It was therefore initially necessary to establish an appropriate cell density specific to palmar fascia fibroblasts to use in subsequent proliferation experiments.

Nodule-derived fibroblasts were seeded into a 96-well culture plate at a range of densities (2-20,000 cells/ well) to determine the optimal limits of detection of fibroblast proliferation by the WST-1 assay (section 2.4.2). The results of the relationship between optical density (absorbance at 450nm) and cell number are illustrated in Figure 1.

At lower fibroblast densities (2-12,000 cells/well), there was a linear relationship between optical density and number of cells seeded in each well, suggesting that the

WST-1 reagent could accurately estimate cell number over this range (Figure 2). However, at densities greater than 12,000 cells/well, optical density was no longer proportional to cell number and would therefore lead to an underestimate of cell number.

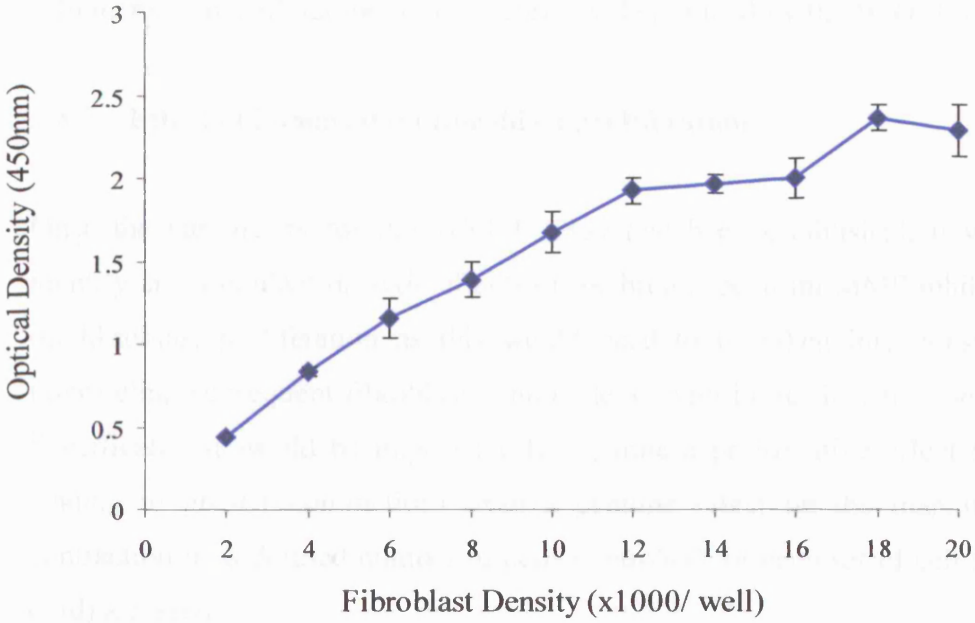

Figure 1. An illustration of the relationship between optical density (absorbance at 450nm) and cell number. Nodule-derived fibroblasts were cultured (n=6 replicates) for 24 hours at various cell concentrations (2-20,000/well). The absorbance was measured spectrophotometrically using the WST-1 assay. Mean ± SEM.

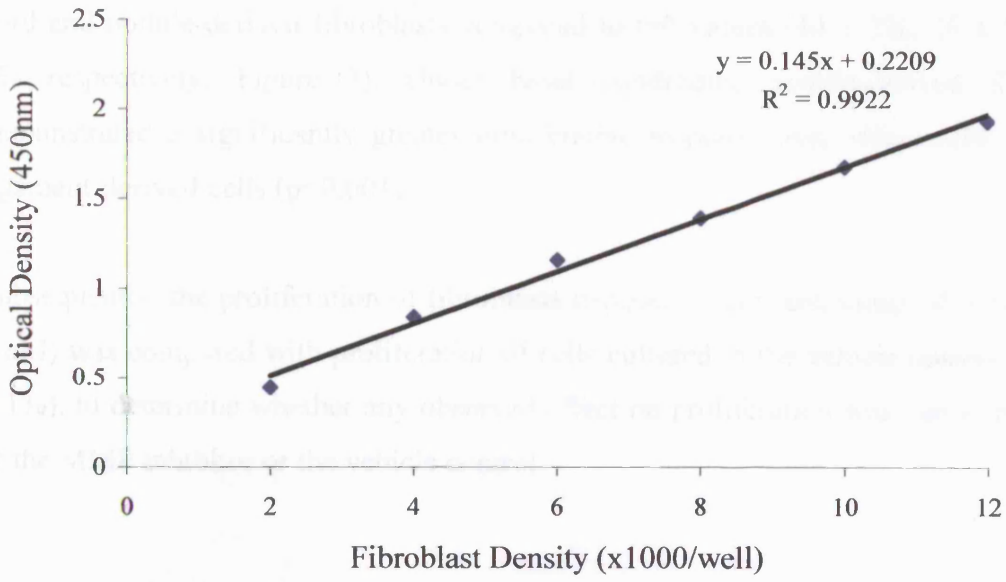

Figure 2. Illustration of the relationship between optical density and cell number at lower cell densities. A linear regression formula is demonstrated and the correlation coefficient (R^2) confirms the linearity of the relationship.

From the results, it therefore appeared that the upper limit for accurate determination of cell number by the WST-1 assay was 12,000 cells/well. For subsequent proliferation assays, it was decided to seed each well with 4,000 cells/well as this density was in the lower-middle range of the linear relationship, enabling both a cell loss and up to a three-fold increase in cell number to be accurately determined by the WST-1 assay.

3.4.2 Effect of ilomastat on fibroblast proliferation

Once the parameters for the WST-1 assay had been established, it was our aim to identify any stimulant or toxic effects of the broad-spectrum MMP inhibitor, ilomastat, on fibroblast proliferation as this would need to be taken into consideration when interpreting subsequent fibroblast contractile activity in our in vitro contraction model. Specifically, it would be impossible to separate a proliferative effect (i.e. more cells leading to greater contraction) from a genuine effect on the magnitude of matrix contraction by a defined number of cells controlled for each set of cell strains (nodule, cord) assessed.

Initially, the response of fibroblasts to normal fibroblast growth medium (NGM) was determined. Exposure to NGM led to proliferation of Dupuytren's and control fibroblasts as evidenced by the increase in OD values at 48 hours for carpal ligament, cord and nodule-derived fibroblasts compared to t=0 values (34 ± 2%, 35 ± 3%, 99 ± 1% respectively, Figure 3). Under basal conditions, nodule-derived fibroblasts demonstrated a significantly greater proliferative response than either cord or carpal ligament-derived cells ($p<0.001$).

Subsequently, the proliferation of fibroblasts exposed to concentrations of ilomastat (0-1mM) was compared with proliferation of cells cultured in the vehicle control (DMSO; 0-1%), to determine whether any observed effect on proliferation was due to the action of the MMP inhibitor or the vehicle control.

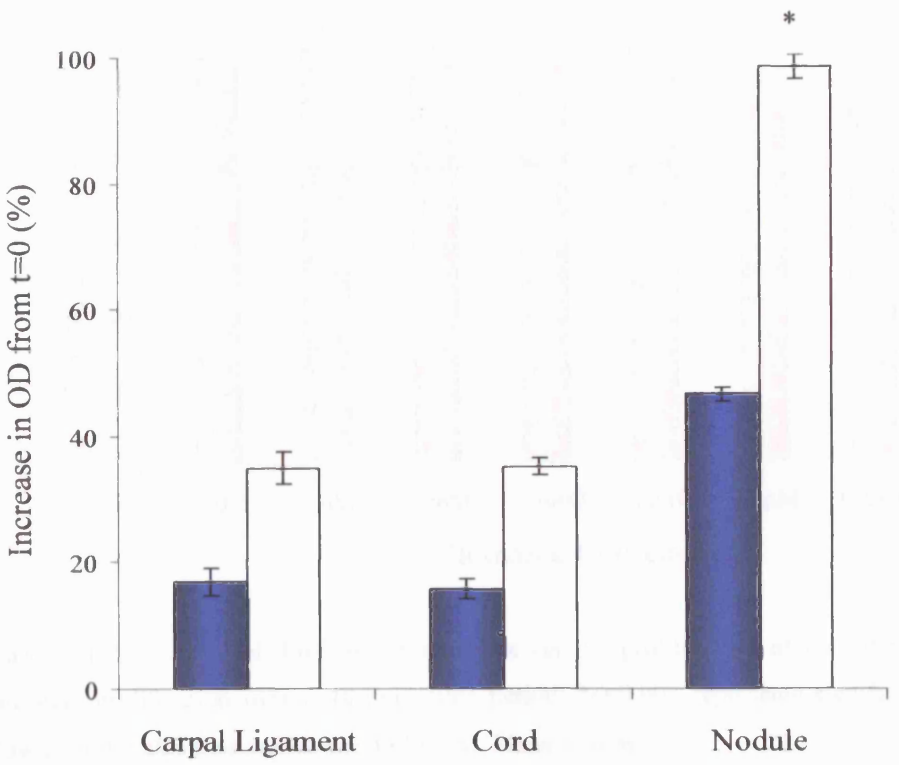

Figure 3. Proliferation of Dupuytren's and control fibroblasts (n=6 replicates) in response to NGM at 24 hours (filled bars) and 48 hours (open bars). *p<0.001 represents a significantly greater proliferative rate for nodule-derived fibroblasts than either cord or carpal ligament-derived cells. Mean ± SEM.

3.4.2.1 Effect of ilomastat on proliferation by cord-derived fibroblasts

The effect of serial dilutions of ilomastat on proliferation of cord-derived fibroblasts is illustrated in Figure 4. Following a 48 hour exposure, ilomastat did not affect cell proliferation at concentrations of 1nM-100μM as OD values were not significantly different from exposure to NGM alone. However, at greater concentrations (1mM), ilomastat induced a 44 ± 1% decrease in absorbance compared with the t=0 value ($p<0.001$). As we have already shown that OD is proportional to cell number, any decrease in OD below the observed t=0 value is indicative of cell death over the 48 hour exposure period. We therefore conclude that ilomastat appears to be cytotoxic at this concentration (1mM).

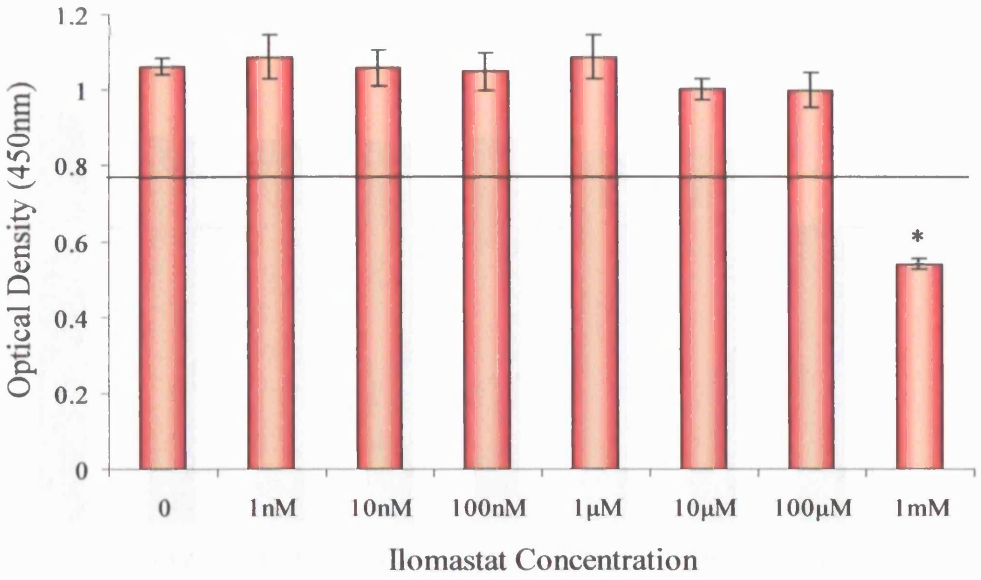

Figure 4. Effect of serial dilutions of ilomastat on the proliferation of cord-derived fibroblast (n=6 replicates) proliferation over a 48 hour time period. *p<0.001 represents significant reduction in OD below the t=0 value (horizontal line, OD 0.78). Mean ± SEM.

However, DMSO is used as a carrier in the preparation of ilomastat and is known to be cytotoxic. In order to determine whether concentrations of DMSO used in the preparation of ilomastat might influence the efficacy of ilomastat independently, we assayed dilutions of DMSO known to be present ($1x10^{-6}$-1%) when ilomastat is tested (Figure 5).

Concentrations of 0.1% DSMO and below did not significantly affect cell proliferation. Exposure to 1% DMSO led to a reduced proliferative response (OD 0.78 ± 0.02) compared to exposure to NGM alone (OD 1.07 ± 0.04, $p<0.001$) over 48 hours. However, the OD values of 1% DMSO were not significantly different from t=0 value (OD 0.78 ± 0.01) suggesting that no cell death occurred. The results indicated that 1% DMSO induced a cytostatic rather than cytotoxic effect on cord-derived fibroblasts and therefore could not account for the cell loss observed on exposure to 1mM ilomastat.

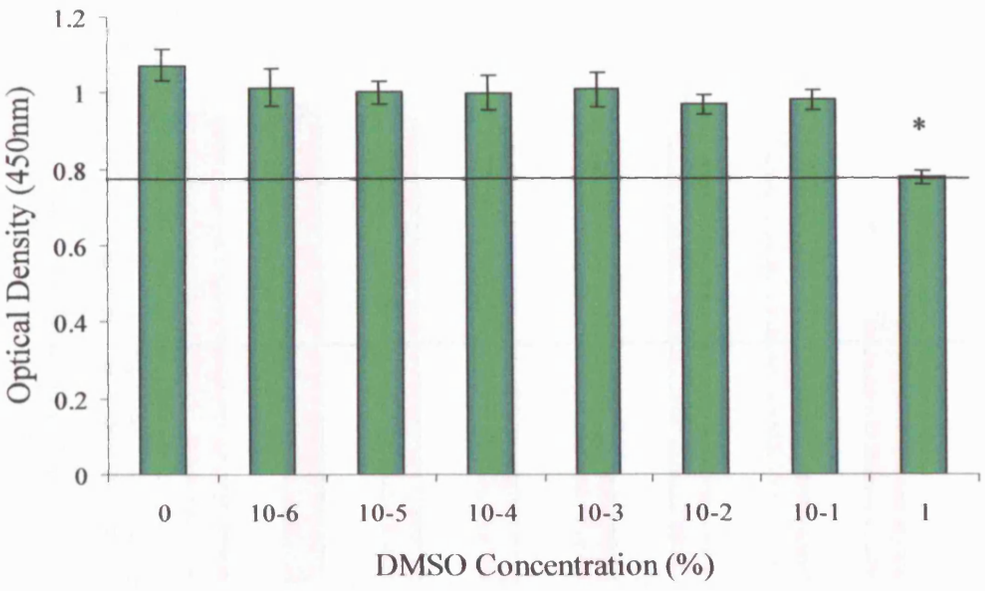

Figure 5. Effect of serial dilutions of DMSO on the proliferation of cord-derived fibroblasts (n=6 replicates) over a 48 hour exposure period. *p<0.001 represents significant reduction in OD below the control value (0, NGM exposure alone). The horizontal line depicts the t=0 value (OD 0.78). Mean ± SEM.

3.4.2.2 Effect of ilomastat on proliferation by nodule-derived fibroblasts

The effect of serial dilutions of ilomastat and DMSO on proliferation of nodule-derived fibroblasts is illustrated in Figure 6. Following a 48hr exposure, ilomastat did not affect cell proliferation at concentrations of 1nM-100μM as OD values were not significantly different from exposure to NGM alone. Exposure to 1mM ilomastat led to a 45 ± 1% decrease ($p<0.001$) in absorbance compared to NGM alone over the 48 hour outcome period indicating a suppression of proliferation. However, the cellular absorbance in response to 1mM ilomastat (0.48 ± 0.02) was not significantly different to the t=0 value (0.45 ± 0.01) suggesting that no cell death occurred.

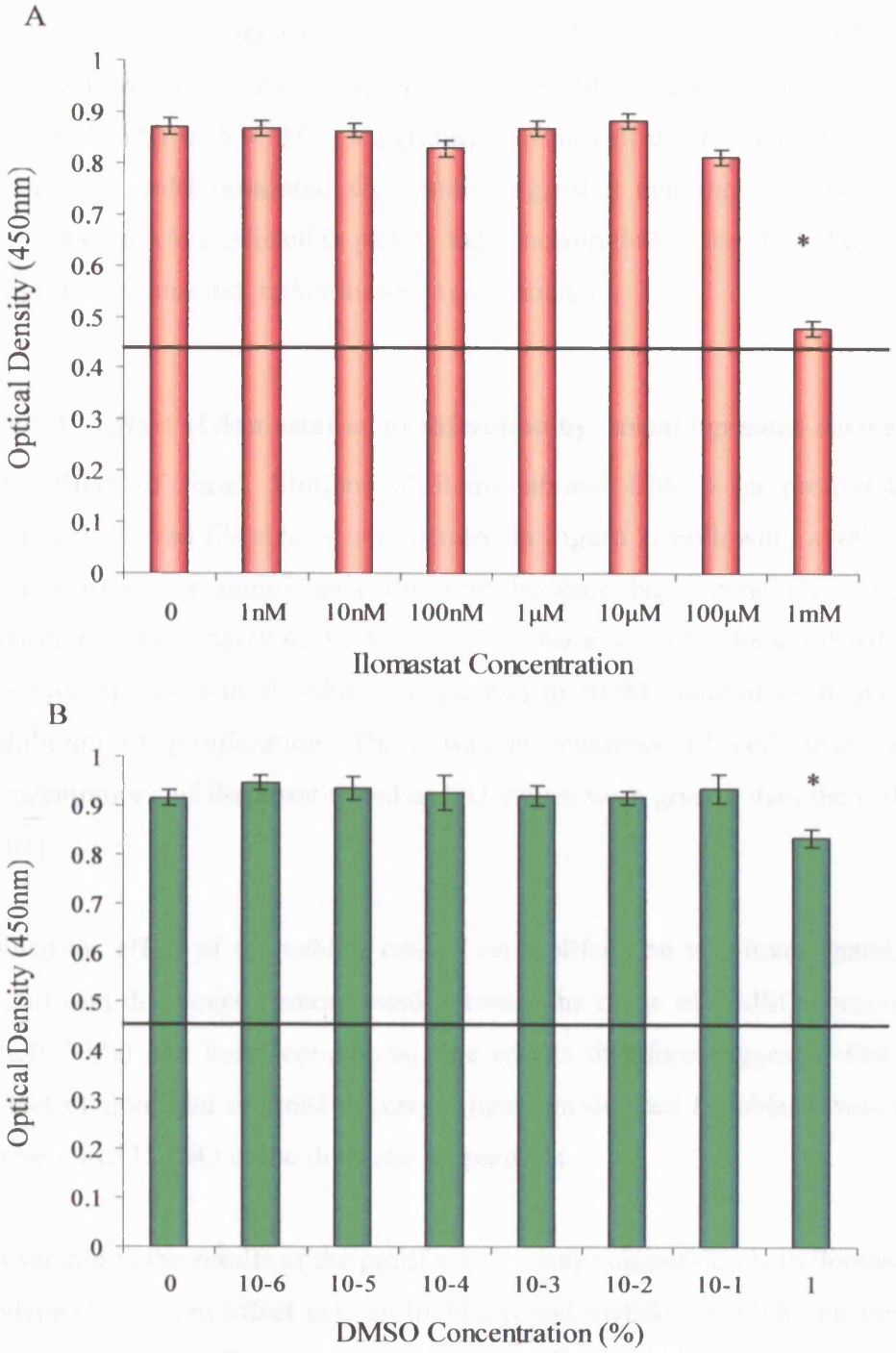

Figure 6. Effect of serial dilutions of ilomastat (panel A) and DMSO (panel B) on the proliferation of nodule-derived fibroblasts (n=6 replicates). *$p<0.001$ represents significant reduction in OD below the basal conditions (NGM exposure alone). The horizontal line represents the t=0 value (0.78) for each graph. Mean ± SEM.

DMSO concentrations of 0.1% and below did not significantly affect cell proliferation, whereas, exposure to 1% DMSO led to a reduced proliferative response (OD 0.83 ± 0.02) compared to exposure to NGM alone (OD 0.92 ± 0.02, $p<0.01$) over 48 hours. However, the OD values in response to 1% DMSO were not significantly different from t=0 value (OD 0.45 ± 0.01) suggesting that no cell death occurred. As 1% DMSO is present in 1mM ilomastat, the results suggested that the suppression of fibroblast proliferation was mediated in part by the concentration of the DMSO in both the vehicle control and ilomastat, rather than ilomastat toxicity.

3.4.2.3 Effect of ilomastat on proliferation by carpal ligament-derived fibroblasts

The effect of serial dilutions of ilomastat and DMSO on proliferation of carpal ligament-derived fibroblasts is illustrated in Figure 7. Following a 48hr exposure, OD values were not significantly different between basal conditions and ilomastat at concentrations 1nM-100μM. However, exposure to 1mM ilomastat led to a 11 ± 1% decrease ($p<0.01$) in absorbance compared to NGM alone at 48 hours suggesting an inhibition of proliferation. There was no evidence of cell death at any of the concentrations of ilomastat tested as OD values were greater than the t=0 value (0.79 ± 0.01).

When the effect of the vehicle control on proliferation was investigated, there was no significant difference demonstrated between the range of DMSO concentrations tested ($1x10^{-6}$-1%) and basal conditions. The results therefore suggested that the cytostatic effect of ilomastat at 1mM on carpal ligament-derived fibroblasts was not due to the presence of DMSO in the ilomastat preparation.

In summary, the results of the proliferation assay suggest that both ilomastat and DMSO independently can affect cell proliferation and viability at high concentrations (1mM ilomastat, 1% DMSO). Furthermore, the effect appears to be cell-type dependent. However, a uniform finding across all cell types was that at lower concentrations of DMSO (0.1% or below) and ilomastat (100μM or below), fibroblasts remained viable and functional.

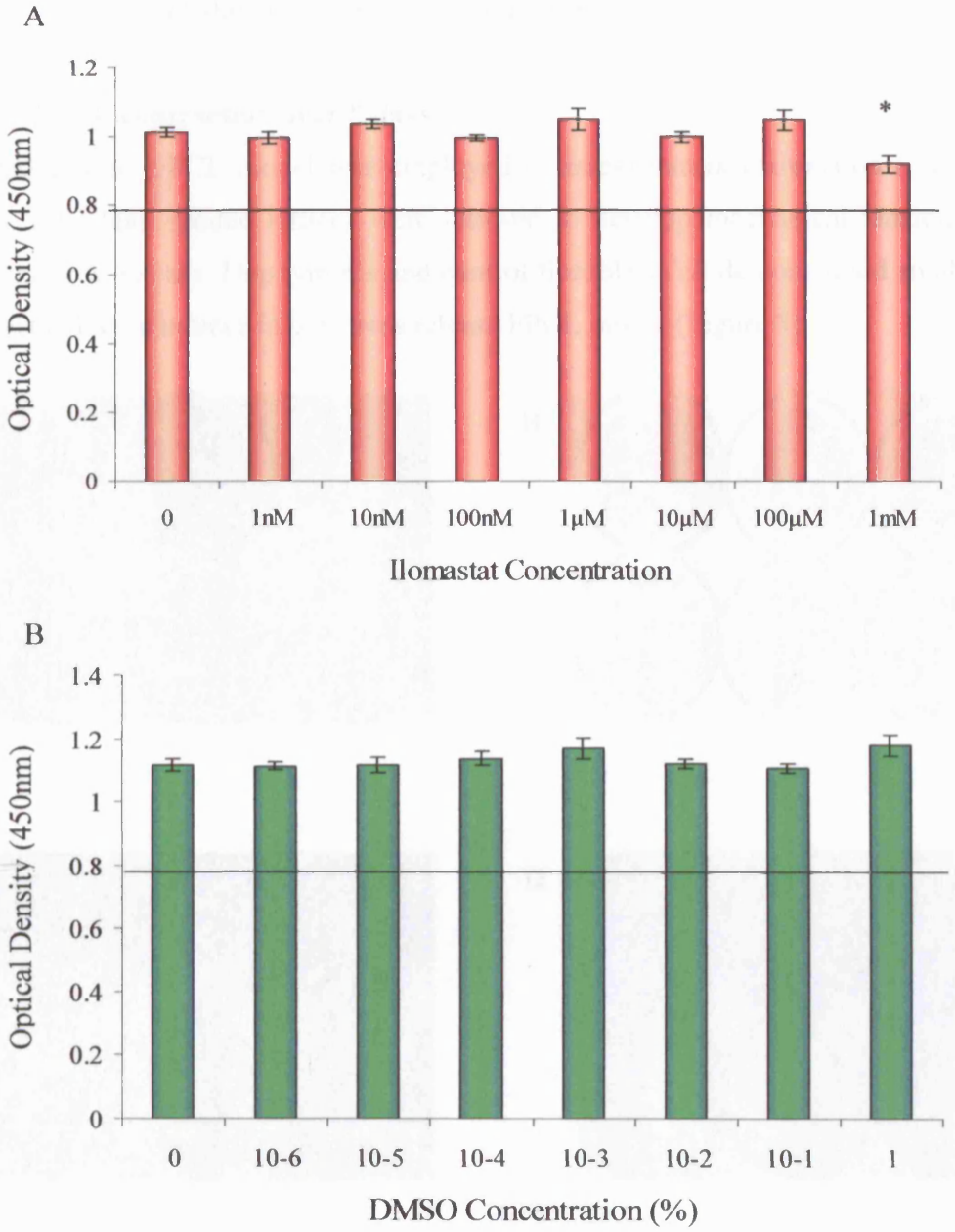

Figure 7. Effect of serial dilutions of ilomastat (panel A) and DMSO (panel B) on the proliferation of carpal ligament-derived fibroblasts (n=6 replicates). *p<0.001 represents significant reduction in OD below the basal conditions (NGM exposure alone). The horizontal line represents the t=0 value (0.79) for each graph. Mean ± SEM.

Having established that 100μM ilomastat was the upper limit at which fibroblasts remained viable and functional, optimal conditions for investigating fibroblast-mediated lattice contraction were determined. Initially, the effect of incubation time was

investigated by measuring lattice contraction under basal conditions over a 5-day time course, aiding establishment of an optimal time course.

3.4.3 FPCL contraction over 5 days

A stress-release FPCL model was employed to assess matrix contraction (see section 2.6.3). Fibroblast-seeded lattices were allowed to develop mechanical tension for 48 hours prior to release. Dupuytren's and control fibroblasts all demonstrated an ability to contract collagen lattices in the stress release FPCL model (Figure 8).

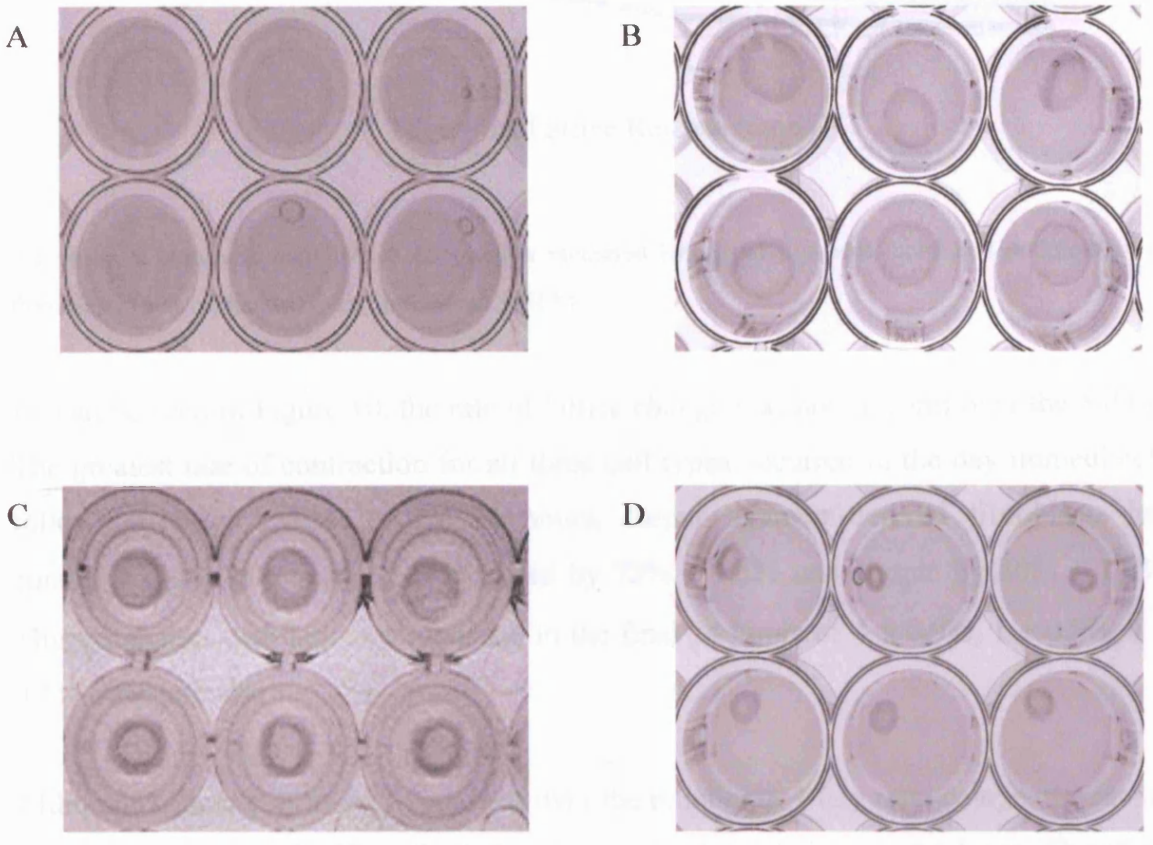

Figure 8. An illustration of lattice contraction by cord-derived fibroblasts. Panel A illustrates stressed lattices (pre-release). Panels B-D illustrate contracting lattices on day 1 (B), day 2 (C) and day 5 (D) following release of attached lattices from the well periphery.

The change in lattice area over time for all three cell types is illustrated in Figure 9. Over the 5-day time course, nodule-derived fibroblasts contracted lattice by 98 ± 0.3% of their original size, cord by 93 ± 0.5% and carpal ligament by 81 ± 0.9% .

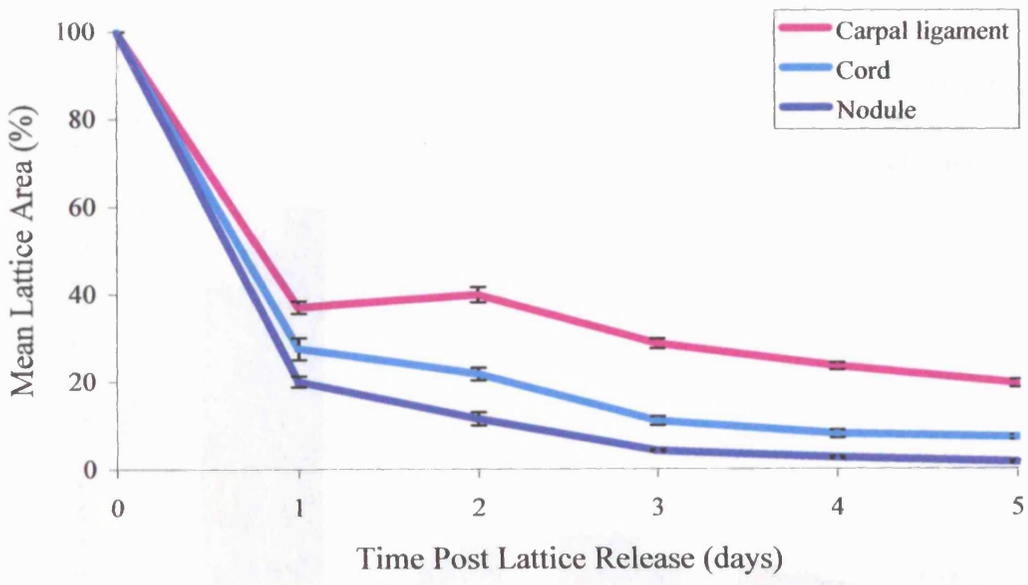

Figure 9. A comparison of lattice contraction mediated by carpal ligament, cord and nodule-derived fibroblasts (n=4 replicates) over time. Mean ± SEM.

As can be seen in Figure 10, the rate of lattice change was not uniform over the 5 days. The greatest rate of contraction for all three cell types occurred in the day immediately following lattice release. After 24 hours, carpal ligament-derived fibroblasts had contracted lattices by 63% ± 1.4%, cord by 72% ± 2.5% and nodule by 80% ± 1.2%. This compared with lattice contraction in the final 24 hours of 4 ± 0.9%, 1 ± 0.5%, 1 ± 0.3%, respectively.

Although lattices continued to contract over the remaining 4-day time course, the rate of contraction was not significantly different between 2 and 5 days post release. Therefore, the end point adopted for this assay was determined to be 48 hours post release as this initial period is the most sensitive to dynamic changes in lattice contraction. Furthermore, a 48 hour incubation time would enable sampling of MMP protein production over the dynamic contraction range and reduce the need for additional media changes and therefore susceptibility to infection.

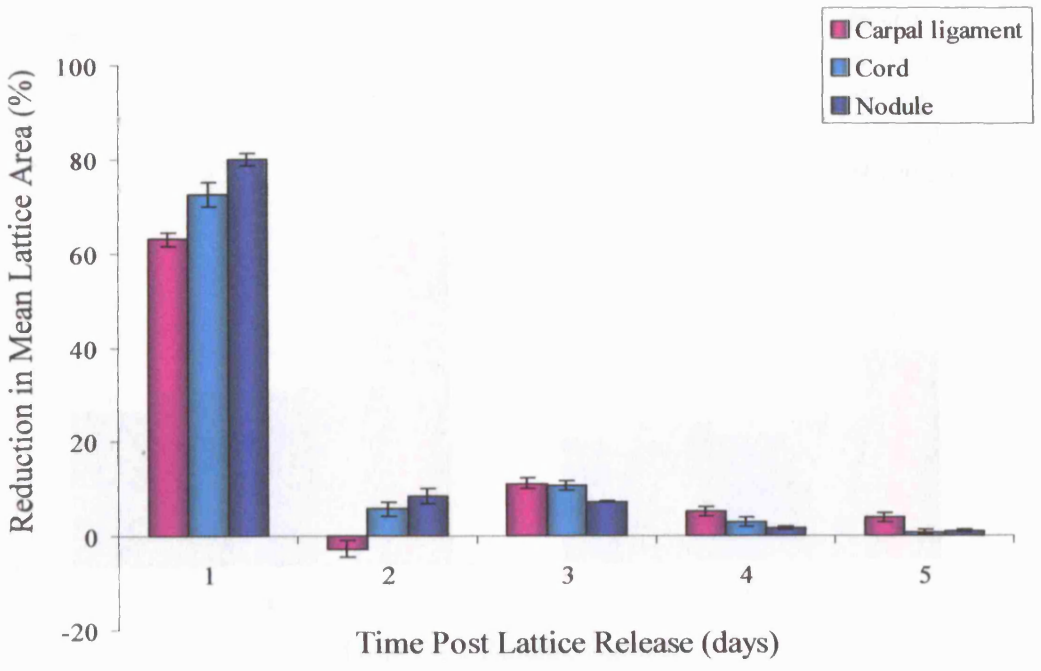

Figure 10. A comparison of change in lattice contraction over time mediated by carpal ligament, cord and nodule-derived fibroblasts (n=4 replicates). Mean ± SEM.

FPCLs were subsequently exposed to serial dilutions of ilomastat up to 100μM to determine the optimal concentration at which ilomastat was effective in the model of matrix contraction (section 2.6.4).

3.4.4 Effect of ilomastat dose on contraction by cord-derived fibroblasts

The results of FPCL contraction by cord-derived fibroblasts exposed to serial concentrations of ilomastat (0-100μM) are illustrated in Figure 11. Following release, lattice contraction by fibroblasts exposed to ilomastat (100nM-10μM) was not significantly different to exposure to NGM alone. However, at greater concentrations (100μM), ilomastat induced a 71 ± 3% suppression ($p<0.001$) of lattice contraction compared to basal conditions (NGM) at 48 hours. The results suggested therefore that there was no dose-response effect at the concentrations tested and that ilomastat was only efficacious at inhibiting lattice contraction at or around 100μM.

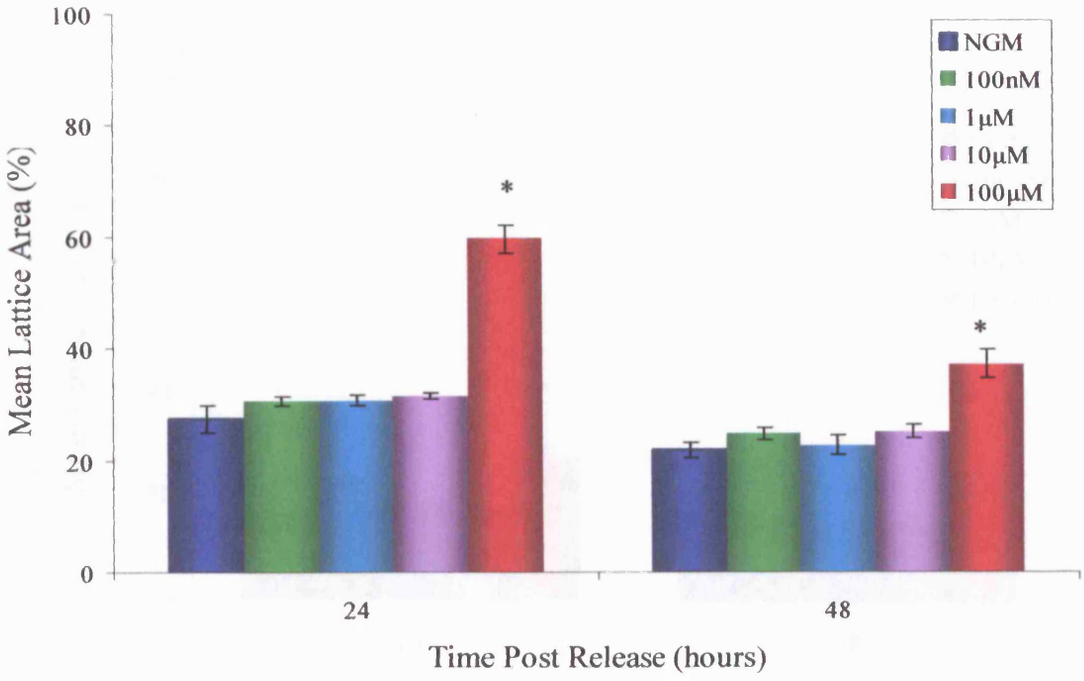

Figure 11. Effect of ilomastat (100nM to 100μM) on lattice contraction by cord-derived fibroblasts (n=4 replicates). *p<0.001 represents a significant difference between ilomastat and NGM treatment. Mean ± SEM.

3.4.5 Effect of ilomastat dose on contraction by nodule-derived fibroblasts

The results of FPCL contraction by nodule-derived fibroblasts exposed to serial concentrations of ilomastat (0-100μM) are illustrated in Figure 12. Following release, lattice contraction by fibroblasts exposed to ilomastat (100nM-10μM) was not significantly different to exposure to NGM alone. However, at greater concentrations (100μM), ilomastat induced a 116 ± 2% suppression ($p<0.001$) of lattice contraction compared to basal conditions (NGM) at 48 hours. As with cord-derived fibroblasts, the results suggested that the magnitude of response to ilomastat did not vary with the concentration of ilomastat tested and that ilomastat was only efficacious at inhibiting lattice contraction at 100μM.

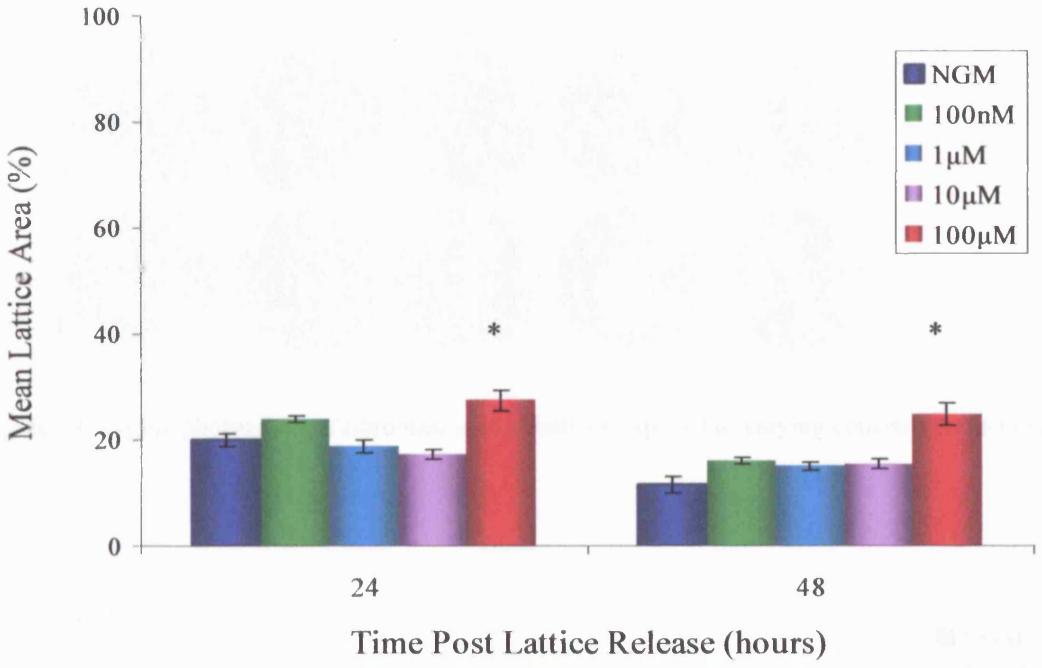

Figure 12. Effect of ilomastat (100nM to 100μM) on lattice contraction by nodule-derived fibroblasts (n=4 replicates). *p<0.001 represents a significant difference between ilomastat and NGM treatment. Mean ± SEM.

3.4.6 Effect of ilomastat dose on contraction by carpal ligament -derived fibroblasts

A graphic illustration of the effect of serial dilutions of ilomastat (0-100μM) on lattice contraction by carpal ligament-derived fibroblasts is demonstrated in Figure 13. In the photograph, lattices exposed to 100μM ilomastat are visibly larger than those exposed to NGM alone. This observation was supported by statistical data based on measurements of mean lattice area over time as illustrated in Figure 14.

Exposure to ilomastat at the highest concentration (100μM) resulted in a 27 ± 4% suppression ($p<0.001$) of lattice contraction compared to basal conditions (NGM) at 48 hours. At 10μM, ilomastat induced an apparent 24 ± 3% suppression of lattice contraction, although this proved not to be significant. In fact, lattice contraction by fibroblasts exposed to all lower doses of ilomastat (100nM-10μM) was not significantly different to exposure to NGM alone.

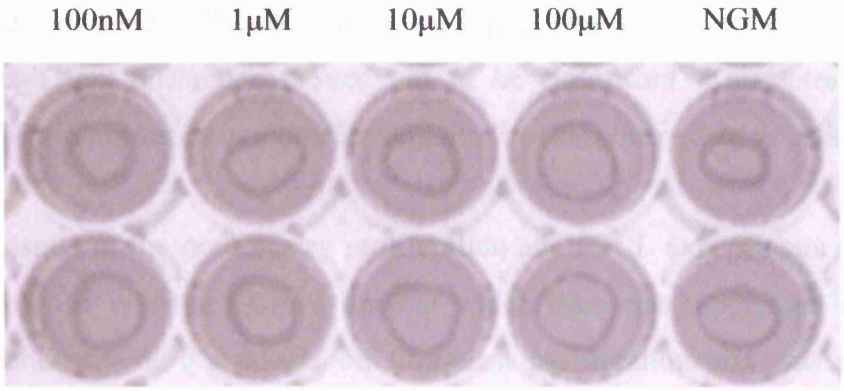

Figure 13. Digital photograph of fibroblast seeded lattices exposed to varying concentrations of ilomastat.

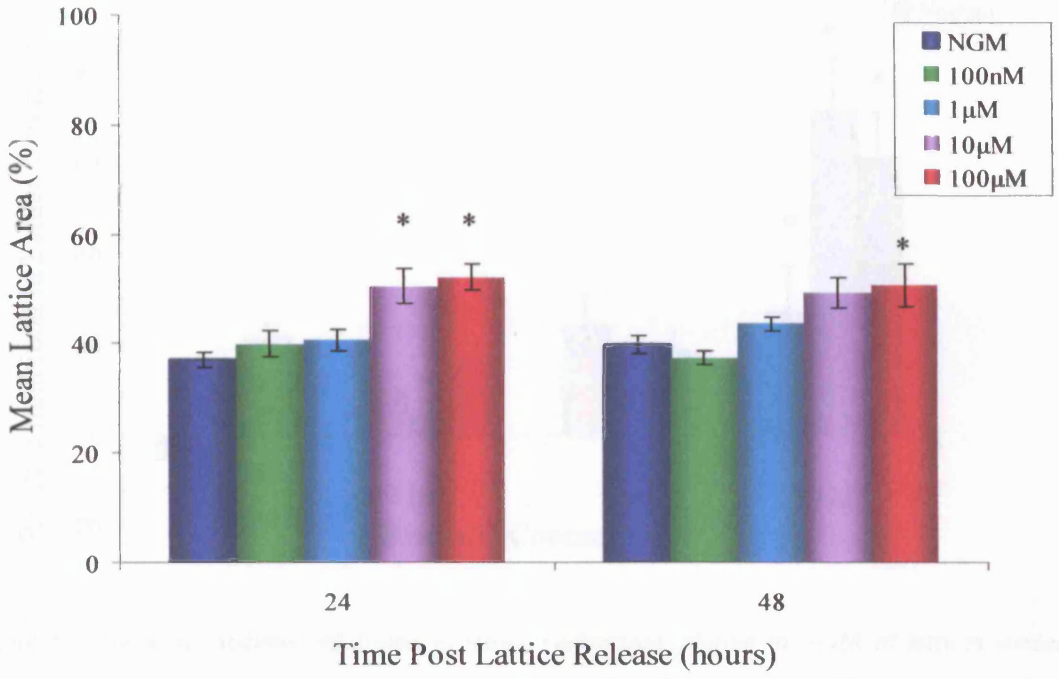

Figure 14. Effect of ilomastat (100nM to 100μM) on lattice contraction by carpal ligament-derived fibroblasts (n=4 replicates). *$p<0.001$ represents a significant difference between ilomastat and NGM treatment. Mean ± SEM.

The results of the relative inhibition achieved by different concentrations of ilomastat on FPCL contraction for all three cell types is illustrated in Figure 15. Relative inhibition was used to described the difference in mean lattice area of ilomastat-exposed lattices

relative to GFM exposure. For both Dupuytren's and control fibroblasts, 100μM ilomastat induced the greatest inhibition in matrix contraction, although for carpal ligament-derived cells, the effect at 10μM was almost as effective as at 100μM, although this difference proved not to be significant. Concentrations in excess of 100μM did not result in a greater magnitude of response (data not shown).

The results of the preliminary proliferation and FPCL experiments suggested therefore that 100μM was the optimal dose at which ilomastat suppressed matrix contraction, independently of it's effects on fibroblast proliferation and was adopted for use in subsequent experiments.

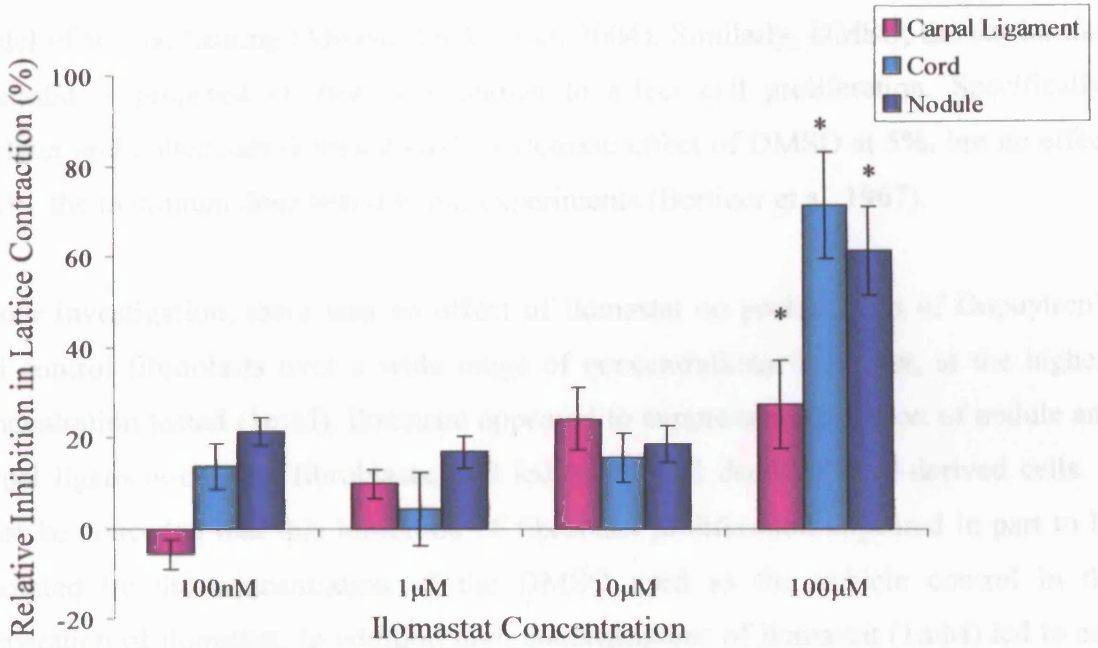

Figure 15. Ilomastat-mediated inhibition in lattice contraction relative to NGM of lattices seeded with carpal ligament, cord and nodule-derived fibroblasts (n=4 replicates). *$p<0.001$ represents a significant difference between ilomastat 100μM and NGM treatment at 48 hours. Mean ± SEM.

3.5 DISCUSSION

Fibroblast proliferation is a key issue when assessing matrix contraction as cell number can influence both the mechanism and extent of lattice contraction (Ehrlich et al. 2000). Synthetic MMP inhibitors have been reported to affect cell proliferation through a cytostatic (cells are growth-arrested but viable) rather than cytotoxic (cell death is induced) effect (Tonn et al. 1999; Coussens et al. 2002). Indeed, the anti-proliferative effect is part of their attraction as anti-cancer agents, although not their principal mode of action. Ilomastat has been shown to affect the pattern of cell proliferation in an experimental model of heart organogenesis (Linask et al. 2005), although, other investigators have found no effect of ilomastat on proliferation of ocular fibroblasts in an FPCL model (Daniels et al. 2003) or keratinocyte proliferation in an experimental model of wound healing (Mirastschijski et al. 2004). Similarly, DMSO, the carrier that ilomastat is prepared in, has been shown to affect cell proliferation. Specifically, Berliner and colleagues demonstrated a cytotoxic effect of DMSO at 5%, but no effect at 1%, the maximum dose tested in our experiments (Berliner et al. 1967).

In our investigation, there was no effect of ilomastat on proliferation of Dupuytren's and control fibroblasts over a wide range of concentrations. However, at the highest concentration tested (1mM), ilomastat appeared to suppress proliferation of nodule and carpal ligament-derived fibroblasts, and led to the cell death of cord-derived cells. It must be conceded that this inhibition of fibroblast proliferation appeared in part to be mediated by the concentration of the DMSO used as the vehicle control in the preparation of ilomastat. In addition high concentrations of ilomastat (1mM) led to cell death of cord derived-cells which appeared to be independent of the effects of the vehicle control. This latter finding was unexpected as cytotoxicity is not generally attributed to MMP inhibitors, although it may have been peculiar to the specific cord strain tested. The pattern of response to 1mM ilomastat could be clarified by increasing the number of samples investigated.

When matrix contraction was observed over a long time course (5 days), it was found that the greatest rate of contraction occurred in the first 24 hours. Investigations have previously found that cells in the stress-release model develop stress fibres and isometric tension during lattice attachment (Grinnell 2003). Once released, lattice

contraction therefore proceeds rapidly. However, over time, mechanical unloading leads to regression of the contractile phenotype slowing of the rate of contraction, which is also compounded by loss of stimulation from growth factors in the media over time. A 48 hour post-release time course was therefore selected for subsequent experiments to capture the most dynamic period of lattice contraction and reduce the chance of infection from multiple media changes.

Previous investigators have demonstrated a dose-response inhibitory effect of ilomastat on FPCL contraction over a similar range of concentrations (1nM-100μM) to our investigation (Daniels et al. 2003). However, we found that diseased and control palmar fascia fibroblasts were only sensitive to ilomastat at the highest concentration tested (100μM). Therefore, 100μM ilomastat was selected as the optimal dose for subsequent experiments as it induced the greatest inhibition of matrix contraction for all three cell types without compromising fibroblast viability or proliferation.

3.6 SUMMARY

- The accurate detection limits of the WST-1 assay were established to range from 2-12,000 fibroblasts/ well.

- The optimal dose of ilomastat at which fibroblasts remained viable and functional was determined to be 100μM by the WST-1 assay.

- Contraction of cord, nodule and carpal ligament fibroblast-seeded lattices was greatest in the first 24 hours following lattice release.

- No dose-response effect for ilomastat (100nM-100μM) was demonstrated.

- The non-toxic dose of ilomastat that achieved the greatest inhibition in lattice contraction was determined to be 100μM.

The next chapter was designed to establish the differences in the contractile abilities of Dupuytren's and control fibroblasts and to determine the effect of the MMP inhibitor, ilomastat, on lattice contraction.

CHAPTER 4

EFFECT OF ILOMASTAT ON MATRIX CONTRACTION IN THE FPCL MODEL

4.1 INTRODUCTION

Contraction is the key pathological component of Dupuytren's disease. MMP activity has been shown to play a critical role in collagen lattice contraction mediated by both ocular and dermal fibroblasts in vitro (Scott et al. 1998; Pins et al. 2000; Sheridan et al. 2001; Daniels et al. 2003). MMP expression has also been demonstrated in fibroblasts derived from normal and diseased palmar fascia (Beckett 2005). Furthermore, there is evidence that MMP expression is upregulated in Dupuytren's tissue (Qian et al. 2004) and that nodule-derived fibroblasts respond to changes in their mechanical environment by overexpressing MMP-1 and MMP-2 in comparison to control cells (Beckett 2005). We therefore determined the importance of MMP activity in matrix contraction by cells derived from both early (nodule) and end-stage (cord) Dupuytren's tissue. Furthermore, we evaluated the efficacy of the broad-spectrum MMP inhibitor, ilomastat, in abrogating this activity, and hence contraction. A stress-release FPCL model (see section 1.13) was selected to evaluate contraction as it provides a good approximation of the mechanical environment of native palmar fascia tissue, which is subjected to constant mechanical stress from digital extension and relaxation from flexion.

4.2 AIMS

The aims of this chapter were two-fold. Firstly, we set out to assess the effect of ilomastat on matrix contraction by Dupuytren's fibroblasts using a stress-release FPCL model of lattice contraction. Secondly, we aimed to determine which MMPs are secreted or expressed on the cell surface during contraction and how their protein levels and enzyme activity are affected by ilomastat.

4.3 METHODS

Once the parameters of the in vitro models were established using unpaired cell strains (chapter 3), all subsequent experiments were conducted using 5 paired cell strains (nodule and cord) with 5 carpal ligament cell strains acting as controls (n=4 replicates/ cell strain/ treatment). Stress-release FPCLs were prepared as previously described (section 2.4.5) and contraction in response to gelatinase-free media (GFM) was compared with exposure to ilomastat (100μM), control peptide (100μM) or vehicle control (0.1% DMSO). The activity and expression of several secreted and membrane-bound MMPs was assessed by western blotting, gelatin zymography and ELISA (section 2.6).

4.4 RESULTS

4.4.1 Maximum lattice contraction under basal conditions

A comparison of the maximum lattice contraction achieved by groups of Dupuytren's (cord and nodule) and control (carpal ligament) fibroblasts under basal conditions (GFM) is illustrated in Figure 1. After 48 hours, nodule-derived fibroblasts contracted lattices (66 ± 2%, mean reduction in lattice area) to a significantly greater extent than either cord (57 ± 2%) or carpal ligament (55 ± 1%). This represented an increase of 20 ± 1% contraction of nodule over carpal ligament ($p<0.001$) and 17 ± 2% over cord ($p<0.001$). There was no significant difference in the extent of contraction between cord and carpal ligament.

As demonstrated in Figure 2, contractile and remodelling activity was greatest in the initial 24 hours compared with the final 24 hours of incubation for both Dupuytren's and control fibroblasts. After 24 hours, carpal ligament-derived fibroblasts had contracted lattices to 94 ± 1% of their final size, cord to 96 ± 2% and nodule to 98 ± 2%. There were no significant differences in the proportion of contraction over the initial or final 24 hours between the three different cell types.

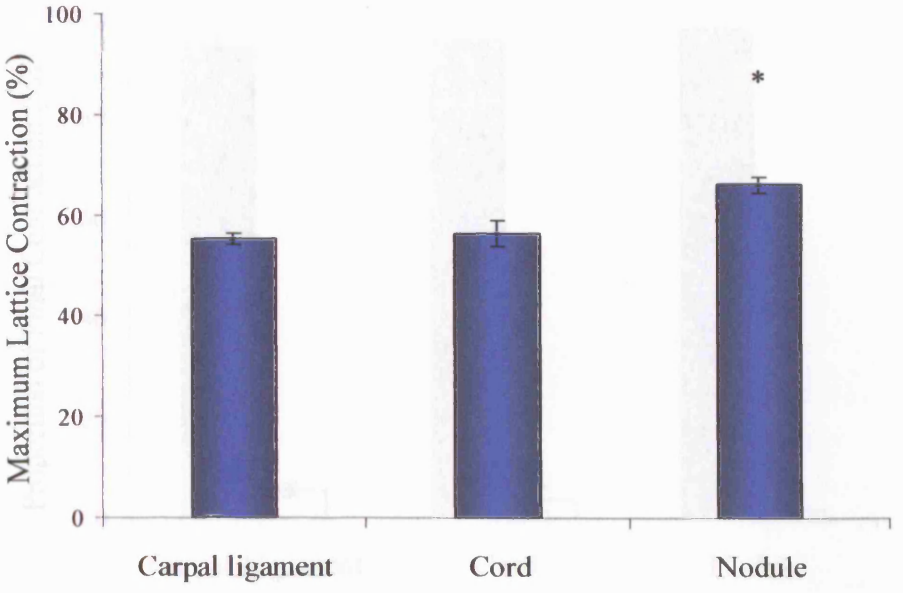

Figure 1. Comparison of contractile activity of multiple cell strains derived from carpal ligament (n=5), Dupuytren's cord (n=5) and nodule (n=5) in response to GFM. *p<0.001 represents a significant difference between nodule and cord or carpal ligament. Mean ± SEM.

Although the majority of contraction appeared to occur over the initial 24-hour incubation period, significant contraction continued over the remaining 24 hours, the magnitude of which depended on the individual cell strains assessed. These results are similar to the contraction profiles observed in the preliminary experiments conducted in chapter 3 (section 3.4.3).

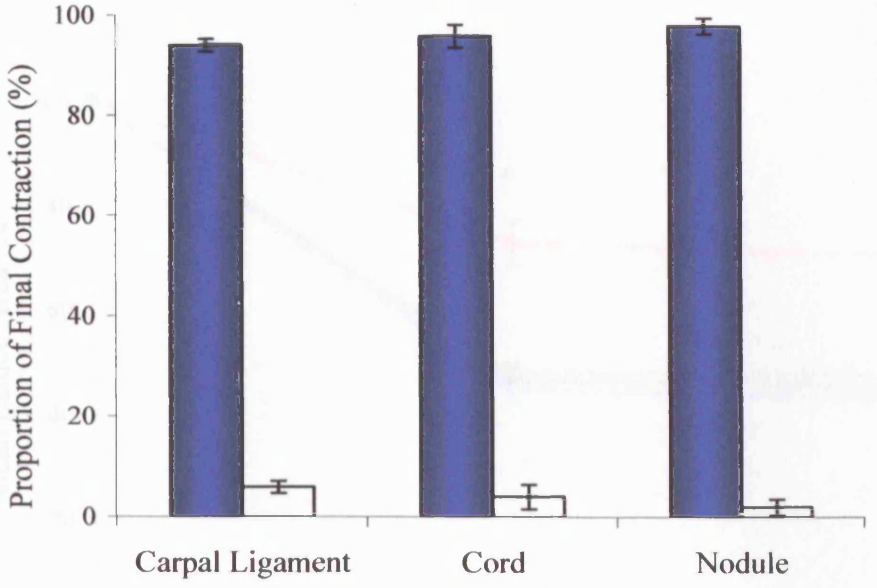

Figure 2. Comparison of contractile activity between fibroblasts (n=5) in the initial 24 hour (closed bars) period after lattice release and the final 24 hours (open bars). Mean ± SEM.

4.4.2 Effect of ilomastat on contraction by cord-derived fibroblasts

A graph illustrating the effect of ilomastat on FPCL contraction by cord-derived fibroblasts is illustrated in Figure 3. On release, fibroblasts contracted lattices to 43 ± 2% of their original size under basal conditions (GFM), 41 ± 2% (control peptide) and 46 ± 2% (vehicle control) after 48 hours. On exposure to ilomastat, lattice contraction by fibroblasts was significantly reduced (69 ± 4%, $p<0.001$) compared to all three control conditions. No significant differences were demonstrated between control groups.

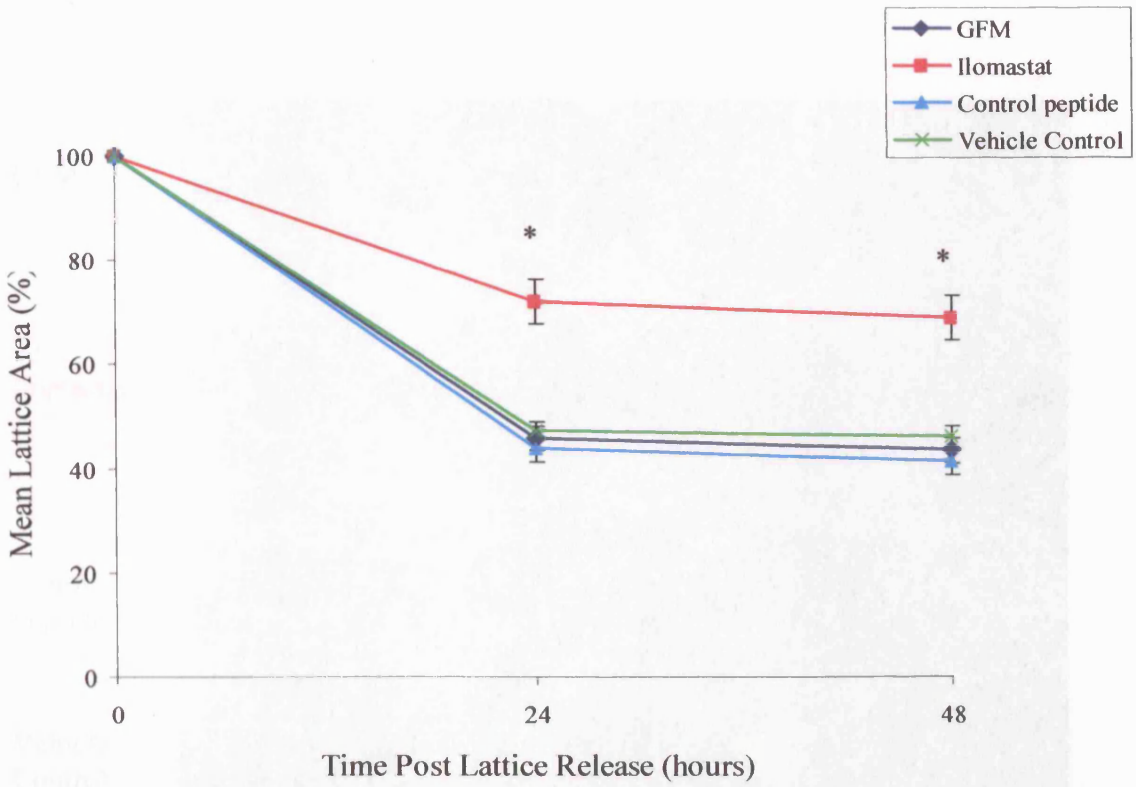

Figure 3. Graph illustrating change in mean area of lattices seeded with cord-derived fibroblasts (n=5) over time. *p<0.001 represents a significant difference between ilomastat exposure and all three control conditions (GFM, control peptide or vehicle control) at 48 hours. Mean ± SEM.

4.4.3 Effect of ilomastat on contraction by nodule-derived fibroblasts

A pictorial example of lattice contraction in response to GFM, ilomastat (100μM), control peptide (100μM), and vehicle control (DMSO 0.1%) is illustrated in Figure 4. Lattices were prepared in quadruplicate and mean lattice area was subsequently calculated as a percentage of the well base area using image analysis software (ImageTool 3.0).

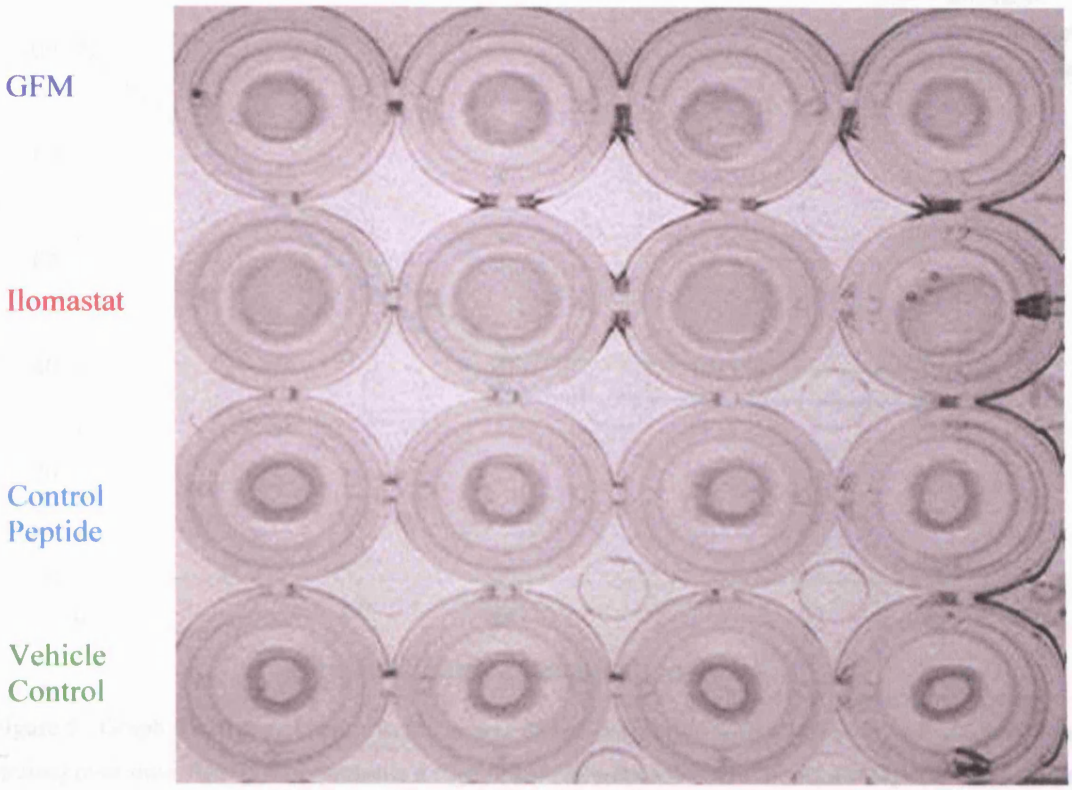

Figure 4. A digital photograph of lattices seeded with nodule-derived fibroblasts 48 hours after release. Rows of lattices were exposed to different test conditions as illustrated.

A graph illustrating the effect of ilomastat on FPCL contraction as estimated by lattice size in proportion to well base is illustrated in Figure 5. On release, nodule-derived fibroblasts contracted lattices to 34 ± 2% (mean ± SEM) of their original size after 48 hours under basal conditions (GFM), 33 ± 2% (control peptide) and 40 ± 2% (vehicle control). However, when exposed to ilomastat, lattice contraction by fibroblasts was inhibited (60 ± 3%). A pair-wise Turkey test revealed that the difference between treatment with ilomastat and the three control conditions was significant ($p<0.001$). However, there were no significant differences between control growth media, control peptide and vehicle control.

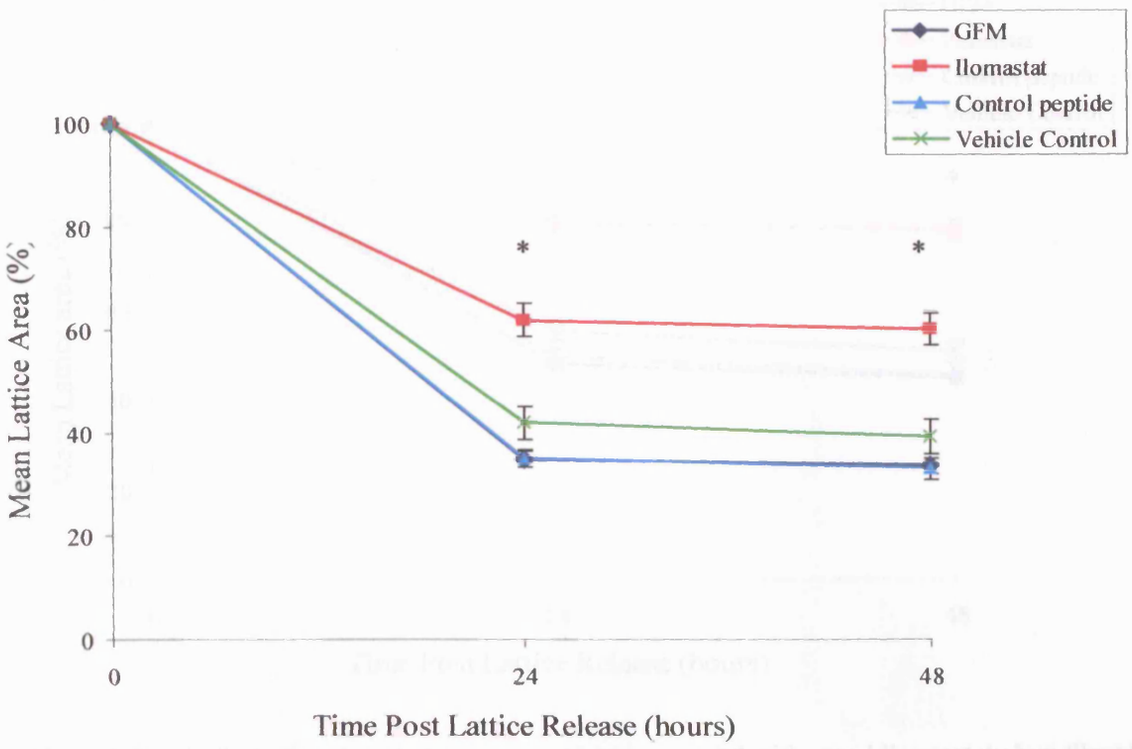

Figure 5. Graph illustrating change in mean area of lattices seeded with nodule-derived fibroblasts (n=5 cell strains) over time. *p<0.001 represents a significant difference between ilomastat exposure and all three control conditions (GFM, control peptide or vehicle control) at 48 hours. Mean ± SEM.

4.4.4 Effect of ilomastat on contraction by carpal ligament-derived fibroblasts

A graph illustrating the effect of ilomastat on FPCL contraction by carpal ligament-derived fibroblasts is illustrated in Figure 6. On release, fibroblasts contracted lattices to 45 ± 1% of their original size after 48 hours under basal conditions (GFM). A similar extent of contraction was observed between fibroblasts exposed to control peptide (45 ± 2%) and vehicle control (50 ± 3%). However, on exposure to ilomastat, fibroblast-mediated lattice contraction was significantly reduced (77 ± 2%, $p<0.05$) compared with the three control conditions.

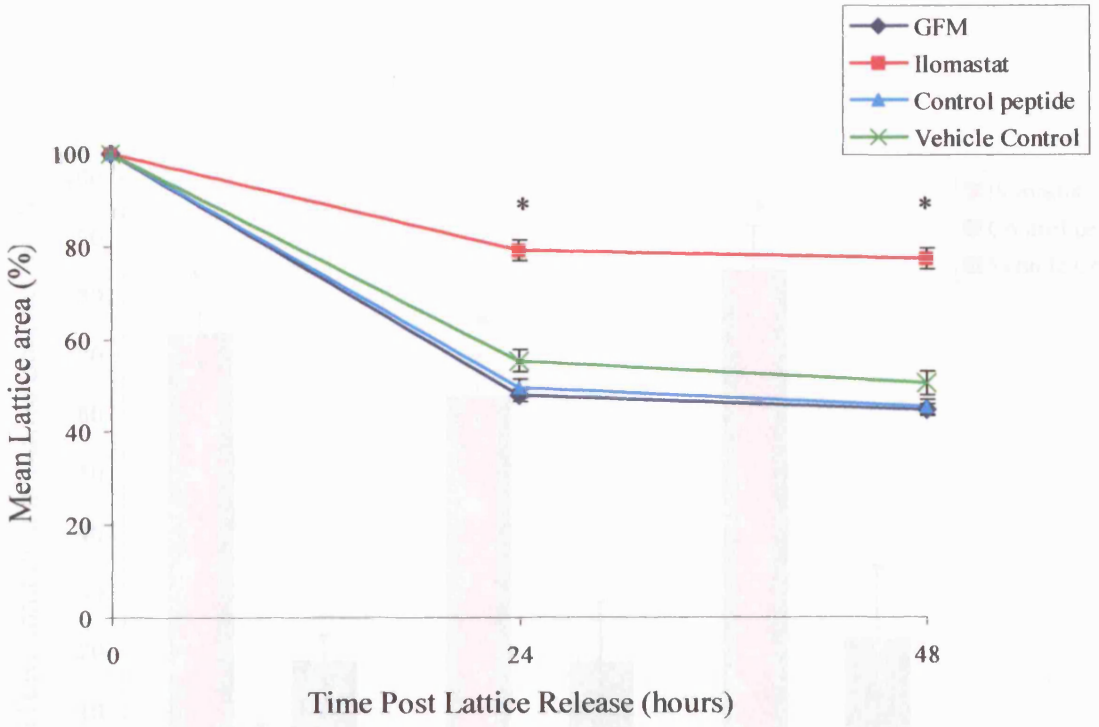

Figure 6. Graph illustrating change in mean area of lattices seeded with carpal ligament-derived fibroblasts (n=5) over time. *p<0.001 represents a significant difference between ilomastat exposure and all three control conditions (GFM, control peptide or vehicle control) at 48 hours. Mean ± SEM.

4.4.5 Differential effect of ilomastat on carpal ligament, cord and nodule

Exposure to ilomastat significantly inhibited lattice contraction after 48 hours by all cell strains assessed compared with exposure to control peptide or vehicle control. Figure 7 demonstrates the relative inhibition of lattice contraction, which was calculated as the difference in lattice contraction relative to basal conditions (GFM). This relative inhibition allowed comparisons in the effectiveness of ilomastat to be made between cord, nodule and carpal ligament.

The relative inhibition of lattice contraction mediated by ilomastat was greater for nodule (84 ± 8%) than cord-derived fibroblasts (58 ± 7%) or carpal ligament (73 ± 6%). However, a one-way ANOVA revealed that there were no significant differences in the extent of inhibition between the different cell types (p=0.097).

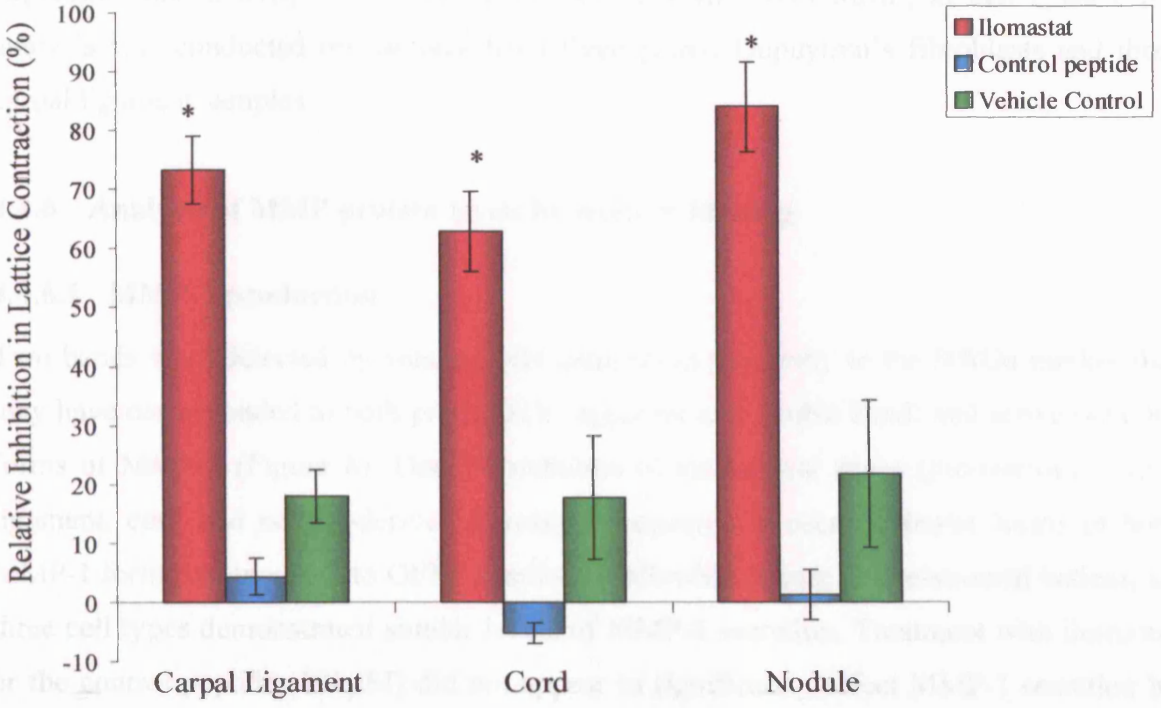

Figure 7. Comparison of inhibition of FPCL contraction relative to basal conditions (GFM). *p<0.05 represents a significant difference between ilomastat-mediated inhibition at 48 hours and control peptide or vehicle control. Mean ± SEM.

The relative inhibition in lattice contraction mediated by control peptide was determined to be 4 ± 3% for carpal ligament, -5 ± 2% for cord and, 1 ± 4% for nodule-derived fibroblasts. This compared to inhibition by the vehicle control of 18 ± 5%, 18 ± 11% and, 22 ± 11%, respectively. We had already demonstrated for each cell type that there were no significant differences in lattice contraction between exposure to GFM, control peptide or vehicle control. Although the relative inhibition by the vehicle control appeared to be greater than control peptide, the differences were not significant as determined by a one-way ANOVA confirming our previous findings.

After establishing the precise effect of ilomastat on matrix contraction mediated by Dupuytren's and control fibroblasts, we subsequently undertook analysis of media collected from stressed lattices (pre-release) as well as contracting lattices to determine the protein levels and pattern of activity of various secreted MMPs. Similarly, we investigated the expression and activity of the membrane-bound MMP, MT1-MMP, in cell lysates. All analysis was conducted on samples from three paired Dupuytren's fibroblasts and three carpal ligament samples.

4.4.6 Analysis of MMP protein levels by western blotting

4.4.6.1 MMP-1 production

Two bands were detected by western blot analysis in proximity to the 50kDa marker that may have corresponded to both pro (55kDa, apparent as a double band) and active (43kDa) forms of MMP-1 (Figure 8). Under conditions of mechanical stress (pre-release), carpal ligament, cord and nodule-derived fibroblasts appeared to secrete similar levels of both MMP-1 forms on exposure to GFM. Similarly, following release of pre-stressed lattices, all three cell types demonstrated similar levels of MMP-1 secretion. Treatment with ilomastat or the control peptide (100μM) did not appear to significantly affect MMP-1 secretion by fibroblasts seeded in either pre-stressed or contracting lattices.

These findings were confirmed objectively by scanning densitometry, which was performed on MMP-1 blots of samples collected from contracting lattices (Figure 9). The mean band densities of both pro and active MMP-1 forms, which correlate to MMP protein level, were calculated. Under basal conditions (GFM), carpal ligament-derived fibroblasts produced similar levels of pro and active MMP-1 (6.8 ± 2.8, 9.4 ± 2.5, respectively, mean band density) compared to cord (7.5 ± 2.5, 7.7 ± 1.6) and nodule (4.7 ± 1.5, 8.6 ± 2.1).

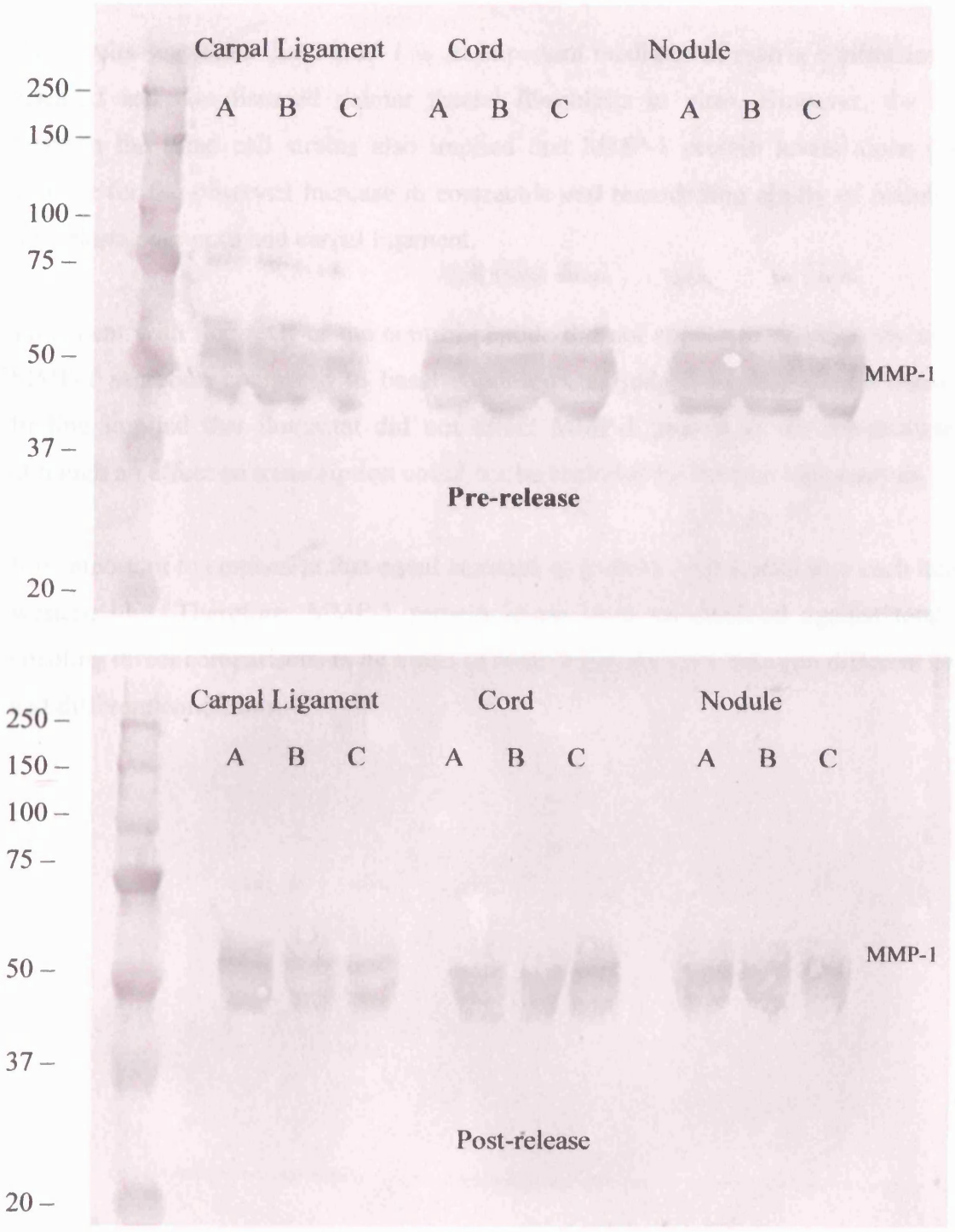

Figure 8. Sample of western blot analysis of MMP-1 production by carpal ligament, cord and nodule-derived fibroblasts seeded within stressed (pre-release) and contracting (post-release) lattices. Lattices were exposed to either GFM (A), ilomastat (B) or control peptide (C). The molecular weight (kDa) of kaleidoscope markers is listed adjacent to the marker bands in left hand column.

The results suggested that MMP-1 is an important mediator of matrix contraction by both diseased and non-diseased palmar fascial fibroblasts in vitro. However, the similarity between the three cell strains also implied that MMP-1 protein levels alone could not account for the observed increase in contractile and remodelling ability of nodule-derived fibroblasts over cord and carpal ligament.

Treatment with ilomastat or the control peptide did not appear to significantly affect pro-MMP-1 secretion compared to basal conditions, as judged by mean band density. This finding implied that ilomastat did not affect MMP-1 protein at the translational level, although an effect on transcription could not be excluded by western blot analysis.

It is important to emphasise that equal amounts of protein were loaded into each lane of the western blot. Therefore, MMP-1 protein levels were standardised against total protein enabling direct comparisons to be made of mean band densities between different cell types and different conditions.

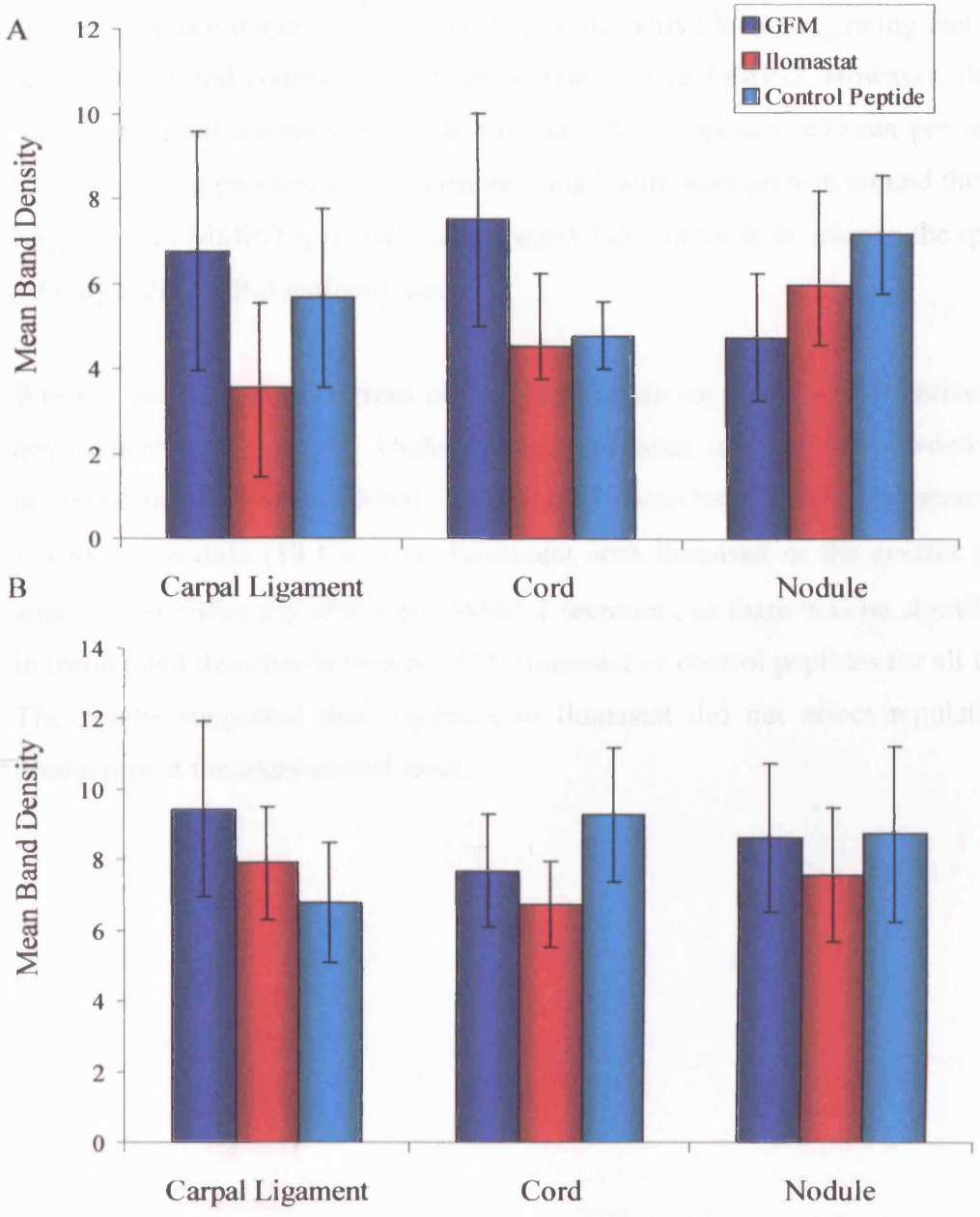

Figure 9. Quantification of MMP-1 protein production of fibroblasts (n=5) seeded in contracting lattices. Panel A demonstrates pro-MMP-1 and panel B active MMP-1 production as determined by mean band density of western blots for fibroblasts exposed to GFM, ilomastat or control peptide. Mean ± SEM.

4.4.6.2 MMP-2 production

A typical western blot analysis of MMP-2 is illustrated in Figure 10. The antibody used to detect MMP-2 is specific to both pro (72kDa) and active (66kDa) forms of the protein. We detected bands most likely corresponding to the active form suggesting that cells seeded in both stressed and contracting lattices secreted active MMP-2. However, the width of the bands suggested the presence of additional MMP-2 species between pro and active form that were being processed. Furthermore, faint bands were present around the 50kDa marker suggestive of MMP-1 (pro and active forms) that pointed to overlap in the specificity of the primary anti-MMP-2 antibody used.

Western blots of samples from contracting lattices were assessed objectively by scanning densitometry (Figure 11). Under basal conditions, carpal ligament-derived fibroblasts produced similar levels of MMP-2 (18.5 ± 2.7 mean band density) compared to cord (14.6 ± 4.6) and nodule (18.1 ± 3.4). Treatment with ilomastat or the control peptide did not appear to significantly affect pro-MMP-2 secretion, as there was no significant difference in mean band densities between GFM, ilomastat or control peptides for all three cell types. The results suggested that exposure to ilomastat did not affect regulation of MMP-2 production at the translational level.

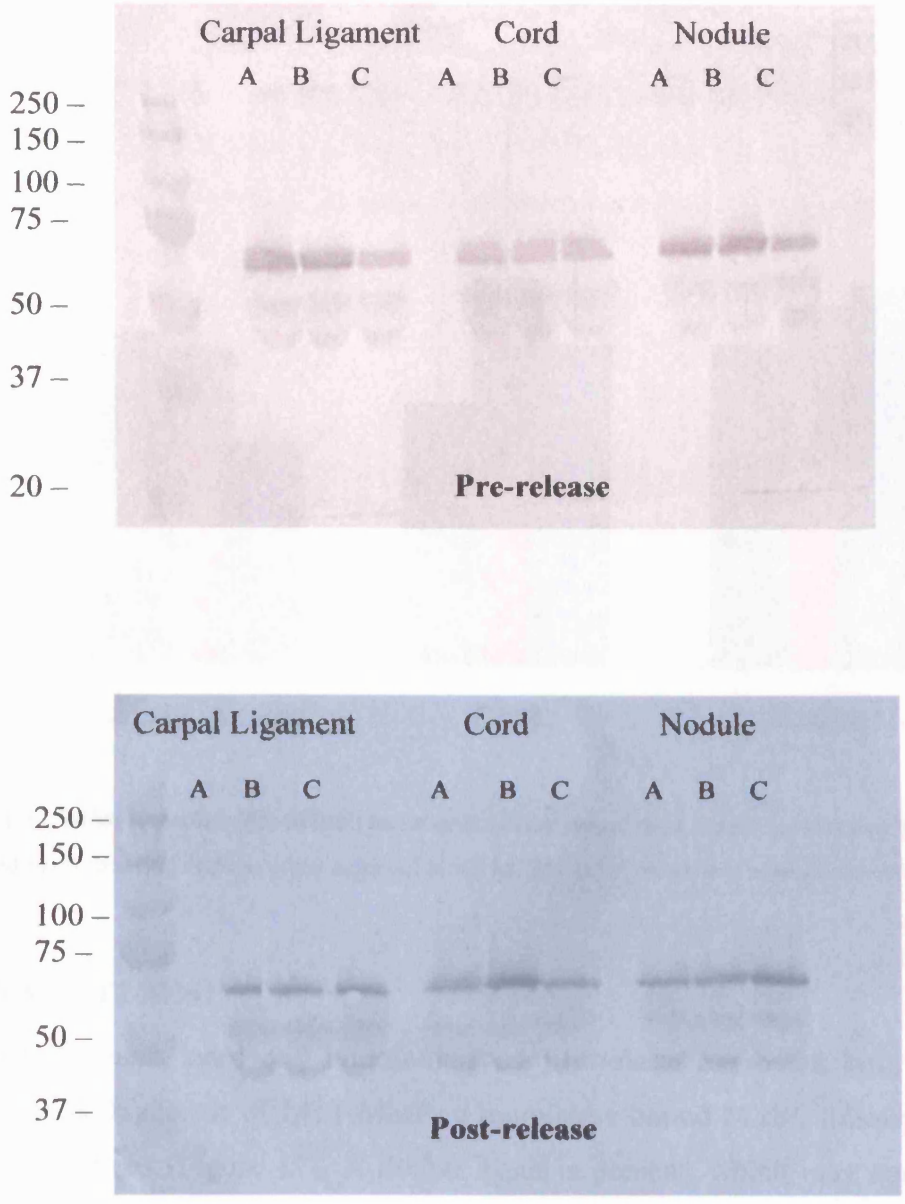

Figure 10. Sample of western blot analysis of MMP-2 production by carpal ligament, cord and nodule-derived fibroblasts seeded within stressed (pre-release) and contracting (post-release) lattices. Lattices were exposed to either GFM (A), ilomastat (B) or control peptide (C). The molecular weight (kDa) of kaleidoscope markers is listed adjacent to the marker bands in left hand column.

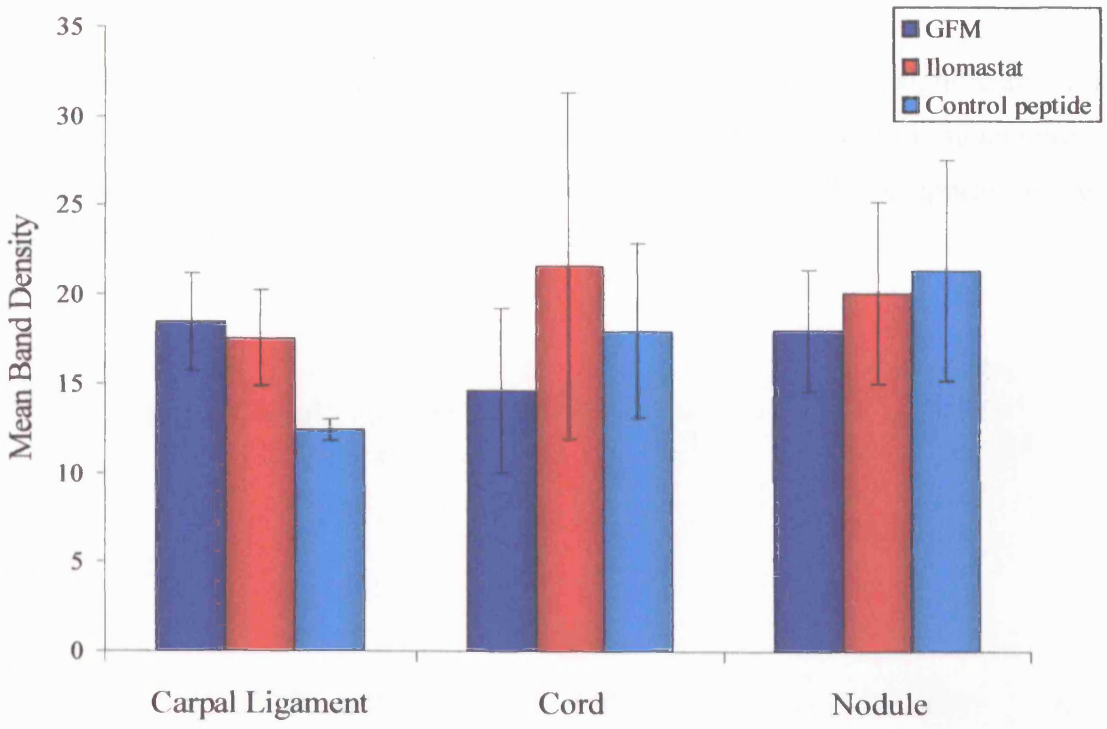

Figure 11. MMP-2 protein production as determined by mean band density of western blots. Fibroblasts (n=3) seeded in contracting lattices were exposed to GFM, ilomastat or control peptide. Mean ± SEM.

4.4.6.3 MT1-MMP

Carpal ligament, cord and nodule-derived fibroblasts expressed both pro (65kDa) and active (63kDa) forms of MT1-MMP, a membrane bound MMP, following release of pre-stressed lattices (Figure 12). A double band is present, which may correlate to both pro (65kDa) and active (63kDa) forms of MT1-MMP. Exposure to ilomastat resulted in the presence of more prominent bands for carpal ligament, cord and nodule-derived fibroblasts suggesting an upregulation of active MT1-MMP compared to basal conditions. This finding was confirmed by analysis of mean active MT1-MMP band densities (Figure 13).

Under basal conditions, mean band densities of active MT1-MMP expression were similar for carpal ligament (7.4 ± 0.8) and cord (5.8 ± 1.4). Although nodule-derived fibroblasts appeared to express far higher levels of active MT1-MMP (10.7 ± 1.4) compared with

either cord or carpal ligament, the difference was not statistically significant (p=0.063).

However, on exposure to ilomastat, mean band densities increased significantly for all three cell types (21 ± 2.2, 20.2 ± 4.2 and 30.7 ± 4.6, respectively), confirming an upregulation of MT1-MMP expression. Treatment with control peptide did not appear to significantly affect MT1-MMP expression.

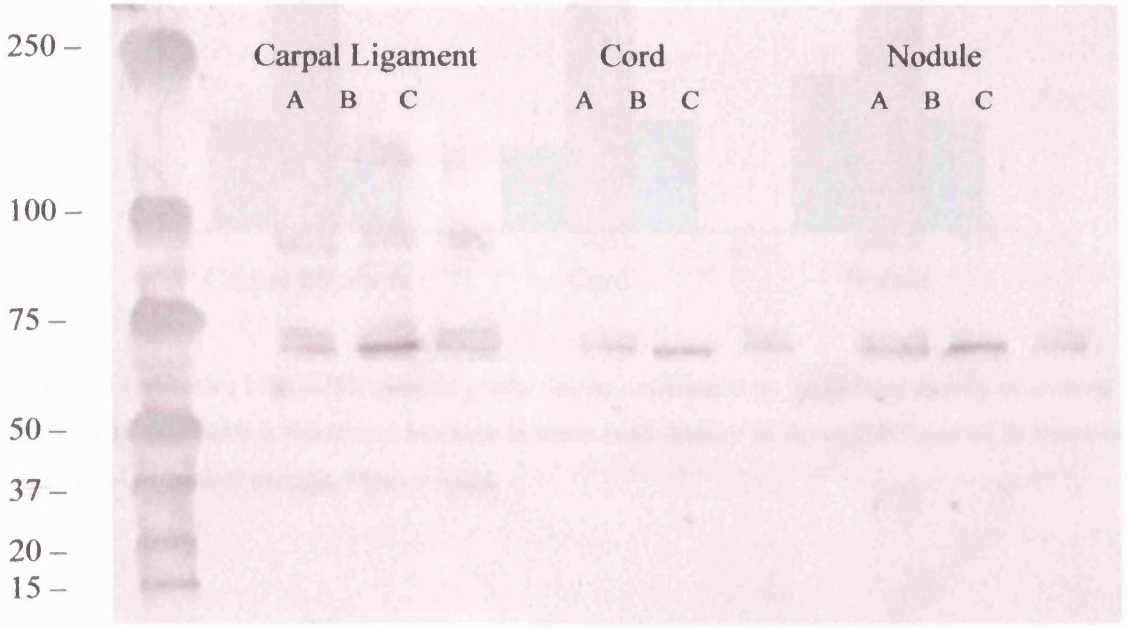

Figure 12. Western blot analysis of MT1-MMP production by carpal ligament, cord and nodule-derived fibroblasts. Lattices were exposed to either GFM (A), ilomastat (B) or control peptide (C). The molecular weight (kDa) of kaleidoscope markers is listed adjacent to the marker bands in left hand column.

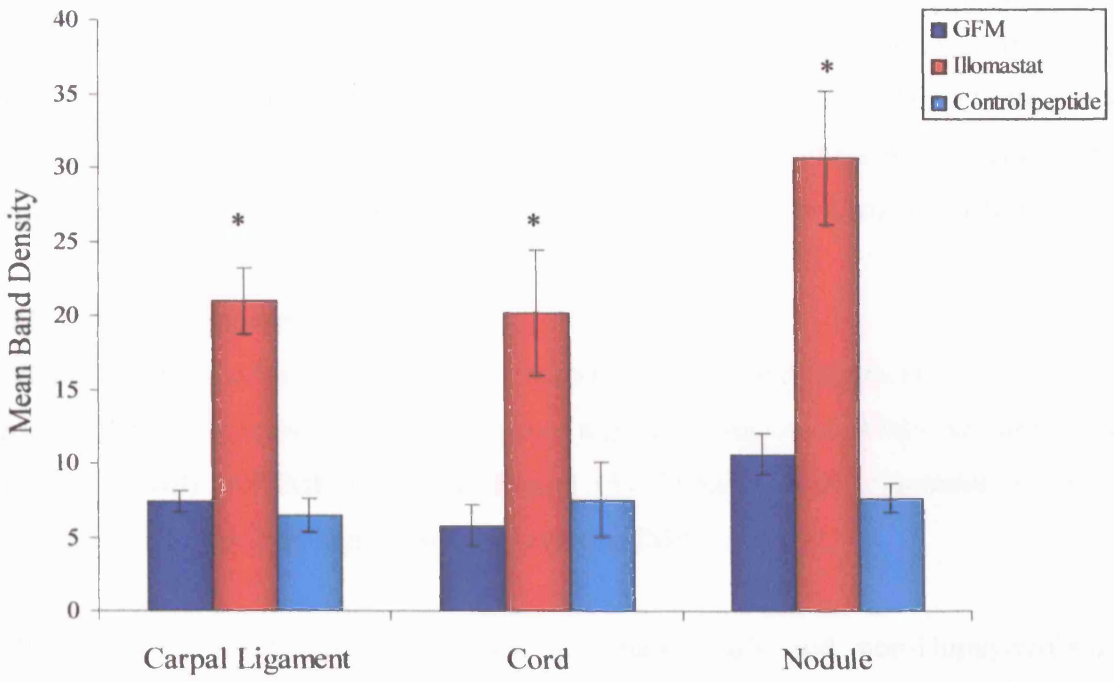

Figure 13. Active MT1-MMP protein production as determined by mean band density of western blots (n=3). *p<0.05 represents a significant increase in mean band density of fibroblasts exposed to ilomastat compared to GFM or control peptide. Mean ± SEM.

Western blot analysis is a method for determining the presence and comparative abundance of proteins, however, it does not yield information on enzyme activity levels associated with MMP expression. Furthermore, western blot analysis proved too insensitive to detect both pro and active forms of MMP-2. By contrast, zymography enables detection of actual gelatinase enzyme activity (MMP-2, MMP-9) through digestion of a gelatin substrate. Zymography was therefore selected to establish levels of MMP-2 enzyme activity.

4.4.7 Gelatin zymography

Under conditions of mechanical stress (pre-release), carpal ligament, cord and nodule-derived fibroblasts released similar levels of a gelatinolytic species into the media that was compatible with proMMP-2 (72kDa; Figure 14). Treatment with ilomastat or the control peptide did not appear to significantly affect proMMP-2 activity.

Following release of stressed lattices, all Dupuytren's and non-Dupuytren's-derived fibroblasts secreted both proMMP-2 and an additional gelatinolytic species compatible with active MMP-2 (66kDa). The presence of active MMP-2 in media collected from lattices post-release suggested that MMP-2 activation was concomitant with lattice contraction under basal conditions. However, bands corresponding to active MMP-2 were absent in lattices exposed to ilomastat for all three cell types, suggesting that ilomastat significantly suppressed MMP-2 enzyme activity. In addition, the results further highlighted the role of active MMP-2 in fibroblast remodelling and contractile behaviour, as lattices exposed to ilomastat produced no detectable active MMP-2 and contracted less than control conditions.

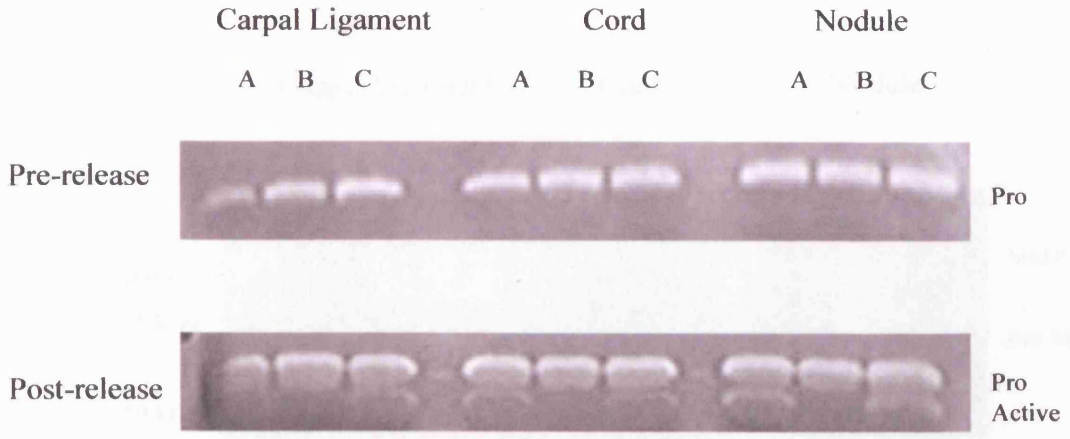

Figure 14. Analysis of gelatinolytic activity produced in conditioned media collected from stressed (pre-release) and contracting (post-release) collagen lattices. Carpal ligament, cord and nodule-derived fibroblasts were exposed to either GFM (A), ilomastat (B) or control peptide (C).

MMP-9, another important gelatinase, was also detected by zymography. However, not all cord, nodule and carpal ligament-derived cell strains appeared to secrete MMP-9 consistently under the same conditions. Furthermore, where present, gelatinolytic bands corresponding to MMP-9 (92kDa) were small indicating less active enzyme in comparison to MMP-2 (Figure 15). Therefore no precise pattern of MMP-9 activity relating to cell type or culture conditions could be identified. The results therefore implied that MMP-9 has a less significant role in contractile behaviour by palmar fascial fibroblasts than MMP-2, which was abundant in all cell lines tested.

Zymography specifically detects gelatinase activity (MMP-2, MMP-9), therefore further analysis by Activity ELISA was required to determine the activity levels of MMP-1 in conditioned media samples, and MT1-MMP in cell lysates derived from contracting lattices.

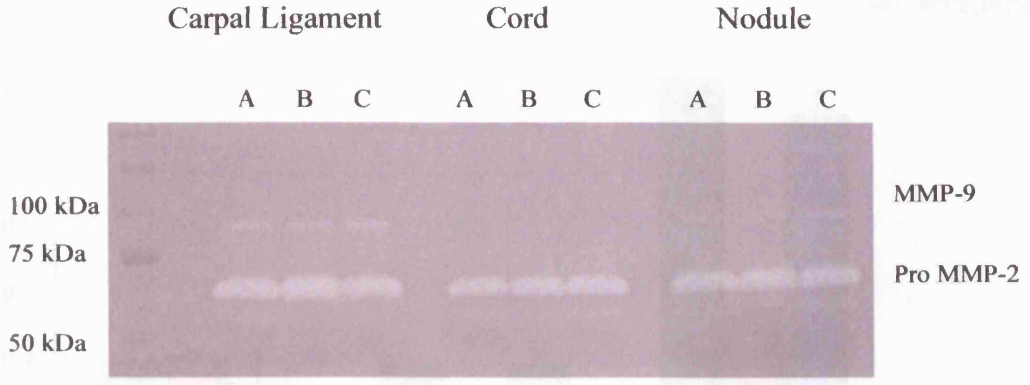

Figure 15. Analysis of gelatinolytic activity produced in conditioned media collected from contracting (post-release) collagen lattices. Carpal ligament, cord and nodule-derived fibroblasts were exposed to either GFM (A), ilomastat (B) or control peptide (C).

4.4.8 Enzyme-Linked Immunosorbent Assay (ELISA)

4.4.8.1 MMP-1 Activity

The results for MMP-1 activity in cell-conditioned media are illustrated in Figure 16. Enzyme activity (panel A) was standardised against sample protein concentration so that direct comparisons between different treatments and cell strains could be made.

Carpal ligament and cord-derived fibroblasts secreted similar levels of active MMP-1 (0.4 ± 0.06ng/mg and 0.39 ± 0.02ng/mg respectively) in post-release contracting lattices. By contrast, nodule-derived fibroblasts appeared to secrete levels of active MMP-1 in excess of double the levels secreted by all other cell strains (1.25 ± 0.18ng/mg; $p<0.05$) of active enzyme.

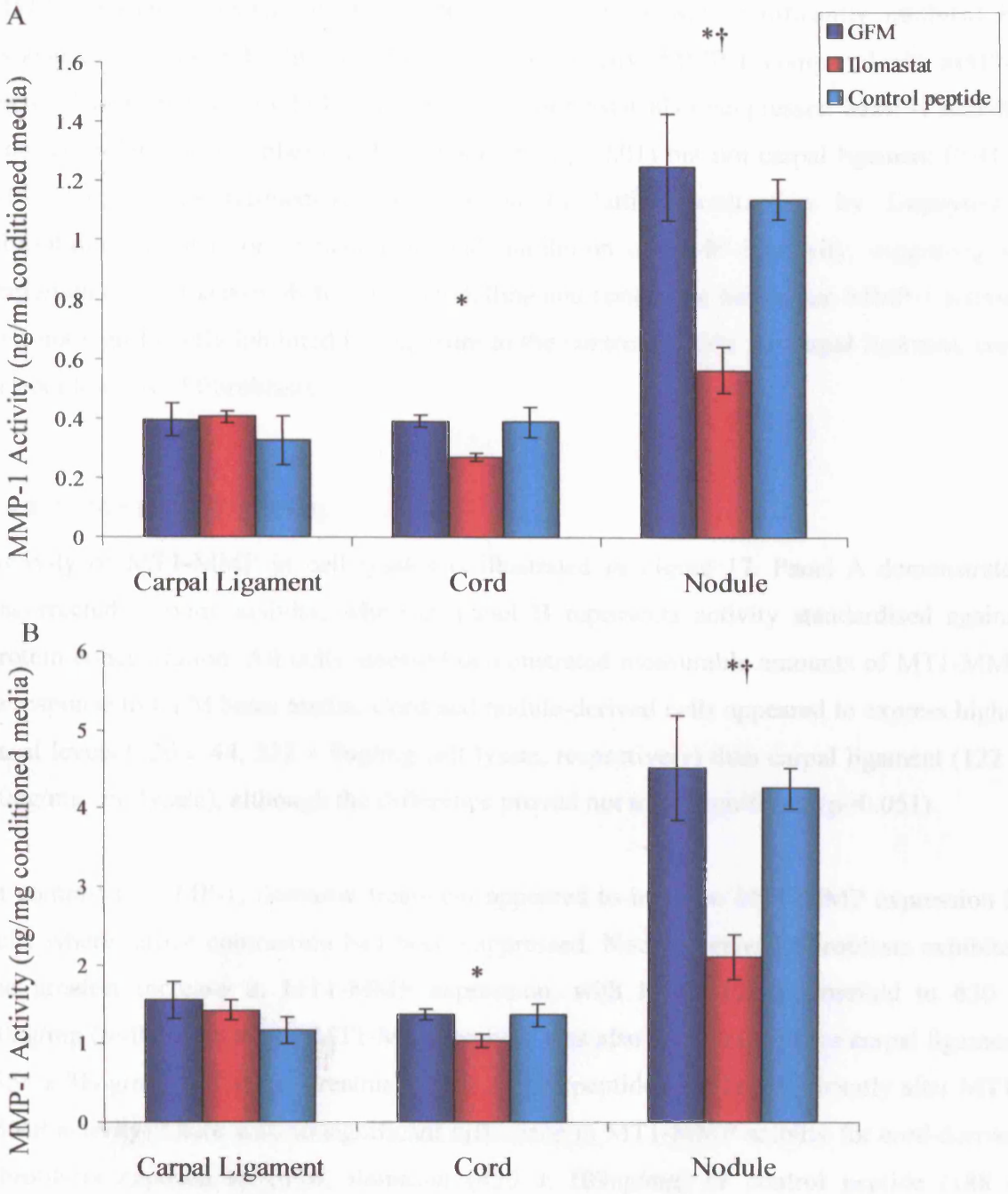

Figure 16. Quantification of MMP-1 activity (ng/ml conditioned media, panel A) and activity standardised against media protein content (ng/mg, panel B). Exposure to ilomastat resulted in a significant (*$p<0.05$) inhibition of MMP-1 activity to compared to GFM or control peptide. †$p<0.05$ represents a significant difference between nodule (n=3) and cord (n=3) or carpal ligament (n=3). Mean ± SEM.

MMP-1 activity secreted by nodule-derived fibroblasts was significantly inhibited by exposure to ilomastat, leading to a 55% reduction in active MMP-1, compared with MMP-1 secreted in response to GFM alone ($p<0.01$). Ilomastat also suppressed MMP-1 activity from cord-derived fibroblasts (0.27 ± 0.02ng/mg, $p<0.01$) but not carpal ligament (0.41 ± 0.02ng/mg). Ilomastat-mediated suppression of lattice contraction by Dupuytren's fibroblasts was therefore concomitant with inhibition of MMP-1 activity, suggesting an important role for active MMP-1 in remodelling and contractile behaviour. MMP-1 activity was not significantly inhibited by exposure to the control peptide for carpal ligament, cord or nodule-derived fibroblasts.

4.4.8.2 MT1-MMP Activity

Activity of MT1-MMP in cell lysates is illustrated in Figure 17. Panel A demonstrates uncorrected enzyme activity, whereas, panel B represents activity standardised against protein concentration. All cells assessed demonstrated measurable amounts of MT1-MMP in response to GFM basal media. Cord and nodule-derived cells appeared to express higher basal levels (220 ± 44, 212 ± 9ng/mg cell lysate, respectively) than carpal ligament (122 ± 10ng/mg cell lysate), although the difference proved not to be significant ($p=0.051$).

In contrast to MMP-1, ilomastat treatment appeared to increase MT1-MMP expression in cells where lattice contraction had been suppressed. Nodule-derived fibroblasts exhibited the greatest increase in MT1-MMP expression, with levels rising threefold to 630 ± 40ng/mg ($p<0.001$). Greater MT1-MMP activity was also demonstrated for carpal ligament (358 ± 38ng/mg, $p<0.001$). Treatment with control peptide did not significantly alter MT1-MMP activity. There was no significant difference in MT1-MMP activity for cord-derived fibroblasts exposed to GFM, ilomastat (430 ± 109ng/mg) or control peptide (188 ± 38ng/mg) as determined by a one-way ANOVA.

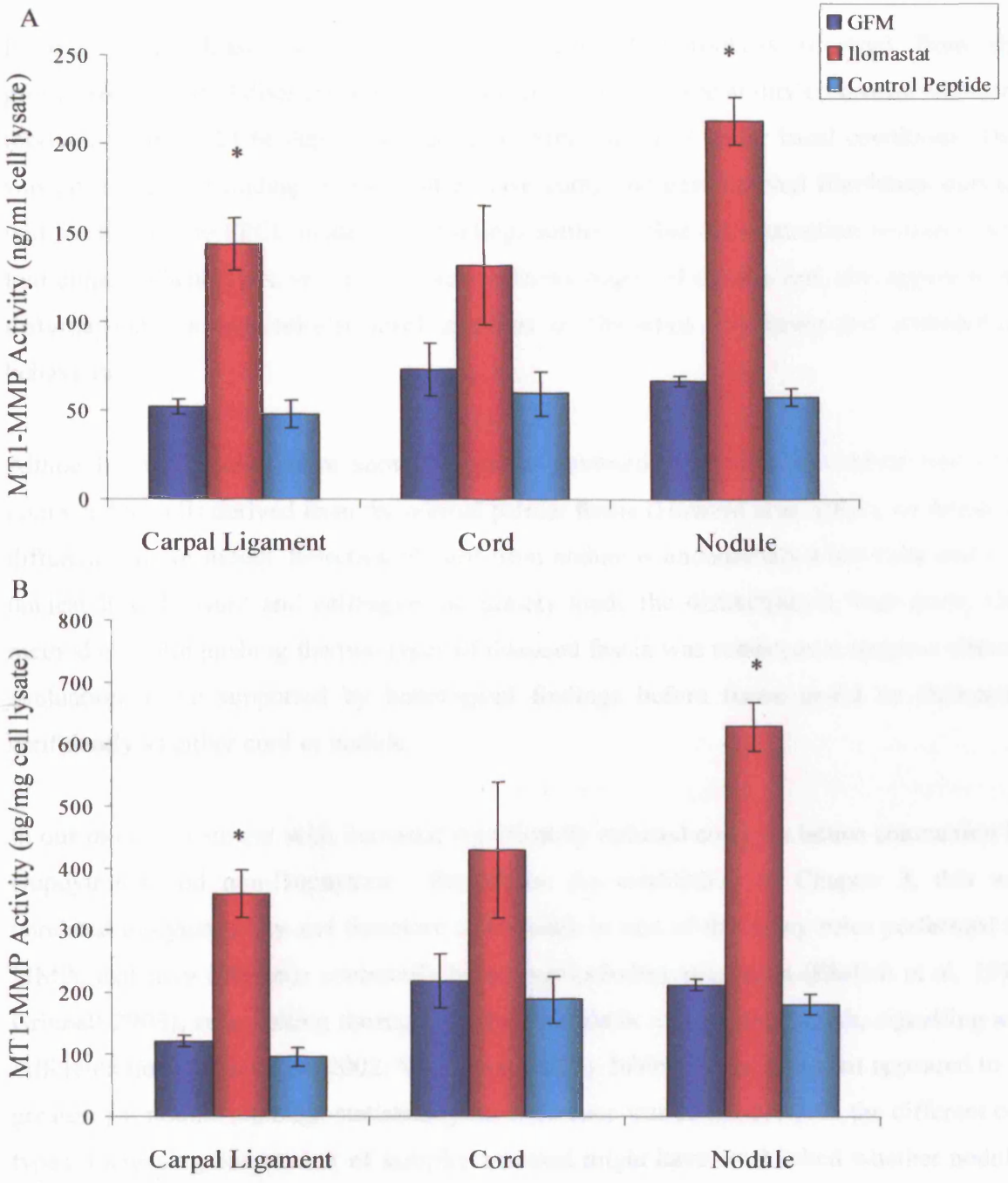

Figure 17. Quantification of MT1-MMP activity (ng/ml cell lysate, n=5, panel A) and activity standardised against lysate protein content (ng/mg cell lysate, n=3, panel B). Exposure to ilomastat resulted in a significant (*$p<0.05$) upregulation of MT1-MMP activity to compared to GFM or control peptide. Mean ± SEM.

4.5 DISCUSSION

In our stress-release FPCL model, nodule-derived fibroblasts (derived from the proliferative stage of disease) demonstrated a greater contractile ability compared with cord (derived from the ECM deposition stage) or carpal ligament under basal conditions. This was an interesting finding as few studies have compared cord-derived fibroblasts directly with nodule in the FPCL model. Our findings further define the distinction between these two clinical phenotypes, which represent different stages of disease and also appear to be distinguishable at the cellular level in terms of fibroblast contractile and remodelling behaviour.

Although some studies have shown a greater contractile capacity of cord-derived cells compared to cells derived from the normal palmar fascia (Howard et al. 2003), we found no difference in our model. Selection of cord from nodule is undoubtedly a key issue and it is unclear how Howard and colleagues accurately made the distinction in their study. Our method of distinguishing the two types of diseased fascia was robust, as it required clinical evaluation to be supported by histological findings before tissue could be delineated confidently as either cord or nodule.

In our model, treatment with ilomastat significantly reduced collagen lattice contraction by Dupuytren's and non-Dupuytren's fibroblasts. As established in Chapter 3, this was unrelated to cytotoxicity and therefore attributable to one of the many roles performed by MMPs that may influence contractile behaviour including migration (Ehrlich et al. 1990; Grinnell 2003), remodelling through removal of matrix molecules, growth, signalling and differentiation (Koike et al. 2002; Visse et al. 2003). Inhibition by ilomastat appeared to be greatest for nodule although statistically no difference was found between the different cell types. Increasing the number of samples assessed might have established whether nodule-derived fibroblasts were indeed more sensitive to inhibition by ilomastat was outside the scope of the present study.

Analysis of media samples collected during lattice contraction demonstrated involvement of several MMPs in this process. Fibroblasts seeded in contracting lattices (post-release) produced MMP-1, MMP-2 and MT1-MMP. The primary substrate of MMP-1 is collagen type 1 and similar to the findings of previous investigators, MMP-1 activity was detected in the media collected from contracting FPCLs (Scott et al. 1998; Derderian et al. 2005). In our study, MMP-1 activity was greatest for nodule-derived fibroblasts, which also contracted lattices to the greatest extent. Treatment with ilomastat inhibited enzymic activity of MMP-1 in Dupuytren's-derived fibroblasts (both nodule and cord) but not the levels of MMP-1 protein secreted. Surprisingly, ilomastat did not affect MMP-1 activity in control carpal ligament fibroblasts as a group, although some individual carpal ligament strains demonstrated a small but significant inhibition in response to ilomastat.

Activation of MMP-2 occurred concomitantly with lattice contraction and ilomastat inhibited MMP-2 at the level of enzyme-substrate interaction in all fibroblasts. MMP-9, which has been shown to be involved in contraction (Defawe et al. 2005), was not consistently detected in our study suggesting that MMP-2 is the dominant gelatinase mediating lattice contraction by palmar fascial fibroblasts. Our results imply utilisation of both MMP-1 and MMP-2 in processing and remodelling of the collagen lattice by Dupuytren's fibroblasts during contraction. Furthermore, regulation of MMPs at the level of activation appears to be a crucial step in determining fibroblast contractile behaviour.

MT1-MMP, a membrane-bound MMP known to mediate activation of proMMP-2 (Deryugina et al. 2001; Visse et al. 2003) was expressed in contracting lattices. Most of the MT1-MMP appeared to be expressed in the active form. Exposure of Dupuytren's fibroblasts to ilomastat resulted in an upregulation of MT1-MMP protein expression and enzymic activity. This may have been the result of a local feedback mechanism – fibroblasts responding to reduced MMP-2 activity by upregulating MT1-MMP expression to increase proMMP-2 activation. These results reinforce the dynamic nature of cell-matrix interactions: even after MMP secretion has occurred, fibroblasts retain the ability to influence their activity in response to matrix signals through membrane-bound enzymes such as MT1-MMP.

4.6 SUMMARY

- Nodule-derived fibroblasts contracted lattices to a significantly greater extent than either cord or carpal ligament.

- Inhibition of MMP activity by ilomastat resulted in a significant suppression of lattice contraction by Dupuytren's and control fibroblasts.

- All cell types secreted similar levels of MMP-1 and MMP-2 under basal conditions.

- Ilomastat suppressed activation of MMP-1 and MMP-2.

- Ilomastat exposure induced an increase in expression and activity of MT1-MMP.

In the next chapter, we investigated fibroblast-mediated contraction using the culture force model to enable precise quantification of force generation by fibroblasts and to establish whether ilomastat had a differential effect on the two components of contraction, namely fibroblast contraction and matrix remodelling. Furthermore, a more in depth analysis of MMP regulation was performed involving assessment of gene expression, protein levels and enzyme activity of both MMPs and their endogenous inhibitors, the TIMPs.

CHAPTER 5

GENERATION OF CONTRACTILE FORCE, MATRIX REMODELLING MMP GENE EXPRESSION AND ACTIVITY: MODULATION BY ILOMASTAT

5.1 INTRODUCTION

It has been postulated that permanent tissue contracture is the result of two distinct processes working in parallel, namely cell-mediated matrix contraction and matrix remodelling (Flint et al. 1990; Tomasek et al. 2002). Although the stress-release FPCL model provides information on overall collagen contraction, it does not allow delineation of the cellular and remodelling components. The culture force monitor was developed to provide actual kinetic information on force generation by fibroblasts embedded in a collagen matrix (Eastwood et al. 1994). However, more recently, modifications to the model have also enabled quantification of the remodelling component, therefore, providing further insight into the mechanics of tissue contracture (Marenzana et al. 2006). The precise role of MMP activity in the two processes of cell-mediated contraction and matrix remodelling has yet to be determined. MMP activity can be regulated at several different levels, therefore, understanding key links in the regulatory chain is an essential pre-requisite to successful development of drugs for therapeutic intervention.

5.2 AIMS

Initially, we set out to determine the effect of ilomastat on force generation by Dupuytren's fibroblasts in the CFM model. We also intended to differentiate the influence of MMP activity on cellular contraction and matrix remodelling. Finally, we aimed to establish how the pattern of MMP and TIMP expression and activity was affected by ilomastat during the process of force generation.

5.3 METHODS

All experiments were conducted using 5 paired Dupuytren's cell strains (nodule and cord) with 5 carpal ligament cell strains acting as controls. Collagen lattices were prepared in the CFM model as previously described (section 2.5) and force generation in response to

gelatinase-free media (GFM) was compared with exposure to ilomastat (100μM) or control peptide (100μM). Addition of Cytochalasin-D (60μM final concentration) allowed differentiation of the cellular and remodelling components. The activity and expression of several secreted and membrane-bound MMPs was assessed by RT-PCR, western blotting and ELISA (sections 2.6-2.7).

5.4 RESULTS

Initially, the model was prepared using acellular collagen lattices to determine whether any force was generated in the system in the absence of fibroblasts. Similarly, cytochalasin-D was added after 48 hours to demonstrate that it did not affect the collagen lattice structure.

5.4.1 Force generation in acellular lattices

A typical contraction profile of an acellular collagen lattice is demonstrated in Figure 1. As can be seen, a small amount of force generation (7 dynes) was observed despite the absence of fibroblasts. This inherent mechanical tension has been demonstrated previously and may have occurred as a result of a humidity imbalance in the system brought about by evaporative losses in the media or lattice (Beckett 2005).

On addition of cytochalasin-D at 48 hours, an initial reduction in measured force was demonstrated. However, this was short-lived and may have been due to the sensitivity of the force transducer to the addition of fluid to the system. The force quickly recovered to it's prior level implying that any effect of cytochalasin-D subsequently observed was the result of a specific effect on cellular processes and not due to an alteration of collagen matrix structure or stiffness.

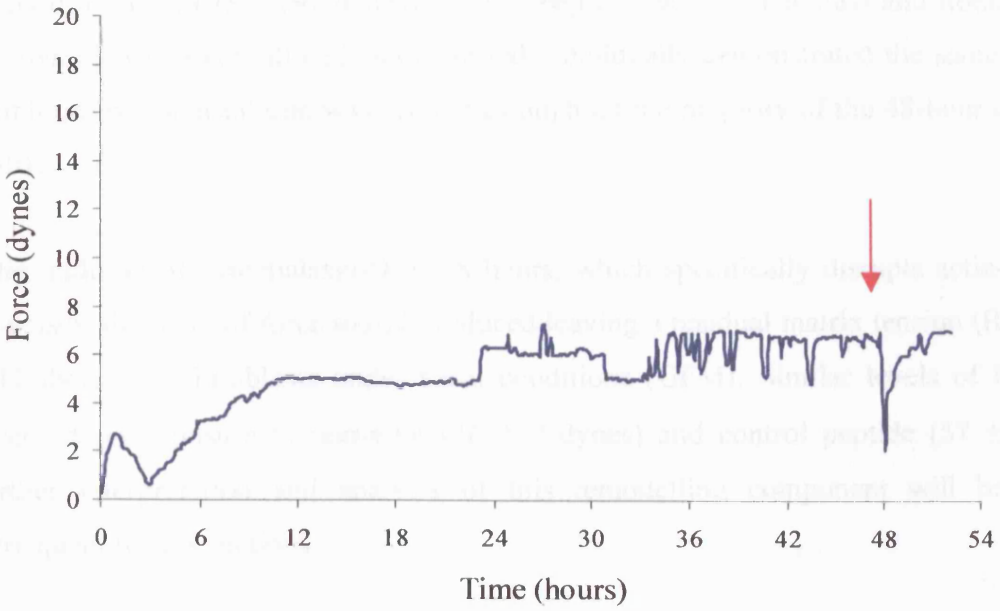

Figure 1. Contraction profile of an acellular collagen lattice. Cytochalasin-D was added to the system after 48 hours (red arrow).

5.4.2 Effect of ilomastat on contraction and remodelling by cord-derived fibroblasts

A graph illustrating the effect of ilomastat on force generation by cord-derived fibroblasts is illustrated in Figure 2. Although, force readings were plotted at 15-minute intervals, the SEM was only displayed at 6-hour intervals to avoid data clutter. Over the first 48 hours, cord-derived fibroblasts exposed to GFM appeared to generate much greater forces than fibroblasts exposed to ilomastat. However, the difference only reached statistical significance at 42 and 48 hours. After 48 hours, fibroblasts developed a significantly greater force both under basal conditions (143 ± 18 dynes, mean ± SEM) and in response to control peptide (141 ± 23 dynes) compared with ilomastat (71 ± 10 dynes, p=0.023). This difference represented a 100% reduction in force generation by fibroblasts exposed to ilomastat.

Although there appears to be a distinct pattern of inhibition by ilomastat, the fact that statistical significance occurred at just two time intervals underlies the considerable inter-

patient variability encountered in contractile responses of cord-derived fibroblasts. This is highlighted by the wide ranges of force generation observed at 48 hours for fibroblasts exposed to GFM (97 – 197 dynes), control peptide (90 – 221 dynes) and ilomastat (47 – 100 dynes). However, all cell strains tested individually demonstrated the same pattern of inhibition by ilomastat that was present throughout the majority of the 48-hour contraction profile.

After addition of cytochalasin-D at 48 hours, which specifically disrupts actin-dependent processes, the level of force sharply reduced leaving a residual matrix tension (RMT) of 44 ± 11 dynes for fibroblasts under basal conditions (GFM). Similar levels of RMT were observed on exposure to ilomastat (26 ± 7 dynes) and control peptide (57 ± 9 dynes). Further interpretation and analysis of this remodelling component will be made in subsequent results sections.

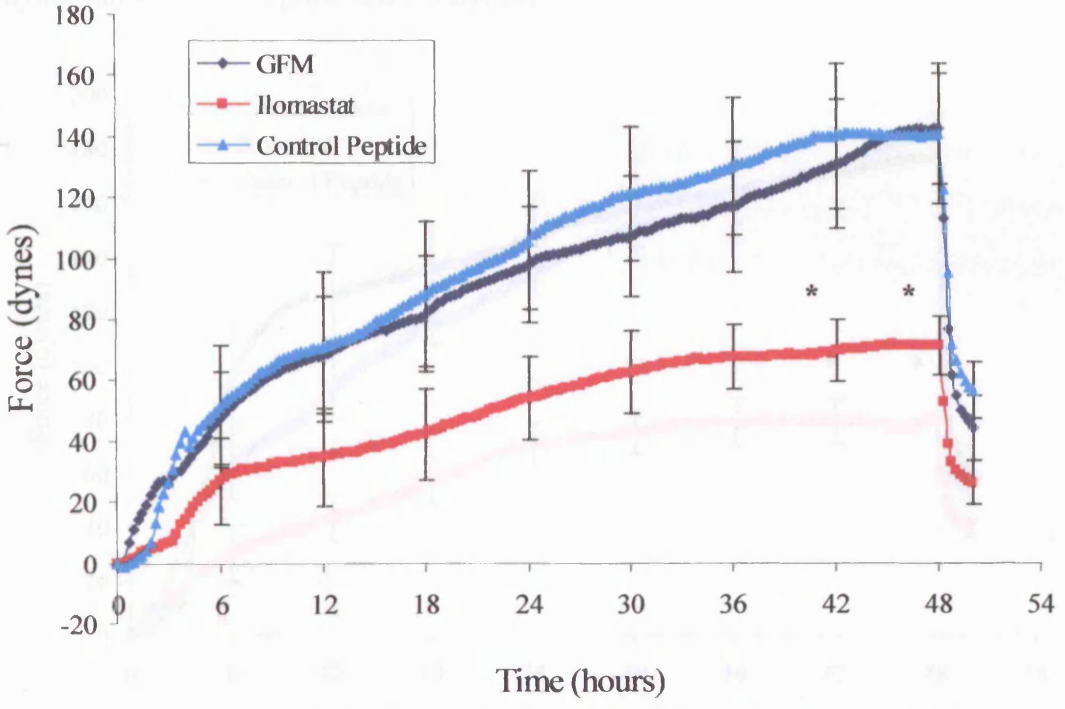

Figure 2. Force generation by cord-derived fibroblasts (n=5) over time. Cytochalasin-D was added to the system after 48 hours. *$p<0.05$ represents a significant difference between ilomastat exposure and control conditions (GFM or control peptide). Mean ± SEM.

5.4.3 Effect of ilomastat on contraction and remodelling by nodule-derived fibroblasts

A graph illustrating the effect of ilomastat on force generation by nodule-derived fibroblasts is illustrated in Figure 3. After 48 hours, nodule-derived fibroblasts generated forces of 176 ± 15 dynes under basal conditions (GFM). However, exposure to ilomastat significantly reduced their ability to generate contractile force (80 ± 8 dynes, $p<0.001$). In fact, a significant difference was first observed at 12 hours ($p=0.03$) and maintained until addition of cytochalasin-D at 48 hours. Exposure to control peptide did not significantly affect maximum force generation (178 ± 17 dynes) compared to basal conditions.

After addition of cytochalasin-D, the level of force maintained by fibroblasts sharply reduced leaving a residual matrix tension (RMT) of 60 ± 11 dynes under basal conditions (GFM). Similar levels of RMT were observed for fibroblasts exposed to ilomastat (40 ± 4 dynes) and control peptide (56 ± 5 dynes).

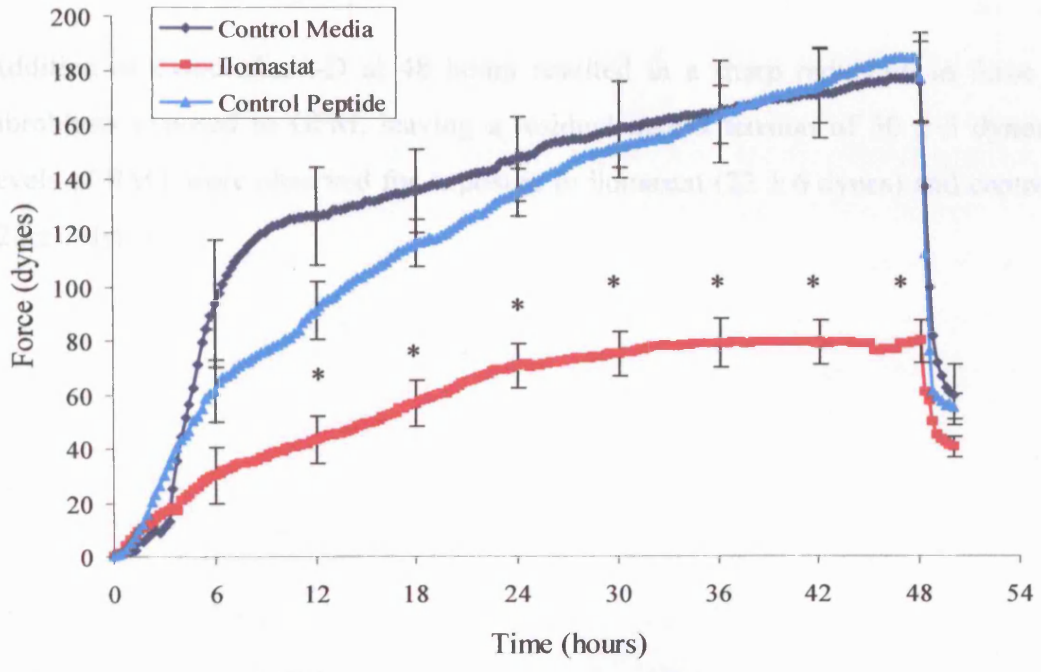

Figure 3. Force generation by nodule-derived fibroblasts (n=5 cell strains) over time. Cytochalasin-D was added to the system after 48 hours. *$p<0.05$ represents a significant difference between ilomastat exposure and control conditions (GFM or control peptide). Mean ± SEM.

5.4.4 Effect of ilomastat on contraction and remodelling by carpal ligament-derived fibroblasts

A graph illustrating the effect of ilomastat on force generation by carpal ligament-derived fibroblasts is illustrated in Figure 4. At 48 hours, fibroblasts generated similar levels of contractile force on exposure to GFM (72 ± 10 dynes) compared to control peptide (78 ± 17 dynes) or ilomastat (51 ± 10 dynes). In fact, throughout the first 48 hours of monitoring, no significant differences were observed between ilomastat and the two control conditions although a pattern of inhibition was evident from the graph. As with cord-derived fibroblasts, all individual carpal ligament strains demonstrated the same pattern of reduced force generation on exposure to ilomastat but collectively, interpatient variability prevented emergence of an overall pattern in the group. This is borne out in the wide standard error bars of individual data points on the graph. Force generation at 48 hours ranged from 48 – 100 dynes in fibroblasts exposed to GFM, 35 – 126 dynes (control peptide) and 22 – 73 dynes (ilomastat).

Addition of cytochalasin-D at 48 hours resulted in a sharp reduction in force level for fibroblasts exposed to GFM, leaving a residual matrix tension of 30 ± 5 dynes. Similar levels of RMT were observed for exposure to ilomastat (22 ± 6 dynes) and control peptide (28 ± 7 dynes).

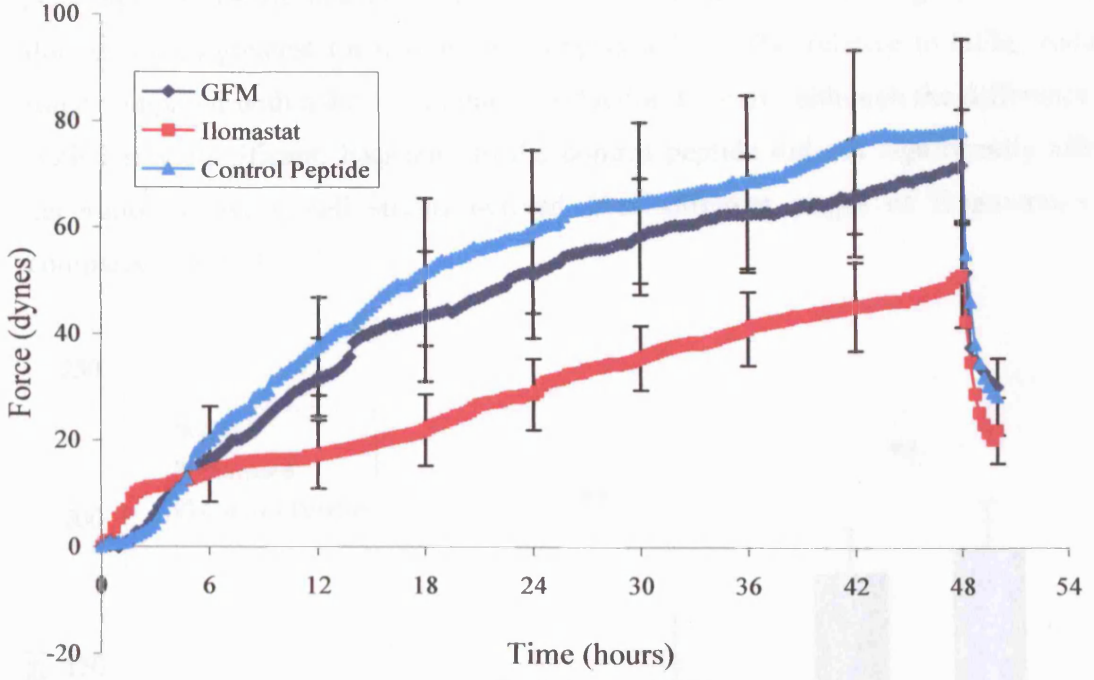

Figure 4. Force generation by carpal ligament-derived fibroblasts (n=5) over time. Fibroblasts were exposed to GFM, control peptide or ilomastat. Cytochalasin-D was added to the system after 48 hours. Mean ± SEM.

The information derived from the use of the culture force monitor lattice contraction model was subsequently analysed further to enable comparisons to be made between the response of Dupuytren's and control fibroblasts to ilomastat in terms of maximum force generation and rate of force development. Similarly, the relative importance of cell-mediated matrix contraction and matrix remodelling between different cell types was investigated.

5.4.5 Comparison between responses of cord, nodule and carpal ligament

5.4.5.1 Maximum force generation

A comparison of the maximum force generated by different cell strains in response to ilomastat and control conditions is illustrated in Figure 5. Under basal conditions (GFM), Dupuytren's-derived fibroblasts generated significantly greater contractile forces than control cells ($p<0.001$), representing an increase over carpal ligament of 246 ± 21% for nodule and 197 ± 25% for cord-derived fibroblasts.

Exposure to ilomastat resulted in a significant ($p<0.05$) reduction in the maximum force generated by nodule and cord-derived fibroblasts but not carpal ligament. Inhibition by ilomastat was greatest for nodule, resulting in a 53 ± 7% (relative to GFM) reduction in force compared with a 49 ± 5% relative reduction for cord, although the difference was not statistically significant. Exposure to the control peptide did not significantly affect force generation between cell strains derived from different stages of Dupuytren's disease compared to GFM.

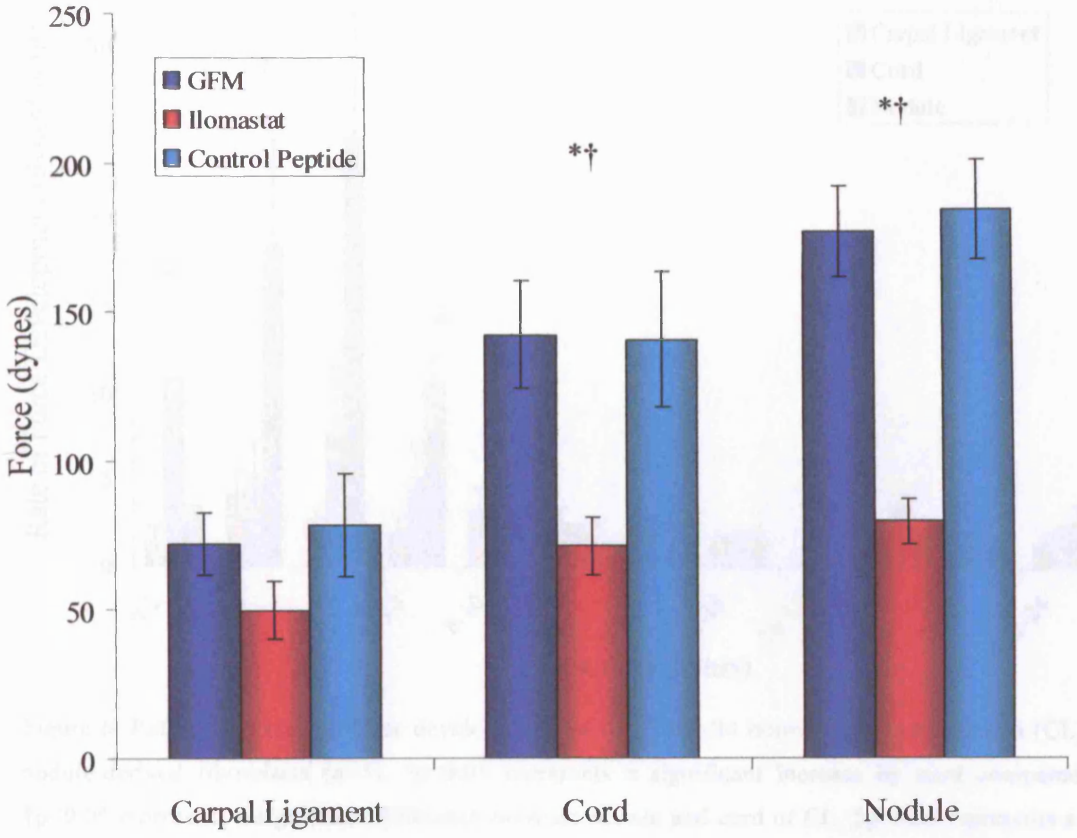

Figure 5. Maximum force generated over a 48-hour time period by carpal ligament (n=5), cord (n=5) and nodule-derived fibroblasts (n=5) in response to GFM, ilomastat or control peptide. †$p<0.05$ represents a significant difference between ilomastat and GFM or control peptide. *$p<0.01$ represents a significant difference in response to GFM between Dupuytren's and carpal ligament fibroblasts. Mean ± SEM.

5.4.5.2 Rate of contraction

The greatest rate of force generation by all three cell strains occurred over the first 24 hours. To further establish the precise relationship between time and force development, we analysed the rate of increase in force at 2 hourly intervals over the first 24 hours. The results of this analysis are demonstrated in Figure 6.

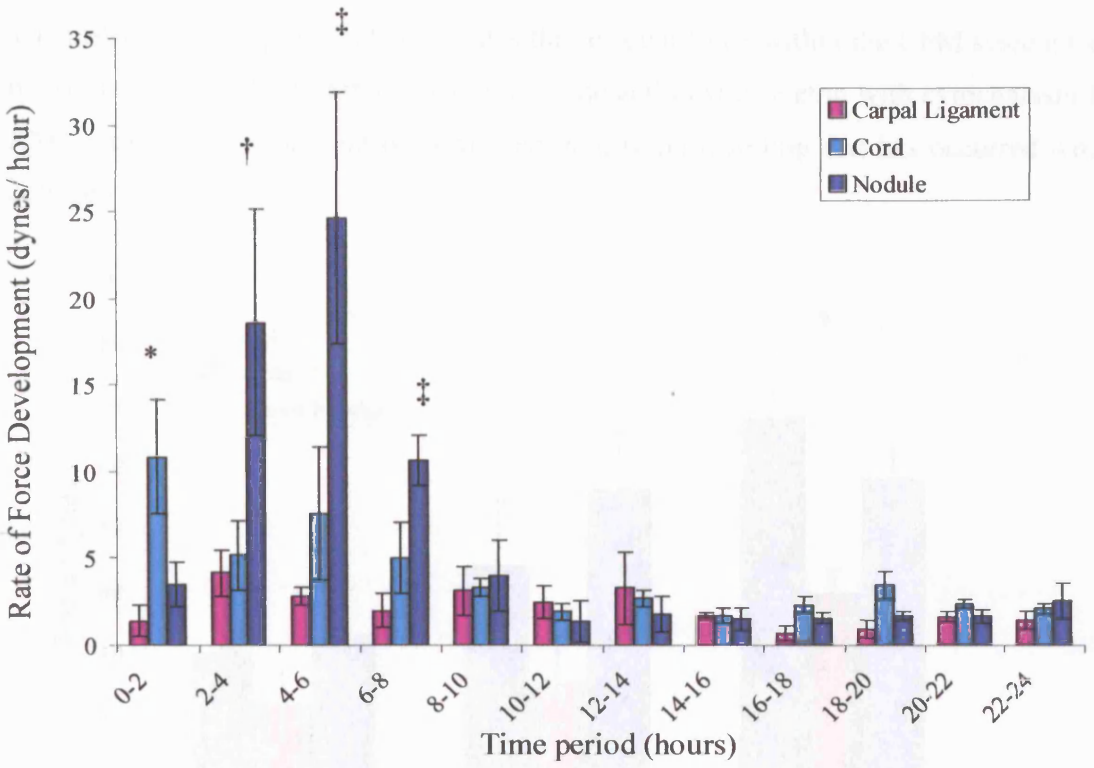

Figure 6. Rate of increase in force development over the first 24 hours for carpal ligament (CL), cord and nodule-derived fibroblasts (n=5). *p<0.05 represents a significant increase by cord compared with CL. †p<0.05 represents a significant difference between nodule and cord or CL. ‡p<0.05 represents a significant increase by nodule compared with CL. Mean ± SEM.

Over the first 2-hour period, cord-derived fibroblasts demonstrated the greatest rate of force generation (11 ± 3 dynes/ hour), contracting to a significantly greater extent than carpal ligament (1 ± 1 dynes/ hour; $p<0.05$), and nodule (4 ± 1 dynes/ hour). Conversely, over the proceeding three 2-hour intervals, nodule-derived fibroblasts developed force at the greatest rate. During the 4-6 hour and 6-8 hour intervals, force generation by nodule-derived

fibroblasts (25 ± 7, 11 ± 1 dynes/ hour, respectively) occurred at a faster rate ($p<0.05$) than carpal ligament (3 ± 1, 2 ± 1 dynes/ hour, respectively), but was not significantly different from cord (8 ± 4, 5 ± 2 dynes/ hour, respectively). After 8 hours, the rate of force generation was reduced and similar for all three cell types.

5.4.5.3 Effect of ilomastat on matrix remodelling

The histogram in Figure 7 demonstrates the residual force within the CFM system (residual matrix tension or RMT) after disruption of the actin cytoskeleton with cytochalasin-D. The RMT represents the amount of permanent matrix remodelling that has occurred within the collagen lattice.

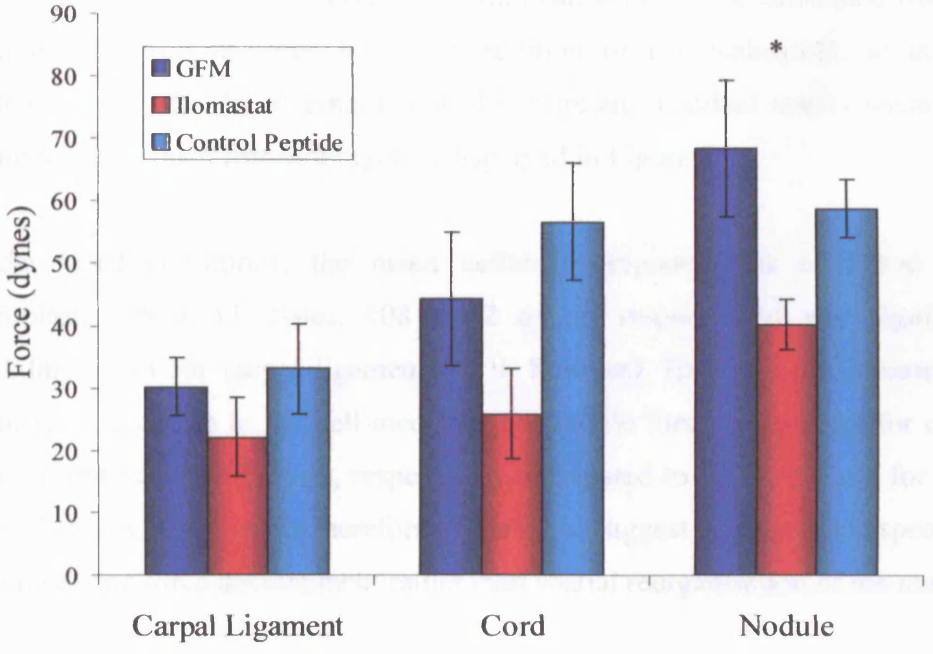

Figure 7. Histogram demonstrating the residual matrix tension of Dupuytren's and control lattices (n=5). Fibroblasts were exposed to either GFM, ilomastat or control peptide. *$p<0.05$ represents a significant increase of nodule over carpal ligament in response to GFM. Mean ± SEM.

Under basal conditions, there were significant differences in the mean RMT values of Dupuytren's and control fibroblasts ($p<0.05$) as revealed by a one-way ANOVA. Nodule-

derived fibroblasts demonstrated an RMT of 69 ± 11 dynes, representing a 127 ± 36% increase over carpal ligament. Further analysis revealed that the RMT of cord-derived fibroblasts (44 ± 11 dynes) was not significantly different from either nodule or carpal ligament (30 ± 5 dynes). The results suggested that nodule-derived fibroblasts were able to mediate greater permanent remodelling of the collagen lattice than carpal ligament. Although exposure to ilomastat tended to result in a lower RMT for all three cell strains, the differences were not significant when compared to either GFM or control peptide. These findings led to the conclusion that whilst ilomastat treatment resulted in a reduction in force generated by cells derived from each different tissue; treatment did not affect permanent matrix remodelling.

The cellular component of force generation can similarly be calculated from the collected data as the drop in force following addition of cytochalasin-D, in other words, the difference between force generated at 48 hours and residual matrix tension. The cellular component for each fibroblast type is displayed in Figure 8.

Under basal conditions, the mean cellular component for cord and nodule-derived fibroblasts (98 ± 11 dynes, 108 ± 12 dynes, respectively) was significantly greater ($p<0.001$) than for carpal ligament (42 ± 8 dynes). Exposure to ilomastat resulted in a significant decrease in the cell-mediated contractile force component for cord and nodule (46 ± 6 dynes, 39 ± 8 dynes, respectively) compared to GFM, but not for carpal ligament (28 ± 8 dynes). The results therefore appeared to suggest that ilomastat specifically targeted cell-mediated force development rather than spatial reorganisation of the matrix.

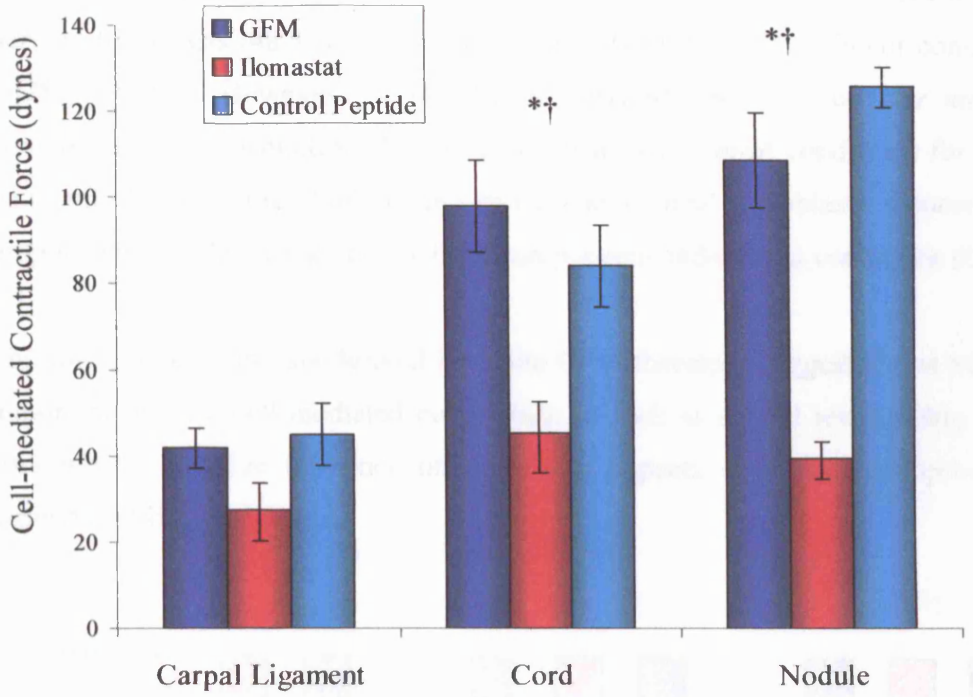

Figure 8. Histogram demonstrating cell-mediated contractile force generated by Dupuytren's and control fibroblasts (n=5). Fibroblasts were exposed to either GFM, ilomastat or control peptide. *$p<0.05$ represents a significant increase by nodule and cord-derived cells compared with carpal ligament in response to GFM. †$p<0.001$ represents a significant difference between treatment with ilomastat and GFM. Mean ± SEM.

As determined by Marenzana and colleagues (Marenzana et al. 2006), the reduction in force following addition of cytochalasin-D is a result of both the disruption of the actin cytoskeleton as well as a recoil force due to the spring-like action of the strain gauge being released. They also demonstrated that the greater the final cell-generated force, the greater the recoil force and therefore total force reduction. This observation implies that the observed RMT is in fact an underestimate of the full extent of matrix remodelling. Furthermore, it suggests that both the remodelling and cellular components might more accurately be expressed as a proportion of the total force generated rather than raw force readings as illustrated in Figure 9.

When the data was analysed in terms of proportions, it was shown that ilomastat exposure resulted in a significant reduction in the cellular component of force generation by nodule-derived fibroblasts (48 ± 6%) compared with either GFM (62 ± 5%) or control peptide (68 ± 2%; $p<0.05$). However, no significant difference between cellular and remodelling components was encountered between ilomastat and control conditions for cord or carpal ligament. Furthermore, both Dupuytren's and control fibroblasts demonstrated similar proportions of cellular and remodelling components under basal conditions (GFM).

The force generation data derived from the CFM therefore suggested that MMP activity is important in both cell-mediated contraction as well as spatial remodelling of the matrix, although the relative influence on these two aspects of force development appears to depend on fibroblast origin.

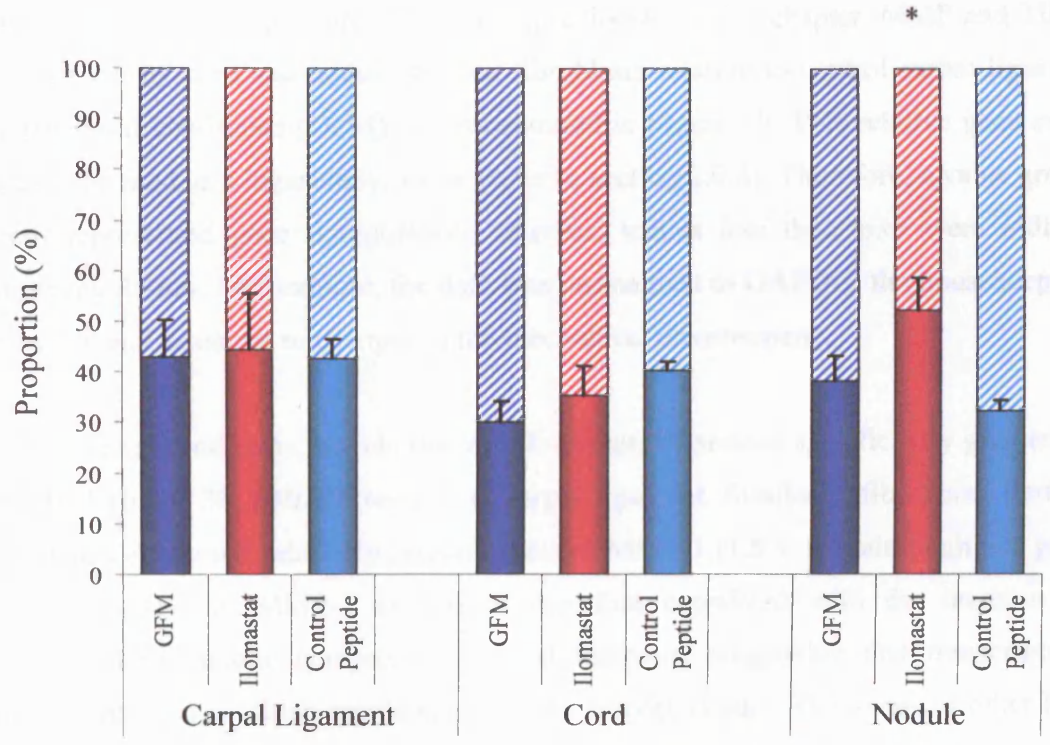

Figure 9. Histogram demonstrating proportion of maximum force generated in terms of RMT (filled) and cellular (dashed) components. *$p<0.05$ represents a significant difference in response to GFM, ilomastat and control peptide (n=5). Mean ± SEM.

The next set of experiments was designed to assess whether changes in mechanical tension in the CFM model were concomitant with changes in MMP expression and activity. Initially, gene expression was determined by RT-PCR to establish whether ilomastat affected MMP and TIMP mRNA levels either directly or indirectly through a feedback mechanism.

5.4.6 RT-PCR: MMP and TIMP gene expression

5.4.6.1 Comparison of gene expression by cord, nodule and carpal ligament

We initially analysed baseline gene expression to determine whether any differences existed between Dupuytren's and control fibroblasts that might correlate with the observed differences in force generation described previously in this chapter. MMP and TIMP gene expression by cord and nodule-derived fibroblasts relative to control carpal ligament cells under basal conditions (GFM) is demonstrated in Figure 10. This relative gene expression was expressed as a logarithmic value (refer to section 2.9.8). Therefore, a value greater than zero represented gene upregulation, whereas, values less than zero were indicative of downregulation. Furthermore, the data was normalised to GAPDH, the housekeeping gene, which is not sensitive to changes in the mechanical environment.

Under basal conditions, nodule-derived fibroblasts expressed significantly greater levels of MMP-1 (6.3 ± 30, $p<0.05$) relative to carpal ligament. Similarly, fibroblasts derived from cord also expressed relatively greater levels of MMP-1 (1.8 ± 10), although this proved not to be significant. MMP-1 expression therefore correlated with the increase in force generated by nodule compared to carpal ligament, suggesting that transcription is an important level at which regulation of MMP activity occurs. The levels of other MMP and TIMP genes investigated were similar between cord, nodule and carpal ligament.

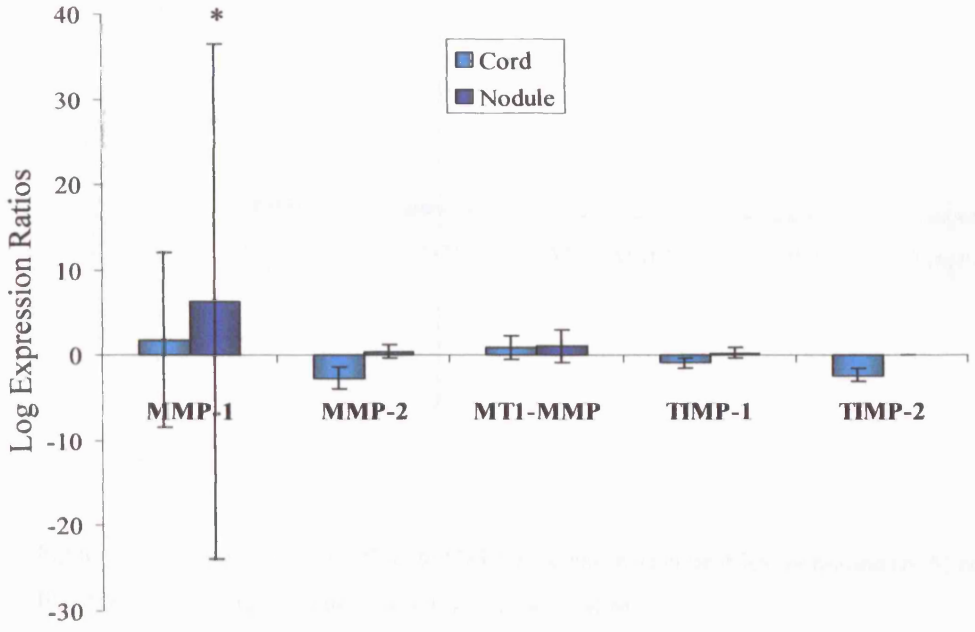

Figure 10. Comparison of MMP and TIMP gene expression by cord (n=5) and nodule (n=5) relative to carpal ligament-derived fibroblasts (n=5) under basal conditions (GFM). *$p<0.05$ represents a significant increase of nodule over carpal ligament. Mean ± SEM.

A direct comparison between gene expression by nodule relative to cord-derived fibroblasts was similarly made to establish whether any differences in baseline gene expression existed between the two Dupuytren's phenotypes. As illustrated in the results in Figure 11, no significant differences were demonstrated in MMP and TIMP gene expression profiles between cord and nodule-derived cells, which mirrored the findings that contractile and remodelling behaviour was similar between the two.

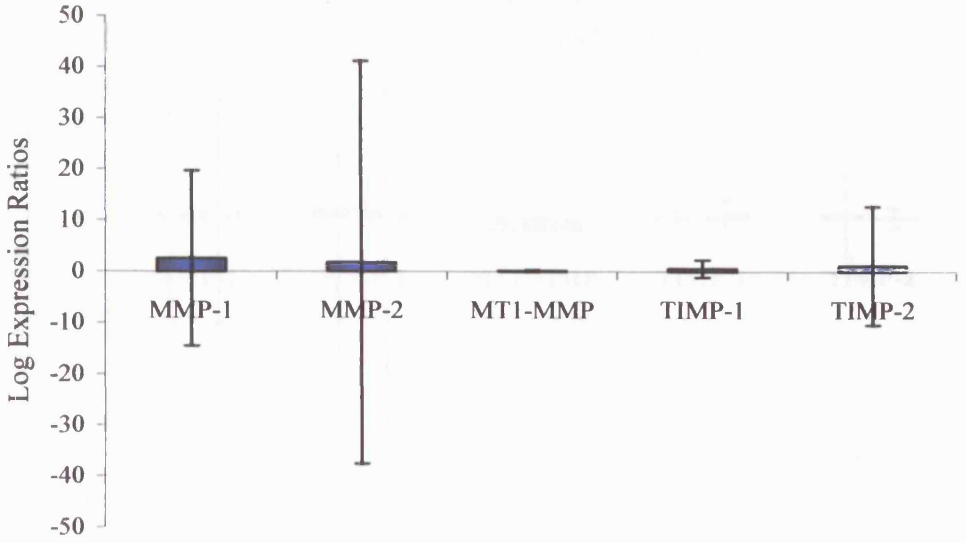

Figure 11. Comparison of MMP and TIMP gene expression profiles by nodule (n=5) relative to cord-derived fibroblasts under basal conditions (GFM). Mean ± SEM.

5.4.6.2 Effect of ilomastat on gene expression by cord-derived fibroblasts

The expression by cord-derived fibroblasts of secreted (MMP-1 and MMP-2) and membrane-bound MMPs (MT1-MMP) as well as TIMPs (TIMP-1 and TIMP-2) is illustrated in Figure 12. Gene expression of cord-derived fibroblasts exposed to ilomastat and control peptide was calculated relative to basal conditions (GFM).

Treatment with ilomastat appeared to result in an upregulation of MMP-1 and MMP-2 (2.3 ± 24.4, 2.4 ± 50, log expression ratios, respectively), although this proved not to be statistically significantly. Similarly, MT1-MMP and the TIMP genes assayed were not affected by exposure to ilomastat. No difference in relative gene expression was observed with exposure to the control peptide.

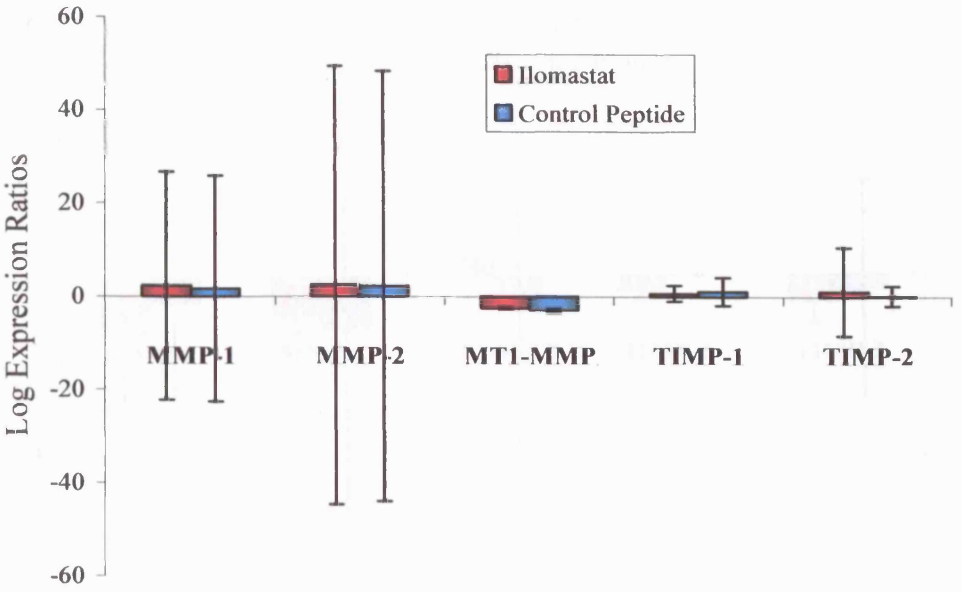

Figure 12. Comparison of MMP and TIMP gene expression by cord-derived fibroblasts (n=5) exposed to either ilomastat or control peptide relative to basal conditions (GFM). Mean ± SEM.

The large variability associated with MMP-1 and MMP-2 expression determined by RT-PCR is notable and mirrors the variability observed in the force generation profiles of cord-derived fibroblasts. This variability reflects underlying differences between patients. Furthermore, it may additionally suggest that although all cord tissue appears superficially homogeneous, it may vary considerably in terms of expression and contractile behaviour with stage of disease.

5.4.6.3 Effect of ilomastat on gene expression by nodule-derived fibroblasts

The expression by nodule-derived fibroblasts of various secreted and expressed MMPs and TIMPs is illustrated in Figure 13. Exposure to ilomastat resulted in a downregulation of MMP-1 and MMP-2 (-1.3 ± 1.6, -0.9 ± 0.5) relative to GFM, although this proved not to be significant. MT1-MMP appeared to be upregulated (0.4 ± 1.4) in response to ilomastat although this too was not significant. Likewise, TIMP gene expression was unaffected by ilomastat and there was no effect of control peptide on any gene. It is notable that the gene expression profiles derived from nodule-derived fibroblasts was associated with less inter-patient variability compared with cord-derived fibroblasts.

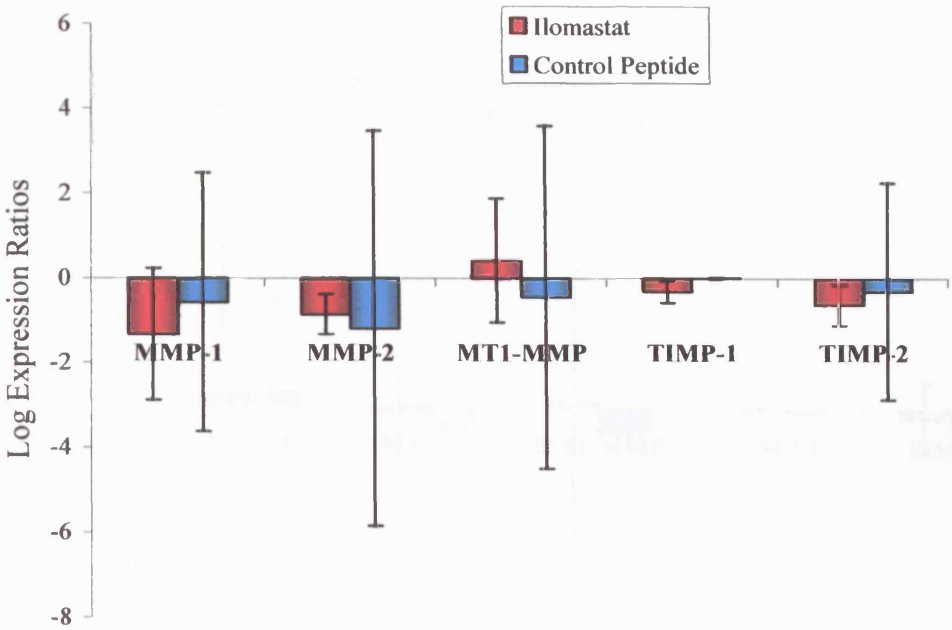

Figure 13. Comparison of MMP and TIMP gene expression by nodule-derived fibroblasts (n=5) exposed to either ilomastat or control peptide relative to basal conditions (GFM). Mean ± SEM.

5.4.6.4 Effect of ilomastat on gene expression by carpal ligament-derived fibroblasts

MMP and TIMP gene expression by carpal ligament-derived fibroblasts is illustrated in Figure 14. Neither ilomastat nor control peptide appeared to affect gene expression relative to basal conditions (GFM). This was borne out statistically as log expression ratios of ilomastat and control peptide treatment proved to be not significantly different from each other.

The results of RT-PCR provided some interesting insights into MMP regulation, suggesting that ilomastat exposure did not affect MMP-1 and MMP-2 at the level of transcription either through a direct inhibitory effect or a feedback mechanism within the 48 hour experimental window. Furthermore, ilomastat-mediated inhibition of MMP activity did not result in a feedback downregulation of TIMP-1 an TIMP-2 gene expression at 48 hours.

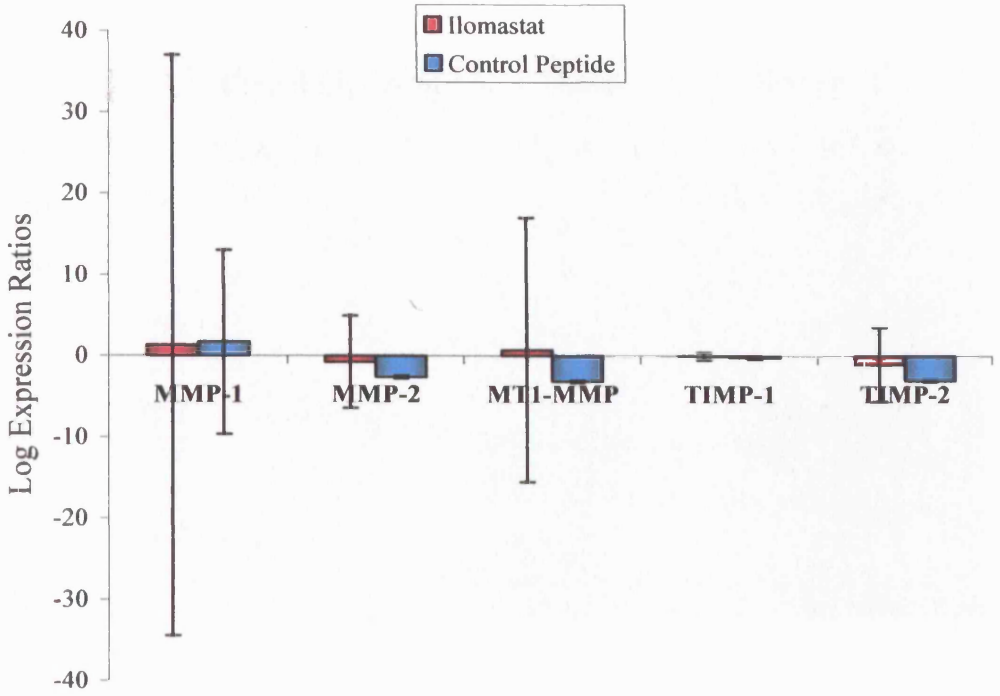

Figure 14. Comparison of MMP and TIMP gene expression by carpal ligament-derived fibroblasts (n=5) exposed to either ilomastat or control peptide relative to basal conditions (GFM). Mean ± SEM.

The results of the RT-PCR established that only nodule-derived fibroblasts exhibited elevated MMP-1 expression corresponding to force generation. Conversely, the gene expression profiles of MMP-2, MT1-MMP, TIMP-1 and TIMP-2 were not significantly different between the three cell strains and not affected by exposure to ilomastat. We subsequently performed western blot analysis to determine whether ilomastat affected MMP and TIMP activity at the protein level.

5.4.7 Western Blot analysis: estimation of MMP and TIMP protein levels

5.4.7.1 MMP-1

Cord, nodule and carpal ligament-derived fibroblasts appeared to secrete similar levels of both pro and active MMP-1 on exposure to GFM (Figure 15). Furthermore, MMP-1 secretion did not appear to be significantly affected by treatment with ilomastat or the

control peptide. The findings suggested that modulation of MMP-1 activity did not occur at the level of translation or was beyond the sensitivity of detection by western blot analysis.

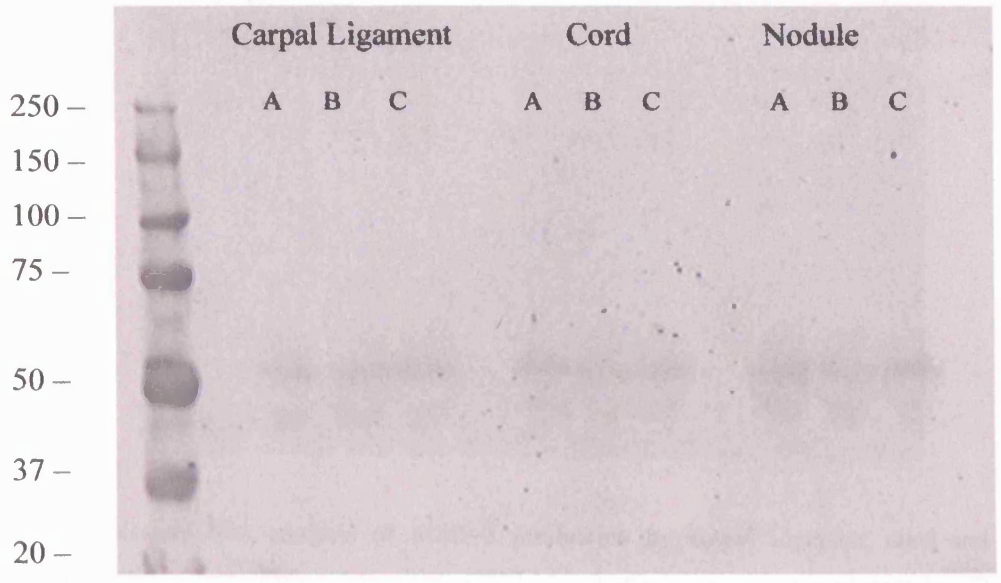

Figure 15. Western blot analysis of pro and active MMP-1 production by carpal ligament, cord and nodule-derived fibroblasts. Lattices were exposed to either GFM (A), ilomastat (B) or control peptide (C). The molecular weight (kDa) of kaleidoscope markers is listed adjacent to the marker bands in left hand column.

5.4.7.2 MMP-2

Only the latent form of MMP-2 (proMMP-2, 72kDa) was detected by western blotting as demonstrated by a sample blot in Figure 16. Some variation was observed in band intensity between different fibroblast types. Therefore, scanning densitometry was performed on all blots to objectively assess proMMP-2 protein levels (Figure 17).

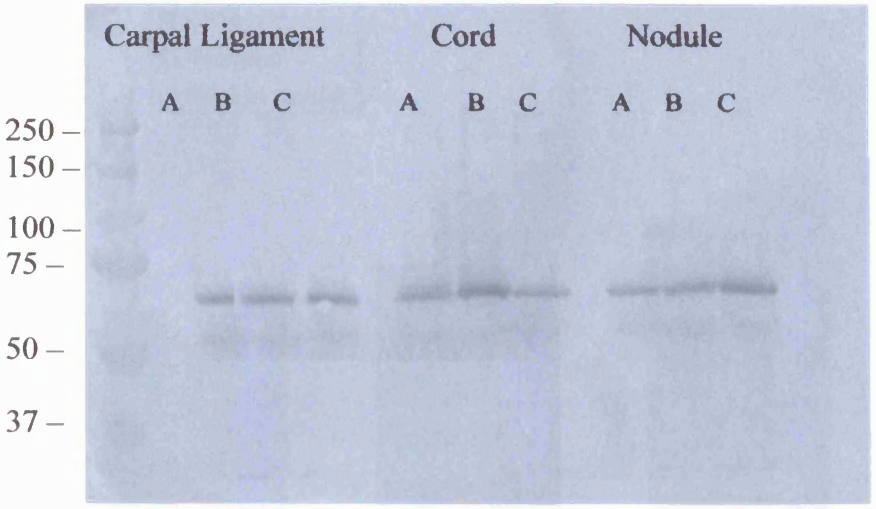

Figure 16. Western blot analysis of MMP-2 production by carpal ligament, cord and nodule-derived fibroblasts. Lattices were exposed to either GFM (A), ilomastat (B) or control peptide (C). The molecular weight (kDa) of kaleidoscope markers is listed adjacent to the marker bands in left hand column.

As determined by scanning densitometry, carpal ligament-derived fibroblasts produced similar levels of proMMP-2 (14.6 ± 0.6 mean band density) compared to cord (17.0 ± 2.3) and nodule-derived cells (19.4 ± 2.1) under basal conditions. Treatment with ilomastat or the control peptide did not appear to significantly affect proMMP-2 secretion, as there was no significant difference in mean band densities between GFM, ilomastat or control peptides by Dupuytren's and control fibroblasts. The results therefore suggested that exposure to ilomastat did not affect regulation of MMP-2 production at the translational level.

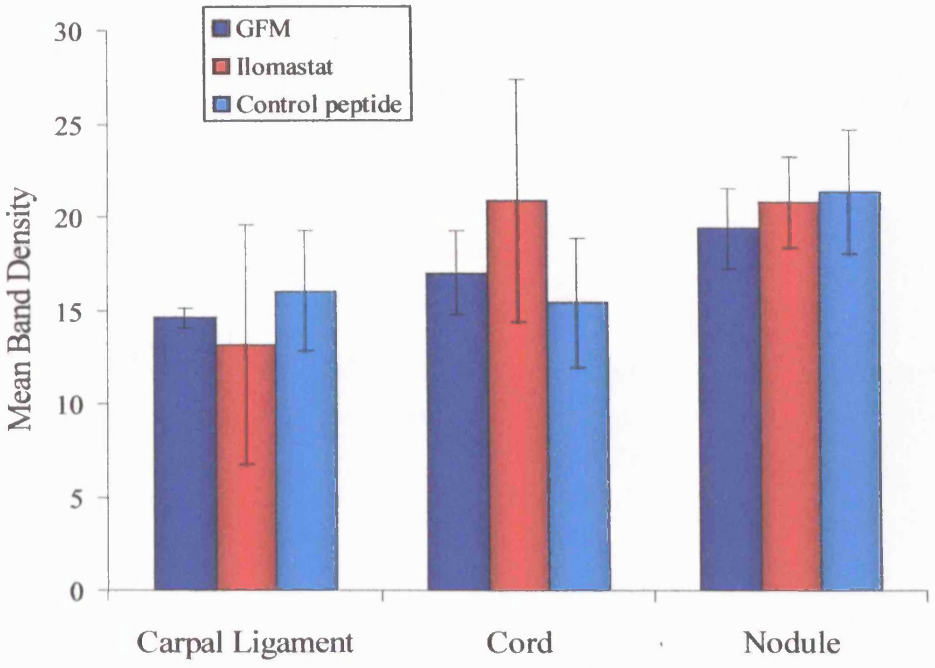

Figure 17. MMP-2 protein production as determined by mean band density of western blots (n=5). Fibroblasts seeded in contracting lattices were exposed to GFM, ilomastat or control peptide. Mean ± SEM.

5.4.7.3 MT1-MMP

MT1-MMP was detected in cell lysates isolated from cord, nodule and carpal ligament-derived fibroblasts as demonstrated in Figure 18. Two prominent bands were detected. The upper one was a double band probably corresponding to pro-MT1-MMP (65kDa) and active MT1-MMP species (63kDa). The lower band (around 55kDa) was not anticipated and may have been due to the primary antibody reacting with MMP-1 species in addition to MT1-MMP. MT1-MMP is expressed on the surface of all cells. Exposure to ilomastat appeared to result in an upregulation of the amount of active MT1-MMP by all three fibroblast strains, but did not affect the levels of pro-enzyme. The findings were confirmed by scanning densitometry as demonstrated in Figure 19.

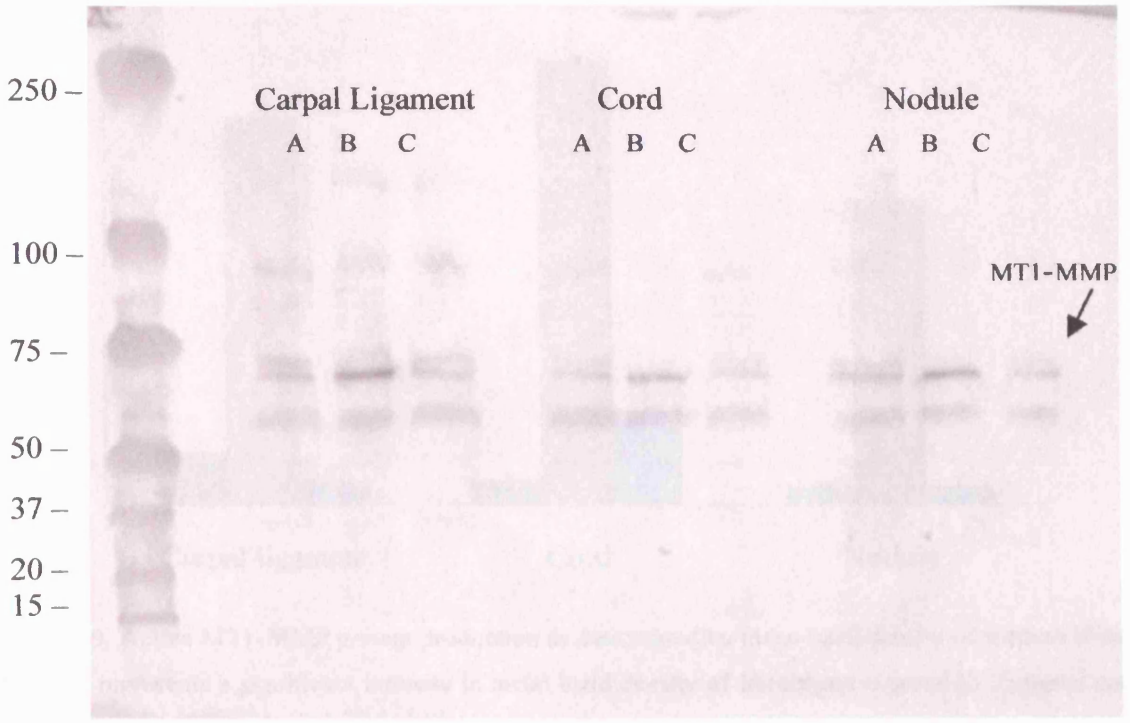

Figure 18. Western blot analysis of pro and active MT1-MMP expression by carpal ligament, cord and nodule-derived fibroblasts in cell lysates. Lattices were exposed to either GFM (A), ilomastat (B) or control peptide (C). The molecular weight (kDa) of kaleidoscope markers is listed adjacent to the marker bands in left hand column.

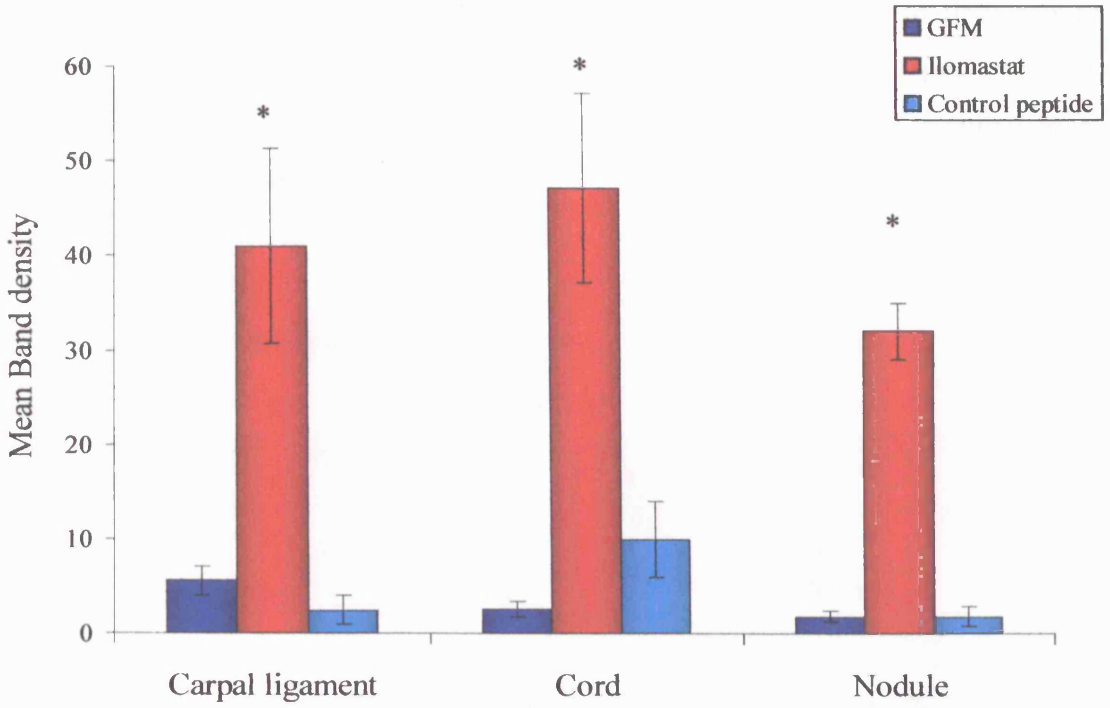

Figure 19. Active MT1-MMP protein production as determined by mean band density of western blots (n=5). *p<0.05 represents a significant increase in mean band density of fibroblasts exposed to ilomastat compared to GFM or control peptide. Mean ± SEM.

Under basal conditions, mean band densities of active MT1-MMP expression were similar for carpal ligament (5.6 ± 1.5), cord (2.6 ± 0.8) and nodule-derived fibroblasts (1.8 ± 0.5). However, on exposure to ilomastat, mean band densities were increased significantly for all three cell types (41 ± 10.2, 47 ± 10.0 and 32 ± 2.9, respectively), confirming an upregulation of MT1-MMP expression. Furthermore, the extent of ilomastat-mediated MT1-MMP upregulation was similar between all three cell strains. Treatment with control peptide did not appear to significantly affect MT1-MMP expression.

5.4.7.4 TIMP-1

A protein corresponding to TIMP-1 (25kDa) was detected in media collected from contracting lattices seeded with both Dupuytren's and control fibroblasts as illustrated in Figure 20. Lower molecular weight markers were more prominent than in previous blots due to the use of a 15% acrylamide separating gel. Similar amounts of TIMP-1 protein appeared to be produced by all three cell strains under basal conditions. Furthermore,

TIMP-1 production did not appear to be influenced by exposure to ilomastat or control peptide. Scanning densitometry was not performed. As with some previous blots, cross-reactivity between the primary antibody and other MMP species resulted in additional bands (possibly pro and active MMP-1).

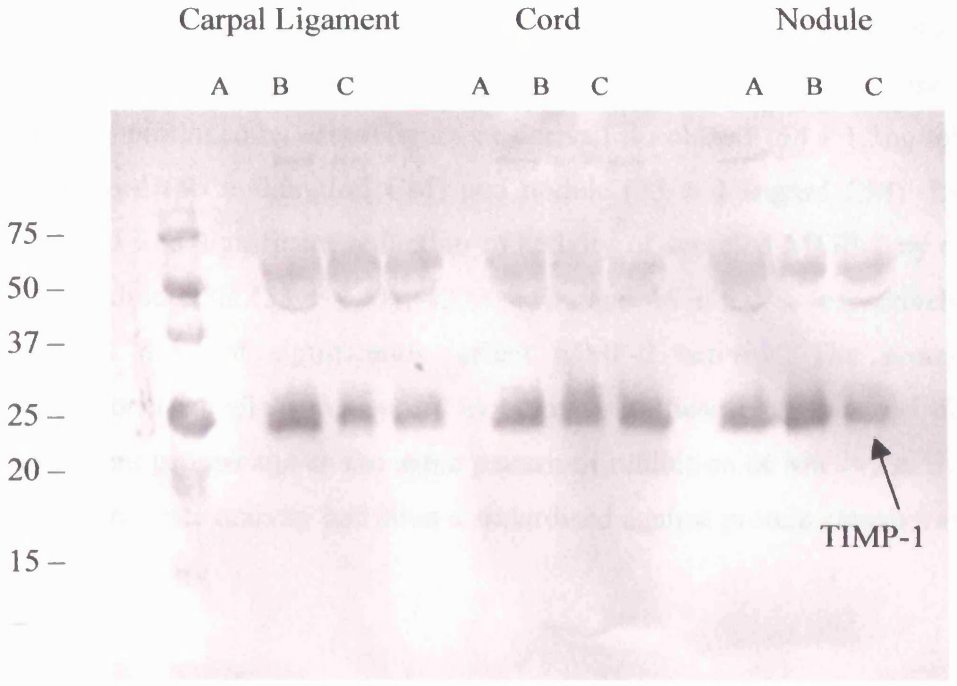

Figure 20. Western blot analysis of TIMP-1 production by carpal ligament, cord and nodule-derived fibroblasts. Lattices were exposed to either GFM (A), ilomastat (B) or control peptide (C). The molecular weight (kDa) of kaleidoscope markers is listed adjacent to the marker bands in left hand column.

5.4.7.5 TIMP-2

Cord, nodule and carpal ligament-derived fibroblasts did not appear to secrete significant levels of TIMP-2 (21kDa) on exposure to either GFM, ilomastat or control peptide as no bands corresponding to TIMP-2 were reliably detected by western blotting.

The results of the western blot analysis implied that exposure to ilomastat does not modulate MMP or TIMP activity at the level of translation. The exception being MT1-MMP, which was found to be modulated at the level of translation but not transcription. We

subsequently performed an activity ELISA to establish the pattern of MT1-MMP and MMP-2 activity by fibroblasts exposed to ilomastat.

5.4.8 Effect of ilomastat on MMP activity

5.4.8.1 MMP-2 activity

Activity of MMP-2 secreted in cell-conditioned media (CM) is illustrated in Figure 22. Panel A demonstrates levels of active enzyme activity. Under basal conditions, MMP-2 activity produced by carpal ligament-derived fibroblasts (53 ± 1.3ng/ml CM) was similar to both cord (55 ± 0.6ng/ml CM) and nodule (53 ± 1.3ng/ml CM). Exposure to ilomastat resulted in a significant reduction in activity of secreted MMP-2 by carpal ligament, cord and nodule cells (53 ± 4.5%, 42 ± 4.7% and 46 ± 5.4%, respectively; $p<0.001$). Control peptide did not significantly affect MMP-2 activity. The protein concentration of conditioned media samples did not vary significantly between different cell strains or treatment groups and so the same pattern of inhibition of MMP-2 activity by ilomastat was observed once activity had been standardised against protein concentration (panel B).

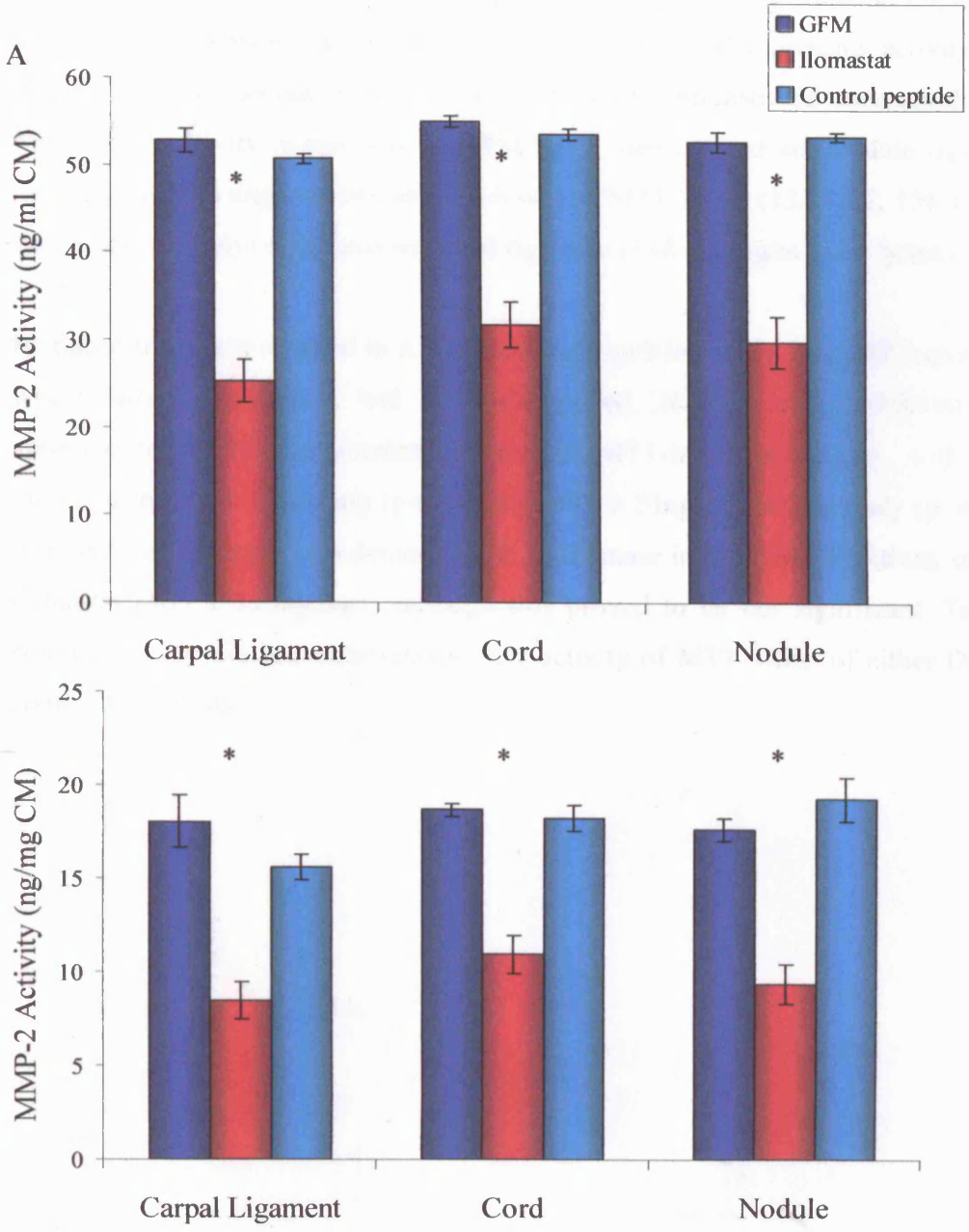

Figure 22. Quantification of MMP-2 activity (ng/ml conditioned media, panel A) and activity standardised against protein content (ng/mg conditioned media, panel B). *$p<0.001$ represents a significant inhibition of MMP-2 activity following ilomastat exposure compared to GFM or control peptide (n=5). Mean ± SEM.

5.4.8.2 MT1-MMP activity

Activity of cell-surface bound MT1-MMP in cell lysates is illustrated in Figure 23. Panel A demonstrates levels of enzyme activity, whereas, panel B represents activity standardised against protein concentration. All cells assessed demonstrated measurable amounts of MT1-MMP activity in response to GFM basal media. Cord and nodule ligament-derived cells appeared to express similar basal levels of MT1-MMP (132 ± 17, 156 ± 18ng/mg cell lysate, respectively) compared to carpal ligament (148 ± 27ng/mg cell lysate).

Ilomastat treatment resulted in a significant upregulation of MT1-MMP expression in cells where lattice contraction had been suppressed. Nodule and cord-derived fibroblasts appeared to exhibit the greatest increase in MT1-MMP expression, with levels rising threefold to 486 ± 140ng/mg ($p<0.05$) and 497 ± 23ng/mg, respectively ($p<0.001$). Carpal ligament-derived cells also demonstrated an increase in MT1-MMP activity on exposure to ilomastat (405 ± 113ng/mg), although this proved to be not significant. Treatment with control peptide did not significantly alter activity of MT1-MMP of either Dupuytren's or control fibroblasts.

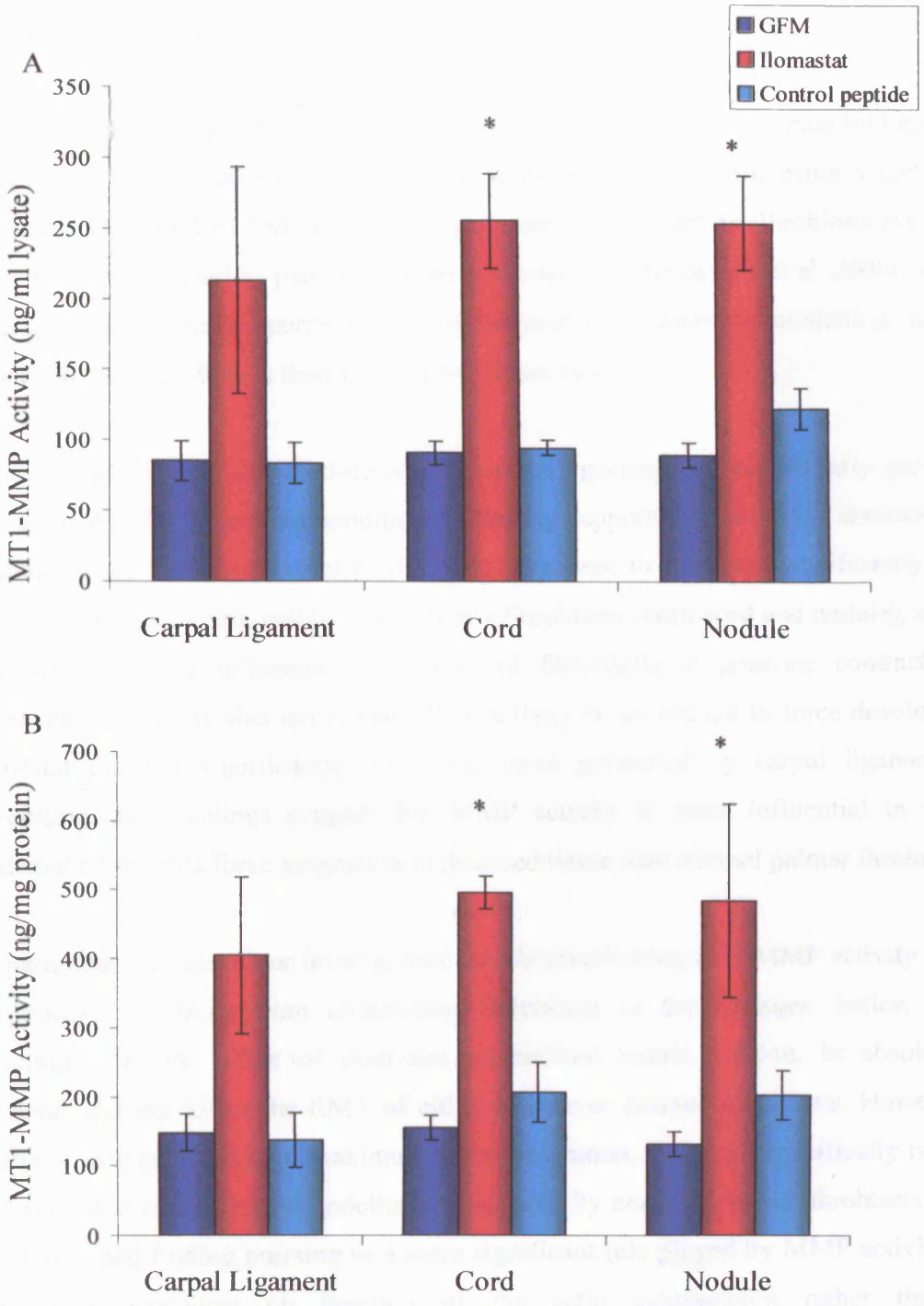

Figure 23. Quantification of levels of MT1-MMP activity (ng/ml cell lysate, panel A) and activity standardised against lysate protein content (ng/mg protein, panel B). *$p<0.05$ represents a significant upregulation of MT1-MMP activity following ilomastat exposure compared to GFM or control peptide (n=5). Mean ± SEM.

5.5 DISCUSSION

Mechanical tension and tissue contracture are two related facets of tissue biology that are important in Dupuytren's disease and can be investigated in vitro using a culture force monitor (CFM). In the CFM model, force generated by contracting fibroblasts is transferred into a force maintained by permanent matrix shortening (Marenzana et al. 2006). This latter process requires spatial reorganisation of the matrix, or matrix remodelling, to achieve actual shortening, which is facilitated by MMP activity.

In our model, nodule and cord-derived fibroblasts generated a significantly greater force than control cells under basal conditions, a finding supported by previous researchers using a culture force monitor (Bisson et al. 2004). Exposure to ilomastat significantly inhibited the maximum force obtained by Dupuytren's fibroblasts (both cord and nodule), suggesting that MMP activity influences the ability of fibroblasts to generate contractile force. However, our results also imply that MMP activity is not critical to force development, as ilomastat did not significantly affect the force generated by carpal ligament-derived fibroblasts. The findings suggest that MMP activity is more influential in fibroblast-mediated contractile force generation in diseased tissue than normal palmar fascia.

Of particular interest to our investigation was in establishing how MMP activity influences the transfer of force from contracting fibroblasts to the collagen lattice. This was determined by the effect of ilomastat on residual matrix tension. In absolute terms, ilomastat did not affect the RMT of either disease or control fibroblasts. However, when analysed as a proportion of maximum force generation, ilomastat specifically reduced the cell-mediated rather than remodelling component by nodule-derived fibroblasts. This was an unexpected finding pointing to a more significant role played by MMP activity in force generation dependent on function of the actin cytoskeleton rather than spatial reorganisation of the matrix. However, with cord and carpal ligament-derived cells, ilomastat appeared to reduce the remodelling component in line with the overall reduction in force generation.

Nodule-derived fibroblasts were found to express higher levels of MMP-1 under normal growth conditions compared to control cells, which correlated with their increased force generation. However, no similar increase in MMP-1 was detected in cord-derived fibroblasts suggesting that force generation is mediated by other MMPs in addition to MMP-1.

Regulation of MMPs has been shown to occur at the level of gene expression (Reuben et al. 2006). Through feedback mechanisms, we might have expected a decrease in TIMP gene expression as a result of the presence of an exogenous inhibitor (ilomastat). Furthermore, an increase in MMP-1 and MMP-2 gene expression in response to inhibition at the level of enzyme activity by ilomastat may have also been anticipated. However, in our experimental models, no difference in gene expression was demonstrated between treatment with ilomastat and control conditions. Due to the nature of the CFM models, only endpoint sampling was feasible, therefore dynamic changes in gene expression may have been missed. This seems a distinct possibility as the most dynamic changes in force generation occurred in the first 10 hours, whereas, gene expression was assessed at 50 hours. Conversely, the 50-hour time course may have been too short to enable differences in transcription to be detected.

Exposure to ilomastat did not influence the secretion of the MMP or TIMP proteins under investigation. However, as demonstrated in the FPCL model of contraction in Chapter 4, treatment with ilomastat resulted in an inhibition of MMP-2 activity, whereas MT1-MMP expression and activity were upregulated, a finding that could relate to the role of MT1-MMP as an activator of proMMP-2. In general, the findings of the MMP and TIMP analysis suggest that within the CFM time course used in our model, regulation of activity was predominantly directed at the level of protein activation rather than transcription or translation.

5.6 SUMMARY

- Nodule and cord-derived fibroblasts demonstrated a greater ability to generate force than carpal ligament in the CFM model.

- The rate of force development was significantly different between Dupuytren's and control cells over the first 8 hours of contraction, but not after 8 hours.

- Ilomastat significantly inhibited force development by Dupuytren's but not control cells.

- Ilomastat did not affect the absolute residual matrix tension values of cord, nodule or carpal ligament-derived fibroblasts. However, in terms of proportion, ilomastat preferentially inhibited cell-mediated contraction compared with matrix remodelling for nodule-derived fibroblasts.

- Nodule-derived fibroblasts expressed greater levels of MMP-1 gene than carpal ligament. However, no difference in gene expression was observed in response to different experimental conditions.

- Ilomastat resulted in an inhibition of MMP-2 activity at the level of enzyme activation.

- Ilomastat resulted in an upregulation of MT1-MMP protein expression and activity but did not affect MMP-1, MMP-2, TIMP-1 or -2 protein levels.

CHAPTER 6

GENERAL DISCUSSION

6.1 OVERVIEW

Dupuytren's disease is a fibrocontractile condition that causes disability through progressive digital contracture. It is a condition that naturally lends itself to scientific research because it is common, accounts for significant morbidity and gives rise to a discrete clinical problem that remains unsolved; namely, the high recurrence rates seen after surgery. In addition, diseased tissue samples are in abundance and readily available for analysis. Looking at the broader perspective, tissue contracture and fibroblast proliferation are common features of many related conditions that are not bound by anatomy or tissue type. The findings from our research may therefore contribute to the wider understanding of these related fibrocontractile disorders, further defining the underlying disease processes and helping to establish solutions.

Our decision to focus our research on the influence of MMP activity in Dupuytren's disease is similarly pertinent. Collectively, the family of MMP enzymes have been the source of much interest and speculation over recent years, as an appreciation of their corollary role in tissue remodelling has unfolded. The precise influence of MMPs in disease processes is undoubtedly more complicated than at first anticipated, but many and varied research initiatives into their therapeutic potential continue.

The problem of recurrence in Dupuytren's following corrective surgery is long-standing. However, in assessing the influence of MMPs, we have selected a novel avenue of research aimed at generating a new solution to an old riddle.

In this chapter, we aim to tie in the various threads that have been investigated in this thesis. Specifically, we will look to clarify differences between cellular activity observed from cord and nodule-derived tissue and seek to correlate these with disease progression. We will also seek to determine the role of MMP activity in remodelling of collagen lattices and generation of contractile force and, discuss the influence of an MMP inhibitor on regulation of MMP activity. We hope to demonstrate how these studies contribute to the greater body of knowledge about Dupuytren's and what further

research it points up. Some of the limitations of this present study have already been acknowledged at various points in the results chapters, however, a few general points will be made at the end of each section.

6.2 CORD AND NODULE – TWINS OR SIBLINGS?

The distinction between cord and nodule is very relevant to the study of Dupuytren's disease. Many researchers have sought to characterise the differences between the two clinical phenotypes, in order more specifically to define their respective roles in the disease's progression. Compared to cord, nodules are often associated with an earlier, active stage of disease in which fibroblasts are more proliferative (Luck 1959), contract collagen lattices to a greater extent (Bisson et al. 2003), express more α-SMA (Dave et al. 2001; Bisson et al. 2003) and demonstrate less intercellular communication (Moyer et al. 2002). However, nodule-derived fibroblasts have also been shown to demonstrate reduced metabolic activity compared to cord (Seyhan et al. 2006), which contradicts the postulation that they form a focus of active disease.

Clearly, selection of cord from nodule is a key issue. We chose a robust method for distinguishing the two phenotypes, in that it relied on clinical appearance to correlate with histological evaluation before a positive identification could be made. However, some researchers have been less stringent in their selection process, often relying purely on macroscopic appearance (Seyhan et al. 2006). Others have grouped all Dupuytren's-derived fibroblasts together in their investigations (Rayan et al. 1994; Tomasek et al. 1995; Wong et al. 2006) or looked at either just cord or nodule respectively (Hurst et al. 1986; Tarpila et al. 1996; Kuhn et al. 2002). Even with a rigorous assessment, the distinction may not be so black and white as cord and nodule often co-occur. Therefore, it is conceivable that pockets of nodule-like fibroblasts may reside within cord tissue and vice versa. Nevertheless, it was important to investigate the two Dupuytren's tissue types separately, to establish whether previously ascribed differences were prevalent in our model and whether a differential sensitivity to MMP inhibition existed.

In support of the findings of previous researchers, we found that fibroblasts derived from nodules demonstrated an increased proliferative response compared to cord and contracted lattices to a greater extent in the FPCL model. However, the differences in contractile ability were not apparent in the CFM model: although nodule-derived fibroblasts generated greater forces on average, the responses were not significantly different from cord, a similar finding to Beckett (Beckett 2005). The wide range of cord-mediated CFM responses suggested that cord tissue is not in fact a distinct entity, but is responsible for a spectrum of fibroblast behaviour that overlaps considerably with nodule tissue. Similarly, the interpatient variability highlighted the difficulty in selecting tissue samples from patients at the same stage of disease and may have masked some important findings.

As well as differences in contractile behaviour, discrepancies between cord and nodule were noted at the molecular level. Specifically, under basal conditions, MMP-1 activity was greater in nodule-derived fibroblasts than cord, which was concurrent with increased lattice contraction. Our findings support the notion that differences between cord and nodule are significant enough to warrant investigation of each in isolation. However, by increasing the number of samples tested and endeavouring to control for disease stage, we may have been able to reduce interpatient variability and further delineate differences between cord and nodule. Such an approach might establish or refute some of the underlying trends that did not reach statistical significance and further illuminate the specific roles of cord and nodule in the development and progression of the disease.

6.3 INFLUENCE OF MMP ACTIVITY ON CONTRACTION, FORCE GENERATION AND REMODELLING

It is well established that MMPs are involved in collagen contraction, matrix organisation and tissue scarring. Furthermore, MMPs are found in normal and diseased palmar fascia, where, it has been speculated they play a role in the development of

contracture (Beckett 2005). Therefore, we sought to assess the efficacy of an MMP inhibitor on Dupuytren's fibroblasts in vitro, as a preliminary investigation into the influence of MMPs on remodelling, and to outline their role in disease pathogenesis.

Ilomastat is a broad-spectrum inhibitor therefore making it a good interventional candidate. This is an important attribute, since as overlapping substrate specificity among MMP family members has been well documented (Sternlicht et al. 2001) and individually, specific MMP-blocking agents have been shown to have little effect on lattice contraction (Sheridan et al. 2001). Furthermore, ilomastat has been found to inhibit matrix contraction by ocular fibroblasts (Daniels et al. 2003), reduce scarring in an experimental model of glaucoma filtration surgery (Wong et al. 2003) and prevent human lens capsular contracture (Wong et al. 2004). In their study, Daniels and colleagues (Daniels et al. 2003) looked at the effect of various MMP inhibitors on collagen contraction, among them ilomastat, BB-94 and CellTech. Whilst all inhibitors reduced contraction, ilomastat was deemed most beneficial, being effective over the widest concentration range, further evidence of its suitability for our investigation.

Of all three FPCL models, the stress-release model was chosen to investigate contraction initially as it is thought to closely mimic the late granulation tissue remodelling phase of wound healing, which has many parallels with Dupuytren's disease (section 1.9.2). Furthermore, as discussed earlier, it provides a good approximation of the mechanical environment of palmar fascia tissue.

In our study, treatment with ilomastat significantly reduced collagen lattice contraction by all tissue-derived fibroblasts in the stress-release FPCL model. As discussed, this was unrelated to cytotoxicity as cells were able to proliferate normally and remain viable at the concentration of ilomastat investigated: 100μM. Furthermore, treatment with the control peptide or vehicle control did not significantly affect matrix contraction compared to basal conditions (GFM). The results suggested that contraction and lattice remodelling by Dupuytren's fibroblasts are highly MMP-dependent processes. However, the fact that ilomastat did not mediate complete inhibition of lattice contraction also

indicates that MMP activity may not be essential for matrix contraction. Conversely, ilomastat, despite conferring broad-spectrum inhibition, may not abrogate activity of some MMPs with overlapping substrate specificities (e.g. MT1-MMP) that assume greater importance once key MMPs are blocked (e.g. MMP-1).

MMP activity was greatest for nodule-derived fibroblasts, correlating with both the increased contractile ability of nodule relative to cord as well as with an apparent increased sensitivity of nodules to inhibition by ilomastat, although the latter finding did not achieve statistical significance. These observations support the postulation that nodules form an active focus of disease, being more involved than cord in the processes leading to contracture.

The CFM model was subsequently selected for investigation of contractile processes to provide actual kinetic information on force generation and to define more narrowly the individual components of cell-mediated contraction and matrix remodelling. Interestingly, the effects of ilomastat on tissue-derived fibroblasts in the CFM model were not uniform. Whilst a clear pattern of inhibition of force generation was demonstrated for cord and nodule, exposure to ilomastat did not significantly affect tension development by carpal ligament-derived fibroblasts.

The results for carpal ligament-derived fibroblasts mirrored findings by a previous investigator using dermal fibroblasts (Phillips et al. 2003). Phillips and colleagues demonstrated that ilomastat (10μM) inhibited lattice contraction by dermal fibroblasts in a free-floating FPCL model, but did not significantly reduce force generation as determined through use of a CFM model. The authors concluded that MMP activity facilitates three-dimensional remodelling, but does not influence cellular force output. Based on our own observations in the two models, it could be similarly argued that MMP activity influences spatial remodelling of the matrix by carpal ligament-derived fibroblasts, but does not affect the generation of tensile strength. A key difference is that in their investigation, Phillips and colleagues used a lower dose of ilomastat (10μM

compared to 100μM). They too may have encountered an inhibition of force development at the higher dose of ilomastat selected for our study.

Ilomastat did, however, reduce force development by cord and nodule-derived fibroblasts suggesting that abnormal MMP activity may be an important feature in the pathogenesis of Dupuytren's disease. Specifically, the findings imply that regulation of tensile force is mediated by MMP activity in diseased, but not in normal palmar fascia. This notion supports the rationale for the therapeutic use of an MMP inhibitor in Dupuytren's disease.

Further insight regarding the influence of MMP activity on both remodelling and force generation can be gleaned through the addition of cytochalasin-D to the CFM system, as established by Marenzana and colleagues (Marenzana et al. 2006). In their seminal paper, they elegantly demonstrated how cytochalasin-D, which specifically targets actin-dependent cellular processes, enables quantification of remodelling processes in the CFM model and, by extension, evaluation of cell-mediated tensile force generation. Specifically, they established that the addition of cytochalasin-D leads to a rapid reduction in force, leaving a residual matrix tension (RMT), which is an approximation of matrix shortening and therefore of remodelling.

In our study, although exposure to ilomastat reduced overall force development by Dupuytren's fibroblasts, it did not affect the magnitude of RMT by either cord or nodule-derived fibroblasts. These findings imply that MMP activity does not directly influence force attributable to spatial reorganisation or shortening of the matrix. Conversely, ilomastat was shown significantly to reduce the cell-mediated contractile force by both cord and nodule-derived fibroblasts, suggesting that MMP activity is directly involved in the generation of tensile strength by fibroblasts.

When the data for cord-derived fibroblasts were analysed in terms of proportion of overall force generation rather than absolute numbers, ilomastat exposure did not affect either the proportion of the remodelling or cellular components. In other words, the two

components reduced in line with the overall decrease in maximum force generation. In summary, the results derived from the CFM imply that MMP activity is an important mediator of both cell-dependent force generation and force retained in the matrix as a result of spatial remodelling. However, the findings also suggest that the relative influence of MMP activity on the two processes depends on fibroblast type or possibly the mechanical environment of the tissue from which the cells are derived. Several investigators have demonstrated that the compliance of tissue from which cells derive affects cellular behaviour including force generation (Wrobel et al. 2002; Peyton et al. 2005). The difference in tissue compliance between normal and diseased palmar fascia may therefore additionally be an important issue.

Interpreting the force generation plot in terms of two components is schematic and practical; however, it does not allow characterisation of all underlying processes. As illustrated in Figure 1, some researchers have considered the development of force in the CFM model to occur in three different phases (Tomasek et al. 2002; Marenzana et al. 2006), an assumption that allows further postulations to be made about the possible role of MMPs.

The initial phase follows cell-seeding and correlates with cell migration, the latter having been associated with force generation by traction (Harris et al. 1981; Ehrlich et al. 1990; Tranquillo 1999). Through matrix softening, MMPs can facilitate the migration of cells through the matrix. The importance of MMP activity on migration has been demonstrated in an experimental model of wound healing (Mirastschijski et al. 2004) and in culture keloid fibroblasts (Fujiwara et al. 2005), thus supporting a role for MMPs in force generated by traction.

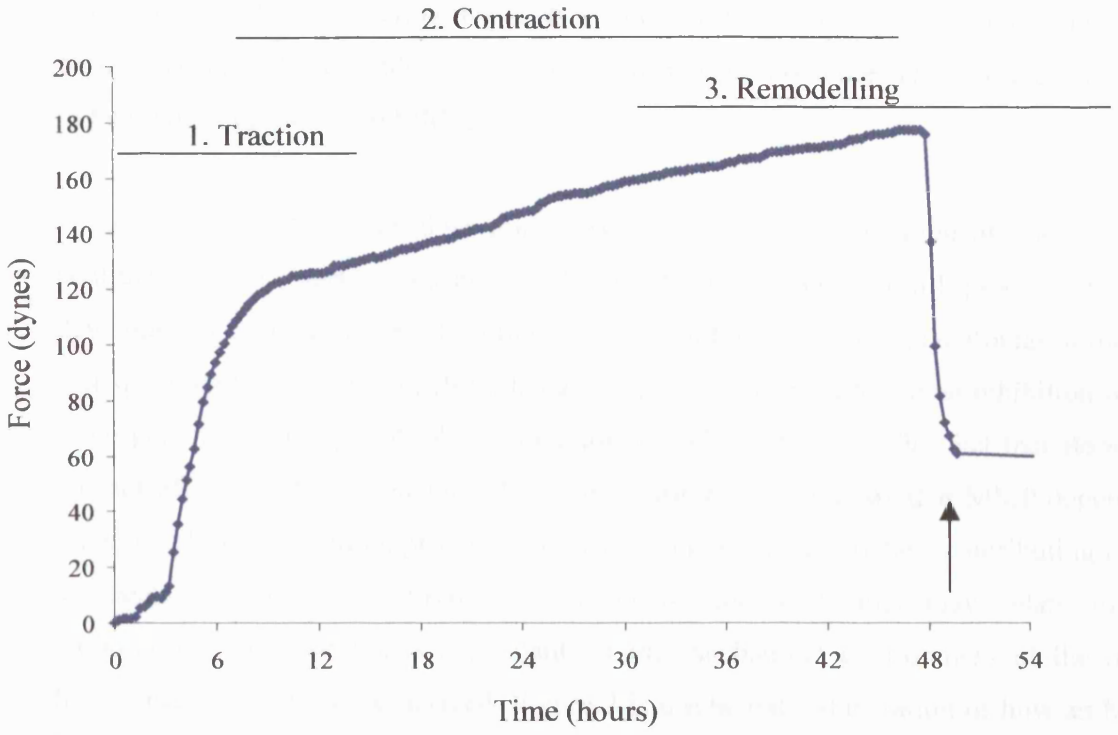

Figure 1. The three phases of force generation in the culture force monitor. The actual beginning and end of each phase is uncertain and not clearly defined. Addition of Cytochalasin-D is marked by an arrow.

As mechanical stress develops at the beginning of the second phase (contraction phase), fibroblasts differentiate into proto-myofibroblasts and myofibroblasts, which can exert contractile force on the extracellular matrix. Cell force during this phase is relatively constant, representing a form of tensional homeostasis (Brown et al. 1998). As well as simple matrix destruction, MMPs have a profound influence on fundamental cellular processes such as proliferation, growth, signalling and differentiation (Koike et al. 2002; Visse et al. 2003), which could indirectly influence contractile force generation. Furthermore, by reducing the mechanical tension generated through traction, an MMP inhibitor would reduce the stimulus for differentiation. In fact, ilomastat has been shown to mediate a reduction in both α-SMA expression and lattice contraction by dermal fibroblasts that was independent of TGF-β, a profibrotic mediator (Mirastschijski et al. 2004).

The final phase, characterised by the RMT, is due to irreversible shortening and remodelling of the collagen lattice such as occur in tissue contracture. Any remodelling process necessarily depends on the removal of matrix molecules and is therefore likely to be highly dependent on MMPs.

Although, the CFM model does not allow the precise differentiation of traction from contraction, our work suggests a role for MMP activity in all phases of force development by Dupuytren's fibroblasts. In contrast to our hypothesis, ilomastat did not just specifically target remodelling behaviour, but it also resulted in an inhibition of the force generated through fibroblast locomotion and contraction. The fact that ilomastat did not affect the force generated by control fibroblasts suggests that MMP-dependent force development is more prominent in diseased tissue and may be a contributing factor to tissue contracture in vivo. As previously discussed, this may relate to the 'conditioning' of fibroblasts dependent on the mechanical environment of the tissue from which the cells were derived. Figure 2 is a schematic illustration of how an MMP inhibitor might target different steps in the process of matrix contraction, based on a synthesis of our own findings, current knowledge about Dupuytren's pathogenesis, and postulations regarding contracture development (Tomasek et al. 2002; Marenzana et al. 2006).

A limitation to our study is that changes in cell number in the two lattice models were not formally assessed. Instead, it was assumed that the results of the proliferation assay on fibroblasts cultured in monolayer would be applicable to fibroblasts seeded in collagen lattices. However, it is feasible that ilomastat may have mediated a different effect, with respect to viability and proliferation, on fibroblasts cultured in two-dimensions as opposed to three-dimensional lattices. In addition, cell number may have varied over the period of mechanical strain. Any such difference may have influenced the contraction and force generation profiles elicited in the two models.

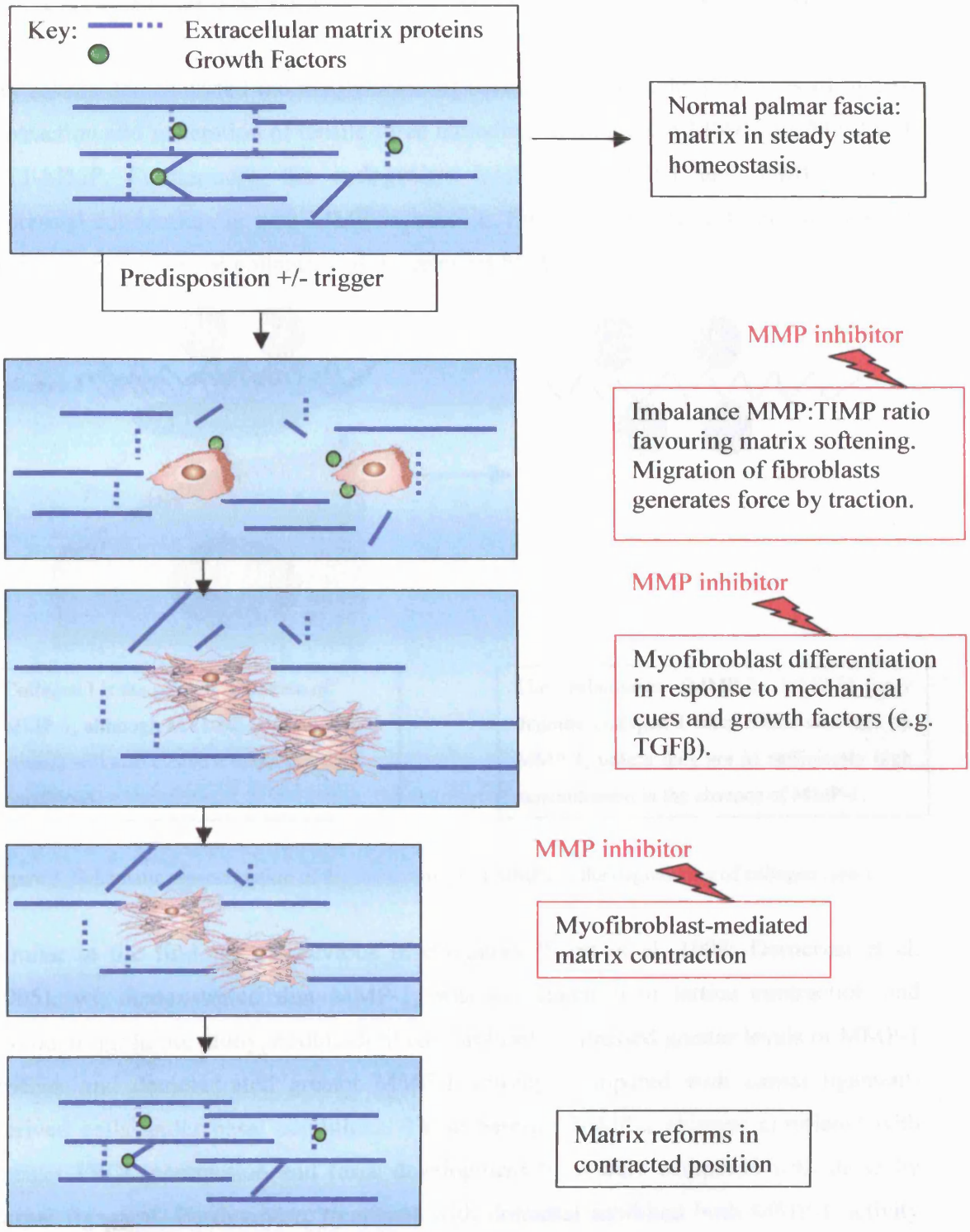

Figure 2. A schematic diagram illustrating the points at which an MMP inhibitor might interrupt the sequence of events leading to permanent matrix shortening.

6.4 PATTERN OF EXPRESSION AND ACTIVITY OF SPECIFIC MMPS

Our results demonstrated the involvement of several MMPs in the processes of matrix contraction and generation of tensile force including, among them MMP-1, MMP-2 and MT1-MMP. Furthermore, the endogenous inhibitors, TIMP-1 and TIMP-2, were expressed concomitantly with MMP expression. Figure 3 provides a brief overview of the interaction between collagen and the relevant MMPs.

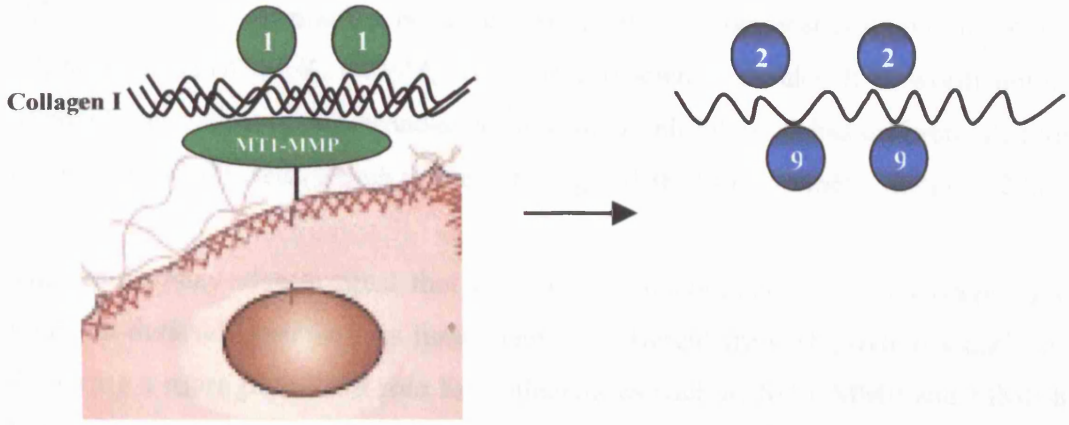

Figure 3. Schematic representation of the involvement of MMPs in the degradation of collagen type I.

Similar to the findings of previous investigators (Scott et al. 1998; Derderian et al. 2005), we demonstrated that MMP-1, was associated with lattice contraction and remodelling. In our study, nodule-derived fibroblasts expressed greater levels of MMP-1 mRNA and demonstrated greater MMP-1 activity, compared with carpal ligament-derived cells under basal conditions. These baseline MMP-1 changes correlated with greater FPCL contraction and force development by nodule compared with those by carpal ligament. Furthermore, treatment with ilomastat inhibited both MMP-1 activity and contraction in Dupuytren's-derived fibroblasts (both nodule and cord). These results

imply utilisation of MMP-1 during matrix contraction and remodelling by Dupuytren's fibroblasts.

The role of MMP-1 in the processing of lattices by control fibroblasts is less clear. Ilomastat did not affect MMP-1 activity by carpal ligament-derived fibroblasts, despite inhibiting FPCL contraction. The possibility that this finding could have been attributable to patient variability and insufficient sampling has already been discussed (Chapter 4). This eventuality is particularly likely, as ilomastat is known to be a potent inhibitor of MMP-1 (K_i 400pM, www.merckbisciences.co.uk). It is worth noting that although ilomastat confers broad-spectrum MMP inhibition, it has different affinities for each of the MMPs with which it interacts (e.g. MMP-2 - K_i 500pM, MMP-3 - 27nM).

The results may also suggest that the balance of collagen type I cleavage by carpal ligament-derived fibroblasts is fundamentally different from Dupuytren's-derived cells, favouring a more prominent role for collagenases such as MT1-MMP and MMP-8 than MMP-1. This is conceivable since tissue-specific MMP activity has been documented to vary between physiological and diseased states (Tchetverikov et al. 2005). As MMP-1 levels were increased in nodule-derived cells, the reduction in MMP activity may have been more pronounced due to the specificity of ilomastat for this mediator compared with other MMP species. Further analysis to identify the role of other collagenases in matrix remodelling by control fibroblasts was beyond the scope of this study but is the subject of ongoing investigations.

ProMMP-2, a gelatinase, was detected in FPCLs under stress (pre-release) in Dupuytren's and in control fibroblasts. By contrast, both pro and active forms were detected in post-release lattices suggesting that activation of MMP-2 was concomitant with lattice contraction. Ilomastat inhibited MMP-2 in all fibroblasts at the level of activation. MMP-1 is involved in proteolytic cleavage of the triple helical structure of type 1 collagen, exposing fragments that are susceptible to gelatinases including MMP-2. Our results imply a role for MMP-2 in processing and remodelling of the collagen lattice by Dupuytren's fibroblasts during contraction.

The importance of MMP-2 in mediating lattice contraction and remodelling by oral mucosal and dermal fibroblasts has been demonstrated in previous studies (Mudera et al. 2000; Stephens et al. 2001). Furthermore, Tarlton and colleagues found a direct relationship between mechanical stress and release of MMP-2 by Dupuytren's tissue in vitro (Tarlton et al. 1998). MMP-9, another gelatinase, has been shown to be upregulated by tendon fibroblasts in response to mechanical loading (Prajapati et al. 2000) and attachment to collagen type 1 (Ritty et al. 2003). However, MMP-9 was not consistently detected in our study, suggesting that MMP-2 is the dominant gelatinase involved in mediating lattice contraction by palmar fascial fibroblasts.

The main pathway for proMMP-2 activation occurs on the cell surface and is mediated by MT1-MMP in association with TIMP-2 (Butler et al. 1998; Wang et al. 2000). Exposure of Dupuytren's fibroblasts to ilomastat resulted in an upregulation of MT1-MMP protein expression and enzymic activity. The results suggest that fibroblasts may have upregulated MT1-MMP expression at the cell surface in response to detection of reduced MMP-2 activity, thereby enhancing proMMP-2 activation. Previous work has demonstratied increased MT1-MMP-dependent activation of proMMP-2 in the presence of marimastat, another synthetic MMP inhibitor (Toth et al. 2000). By contrast, TIMP-2 levels were not affected by treatment with ilomastat. TIMP-2 is a known inhibitor of MT1-MMP, and although essential for proMMP-2 activation, an excess of TIMP-2 can actually prevent the activation process (Nagase et al. 2006). A further possibility is that MT1-MMP was upregulated in response to reduced MMP-1 activity, as MT1-MMP has the capacity to digest interstitial collagens (Ohuchi et al. 1997) and has been shown to influence cellular migration through collagen lattices (Koike et al. 2002).

The net balance between MMP and TIMP activity has been identified as an important determinant of tissue homeostasis (Stephens et al. 2001; Nakatani et al. 2006) and therefore, modulation of MMP activity by an exogenous inhibitor might have been expected to result in changes in TIMP levels. However, the expression and protein levels of the two endogenous inhibitors, TIMP-1 and TIMP-2, were not affected by treatment

with ilomastat in either Dupuytren's or control fibroblasts. Our investigation, however, did not rule out changes at the level of TIMP-1 and TIMP-2 enzyme activity. This is especially pertinent as our analysis of the various points in the regulatory chain from transcription to protein activation suggested that, with the exception of MT1-MMP, changes in MMP activity mediated by ilomastat exposure were predominantly manifested at the level of extracellular proteolytic activation. Analysis of TIMP-1 and TIMP-2 activity was beyond the scope of our study, but may have further illuminated the nature of cell-matrix interactions, especially with regard to proMMP-2 activation and the net balance between MMP and TIMP activity.

The differences between TIMP-1 and TIMP-2 levels in Dupuytren's and in control patients have been investigated previously. Ulrich and colleagues demonstrated elevated TIMP-1 serum levels in Dupuytren's patients compared to controls (Ulrich et al. 2003). However, a limitation to Ulrich's study is that snapshot systemic enzyme levels may be a poor correlate of localised tissue activity, since many external factors can influence MMP expression (Parsons et al. 1997; Meisser et al. 2005). In our model, Dupuytren's-derived fibroblasts exhibited similar levels of both TIMP-1 and TIMP-2, compared to controls.

In another study, the effect of mechanical tension on MMP and TIMP expression was investigated using a CFM model (Beckett 2005). Introduction of a mechanical load to the system resulted in an upregulation of TIMP-1 gene expression by carpal ligament, but not by Dupuytren's-derived fibroblasts. Conversely, nodule-derived fibroblasts responded by upregulating MMP-1 and MMP-2 expression. The results suggested that the net balance between MMP and TIMP activity was modified in response to a mechanical stimulus, favouring an increase in matrix turnover by Dupuytren's fibroblasts. Interestingly, when a static load was applied in Beckett's study, no differences in either TIMP-1 or TIMP-2 expression were encountered between Dupuytren's and control fibroblasts, which corroborated with our findings.

Mechanical load has also previously been identified as an important mediator of MMP and TIMP gene expression by dermal fibroblasts (Mudera et al. 2000) and by osteoblasts (Jansen et al. 2006). A limitation to the CFM model is that only endpoint sampling is possible due to the sensitive nature of the equipment. In essence, analysis of gene expression, protein levels and enzyme activity were therefore only possible at the termination of the experiment. However, our investigation demonstrated that force development by Dupuytren's fibroblasts occurred at a significantly greater rate than control carpal ligament cells only for the first ten hours. Differences in expression and activity of MMPs may therefore have only been apparent during the most dynamic period of development of mechanical tension (0 - 10 hours) in the CFM model.

6.5 ILOMASTAT – THERAPEUTIC POTENTIAL?

The past decade has seen the accumulation of a body of evidence pointing to a central role for MMPs in both biological and pathological processes (Lemaitre et al. 2006; Nagase et al. 2006). Based on some of this early work, the therapeutic potential of targeting MMP activity has been investigated in several diseases, notably cancer and rheumatoid arthritis (Egeblad et al. 2002; Mengshol et al. 2002). However, clinical trials have not yet demonstrated any clear benefit of MMP inhibitors in improving patient outcomes (Baker et al. 2002; Coussens et al. 2002). As discussed in the introduction, this relates partly to trial design, and partly to the complex and diverse roles performed by MMPs in vivo. It is anticipated that an understanding of the precise MMP abnormality involved in disease progression, as well as the selection of an inhibitor with appropriate specificity, will yield successful results.

With regard to Dupuytren's, the use of synthetic MMP inhibitors aimed at preventing disease recurrence and progression constitutes an attractive strategy. Dupuytren's fibroblasts demonstrate abnormal contractile and remodelling behaviour compared to controls in vitro (Bisson et al. 2004; Beckett et al. 2005). This behaviour has, in turn, been associated with an abnormal pattern of MMP expression (Beckett et al. 2005). In

our study, inhibition of MMP-1 and MMP-2 activity by ilomastat accompanied a reduction in lattice contraction and in force generation mediated by Dupuytren's fibroblasts.

Clinically, nodules precede cords, and some have conjectured that the nodule is the initial trigger for contracture development (Chiu et al. 1978). Our results demonstrate that nodule-derived fibroblasts mediate greater lattice contraction than cord and were more sensitive to inhibition by ilomastat. These findings imply that intervention with an MMP inhibitor might be best directed at an early stage of the disease when nodules predominate. By specifically targeting nodules, it may be possible to prevent the progression to contracture and thus avoid the need for surgery.

Critics will draw attention to circumstantial evidence derived from the observations of Hutchinson of patients enrolled in a clinical trial investigating the effects on advanced gastric adenocarcinoma of marimastat, a hydroxamate MMP inhibitor with specificity against MMP- and MMP-9 (Hutchinson et al. 1998). Three out of twelve patients were noted to develop a Dupuytren's-like condition. However, the evidence is at best anecdotal. In particular, it is unclear whether patients were screened for Dupuytren's prior to the beginning of the trial: Dupuytren's would not be an uncommon finding in such an elderly cohort of patients. Furthermore, the condition described in the trial resolved on withdrawal of marimastat, which suggests a fundamental difference from Dupuytren's, which by definition results in permanent tissue contracture. Nonetheless, the findings are intriguing and highlight the fact that we do not yet fully comprehend the complete diversity of roles performed by MMPs in tissue homeostasis.

Our results suggest a critical role for MMP activity in matrix processing and organisation by Dupuytren's fibroblasts in vitro, suggesting that inhibition of MMP activity may well reduce contracture in vivo, by reducing fibroblast-mediated matrix contraction and remodelling. Obviously, the step from in-vitro results to proven clinical benefit is not insignificant. The importance of selecting an inhibitor with appropriate

specificity has already been highlighted and might require further work to establish more precisely the MMP and TIMP abnormalities underlying Dupuytren's.

Of critical importance, ilomastat, or the chosen MMP inhibitor, must be shown to be safe when administered in vivo. Unfortunately, an experimental model of Dupuytren's disease does not exist. However, MMP inhibitors (MPI) are in general thought to induce few serious complications. In particular, ilomastat has been shown to be safe in vivo in an experimental model of otitis media (Antonelli et al. 2003) and glaucoma filtration surgery (Wong et al. 2003). Minor side effects such as arthritis and myalgia are commonly described for MPIs (Wall et al. 2004) and are often attributed to the inhibition of sheddases. It may therefore be useful to evaluate and make comparisons with newer MPIs, such as BMS-275291, that lack antisheddase activity and have been shown to be well tolerated by patients enrolled in clinical trials (Lara et al. 2006).

6.6 CONCLUDING REMARKS

As suggested by its numerous associations and putative causes, Dupuytren's contracture may be the final pathway for several different aetiologies. Therefore, a broad approach to investigating the molecular basis of this condition is indicated. Previous work by other researchers has been directed towards abnormalities in growth factors, extracellular matrix proteins, and even free radicals. In carrying out this study, we have achieved what we set out to do: we have completed another piece of the puzzle and outlined a new strategy for tackling disease progression and recurrence. Specifically, we have made a rigorous assessment of the influence of MMP activity on matrix organisation by Dupuytren's fibroblasts, through the use of two distinct models of collagen lattice contraction.

The supposition that MMP activity may play a pivotal role in the development of contracture has been made previously (Tomasek et al. 2002; Beckett 2005). We have now delivered some robust experimental evidence to suggest that inhibition of MMP

activity can reduce matrix contraction and remodelling by Dupuytren's fibroblasts. It may therefore be effective in reducing contracture in vivo.

6.7 PROPOSAL FOR FUTURE WORK

Our study yielded interesting results that merited further investigation. However, the scope of the project was inevitably limited by time constraints. Based on an analysis of our findings, there are several experimental threads that could be picked up and pursued in further studies. They include further in-vitro work as a basis for another MD project, as well as the progressing to a clinical model.

Future work might take a more searching look at the role of MMP activity in force development by Dupuytren's fibroblasts. As mentioned previously, force is thought to be initially generated through fibroblast locomotion and contraction, but it was not possible to differentiate respective responsibility through the model we used in our project. It would, however, be possible to determine the effect of ilomastat on the movement of Dupuytren's fibroblasts through the matrix by means of migration assays using a confocal microscope. This would enable an assessment to be made of force generated by traction. Furthermore, an examination of α-SMA expression by contracting fibroblasts exposed to ilomastat might indicate whether any effect on cell-mediated contraction was independent of myofibroblast differentiation. This could be established through a combination of PCR, western blotting and immunohistochemical staining.

As alluded to earlier, MMP expression has been shown to be mechano-sensitive (Mudera et al. 2000). In our model, fibroblast contractile activity and changes in rate of force development were greatest early on. It would therefore be interesting to sample lattices and media at an early stage, perhaps after 6 or 8 hours. This would permit an investigation of the transient differences in mRNA expression and in intracellular signalling proteins such as protein kinases, arising between different cell strains and in response to ilomastat.

Ultimately, the goal is to assess the effect of an MMP inhibitor in preventing recurrence in patients undergoing surgery for Dupuytren's contracture. This could be established by a randomised controlled trial. However, before undertaking a clinical trial, several considerations must be addressed. First and foremost, the MMP inhibitor must be shown to be safe when administered in vivo. Subsequently, a suitable dosage regime, point of intervention and mode of delivery will need to be worked out, so that diseased tissue can be targeted effectively with minimal systemic impact.

REFERENCES

Adams, J. C. and F. M. Watt (1993). "Regulation of development and differentiation by the extracellular matrix." Development **117**(4): 1183-98.

Alioto, R. J., R. N. Rosier, R. I. Burton and J. E. Puzas (1994). "Comparative effects of growth factors on fibroblasts of Dupuytren's tissue and normal palmar fascia." J Hand Surg [Am] **19**(3): 442-52.

Antonelli, P. J., G. S. Schultz, D. J. Sundin, P. A. Pemberton and P. J. Barr (2003). "Protease inhibitors alpha1-antitrypsin and ilomastat are not ototoxic in the chinchilla." Laryngoscope **113**(10): 1764-9.

Arafa, M., J. Noble, S. G. Royle, I. A. Trail and J. Allen (1992). "Dupuytren's and epilepsy revisited." J Hand Surg [Br] **17**(2): 221-4.

Armstrong, J. R., J. S. Hurren and A. M. Logan (2000). "Dermofasciectomy in the management of Dupuytren's disease." J Bone Joint Surg Br **82**(1): 90-4.

Arnoczky, S. P., T. Tian, M. Lavagnino and K. Gardner (2004). "Ex vivo static tensile loading inhibits MMP-1 expression in rat tail tendon cells through a cytoskeletally based mechanotransduction mechanism." J Orthop Res **22**(2): 328-33.

Attali, P., O. Ink, G. Pelletier, C. Vernier, F. Jean, L. Moulton and J. P. Etienne (1987). "Dupuytren's contracture, alcohol consumption, and chronic liver disease." Arch Intern Med **147**(6): 1065-7.

Augoff, K., J. Kula, J. Gosk and R. Rutowski (2005). "Epidermal growth factor in Dupuytren's disease." Plast Reconstr Surg **115**(1): 128-33.

Badalamente, M. A. and L. C. Hurst (1999). "The biochemistry of Dupuytren's disease." Hand Clin **15**(1): 35-42, v-vi.

Badalamente, M. A., L. C. Hurst and V. R. Hentz (2002). "Collagen as a clinical target: nonoperative treatment of Dupuytren's disease." J Hand Surg [Am] **27**(5): 788-98.

Badalamente, M. A., S. P. Sampson, L. C. Hurst, A. Dowd and K. Miyasaka (1996). "The role of transforming growth factor beta in Dupuytren's disease." J Hand Surg [Am] **21**(2): 210-5.

Bailey, A. J., S. Bazin, T. J. Sims, M. Le Lous, C. Nicoletis and A. Delaunay (1975). "Characterization of the collagen of human hypertrophic and normal scars." Biochim Biophys Acta **405**(2): 412-21.

Bailey, A. J., J. F. Tarlton, J. Van der Stappen, T. J. Sims and A. Messina (1994). "The continuous elongation technique for severe Dupuytren's disease. A biochemical mechanism." J Hand Surg [Br] **19**(4): 522-7.

Baird, K. S., J. F. Crossan and S. H. Ralston (1993). "Abnormal growth factor and cytokine expression in Dupuytren's contracture." J Clin Pathol **46**(5): 425-8.

Baker, A. H., D. R. Edwards and G. Murphy (2002). "Metalloproteinase inhibitors: biological actions and therapeutic opportunities." J Cell Sci **115**(Pt 19): 3719-27.

Bayat, A., J. S. Watson, J. K. Stanley, M. W. Ferguson and W. E. Ollier (2003). "Genetic susceptibility to dupuytren disease: association of Zf9 transcription factor gene." Plast Reconstr Surg **111**(7): 2133-9.

Beckett, K. (2005). "The Progression from Contraction to Contracture in Dupuytren's Derived Fibroblasts: a Study of the Cellular and Molecular Events." MD thesis, UCL.

Beckett, K., M. Bisson, V. Mudera, D. A. McGrouther and A. O. Grobbelaar (2005). "A hypothesis for the progression of Dupuytren's Contracture [abstract]." J Hand Surg [Br] **30 (Suppl 1)**: 28.

Bell, E., B. Ivarsson and C. Merrill (1979). "Production of a tissue-like structure by contraction of collagen lattices by human fibroblasts of different proliferative potential in vitro." Proc Natl Acad Sci U S A **76**(3): 1274-8.

Berliner, D. L. and A. G. Ruhmann (1967). "The influence of dimethyl sulfoxide on fibroblastic proliferation." Ann N Y Acad Sci **141**(1): 159-64.

Bisson, M. A., D. A. McGrouther, V. Mudera and A. O. Grobbelaar (2003). "The different characteristics of Dupuytren's disease fibroblasts derived from either nodule or cord: expression of alpha-smooth muscle actin and the response to stimulation by TGF-beta1." J Hand Surg [Br] **28**(4): 351-6.

Bisson, M. A., V. Mudera, D. A. McGrouther and A. O. Grobbelaar (2004). "The contractile properties and responses to tensional loading of Dupuytren's disease--derived fibroblasts are altered: a cause of the contracture?" Plast Reconstr Surg **113**(2): 611-21; discussion 622-4.

Bramhall, S. R., A. Rosemurgy, P. D. Brown, C. Bowry and J. A. Buckels (2001). "Marimastat as first-line therapy for patients with unresectable pancreatic cancer: a randomized trial." J Clin Oncol **19**(15): 3447-55.

Brickley-Parsons, D., M. J. Glimcher, R. J. Smith, R. Albin and J. P. Adams (1981). "Biochemical changes in the collagen of the palmar fascia in patients with Dupuytren's disease." J Bone Joint Surg Am **63**(5): 787-97.

Brown, P. D. (2000). "Ongoing trials with matrix metalloproteinase inhibitors." Expert Opin Investig Drugs **9**(9): 2167-77.

Brown, R. A., R. Prajapati, D. A. McGrouther, I. V. Yannas and M. Eastwood (1998). "Tensional homeostasis in dermal fibroblasts: mechanical responses to mechanical loading in three-dimensional substrates." J Cell Physiol **175**(3): 323-32.

Bulstrode, N. W., M. Bisson, B. Jemec, A. L. Pratt, D. A. McGrouther and A. O. Grobbelaar (2004). "A prospective randomised clinical trial of the intra-operative use of 5-fluorouracil on the outcome of dupuytren's disease." J Hand Surg [Br] **29**(1): 18-21.

Bulstrode, N. W., B. Jemec and P. J. Smith (2005). "The complications of Dupuytren's contracture surgery." J Hand Surg [Am] **30**(5): 1021-5.

Butler, G. S., M. J. Butler, S. J. Atkinson, H. Will, T. Tamura, S. Schade van Westrum, T. Crabbe, J. Clements, M. P. d'Ortho and G. Murphy (1998). "The TIMP2 membrane type 1 metalloproteinase "receptor" regulates the concentration and efficient activation of progelatinase A. A kinetic study." J Biol Chem **273**(2): 871-80.

Cheema, U., S. Y. Yang, V. Mudera, G. G. Goldspink and R. A. Brown (2003). "3-D in vitro model of early skeletal muscle development." Cell Motil Cytoskeleton **54**(3): 226-36.

Chiquet, M., M. Matthisson, M. Koch, M. Tannheimer and R. Chiquet-Ehrismann (1996). "Regulation of extracellular matrix synthesis by mechanical stress." Biochem Cell Biol **74**(6): 737-44.

Chiquet, M., A. S. Renedo, F. Huber and M. Fluck (2003). "How do fibroblasts translate mechanical signals into changes in extracellular matrix production?" Matrix Biol **22**(1): 73-80.

Chiu, H. F. and R. M. McFarlane (1978). "Pathogenesis of Dupuytren's contracture: a correlative clinical-pathological study." J Hand Surg [Am] **3**(1): 1-10.

Choquet, D., D. P. Felsenfeld and M. P. Sheetz (1997). "Extracellular matrix rigidity causes strengthening of integrin-cytoskeleton linkages." Cell **88**(1): 39-48.

Citron, N. and A. Hearnden (2003). "Skin tension in the aetiology of Dupuytren's disease; a prospective trial." J Hand Surg [Br] **28**(6): 528-30.

Citron, N. D. and V. Nunez (2005). "Recurrence after surgery for Dupuytren's disease: a randomized trial of two skin incisions." J Hand Surg [Br] **30**(6): 563-6.

Conway, J. G., J. A. Wakefield, R. H. Brown, B. E. Marron, L. Sekut, S. A. Stimpson, A. McElroy, J. A. Menius, J. J. Jeffreys, R. L. Clark and et al. (1995). "Inhibition of cartilage and bone destruction in adjuvant arthritis in the rat by a matrix metalloproteinase inhibitor." J Exp Med **182**(2): 449-57.

Cordova, A., M. Tripoli, B. Corradino, P. Napoli and F. Moschella (2005). "Dupuytren's contracture: an update of biomolecular aspects and therapeutic perspectives." J Hand Surg [Br] **30**(6): 557-62.

Coussens, L. M., B. Fingleton and L. M. Matrisian (2002). "Matrix metalloproteinase inhibitors and cancer: trials and tribulations." Science **295**(5564): 2387-92.

Critchley, E. M., S. D. Vakil, H. W. Hayward and V. M. Owen (1976). "Dupuytren's disease in epilepsy: result of prolonged administration of anticonvulsants." J Neurol Neurosurg Psychiatry **39**(5): 498-503.

Daniels, J. T., A. D. Cambrey, N. L. Occleston, Q. Garrett, R. W. Tarnuzzer, G. S. Schultz and P. T. Khaw (2003). "Matrix metalloproteinase inhibition modulates fibroblast-mediated matrix contraction and collagen production in vitro." Invest Ophthalmol Vis Sci **44**(3): 1104-10.

Darby, I., O. Skalli and G. Gabbiani (1990). "Alpha-smooth muscle actin is transiently expressed by myofibroblasts during experimental wound healing." Lab Invest **63**(1): 21-9.

Dave, S. A., D. R. Banducci, W. P. Graham, 3rd, G. M. Allison and H. P. Ehrlich (2001). "Differences in alpha smooth muscle actin expression between fibroblasts derived from Dupuytren's nodules or cords." Exp Mol Pathol **71**(2): 147-55.

Defawe, O. D., R. D. Kenagy, C. Choi, S. Y. Wan, C. Deroanne, B. Nusgens, N. Sakalihasan, A. Colige and A. W. Clowes (2005). "MMP-9 regulates both positively and negatively collagen gel contraction: a nonproteolytic function of MMP-9." Cardiovasc Res **66**(2): 402-9.

Derderian, C. A., N. Bastidas, O. Z. Lerman, K. A. Bhatt, S. E. Lin, J. Voss, J. W. Holmes, J. P. Levine and G. C. Gurtner (2005). "Mechanical strain alters gene

expression in an in vitro model of hypertrophic scarring." Ann Plast Surg **55**(1): 69-75; discussion 75.

Deryugina, E. I., B. Ratnikov, E. Monosov, T. I. Postnova, R. DiScipio, J. W. Smith and A. Y. Strongin (2001). "MT1-MMP initiates activation of pro-MMP-2 and integrin alphavbeta3 promotes maturation of MMP-2 in breast carcinoma cells." Exp Cell Res **263**(2): 209-23.

Eastwood, M., D. A. McGrouther and R. A. Brown (1994). "A culture force monitor for measurement of contraction forces generated in human dermal fibroblast cultures: evidence for cell-matrix mechanical signalling." Biochim Biophys Acta **1201**(2): 186-92.

Eastwood, M., V. C. Mudera, D. A. McGrouther and R. A. Brown (1998). "Effect of precise mechanical loading on fibroblast populated collagen lattices: morphological changes." Cell Motil Cytoskeleton **40**(1): 13-21.

Eastwood, M., R. Porter, U. Khan, G. McGrouther and R. Brown (1996). "Quantitative analysis of collagen gel contractile forces generated by dermal fibroblasts and the relationship to cell morphology." J Cell Physiol **166**(1): 33-42.

Egeblad, M. and Z. Werb (2002). "New functions for the matrix metalloproteinases in cancer progression." Nat Rev Cancer **2**(3): 161-74.

Ehrlich, H. P., A. Desmouliere, R. F. Diegelmann, I. K. Cohen, C. C. Compton, W. L. Garner, Y. Kapanci and G. Gabbiani (1994). "Morphological and immunochemical differences between keloid and hypertrophic scar." Am J Pathol **145**(1): 105-13.

Ehrlich, H. P. and J. B. Rajaratnam (1990). "Cell locomotion forces versus cell contraction forces for collagen lattice contraction: an in vitro model of wound contraction." Tissue Cell **22**(4): 407-17.

Ehrlich, H. P. and T. Rittenberg (2000). "Differences in the mechanism for high- versus moderate-density fibroblast-populated collagen lattice contraction." J Cell Physiol **185**(3): 432-9.

Elsdale, T. and J. Bard (1972). "Collagen substrata for studies on cell behavior." J Cell Biol **54**(3): 626-37.

Fitzgerald, A. M., J. J. Kirkpatrick and I. L. Naylor (1999). "Dupuytren's disease. The way forward?" J Hand Surg [Br] **24**(4): 395-9.

Flint, M. H. and C. A. Poole (1990). "Contraction and contracture, in Mc Farlane RM, Mc Grouther DA, Flint MH (eds): *Dupuytren's Disease*. Edinburgh, Churchill Livingstone." (104-16).

Foucher, G., C. Cornil and E. Lenoble (1992). "Open palm technique for Dupuytren's disease. A five-year follow-up." Ann Chir Main Memb Super **11**(5): 362-6.

Foucher, G., J. Medina and R. Navarro (2003). "Percutaneous needle aponeurotomy: complications and results." J Hand Surg [Br] **28**(5): 427-31.

Fujiwara, M., Y. Muragaki and A. Ooshima (2005). "Keloid-derived fibroblasts show increased secretion of factors involved in collagen turnover and depend on matrix metalloproteinase for migration." Br J Dermatol **153**(2): 295-300.

Gabbiani, G. (2003). "The myofibroblast in wound healing and fibrocontractive diseases." J Pathol **200**(4): 500-3.

Gabbiani, G., C. Chaponnier and I. Huttner (1978). "Cytoplasmic filaments and gap junctions in epithelial cells and myofibroblasts during wound healing." J Cell Biol **76**(3): 561-8.

Gabbiani, G., B. J. Hirschel, G. B. Ryan, P. R. Statkov and G. Majno (1972). "Granulation tissue as a contractile organ. A study of structure and function." J Exp Med **135**(4): 719-34.

Gabbiani, G. and G. Majno (1972). "Dupuytren's contracture: fibroblast contraction? An ultrastructural study." Am J Pathol **66**(1): 131-46.

Gabbiani, G., G. B. Ryan and G. Majne (1971). "Presence of modified fibroblasts in granulation tissue and their possible role in wound contraction." Experientia **27**(5): 549-50.

Garbisa, S., G. Scagliotti, L. Masiero, C. Di Francesco, C. Caenazzo, M. Onisto, M. Micela, W. G. Stetler-Stevenson and L. A. Liotta (1992). "Correlation of serum metalloproteinase levels with lung cancer metastasis and response to therapy." Cancer Res **52**(16): 4548-9.

Gelberman, R. H., D. Amiel, R. M. Rudolph and R. M. Vance (1980). "Dupuytren's contracture. An electron microscopic, biochemical, and clinical correlative study." J Bone Joint Surg Am **62**(3): 425-32.

Giannelli, G., J. Falk-Marzillier, O. Schiraldi, W. G. Stetler-Stevenson and V. Quaranta (1997). "Induction of cell migration by matrix metalloprotease-2 cleavage of laminin-5." Science **277**(5323): 225-8.

Glimcher, M. J. and H. M. Peabody (1990). "Collagen organization, in Mc Farlane RM, Mc Grouther DA, Flint MH (eds): *Dupuytren's Disease*. Edinburgh, Churchill Livingstone." 72-85.

Godtfredsen, N. S., H. Lucht, E. Prescott, T. I. Sorensen and M. Gronbaek (2004). "A prospective study linked both alcohol and tobacco to Dupuytren's disease." J Clin Epidemiol **57**(8): 858-63.

Gonzalez, A. M., M. Buscaglia, R. Fox, A. Isacchi, P. Sarmientos, J. Farris, M. Ong, D. Martineau, D. A. Lappi and A. Baird (1992). "Basic fibroblast growth factor in Dupuytren's contracture." Am J Pathol **141**(3): 661-71.

Grinnell, F. (1994). "Fibroblasts, myofibroblasts, and wound contraction." J Cell Biol **124**(4): 401-4.

Grinnell, F. (1999). "Signal transduction pathways activated during fibroblast contraction of collagen matrices." Curr Top Pathol **93**: 61-73.

Grinnell, F. (2000). "Fibroblast-collagen-matrix contraction: growth-factor signalling and mechanical loading." Trends Cell Biol **10**(9): 362-5.

Grinnell, F. (2003). "Fibroblast biology in three-dimensional collagen matrices." Trends Cell Biol **13**(5): 264-9.

Grinnell, F. and C. H. Ho (2002). "Transforming growth factor beta stimulates fibroblast-collagen matrix contraction by different mechanisms in mechanically loaded and unloaded matrices." Exp Cell Res **273**(2): 248-55.

Guidry, C. and F. Grinnell (1987). "Contraction of hydrated collagen gels by fibroblasts: evidence for two mechanisms by which collagen fibrils are stabilized." Coll Relat Res **6**(6): 515-29.

Hande, K. R., M. Collier, L. Paradiso, J. Stuart-Smith, M. Dixon, N. Clendeninn, G. Yeun, D. Alberti, K. Binger and G. Wilding (2004). "Phase I and pharmacokinetic study of prinomastat, a matrix metalloprotease inhibitor." Clin Cancer Res **10**(3): 909-15.

Haralson, M. A. and J. R. Hassell (1995). "The Extracellular matrix - an overview. In The extracellular matrix - a practical approach. Edited by Haralson and Hassell, IRL Oxford University Press." (1-30).

Haro, H., H. C. Crawford, B. Fingleton, K. Shinomiya, D. M. Spengler and L. M. Matrisian (2000). "Matrix metalloproteinase-7-dependent release of tumor necrosis factor-alpha in a model of herniated disc resorption." J Clin Invest **105**(2): 143-50.

Harris, A. K., D. Stopak and P. Wild (1981). "Fibroblast traction as a mechanism for collagen morphogenesis." Nature **290**(5803): 249-51.

Harter, L. V., K. A. Hruska and R. L. Duncan (1995). "Human osteoblast-like cells respond to mechanical strain with increased bone matrix protein production independent of hormonal regulation." Endocrinology **136**(2): 528-35.

Higuchi, R., C. Fockler, G. Dollinger and R. Watson (1993). "Kinetic PCR analysis: real-time monitoring of DNA amplification reactions." Biotechnology (N Y) **11**(9): 1026-30.

Hinz, B., G. Celetta, J. J. Tomasek, G. Gabbiani and C. Chaponnier (2001). "Alpha-smooth muscle actin expression upregulates fibroblast contractile activity." Mol Biol Cell **12**(9): 2730-41.

Holmbeck, K., P. Bianco, J. Caterina, S. Yamada, M. Kromer, S. A. Kuznetsov, M. Mankani, P. G. Robey, A. R. Poole, I. Pidoux, J. M. Ward and H. Birkedal-Hansen (1999). "MT1-MMP-deficient mice develop dwarfism, osteopenia, arthritis, and connective tissue disease due to inadequate collagen turnover." Cell **99**(1): 81-92.

Howard, J. C., V. M. Varallo, D. C. Ross, J. H. Roth, K. J. Faber, B. Alman and B. S. Gan (2003). "Elevated levels of beta-catenin and fibronectin in three-dimensional collagen cultures of Dupuytren's disease cells are regulated by tension in vitro." BMC Musculoskelet Disord **4**: 16.

Hu, F. Z., A. Nystrom, A. Ahmed, M. Palmquist, R. Dopico, I. Mossberg, J. Gladitz, M. Rayner, J. C. Post, G. D. Ehrlich and R. A. Preston (2005). "Mapping of an autosomal dominant gene for Dupuytren's contracture to chromosome 16q in a Swedish family." Clin Genet **68**(5): 424-9.

Hueston, J. T. (1962). "Further studies on the incidence of Dupuytren's contracture." Med J Aust **49(1)**: 586-8.

Hueston, J. T. (1963). "Recurrent Dupuytren's contracture." Plast Reconstr Surg **31**: 66-9.

Hueston, J. T., J. V. Hurley and S. Whittingham (1976). "The contracting fibroblast as a clue to Dupuytren's contracture." Hand **8**(1): 10-2.

Hurst, L. C., M. A. Badalamente and J. Makowski (1986). "The pathobiology of Dupuytren's contracture: effects of prostaglandins on myofibroblasts." J Hand Surg [Am] **11**(1): 18-23.

Hutchinson, J. W., G. M. Tierney, S. L. Parsons and T. R. Davis (1998). "Dupuytren's disease and frozen shoulder induced by treatment with a matrix metalloproteinase inhibitor." J Bone Joint Surg Br **80**(5): 907-8.

Itoh, T., H. Matsuda, M. Tanioka, K. Kuwabara, S. Itohara and R. Suzuki (2002). "The role of matrix metalloproteinase-2 and matrix metalloproteinase-9 in antibody-induced arthritis." J Immunol **169**(5): 2643-7.

Jain, A., F. Brennan and J. Nanchahal (2002). "Treatment of rheumatoid tenosynovitis with cytokine inhibitors." Lancet **360**(9345): 1565-6.

Jansen, J. H., H. Jahr, J. A. Verhaar, H. A. Pols, H. Chiba, H. Weinans and J. P. van Leeuwen (2006). "Stretch-induced modulation of matrix metalloproteinases in mineralizing osteoblasts via extracellular signal-regulated kinase-1/2." J Orthop Res **24**(7): 1480-8.

Jemec, B., A. O. Grobbelaar, G. D. Wilson, P. J. Smith, R. Sanders and D. A. McGrouther (1999). "Is Dupuytren's disease caused by an imbalance between proliferation and cell death?" J Hand Surg [Br] **24**(5): 511-4.

Jones, G. C., A. N. Corps, C. J. Pennington, I. M. Clark, D. R. Edwards, M. M. Bradley, B. L. Hazleman and G. P. Riley (2006). "Expression profiling of metalloproteinases and tissue inhibitors of metalloproteinases in normal and degenerate human achilles tendon." Arthritis Rheum **54**(3): 832-42.

Jones, G. E. and J. A. Witkowski (1979). "Reduced adhesiveness between skin fibroblasts from patients with Duchenne muscular dystrophy." J Neurol Sci **43**(3): 465-70.

Keilholz, L., M. H. Seegenschmiedt and R. Sauer (1996). "Radiotherapy for prevention of disease progression in early-stage Dupuytren's contracture: initial and long-term results." Int J Radiat Oncol Biol Phys **36**(4): 891-7.

Ketchum, L. D. and T. K. Donahue (2000). "The injection of nodules of Dupuytren's disease with triamcinolone acetonide." J Hand Surg [Am] **25**(6): 1157-62.

Koike, T., R. B. Vernon, M. A. Hamner, E. Sadoun and M. J. Reed (2002). "MT1-MMP, but not secreted MMPs, influences the migration of human microvascular endothelial cells in 3-dimensional collagen gels." J Cell Biochem **86**(4): 748-58.

Kozma, E. M., K. Olczyk, G. Wisowski, A. Glowacki and R. Bobinski (2005). "Alterations in the extracellular matrix proteoglycan profile in Dupuytren's contracture affect the palmar fascia." J Biochem (Tokyo) **137**(4): 463-76.

Kuhn, M. A., X. Wang, W. G. Payne, F. Ko and M. C. Robson (2002). "Tamoxifen decreases fibroblast function and downregulates TGF(beta2) in dupuytren's affected palmar fascia." J Surg Res **103**(2): 146-52.

Lambert, C. A., A. C. Colige, C. Munaut, C. M. Lapiere and B. V. Nusgens (2001). "Distinct pathways in the over-expression of matrix metalloproteinases in human fibroblasts by relaxation of mechanical tension." Matrix Biol **20**(7): 397-408.

Lara, P. N., Jr., W. M. Stadler, J. Longmate, D. I. Quinn, J. Wexler, M. Van Loan, P. Twardowski, P. H. Gumerlock, N. J. Vogelzang, E. E. Vokes, H. J. Lenz, J. H. Doroshow and D. R. Gandara (2006). "A randomized phase II trial of the matrix metalloproteinase inhibitor BMS-275291 in hormone-refractory prostate cancer patients with bone metastases." Clin Cancer Res **12**(5): 1556-63.

Lemaitre, V. and J. D'Armiento (2006). "Matrix metalloproteinases in development and disease." Birth Defects Res C Embryo Today **78**(1): 1-10.

Li, B. H., P. Zhao, S. Z. Liu, Y. M. Yu, M. Han and J. K. Wen (2005). "Matrix metalloproteinase-2 and tissue inhibitor of metallo-proteinase-2 in colorectal carcinoma invasion and metastasis." World J Gastroenterol **11**(20): 3046-50.

Lin, C. Q. and M. J. Bissell (1993). "Multi-faceted regulation of cell differentiation by extracellular matrix." Faseb J **7**(9): 737-43.

Linask, K. K., M. Han, D. H. Cai, P. R. Brauer and S. M. Maisastry (2005). "Cardiac morphogenesis: matrix metalloproteinase coordination of cellular mechanisms underlying heart tube formation and directionality of looping." Dev Dyn **233**(3): 739-53.

Lindahl, G. E., R. C. Chambers, J. Papakrivopoulou, S. J. Dawson, M. C. Jacobsen, J. E. Bishop and G. J. Laurent (2002). "Activation of fibroblast procollagen alpha 1(I) transcription by mechanical strain is transforming growth factor-beta-dependent and involves increased binding of CCAAT-binding factor (CBF/NF-Y) at the proximal promoter." J Biol Chem **277**(8): 6153-61.

Ling, R. S. (1963). "The Genetic Factor in Dupuytren's Disease." J Bone Joint Surg Br **45**: 709-18.

Luck, J. V. (1959). "Dupuytren's contracture; a new concept of the pathogenesis correlated with surgical management." J Bone Joint Surg Am **41-A**(4): 635-64.

Makela, E. A., H. Jaroma, A. Harju, S. Anttila and J. Vainio (1991). "Dupuytren's contracture: the long-term results after day surgery." J Hand Surg [Br] **16**(3): 272-4.

Malemud, C. J. (2006). "Matrix metalloproteinases (MMPs) in health and disease: an overview." Front Biosci **11**: 1696-701.

Mannello, F., G. Tonti and S. Papa (2005). "Matrix metalloproteinase inhibitors as anticancer therapeutics." Curr Cancer Drug Targets **5**(4): 285-98.

Marenzana, M., N. Wilson-Jones, V. Mudera and R. A. Brown (2006). "The origins and regulation of tissue tension: Identification of collagen tension-fixation process in vitro." Exp Cell Res **312**(4): 423-33.

Matthews, P. (1979). "Familial Dupuytren's contracture with predominantly female expression." Br J Plast Surg **32**(2): 120-3.

McCann, B. G., A. Logan, H. Belcher, A. Warn and R. M. Warn (1993). "The presence of myofibroblasts in the dermis of patients with Dupuytren's contracture. A possible source for recurrence." J Hand Surg [Br] **18**(5): 656-61.

McFarlane, R. M. (1983). "The current status of Dupuytren's disease." J Hand Surg [Am] **8**(5 Pt 2): 703-8.

McFarlane, R. M. (1990). "Is Dupuytren's disease a neoplasm? In McFarlane RM, McGrouther DA, Flint MH (eds): Dupuytren's Disease: Biology and Treatment, Vol 5, The Hand and Upper Limb Series. Edinburgh, Churchill Livingstone." 229-290.

McFarlane, R. M. (1991). "Dupuytren's disease: relation to work and injury." J Hand Surg [Am] **16**(5): 775-9.

McGrouther, D. A. (1982). "The microanatomy of Dupuytren's contracture." Hand **14**(3): 215-36.

Meisser, A., M. Cohen and P. Bischof (2005). "Concentrations of circulating gelatinases (matrix metalloproteinase-2 and -9) are dependent on the conditions of blood collection." Clin Chem **51**(1): 274-6.

Meister, P., J. M. Gokel and K. Remberger (1979). "Palmar fibromatosis-"Dupuytren's contracture". A comparison of light electron and immunofluorescence microscopic findings." Pathol Res Pract **164**(4): 402-12.

Mengshol, J. A., K. S. Mix and C. E. Brinckerhoff (2002). "Matrix metalloproteinases as therapeutic targets in arthritic diseases: bull's-eye or missing the mark?" Arthritis Rheum **46**(1): 13-20.

Menzel, E. J., H. Piza, C. Zielinski, A. T. Endler, C. Steffen and H. Millesi (1979). "Collagen types and anticollagen-antibodies in Dupuytren's disease." Hand **11**(3): 243-8.

Messina, A. and J. Messina (1993). "The continuous elongation treatment by the TEC device for severe Dupuytren's contracture of the fingers." Plast Reconstr Surg **92**(1): 84-90.

Meyer, M. and D. A. McGrouther (1991). "A study relating wound tension to scar morphology in the pre-sternal scar using Langers technique." Br J Plast Surg **44**(4): 291-4.

Mirastschijski, U., C. J. Haaksma, J. J. Tomasek and M. S. Agren (2004). "Matrix metalloproteinase inhibitor GM 6001 attenuates keratinocyte migration, contraction and myofibroblast formation in skin wounds." Exp Cell Res **299**(2): 465-75.

Moermans, J. P. (1996). "Long-term results after segmental aponeurectomy for Dupuytren's disease." J Hand Surg [Br] **21**(6): 797-800.

Moyer, K. E., D. R. Banducci, W. P. Graham, 3rd and H. P. Ehrlich (2002). "Dupuytren's disease: physiologic changes in nodule and cord fibroblasts through aging in vitro." Plast Reconstr Surg **110**(1): 187-93; discussion 194-6.

Mudera, V. C., R. Pleass, M. Eastwood, R. Tarnuzzer, G. Schultz, P. Khaw, D. A. McGrouther and R. A. Brown (2000). "Molecular responses of human dermal fibroblasts to dual cues: contact guidance and mechanical load." Cell Motil Cytoskeleton **45**(1): 1-9.

Mudgett, J. S., N. I. Hutchinson, N. A. Chartrain, A. J. Forsyth, J. McDonnell, Singer, II, E. K. Bayne, J. Flanagan, D. Kawka, C. F. Shen, K. Stevens, H. Chen, M. Trumbauer and D. M. Visco (1998). "Susceptibility of stromelysin 1-deficient mice to collagen-induced arthritis and cartilage destruction." Arthritis Rheum **41**(1): 110-21.

Murrell, G. A., M. J. Francis and L. Bromley (1987). "Free radicals and Dupuytren's contracture." Br Med J (Clin Res Ed) **295**(6610): 1373-5.

Murrell, G. A., M. J. Francis and L. Bromley (1991). "The collagen changes of Dupuytren's contracture." J Hand Surg [Br] **16**(3): 263-6.

Nagase, H., R. Visse and G. Murphy (2006). "Structure and function of matrix metalloproteinases and TIMPs." Cardiovasc Res **69**(3): 562-73.

Nagase, H. and J. F. Woessner (1999). "Matrix Metalloproteinases." The Journal of Biological Chemistry **274**(31): 21491-21494.

Nakatani, S., M. Ikura, S. Yamamoto, Y. Nishita, S. Itadani, H. Habashita, T. Sugiura, K. Ogawa, H. Ohno, K. Takahashi, H. Nakai and M. Toda (2006). "Design and

synthesis of novel metalloproteinase inhibitors." Bioorg Med Chem **14**(15): 5402-22.

Neely, A. N., C. E. Clendening, J. Gardner, D. G. Greenhalgh and G. D. Warden (1999). "Gelatinase activity in keloids and hypertrophic scars." Wound Repair Regen **7**(3): 166-71.

Ohuchi, E., K. Imai, Y. Fujii, H. Sato, M. Seiki and Y. Okada (1997). "Membrane type 1 matrix metalloproteinase digests interstitial collagens and other extracellular matrix macromolecules." J Biol Chem **272**(4): 2446-51.

Parsons, M., E. Kessler, G. J. Laurent, R. A. Brown and J. E. Bishop (1999). "Mechanical load enhances procollagen processing in dermal fibroblasts by regulating levels of procollagen C-proteinase." Exp Cell Res **252**(2): 319-31.

Parsons, S. L., S. A. Watson, P. D. Brown, H. M. Collins and R. J. Steele (1997). "Matrix metalloproteinases." Br J Surg **84**(2): 160-6.

Peyton, S. R. and A. J. Putnam (2005). "Extracellular matrix rigidity governs smooth muscle cell motility in a biphasic fashion." J Cell Physiol **204**(1): 198-209.

Pfaffl, M. W., G. W. Horgan and L. Dempfle (2002). "Relative expression software tool (REST) for group-wise comparison and statistical analysis of relative expression results in real-time PCR." Nucleic Acids Res **30**(9): e36.

Phillips, J. A., C. A. Vacanti and L. J. Bonassar (2003). "Fibroblasts regulate contractile force independent of MMP activity in 3D-collagen." Biochem Biophys Res Commun **312**(3): 725-32.

Pins, G. D., M. E. Collins-Pavao, L. Van De Water, M. L. Yarmush and J. R. Morgan (2000). "Plasmin triggers rapid contraction and degradation of fibroblast-populated collagen lattices." J Invest Dermatol **114**(4): 647-53.

Pittet, B., L. Rubbia-Brandt, A. Desmouliere, A. P. Sappino, P. Roggero, S. Guerret, J. A. Grimaud, R. Lacher, D. Montandon and G. Gabbiani (1994). "Effect of gamma-interferon on the clinical and biologic evolution of hypertrophic scars and Dupuytren's disease: an open pilot study." Plast Reconstr Surg **93**(6): 1224-35.

Prajapati, R. T., B. Chavally-Mis, D. Herbage, M. Eastwood and R. A. Brown (2000). "Mechanical loading regulates protease production by fibroblasts in three-dimensional collagen substrates." Wound Repair Regen **8**(3): 226-37.

Qian, A., R. A. Meals, J. Rajfer and N. F. Gonzalez-Cadavid (2004). "Comparison of gene expression profiles between Peyronie's disease and Dupuytren's contracture." Urology **64**(2): 399-404.

Rayan, G. M. (1999). "Clinical presentation and types of Dupuytren's disease." Hand Clin **15**(1): 87-96, vii.

Rayan, G. M. and J. J. Tomasek (1994). "Generation of contractile force by cultured Dupuytren's disease and normal palmar fibroblasts." Tissue Cell **26**(5): 747-56.

Reuben, P. M. and H. S. Cheung (2006). "Regulation of matrix metalloproteinase (MMP) gene expression by protein kinases." Front Biosci **11**: 1199-215.

Riley, G. P., V. Curry, J. DeGroot, B. van El, N. Verzijl, B. L. Hazleman and R. A. Bank (2002). "Matrix metalloproteinase activities and their relationship with collagen remodelling in tendon pathology." Matrix Biol **21**(2): 185-95.

Ritter, M. A. (1973). "The anatomy and function of the palmar fascia." Hand **5**(3): 263-7.

Ritty, T. M. and J. Herzog (2003). "Tendon cells produce gelatinases in response to type I collagen attachment." J Orthop Res **21**(3): 442-50.

Rodrigo, J. J., J. J. Niebauer, R. L. Brown and J. R. Doyle (1976). "Treatment of Dupuytren's contracture. Long-term results after fasciotomy and fascial excision." J Bone Joint Surg Am **58**(3): 380-7.

Rombouts, J. J., H. Noel, Y. Legrain and E. Munting (1989). "Prediction of recurrence in the treatment of Dupuytren's disease: evaluation of a histologic classification." J Hand Surg [Am] **14**(4): 644-52.

Rosemurgy, A., J. Harris, A. Langleben, E. Casper, S. Goode and H. Rasmussen (1999). "Marimastat in patients with advanced pancreatic cancer: a dose-finding study." Am J Clin Oncol **22**(3): 247-52.

Rosenbaum, E., M. Zahurak, V. Sinibaldi, M. A. Carducci, R. Pili, M. Laufer, T. L. DeWeese and M. A. Eisenberger (2005). "Marimastat in the treatment of patients with biochemically relapsed prostate cancer: a prospective randomized, double-blind, phase I/II trial." Clin Cancer Res **11**(12): 4437-43.

Ross, D. C. (1999). "Epidemiology of Dupuytren's disease." Hand Clin **15**(1): 53-62, vi.

Sambrook, J. (1989). "Sambrook J, Fritsch EF, Maniatis T. Molecular cloning: a laboratory manual. 2nd Ed Cold Spring Harbor Laboratory press volume 3 pp E5."

Schmalfeldt, B., D. Prechtel, K. Harting, K. Spathe, S. Rutke, E. Konik, R. Fridman, U. Berger, M. Schmitt, W. Kuhn and E. Lengyel (2001). "Increased expression of matrix metalloproteinases (MMP)-2, MMP-9, and the urokinase-type plasminogen activator is associated with progression from benign to advanced ovarian cancer." Clin Cancer Res **7**(8): 2396-404.

Scott, K. A., E. J. Wood and E. H. Karran (1998). "A matrix metalloproteinase inhibitor which prevents fibroblast-mediated collagen lattice contraction." FEBS Lett **441**(1): 137-40.

Serini, G. and G. Gabbiani (1999). "Mechanisms of myofibroblast activity and phenotypic modulation." Exp Cell Res **250**(2): 273-83.

Seyhan, H., J. Kopp, S. Schultze-Mosgau and R. E. Horch (2006). "Increased metabolic activity of fibroblasts derived from cords compared with nodule fibroblasts sampling from patients with Dupuytren's contracture." Plast Reconstr Surg **117**(4): 1248-52.

Sheetz, M. P., D. P. Felsenfeld and C. G. Galbraith (1998). "Cell migration: regulation of force on extracellular-matrix-integrin complexes." Trends Cell Biol **8**(2): 51-4.

Shelley, W. B. and E. D. Shelley (1993). "Response of Dupuytren's contracture to high-potency topical steroid." Lancet **342**(8867): 366.

Sheridan, C. M., N. L. Occleston, P. Hiscott, C. H. Kon, P. T. Khaw and I. Grierson (2001). "Matrix metalloproteinases: a role in the contraction of vitreo-retinal scar tissue." Am J Pathol **159**(4): 1555-66.

Sier, C. F., F. J. Kubben, S. Ganesh, M. M. Heerding, G. Griffioen, R. Hanemaaijer, J. H. van Krieken, C. B. Lamers and H. W. Verspaget (1996). "Tissue levels of matrix metalloproteinases MMP-2 and MMP-9 are related to the overall survival of patients with gastric carcinoma." Br J Cancer **74**(3): 413-7.

Skiles, J. W., N. C. Gonnella and A. Y. Jeng (2004). "The design, structure, and clinical update of small molecular weight matrix metalloproteinase inhibitors." Curr Med Chem **11**(22): 2911-77.

Smith, M. R., H. Kung, S. K. Durum, N. H. Colburn and Y. Sun (1997). "TIMP-3 induces cell death by stabilizing TNF-alpha receptors on the surface of human colon carcinoma cells." Cytokine **9**(10): 770-80.

Steinberg, B. M., K. Smith, M. Colozzo and R. Pollack (1980). "Establishment and transformation diminish the ability of fibroblasts to contract a native collagen gel." J Cell Biol **87**(1): 304-8.

Stephens, P., K. J. Davies, N. Occleston, R. D. Pleass, C. Kon, J. Daniels, P. T. Khaw and D. W. Thomas (2001). "Skin and oral fibroblasts exhibit phenotypic differences in extracellular matrix reorganization and matrix metalloproteinase activity." Br J Dermatol **144**(2): 229-37.

Sternlicht, M. D. and Z. Werb (2001). "How matrix metalloproteinases regulate cell behavior." Annu Rev Cell Dev Biol **17**: 463-516.

Stiles, P. J. (1966). "Ultrasonic therapy in Dupuytren's contracture." J Bone Joint Surg Br **48**(3): 452-4.

Streuli, C. (1999). "Extracellular matrix remodelling and cellular differentiation." Curr Opin Cell Biol **11**(5): 634-40.

Tarlton, J. F., P. Meagher, R. A. Brown, D. A. McGrouther, A. J. Bailey and A. Afoke (1998). "Mechanical stress in vitro induces increased expression of MMPs 2 and 9 in excised Dupuytren's disease tissue." J Hand Surg [Br] **23**(3): 297-302.

Tarpila, E., M. R. Ghassemifar, S. Wingren, M. Agren and L. Franzen (1996). "Contraction of collagen lattices by cells from Dupuytren's nodules." J Hand Surg [Br] **21**(6): 801-5.

Tchetverikov, I., L. S. Lohmander, N. Verzijl, T. W. Huizinga, J. M. TeKoppele, R. Hanemaaijer and J. DeGroot (2005). "MMP protein and activity levels in synovial fluid from patients with joint injury, inflammatory arthritis, and osteoarthritis." Ann Rheum Dis **64**(5): 694-8.

Terek, R. M., W. A. Jiranek, M. J. Goldberg, H. J. Wolfe and B. A. Alman (1995). "The expression of platelet-derived growth-factor gene in Dupuytren contracture." J Bone Joint Surg Am **77**(1): 1-9.

Thannickal, V. J., G. B. Toews, E. S. White, J. P. Lynch, 3rd and F. J. Martinez (2004). "Mechanisms of pulmonary fibrosis." Annu Rev Med **55**: 395-417.

Tomasek, J. and G. M. Rayan (1995). "Correlation of alpha-smooth muscle actin expression and contraction in Dupuytren's disease fibroblasts." J Hand Surg [Am] **20**(3): 450-5.

Tomasek, J. J., G. Gabbiani, B. Hinz, C. Chaponnier and R. A. Brown (2002). "Myofibroblasts and mechano-regulation of connective tissue remodelling." Nat Rev Mol Cell Biol **3**(5): 349-63.

Tonn, J. C., S. Kerkau, A. Hanke, H. Bouterfa, J. G. Mueller, S. Wagner, G. H. Vince and K. Roosen (1999). "Effect of synthetic matrix-metalloproteinase inhibitors on invasive capacity and proliferation of human malignant gliomas in vitro." Int J Cancer **80**(5): 764-72.

Toth, M., M. M. Bernardo, C.M. Overall, Y.A. DeClerck, H.Tschesche, M.L. Cher, S. Brown, S. Mobashery, R. Fridman, R. (2000). "Tissue inhibitor of metalloproteinase (TIMP)-2 acts synergistically with synthetic matrix metalloproteinase (MMP) inhibitors but not with TIMP-4 to enhance the (Membrane type 1)-MMP-dependent activation of pro-MMP-2." J Biol Chem **275**(52): 41415-23.

Tranquillo, R. T. (1999). "Self-organization of tissue-equivalents: the nature and role of contact guidance." Biochem Soc Symp **65**: 27-42.

Tse, R., J. Howard, Y. Wu and B. S. Gan (2004). "Enhanced Dupuytren's disease fibroblast populated collagen lattice contraction is independent of endogenous active TGF-beta2." BMC Musculoskelet Disord **5**(1): 41.

Ulrich, D., K. Hrynyschyn and N. Pallua (2003). "Matrix metalloproteinases and tissue inhibitors of metalloproteinases in sera and tissue of patients with Dupuytren's disease." Plast Reconstr Surg **112**(5): 1279-86.

van der Rest, M. and R. Garrone (1991). "Collagen family of proteins." Faseb J **5**(13): 2814-23.

Vande Berg, J. S., R. H. Gelberman, R. Rudolph, D. Johnson and P. Sicurello (1984). "Dupuytren's disease: comparative growth dynamics and morphology between cultured myofibroblasts (nodule) and fibroblasts (cord)." J Orthop Res **2**(3): 247-56.

Visse, R. and H. Nagase (2003). "Matrix metalloproteinases and tissue inhibitors of metalloproteinases: structure, function, and biochemistry." Circ Res **92**(8): 827-39.

Wall, L., D. C. Talbot, P. Bradbury and D. I. Jodrell (2004). "A phase I and pharmacological study of the matrix metalloproteinase inhibitor BB-3644 in patients with solid tumours." Br J Cancer **90**(4): 800-4.

Wang, Z., R. Juttermann and P. D. Soloway (2000). "TIMP-2 is required for efficient activation of proMMP-2 in vivo." J Biol Chem **275**(34): 26411-5.

Wojtowicz-Praga, S., J. Torri, M. Johnson, V. Steen, J. Marshall, E. Ness, R. Dickson, M. Sale, H. S. Rasmussen, T. A. Chiodo and M. J. Hawkins (1998). "Phase I

trial of Marimastat, a novel matrix metalloproteinase inhibitor, administered orally to patients with advanced lung cancer." J Clin Oncol **16**(6): 2150-6.

Wong, M. and V. Mudera (2006). "Feedback inhibition of high TGF-beta1 concentrations on myofibroblast induction and contraction by Dupuytren's fibroblasts." J Hand Surg [Br] **31**(5): 473-83.

Wong, T. T., J. T. Daniels, J. G. Crowston and P. T. Khaw (2004). "MMP inhibition prevents human lens epithelial cell migration and contraction of the lens capsule." Br J Ophthalmol **88**(7): 868-72.

Wong, T. T., A. L. Mead and P. T. Khaw (2003). "Matrix metalloproteinase inhibition modulates postoperative scarring after experimental glaucoma filtration surgery." Invest Ophthalmol Vis Sci **44**(3): 1097-103.

Wrobel, L. K., T. R. Fray, J. E. Molloy, J. J. Adams, M. P. Armitage and J. C. Sparrow (2002). "Contractility of single human dermal myofibroblasts and fibroblasts." Cell Motil Cytoskeleton **52**(2): 82-90.

Zucker, S. and J. Vacirca (2004). "Role of matrix metalloproteinases (MMPs) in colorectal cancer." Cancer Metastasis Rev **23**(1-2): 101-17.